THE ASTROPHYSICAL JOURNAL

AN INTERNATIONAL REVIEW OF SPECTROSCOPY AND ASTRONOMICAL PHYSICS

VOLUME 93 MAY 1941 NUMBER 3

THE DYNAMICS OF THE INTERSTELLAR MEDIUM

I. LOCAL EQUILIBRIUM

LYMAN SPITZER, JR.

ABSTRACT

The physical properties of the interstellar medium, especially those which depend on the presence of small dust particles, are examined in detail. It is shown that if the electron density is as great as 10^{-3} per cm^3 the charge on a dust particle will be determined by collisions with rapidly moving electrons rather than by photoelectric ionizations; a small particle will, in such a case, be charged to -2 volts, independently of its radius. Any deviations from equipartition of kinetic energy between all the interstellar particles will be reduced by $1/e$ within at most 10^4 years if there is 1 proton per cm^3, and within 4×10^5 years if no ionized H is present but if 10^{-3} Ca^{++} ions per cm^3 or their equivalent are assumed. The random velocities of dust particles should, therefore, be extremely small, and the mean free path should not be greater than a few astronomical units. The viscosity of the interstellar medium is evaluated and is shown to be negligible; in the neighborhood of stars whose random motion does not exceed 10 km/sec the medium will not acquire any net momentum. The rate of diffusion of interstellar particles is also very low, and mixing of the various constituents in 10^9 years is restricted to a few parsecs.

Recent work,[1] though by no means precise, indicates that the average density of interstellar matter is about 10^{-24} gm/cm^3 in order of magnitude, that a substantial fraction of this is in the form of metallic particles of various radii,[2,3] ranging around 10^{-5} cm, and that the remainder includes neutral and ionized atoms[4] and molecules.[5] The distribution of the small "dust" particles is very spotty, such particles apparently occurring in clouds in the galactic plane.[6,7]

The presence of dust particles implies that the physical state of such a medium may be somewhat different from that discussed in the classical work by Eddington,[8] in which only atoms were assumed to be abundant. It is of interest to investigate anew the physi-

[1] F. H. Seares, *Pub. A.S.P.*, **52**, 80, 1940; "Symposium on Interstellar Absorption," *Ann. d'astrophysique*, **1**, 21, 1938. These two surveys contain extensive bibliographies.

[2] C. Schalén, *Uppsala Ann.*, **1**, No. 2, 1939.

[3] J. L. Greenstein, *Harvard Circ.*, No. 422, 1937.

[4] P. W. Merrill, R. F. Sanford, O. C. Wilson, and C. G. Burwell, *Ap. J.*, **86**, 274, 1937.

[5] A. McKellar, *Pub. A.S.P.*, **52**, 187, 1940.

[6] Joel Stebbins, C. M. Huffer, and A. E. Whitford, *Ap. J.*, **92**, 193, 1940.

[7] A. Hunter and E. G. Martin, *M.N.*, **100**, 669, 1940.

[8] *Internal Constitution of Stars*, p. 371, Cambridge U. Press, 1930.

cal conditions of the interstellar medium. The available observations suffice for a general picture, although perhaps a somewhat incomplete one. Such an investigation is of value partly as a guide to further research, partly as a necessary preliminary to the discussion of the role of interstellar matter in problems of galactic structure and stellar evolution.[9] The local equilibrium of dust and atoms is considered here. The effects of radiation pressure, the physical conditions within clouds of dust, and the galactic equilibrium of interstellar matter will be treated in subsequent papers now in preparation.

In the first of the following four sections the relative abundances of the different particles in interstellar space are discussed, and values are chosen as a basis for the remaining calculations. The second section is devoted to a discussion of the ionization of the various particles, especially the negative charge produced on dust particles by the capture of electrons. The relatively rapid approach of the interstellar particles to an equipartition of kinetic energy is treated in section 3. Section 4 investigates the viscosity of the medium.

1. THE CONSTITUENTS OF THE MEDIUM

The relative abundances of the various atoms, molecules, and dust particles in interstellar space are of primary importance in a discussion of the physical conditions of the interstellar medium. Present data provide lower and upper limits for all the constituents of the medium. The most important datum in this respect is the Oort limit[10] for the density of matter in the neighborhood of the sun; when the density of known stars is subtracted, this gives 3×10^{-24} gm/cm^3 as the maximum mean density of interstellar matter.

A lower limit for the density of dust is fixed by the observations of selective absorption. Greenstein[3] finds that a density of 2×10^{-25} gm/cm^3 would be consistent with the data. Apparently no density much less than 10^{-25} gm/cm^3 would be admissible. This is a mean density and is certainly exceeded at some points in space.

A lower limit of the density of atoms is afforded by measurements of interstellar line absorption and of *H* line emission. The observed strengths of the D lines require an average density[11] of 10^{-31} gm/cm^3 for neutral *Na*. For any assumed electron density the corresponding number of Na^+ atoms may be calculated from the energy density of ultraviolet radiation.

The most thorough investigation of this sort has been carried through by Dunham.[12] From Dunham's tables computed for a moderate selective absorption it follows that, if the interstellar medium is assumed to consist wholly of sodium atoms, then Na^+ will be 2×10^6 as abundant as *Na*, corresponding roughly to 6×10^{-3} electrons per cm^3 and to a space density of 2×10^{-25} gm/cm^3. This value can be reduced to 10^{-25} gm/cm^3, half sodium, half hydrogen, by the addition of 3×10^{-2} protons per cm^3 to increase the electron density. Any further increase in the amount of hydrogen will lead to a net increase in the density of sodium plus hydrogen.

As Dunham has pointed out, however, the ionization formula used neglects the fact that ionization in interstellar space occurs from the ground state only, and gives a relative ionization which is several times too great for a given electron pressure; lack of accurate *gf*-values for the relevant transitions makes the error somewhat indeterminate, but it can scarcely exceed a factor of 10. Even with this maximum allowance for error the minimum density of sodium and hydrogen consistent with the observed strengths of the D lines and the calculated intensity of the ultraviolet ionizing radiation is 3×10^{-26} gm/cm^3; we may, accordingly, take this value as a lower limit for the density of atoms in space.

The best evidence of the density of interstellar hydrogen is provided by the data of

[9] F. Hoyle and R. A. Lyttleton, *Proc. Cambridge Phil. Soc.*, **35**, 592, 1939.

[10] J. A. Oort, *B.A.N.*, No. 238, 1932.

[11] O. C. Wilson and P. W. Merrill, *Ap. J.*, **86**, 44, 1937.

[12] *Proc. Amer. Phil. Soc.*, **81**, 277, 1939.

Struve and Elvey[13] on $H\alpha$ emission in Cygnus and Cepheus. An analysis of these observations by B. Strömgren[14] indicates a value of 3 atoms per cm^3, or 5×10^{-24} gm/cm^3 of ionized H in these regions.

The strength of interstellar H and K relative to the line of neutral *Ca* at λ 4227 determines the electron density and provides a further confirmation of the high value found by Strömgren. Although the observations are not definitive, a ratio of 3500 Ca^+ atoms to each *Ca* atom seems indicated by the line strengths[12] and the curve of growth empirically constructed from the intensities of the *Na* lines. This fact, together with the energy density of interstellar radiation computed by Dunham, gives an electron density of about 10 per cm^3. Since the ionization formula used yields a value of the electron density which is several times too large, this result is in rough agreement with the work of Struve and Strömgren.

The observations of short-wave radio waves emanating from the galactic center have been attributed[15] to the effect of free-free electron transitions in interstellar space, and a density of 1 electron per cm^3 has been shown to be compatible with the data, for the most part. Until the observational discrepancies in this field have been clarified, however, the results are not reliable.

As has been pointed out by Swings and Rosenfeld,[16] the identification[5] of lines from interstellar *NaH*, *CH*, and *CN* is a verification both of a relatively high abundance of atoms in general and of hydrogen in particular. Since the process of molecular formation in space is not yet understood, this argument also is not very trustworthy.

The evidence presented by the relative ionization of *Ca* atoms and the intensity of *H* emission indicates that the density of interstellar atoms is nearer to the Oort limit than to the lower limit of 3×10^{-26} gm/cm^3 found above. We shall assume in the following that (1) the density of hydrogen is 1.7×10^{-24} gm/cm^3, or 1 atom per cm^3; (2) the density of dust particles is between 10^{-24} and 10^{-25} gm/cm^3; (3) the density of other atoms and molecules is considerably less than that of hydrogen. Assumption 3 does not affect the results for the most part.

While assumptions 1 and 2 are good approximations for mean densities, regions probably exist in which neither is fulfilled. The following considerations may be expected to have a certain mean validity. The effect of deviations from the densities here assumed will be discussed in a later paper.

2. IONIZATION

It is well known that most interstellar atoms must be ionized. Hydrogen atoms, however, present a special case, owing to their high abundance. As Strömgren[14] has pointed out, hydrogen ionization is strongly affected by the fact that neutral *H* absorbs heavily any radiation beyond the Lyman limit. If the hydrogen a short distance away from a star is not almost entirely ionized, this absorption will be so great that hydrogen a short distance farther away from the source of the ionizing radiation will not be ionized at all. Hence, interstellar hydrogen will be sharply divided into regions of neutral *H* which we shall call *H* I regions, and *H* II regions of almost completely ionized hydrogen.

Each star will be surrounded by an *H* II region which, if the hydrogen density is uniform, will be spherical. The radius s_0 of such a region is a function primarily of the spectral type of the star and has been computed by Strömgren. With the assumed abundance of 1 hydrogen atom per cm^3, these values range from 7.2 parsecs for a B3 star to 140 parsecs for one of type O5. The distinction between *H* I and *H* II regions is one of great importance, since the electron density, the intensity of *H* emission lines, and the relative abundance of neutral atoms of relatively low ionization potential will clearly be less in *H* I than in *H* II. The absorption of ionizing radiation by other atoms is unim-

[13] *Ap. J.*, **88**, 364, 1938.

[14] *Ap. J.*, **89**, 526, 1939.

[15] L. G. Henyey and P. C. Keenan, *Ap. J.*, **91**, 625, 1940.

[16] *Ap. J.*, **86**, 483, 1937.

portant, since the values of s_0 for atoms less abundant than hydrogen and of lower ionization potential are greater than the distances between the stars.

An interstellar dust particle will also have a net electrostatic charge in general, the sign of this charge depending upon the physical conditions. The possible influences producing such a charge are cosmic rays, ultraviolet stellar radiation, and direct collisions with atomic ions and electrons.

The influence of cosmic rays, discussed by Corlin[17] in the case of meteorites, is quite negligible compared to the effect of electron collisions. The total number of primary cosmic ray particles entering the upper atmosphere of the earth is 0.09 per cm^2 per sec.[18] The number of electrons crossing a square centimeter in a second will equal $\frac{1}{4}n_e v_e$; even if n_e, the number of electrons per cm^3, is as low as 10^{-4} and the velocity, v_e, is 10^7 cm/sec, corresponding to an electron temperature of 200°, $\frac{1}{4}n_e v_e$ will equal 2.5×10^2, or roughly 3×10^3 as great as the corresponding quantity for cosmic rays.

The effect on a dust particle of a collision with a single cosmic ray particle will not be large in any case. A particle of radius 10^{-5} cm corresponds to less than 1 cm of air and will be much too small to produce a cosmic ray shower. The only important effect of the passage of a cosmic ray will be to ionize the atoms inside the dust particles; i.e., recoil electrons will be produced by the cosmic ray. The ionization produced by a typical cosmic ray amounts to roughly 50 electrons per cm in air. Hence, in iron the ionization produced will be less than 10^6 electrons per cm, and in a sphere of radius 10^{-5} cm at most 20 free electrons will be produced by the passage of a single cosmic ray. Since the average energy of the electrons is small—10 or 20 electron volts in order of magnitude—most of these electrons will be stopped before they have reached the surface, and very few will leave the dust particle entirely. A cosmic-ray encounter is, therefore, no more effective in ionizing a dust particle than is an encounter with an electron. Since encounters with cosmic rays are much less frequent than those with electrons, we may neglect them.

It is rather the simple processes of electron collision and photoelectric ionization that are responsible for the charge on an absorbing particle. The photoelectric effect is well known and requires no qualitative explanation. It is perhaps not so clear that in the absence of this phenomenon a dust particle will acquire a charge simply from encounters with electrons and protons, even though positive and negative particles are assumed to be equally numerous. Electron velocities are much greater than those of atoms; the number of collisions with electrons will be much greater than those with positive ions. Any electron which hits a particle is almost certain to penetrate and to be retained by the particle.

It is less certain whether positive ions are necessarily retained by a particle after a collision. We shall assume in this section that they are retained and that only neutral entities can leave a dust particle, except for electrons which may be ejected by the absorption of a quantum of radiation; this assumption gives a lower limit for the negative charge on a dust particle.

The final electric charge on a dust particle must be such that a steady state is reached, with electrons repelled, and positive ions attracted; the total change of charge per unit time from all sources must equal zero.

The cross-section $\pi\sigma_i^2$ for the capture of an ion of charge Q_i, mass m_i, and velocity v_i by a stationary dust particle may be found simply. If V_r is the relative velocity at grazing collision, the conservation of energy and angular momentum yields the equations

$$\tfrac{1}{2}m_i v_i^2 = \tfrac{1}{2}m_i V_r^2 + \frac{Q_i Q_d}{\sigma}\,, \tag{1}$$

$$\sigma_i v_i = \sigma V_r\,, \tag{2}$$

[17] *Zs. f. Ap.*, **15**, 259, 1938.

[18] I. S. Bowen, R. A. Millikan, and H. V. Neher, *Phys. Rev.*, **53**, 217, 1938.

where σ is the geometrical radius of the dust particle and Q_d is its electric charge. Eliminating V_r from equations (1) and (2), we find

$$\pi\sigma_i^2 = \pi\sigma^2\left(1 - \frac{2Q_iQ_d}{\sigma m_i v_i^2}\right). \tag{3}$$

Let Γ_i denote the total number of ions of type i captured per second by a dust particle. To calculate Γ_i we multiply equation (3) by $n_i v_i$, where n_i is the number of ions of type i per cm^3, and average over a Maxwellian velocity distribution; the average extends only over those values for which σ_i^2 is positive. The integration is elementary and gives

$$\Gamma_i = 4\left(\frac{\pi}{3}\right)^{1/2}\frac{n_i\sigma^2E_i^{1/2}}{m_i^{1/2}} \times \begin{cases} 1 - \gamma_i & \gamma_i < 0\,, \\ e^{-\gamma_i} & \gamma_i > 0\,, \end{cases} \tag{4}$$

where

$$\gamma_i = \frac{3Q_iQ_d}{2\sigma E_i} = \frac{3VZ_i}{2E_i}\,; \tag{5}$$

E_i and E_i denote the mean kinetic energy of the particles of type i in ergs and in electron volts, respectively; V is the electrical potential of the dust particle in volts; Z_i is the ionic charge Q_i in units of the charge of the proton.

The number of photoelectrons ejected per second will be roughly $\pi\sigma^2Uc\zeta\chi/h\nu_t$, where ν_t is the threshold frequency, U is the total energy density of radiation per cm^3, ζ is the fraction of the total radiant energy which has a frequency greater than ν_t, and χ is the efficiency of such radiation in ejecting electrons. Since, as we shall see below, the dust particles will be negatively charged in general, all the photoelectrons will escape.

The assumption of a steady state requires that the total charge gained by the particle per second must vanish. If we assume equipartition of kinetic energy, E_i must be independent of i and may be replaced by E. If we also assume that protons are the only positive ions present, we find from equation (4)

$$1 + \gamma + K = \left(\frac{m_p}{m_e}\right)^{1/2}e^{-\gamma}\,, \tag{6}$$

where subscripts e and p refer to electrons and protons, respectively; γ is equal to γ_e and $-\gamma_p$, where these quantities are defined in equation (5); K is defined by

$$K = \frac{(6\pi)^{1/2}Uc\zeta\chi}{4h\nu_t n_e(\overline{v_p^2})^{1/2}}\,. \tag{7}$$

The quantity K is the ratio of the number of electrons ejected per second, photoelectrically, to the number of protons which would be captured per second by direct collision if the dust particle were neutral. For most substances the photoelectric threshold lies at less than 2000 A. With Dunham's value[12] of 5.2×10^{-13} ergs/cm^3 for U, and a root mean square proton velocity of 1.6×10^6 cm/sec, corresponding to a temperature of 10,000°, we see that K is less than $10^3\zeta\chi/n_e$. Since only about 3×10^{-2} of the total radiant energy in space is of wave length shorter than 2000 A, and since the efficiency χ of radiation in producing photoelectrons is rarely as high as 10^{-3}, it follows that $\zeta\chi$ will be less than 10^{-5}, in all probability. Hence, in *H* II, where n_e is unity, K will be much less than unity. Even in *H* I, where the electrons come from elements other than hydrogen and where n_e is roughly 10^{-3}, K will not be greater than 10 at the most.

In H II, therefore, we may neglect K; if we set m_p/m_e equal to 1840, equation (6) has the numerical solution 2.51 for γ. Even if K is as great as 10, the value of γ is reduced by less than 50 per cent from this value. If heavy positive ions are considered, the value of γ is not greatly changed. We shall therefore assume that γ equals 2.5 in general.

From equation (5) we see that the value of γ determines the ratio of the potential of the dust particle in volts to the mean kinetic energy of the electron in electron volts. Since Z_i is -1 for an electron, we have

$$V = -\tfrac{2}{3}\gamma E = -1.67E. \tag{8}$$

If the electron velocities correspond to a temperature T, E is given by

$$E = 1.29 \times 10^{-4} T. \tag{9}$$

If T is 10,000°, a dust particle will, therefore, be charged to a potential of -2.2 volts. Unless the number of electrons per cm^3 is much below 10^{-3}, we may conclude that any small compound particle will be charged to a potential of about -2 volts, independently of its composition or its radius. If the radius σ of the particle is 10^{-5} cm, its charge will be $150e$. If n_e is so small that K exceeds $(m_p/m_e)^{1/2}$, or 43, the dust particles will have a positive charge.

These results are in disagreement with those of Jung,[19] who concludes that dust particles are positively charged, in general. Jung assumes that χ is unity; i.e., that each quantum of frequency greater than ν_t which hits a dust particle produces a photoelectron. In addition, his electron densities are somewhat less than those considered here. These two assumptions lead to a value of K (eq. [7], above) which is too great by a factor of 10^4, even in H I regions.

The collisions which are responsible for the charge on a dust particle will also produce a de-ionizing effect on the interstellar atoms. An ion which collides with a negatively charged dust particle is likely to take an electron with it when it leaves—if, in fact, it leaves at all. With the assumed density of dust, however, the effect is small, though it may become important in dust clouds. A more detailed discussion of this de-ionization by dust is postponed to a subsequent paper, together with the other effects of high dust densities.

3. EQUIPARTITION OF KINETIC ENERGY

The rate at which energy is equalized between particles of different mass has been calculated[20] for the gravitational case. For distant encounters interstellar dust particles, as well as ions, will interact as point charges. For such encounters the forces vary as the inverse square of the separation, and the gravitational analysis may be applied directly, provided the gravitational constant G is replaced by Q_1Q_2/m_1m_2, where Q_1, Q_2, m_1, and m_2 are the charges and masses of the two kinds of interacting particles. The direct inelastic collisions between dust and atoms, of the type discussed in the preceding section, are much less frequent than the more distant encounters; these direct collisions will pro-

[19] *A.N.*, **263**, 425, 1937.

[20] L. Spitzer, Jr., *M.N.*, **100**, 396, 1940. Dr. Chandrasekhar has kindly pointed out (private communication) that this analysis neglects a term in dE/dt which, while zero on the average, is very much greater in any one encounter than the term retained. Thus, statistical fluctuations in the neglected term may make this term an important one for a single star. The influence of this term clearly becomes negligible if the average rate of change of energy of a large number of stars is considered, since statistical fluctuations of the average value of dE/dt for N stars will decrease as $1/N^{1/2}$. In the present case, the number of dust particles per cubic parsec is roughly 10^{44} and is obviously sufficiently large to make any statistical fluctuations wholly negligible.

duce a dissipation of energy and a consequent reduction of the equilibrium velocities, but their effect on the rate of equipartition of energy is small and may be neglected.

We shall assume, then, that interstellar particles interact as point charges. If we consider two types of particles, denoted by subscripts 1 and 2, and assume that the kinetic energies of the two types have Maxwellian distributions with mean values E_1 and E_2, then we have the equation

$$\frac{dE_1}{dt} = \beta n_2 \frac{E_2 - E_1}{\left(\frac{E_2}{m_2} + \frac{E_1}{m_1}\right)^{3/2}}, \tag{10}$$

where n_2 is the number of particles of type 2 per cm^3; β is defined by

$$\beta = \frac{2(3\pi)^{1/2} Q_1^2 Q_2^2}{m_1 m_2} \log\left(1 + \frac{v^4 \mu^2 R_e^2}{Q_1^2 Q_2^2}\right). \tag{11}$$

In the argument of the logarithm in equation (11), v^4 may be taken as the square of the larger of the two mean square velocities; μ is the reduced mass; R_e is the maximum distance at which an encounter is effective, which we may, somewhat arbitrarily, take equal to $n_1^{-1/3}$ or $n_2^{-1/3}$, whichever is the smaller.

Let us take m_i equal to $A_i m_0$, where m_0 is the mass of unit atomic weight, and Q_i equal to $Z_i e$, where e is the charge on the proton; i refers to an ion of any particular type. The logarithmic term then becomes

$$\log_e\left(\frac{v^4 \mu^2 R_e^2}{Q_1^2 Q_2^2}\right) = 32.9\left(1 + \frac{1}{7.1}\log_{10}\frac{E}{Z_1 Z_2} + \frac{1}{21}\log_{10}\frac{1}{n}\right). \tag{12}$$

The approximate terms in the parentheses are small: if we neglect them, we have from equations (10) and (11)

$$\frac{dE_1}{dt} = 4.15 \times 10^{-6} n_2 \frac{Z_1^2 Z_2^2}{A_1 A_2} \frac{E_2 - E_1}{\left(\frac{E_2}{A_2} + \frac{E_1}{A_1}\right)^{3/2}} \text{ sec}^{-1}, \tag{13}$$

where E_i is again the mean kinetic energy, in electron volts, of all particles of type i and is numerically equal to $E_i/1.59 \times 10^{-12}$.

Let the particles of type 2 be those of the relatively greater velocity; i.e., let E_2/A_2 exceed E_1/A_1. If E_2 is relatively constant, equation (13) may be integrated directly. This will be the case if (1) the energy density $n_2 E_2$ of particles of type 2 exceeds $n_1 E_1$ (a mass abundance $n_2 A_2$ greater than $n_1 A_1$ implies this, of course); (2) the energy E_2 is kept constant by other means; or (3) the deviations from equipartition are small. If we neglect E_1/A_1 in the denominator of equation (13) and assume that E_2 is constant, we integrate to find

$$E_2 - E_1 = Ce^{-t/t_e}, \tag{14}$$

where C is a constant and t_e, the time of equipartition, is given by

$$t_e = 2.4 \times 10^5 \frac{A_1 E_2^{3/2}}{A_2^{1/2} Z_1^2 Z_2^2 n_2} \text{ sec} . \tag{15}$$

If the faster particles are also the more massive, equation (14) is valid only until such time as the less massive particles have attained velocities comparable with those of the heavier ones. If the faster particles have a smaller energy density than the slower, E_2 will change relatively much more than E_1, equation (14) is no longer valid, and the approach to equipartition is not exponential.

Another time of relevance is the relaxation time τ, defined ideally as the time in which deviations from a Maxwellian velocity distribution for particles all of a particular type fall to $1/e$ of their initial value. From the approximate formula in the gravitational case,[21] we find, with the same substitutions as before

$$\tau = 3.6 \times 10^5 \frac{A^{1/2} E^{3/2}}{Z^4 n} \text{ sec} . \tag{16}$$

This quantity is roughly equal to the value of t_e found from equation (15) when particles 1 and 2 are assumed identical; this agreement provides a rough check on the calculation of both quantities.

The velocities of protons are at least equal to those of dust particles. Hence, a mass abundance of dust less than that of H^+ implies that the energy density of dust is less than

TABLE 1

	Electrons	Protons	Ca^{++}	Dust
H I n	2.0×10^{-3}		1.0×10^{-3}	2.0×10^{-11}
ρ	1.8×10^{-30}		6.6×10^{-26}	6.5×10^{-25}
τ	0.19 yr.		6.7 yr.	2.3×10^5 yr.
t_e			2.4×10^3 yr.	3.8×10^5 yr.
l	28 A.U.		3.5 A.U.	5.4 A.U.
H II n	1.0	1.0	1.0×10^{-3}	2.0×10^{-11}
ρ	9.0×10^{-28}	1.7×10^{-24}	6.6×10^{-26}	6.5×10^{-25}
τ	3.4 hr.	150 hr.	6.7 yr.	2.3×10^5 yr.
t_e		0.48 yr.	0.11 yr.	9.7×10^3 yr.
l	0.056 A.U.	0.056 A.U.	0.058 A.U.	0.23 A.U.

that of H^+. In this case equation (15) is applicable. In *H* I the hydrogen atoms are not ionized, and equation (15) applies only if the dust velocities are not greater than a few kilometers a second. Values of τ and t_e for typical interstellar particles in both *H* I and *H* II are given in Table 1, calculated for a velocity temperature of 10,000°.

The quantities n and ρ are the space densities in number of particles per cm³ and in gm/cm³, respectively, for each type of particle, and represent typical cases for the population of interstellar space. While the number of Ca^{++} atoms per cm³ is not likely

[21] *Ibid.*, eqs. (11), (15), and (17*a*). Dr. Chandrasekhar has recently computed in detail (*Ap. J.*, **93**, 285, 1941) values of a relaxation time T_E, defined as the time in which the root mean square exchange of energy by a particular star just equals the energy of that star. From his results we find that in an assembly of identical stars ($\mu = 1$) a star whose velocity is equal to the root mean square velocity ($x_0 = 1.22$) will have a relaxation time such that $T_E = 1.15\,\tau$, where τ is taken from the equation cited above.

to be as high as 10^{-3}, that of all atoms other than hydrogen and helium is probably of this order of magnitude, at least. The dust particles are assumed to be spheres of radius 10^{-5} cm, with a density of 7.8 gm/cm^3, corresponding to metallic *Fe*. The symbol d will be used to denote the density of matter within a particle to avoid confusion with ρ, the mass of matter actually present in a cm^3 of interstellar space.

The third row gives the values of the time of relaxation τ for interaction with similar particles only. The values of t_e in the fourth row refer in each case to interactions with the next lightest particle present, except for dust particles in *H* II, where protons are more effective than Ca^{++} ions. Collisions between dust and neutral *H* atoms in *H* I will diminish t_e somewhat from the value for dust given in the table. The time of equipartition for collisions of neutral atoms with a dust particle is approximately $m_d/\pi\sigma^2 n_H m_H v_H$, where subscripts *H* refer to the neutral atom, and m_d is the mass of the dust particle; with one *H* atom per cm^3 the time of equipartition for atomic collisions alone is equal to 1.2×10^6 years. With the assumed densities the effect of neutral atoms is therefore not important.

Rough determinations of the mean free path l are given in astronomical units in the last row of the table. Each value is simply the product of the root mean square velocity for each particle at 10,000° and the corresponding value of either τ or t_e, whichever is the smaller.

Since A_i/Z_i^2 varies as σd for a dust particle, it is evident from equation (15) that dust particles of smaller radius and lesser density than the values assumed will come into equipartition with atoms even more rapidly than is indicated in Table 1. Dust particles of much larger radius will have a correspondingly greater value of t_e, but such particles cannot be abundant and will produce little observable effect in any case. For all practical purposes we may conclude that deviations from equipartition of kinetic energy between all the interstellar particles will be reduced to $1/e$ of their initial value within at most 10^4 years if the hydrogen is ionized, and within at most 4×10^5 years if it is not. The random velocities of the larger particles will be very low. An *Fe* particle of radius 10^{-5} cm should have a velocity of 11 cm/sec at 10,000°, or less than a mile an hour.

The equilibrium velocity temperature of the interstellar particles is rather uncertain. Photoelectric ionizations and electron captures would lead to a temperature roughly equal to the color temperature of the ionizing radiation. In *H* II this would correspond to at least 20,000° for the most part, since the color temperatures of the O and early B stars are of this order.

As has been pointed out above, direct collisions between dust particles and neutral atoms will tend to reduce the equilibrium temperature, as such collisions will, in general, dissipate energy. In the *H* II regions, where the hydrogen is largely ionized, the fall of temperature arising from this cause should not be large, however, though it may be important in *H* I regions. This and other effects of high dust densities will be discussed in more detail in another paper, to appear shortly.

There is little observational evidence on velocity temperatures. The velocity of dust particles is apparently not observable. The temperatures of *H* I regions are also difficult to determine, as such regions do not contribute appreciably to the formation of absorption or emission lines. Greenstein and Henyey[22] have found a value of 5000° for the electron temperature of the Orion nebula—presumably an *H* II region—by a comparison of the relative strengths of the Balmer lines and the emission beyond the Balmer limit; the determination is somewhat uncertain, however.

The atomic velocities derived from absorption-line data present an outstanding discrepancy with the equipartition of energy found in this section. The slow decrease of the K to H doublet ratio as H increases can apparently be explained only as a result of a Doppler width of 22 km/sec for each line,[23] corresponding to a velocity temperature of

[22] *Ap. J.*, **89**, 653, 1939.

[23] O. C. Wilson, *Ap. J.*, **90**, 244, 1939.

860,000°. The ratio of D_2 to D_1 decreases more rapidly with increasing D_1, indicating saturation with a smaller Doppler width of 7.5 km/sec, yielding a temperature of 52,000°. Although there are several possible explanations for this result, none of them seems very plausible. The observations are of great theoretical importance, and it is to be hoped that they may be repeated and extended.

4. VISCOSITY

Although equipartition of energy probably exists in any small region of interstellar space, large-scale turbulence or galactic currents are not ruled out for this reason. The existence of equipartition and of a short mean free path implies rather that the interstellar medium behaves as a perfect gas and that the ordinary equations for a viscous medium are applicable.

For such a gas the coefficient of viscosity η is approximately given by the formula

$$\eta = \tfrac{1}{3}\Sigma_i \rho_i l_i (\overline{v_i^2})^{1/2}, \tag{17}$$

summed over all the constituents of the medium; l_i is the mean free path for the particles of type i. The mean square velocity may be set equal to its equilibrium value, $3kT/m_i$. Substituting the values from Table 1 into equation (17), we find that in H II only protons contribute significantly to the viscosity, and we have $\eta = 7.4 \times 10^{-7}$. In H I neutral H is responsible for a great increase in the viscosity; for a density of 1 atom per cm^3, a collision radius of 10^{-8} cm, and a temperature of 10,000°, we find that η is 2.8×10^{-3}. These values depend on the assumed equipartition of kinetic energy for dust particles, since rapidly moving heavy particles of this sort would yield a considerably greater viscosity.

It may be shown[24] that inequalities in angular momentum will be reduced to half their value in a time comparable with $\rho r^2/\eta$. If we let ρ equal 1.7×10^{-24} gm/cm^3, we find that in 10^9 years inequalities in angular velocity will be reduced to half their value over 0.038 parsec in H II and over 2.3 parsecs in H I. It is evident that any interstellar currents over regions greater than a few parsecs will not be damped out by viscosity during the short time scale. Over 10^8 years the shearing effect of galactic rotation will tend to distort and dissipate any large-scale currents, but any such currents formed more recently than 10^8 years would apparently have survived.

Another consequence of the low value for η is that the flow of the interstellar medium past stars will resemble that of a perfect, nonviscous fluid at a distance from the star of a few hundredths of an astronomical unit or more. This follows at once from the size of the Reynolds number, $\rho v R/\eta$, which is small for viscous flow, and greater than unity for nonviscous flow; R, the relevant linear dimension for the flow under discussion, may here be set equal to the distance of the star at closest approach. The relevant value of η in this case is that for H II, since hydrogen atoms near a star will be ionized in general. Hence, in most cases we may wholly neglect the viscosity of the interstellar medium.

In addition, the interstellar medium will show some tendency to behave as an incompressible fluid as the stars pass through it. It is well known that a gas will flow without much change in density around a body whose velocity relative to the gas is less than the velocity of sound in the gas. For a medium of protons and electrons at 10,000°, the velocity of sound is 17 km/sec, which is greater than the random velocities of many stars, particularly the more massive ones. Here, as before, ionized, rather than neutral, H is relevant near stars. The dust particles produce no effect, as their velocities will be largely controlled by the atoms present. Encounters of atoms with stars differ, of course, from the usual aerodynamical problems in that the star interacts directly with atoms

[24] J. H. Jeans, *Astronomy and Cosmogony*, p. 261, (Cambridge U. Press, 1928).

at a distance rather than indirectly through pressure effects. Even near a very slowly moving star the pressure and density of interstellar matter will therefore depend on the potential energy and hence on the distance from the star. But neither the pressure nor the density should show much variation with direction from the star. It follows that in such a case the vector force on the medium must vanish when integrated over the spherically symmetrical distribution of interstellar matter. Hence, a star with a random velocity of 10 km/sec or less will impart very little net momentum to the interstellar medium.

It is evident, also, from the mean free paths in Table 1 that the rate of diffusion of interstellar matter is quite negligible. In 10^9 years any mixing of the various constituents of the medium will be limited to a range of a few parsecs at most, and any initial large-scale inhomogeneity in the relative concentrations of different atoms must still persist.

It is a very real pleasure to express here my great indebtedness to Dr. B. J. Bok, Dr. J. L. Greenstein, and Dr. O. C. Wilson for critical comments on the manuscripts of this and subsequent papers and for many helpful suggestions.

YALE UNIVERSITY
February 1940

DISPLACEMENTS OF LINES IN THE SPECTRA OF LONG-PERIOD VARIABLES*

PAUL W. MERRILL

ABSTRACT

Wave lengths of absorption lines in Me spectra suitable for velocity measurements with moderate dispersion are listed in Table 1.

Data concerning periodic variations in the displacements of the dark lines, although meager, indicate that, within two months of maximum light, changes in velocity do not exceed a very few kilometers per second. The mean measured displacements of the dark lines are assumed to represent the true stellar velocities.

The emission lines, as is well known, are regularly shifted 0.1 or 0.2 A toward the violet with respect to the absorption spectrum. These shifts, measured in 72 stars (Table 3), are plotted against spectral type in Figure 1 and against period in Figure 2. The relationship with period furnishes the best method of correcting the radial velocities determined from bright lines alone.

A statistical discussion of the radial velocities of 133 long-period variables of spectral classes Me and Se was published in 1923.[1] Since then the number of stars observed has been more than doubled, and a second discussion is soon to be made. It therefore seems desirable to re-examine the relationships between the measured line displacements and the true stellar motions. Two problems arise: (1) Do the displacements of dark lines at time of maximum light correspond exactly to the radial velocity of the center of the star? (2) What is the best method of correcting the velocities derived from the bright lines for the systematic displacements of these lines relative to the absorption spectrum?

The purpose of the present *Contribution* is not only to deal with these two questions and thus to clear the way for a discussion of the galactic motions of long-period variables but also to present facts of intrinsic interest for the study of the obscure physical phenomena in the atmospheres of these remarkable objects.

ABSORPTION LINES

The Mount Wilson measurements of absorption lines have been made on plates taken with a one-prism spectrograph and 18-inch camera, dispersion at $H\gamma$, 35 A/mm, at $H\zeta$, 24 A/mm. About two-thirds of the spectrograms were obtained with the 100-inch telescope, one-third with the 60-inch. Since March, 1937, the Cramer Hi-Speed Special emulsion has been regularly used; in previous years, either Eastman 40 or Imperial Eclipse Soft. Recent spectrograms, compared with the earlier ones, have considerably greater density in the region extending for several hundred angstrom units from $H\delta$ toward the ultraviolet. The increased density, which is of considerable value in the measurement of radial velocity, is due largely to improved transmission in this spectral region of the telescope and spectrograph.

The absorption lines used for measurements of velocity are those given in *Mount Wilson Contributions*, No. 265,[2] Table IV, with the addition of about 70 metallic lines (laboratory wave lengths) mainly in the region $\lambda\lambda$ 3750–4000.

The revised list of wave lengths in Table 1 is recommended for future use in velocity measurements of Me spectra with dispersion about 35 A/mm at $H\gamma$. Laboratory determinations were adopted unless the mean residuals from the stellar spectrograms definitely indicated a different value. For these modified values, probably caused by

* *Contributions from the Mount Wilson Observatory, Carnegie Institution of Washington*, No. 644.

[1] P. W. Merrill, *Mt. W. Contr.*, No. 264; *Ap. J.*, **58**, 215, 1923.

[2] P. W. Merrill, *Ap. J.*, **58**, 195, 1923.

blends, the chemical symbol is in parenthesis. Those wave lengths without chemical symbols correspond to unidentified stellar lines frequently measured. One-half the plate measurements and nearly all the computations which underlie Table 1 have been made by Miss Cora G. Burwell.

TABLE 1

ABSORPTION LINES FOR VELOCITY MEASUREMENTS IN SPECTRA OF CLASS Me

3752.78	(*Ti*)	3982.48	*Ti*	4200.06	(*Fe*)
53.65	(*Ti, Fe*)			02.11	(*Fe*)
58.24	*Fe*	89.78*	*Ti*	03.66	
75.66	(*Ni, Ti?*)	98.64	*Ti*	04.97	
93.62	(*Ni, V*)	4008.93	*Ti*	06.70	*Fe*
95.00	*Fe*	20.54	(*Sc?*)	15.82	(*Sr* II, *Fe*)
3808.48	(*V*)	23.69	*Sc*	26.73	*Ca*
12.96	*Fe?*	24.61	(*Ti*)	32.60	(*Fe*)
13.49	*V*	26.97		34.12	(*V*)
15.80	(*Fe?*)	30.81	(*Mn*)	54.30	(*Cr*)
24.44	*Fe*	33.07	*Mn*	58.32	*Fe*
25.93	(*Fe*)	34.57	(*Mn*)	60.48	*Fe*
28.63	(*V*)	35.87	(*Mn*)	74.80	*Cr*
44.39	(*V*)	41.30	(*Mn*)	82.71	*Ti?*
47.28	(*V*)	44.18	(*K*)	85.87	(*Ti?*)
50.88	(*Co*)	45.89	(*Fe*)	89.60	(*Cr, Ca?*)
67.65	(*V*)	48.76	*Mn*	91.43	(*Fe*)
72.57	(*Fe?*)	54.83		94.25	(*Fe*)
75.18	(*V, Ti?*)	63.75	(*Fe*)	99.08	(*Ca*)
75.96	(*V*)	76.35	(*Fe*)	4300.82	(*Ti*)
78.58	*Fe*	77.77	(*Sr* II)	02.68	(*Ca*)
83.29	*Cr, Fe*	90.52	(*V*)	06.05	(*Ti*)
86.34	(*Fe*)	92.46	(*V*)	07.74	(*Fe, Ca?*)
90.07	(*V*)	4105.04	(*V*)	14.64	(*Ti*)
		09.64	(*V*)	25.88	(*Fe*)
92.86*	*V*	11.79	*V*	30.02	*V*
95.66	*Fe*	13.72		32.75	(*V*)
99.71	*Fe*	15.19	*V*	37.48	(*Cr*)
3902.25	*V*	16.58	(*V*)	44.43	(*Cr*)
06.44	(*Fe*)	18.60	(*Co?*)	47.24	*Fe*
08.70	(*Cr*)	21.64		68.04	*V*
09.91	(*Co, V*)	23.61	(*V*)	75.93	*Fe*
11.87	(*Sc?*)	28.07	*V*	79.37	(*V*)
20.26	*Fe*	29.76		83.64	(*Fe*)
22.91	*Fe*	32.09	(*V*)	84.25	(*Fe, V*)
24.53	*Ti*	34.40	(*V*)	84.72	*V*
27.92	*Fe*	39.89	(*Fe*)	95.23	*V*
44.12	(*Al*)	47.67	*Fe*	4404.87	(*Fe*)
47.78	(*Ti*)	49.76	*Fe?*	27.31	*Fe*
48.78	(*Ti*)	52.31	(*Fe?*)	62.03	(*Fe*)
50.34	*Ti*	74.00		82.13	(*Fe*)
58.14	(*Ti*)	79.54	(*V?*)	94.34	
61.53	*Al*	90.77	(*Co*)	96.59	
79.52	*Co?*	94.95			
81.76	*Ti*	98.52			

* The average weights of the results in the three portions of the table are roughly 2, 5, and 25, respectively.

Variation with phase.—A. H. Joy's measurements in the spectrum of *o* Ceti[3] showed that during the light-cycle the displacement of the bright lines varied about 10 km/sec, following a curve having approximately the same shape and phase as the light-curve. No other variable with a comparable period has been adequately investigated. The

[3] *Mt. W. Contr.*, No. 311; *Ap. J.*, **63**, 281, 1926.

published material on four variables with shorter periods is summarized in P. W. Merrill, *Spectra of Long-Period Variable Stars*[4] (p. 61, Table 16).

In the present investigation the emphasis has been upon including numerous stars rather than upon extensive observations of individual objects. For several stars, however, a few additional data bearing on variation with phase have been obtained.

All available data concerning U Orionis, R Hydrae, and R Cassiopeiae are summarized in Table 2. For R Hydrae alone do the results indicate a velocity-curve similar to that found by Joy for *o* Ceti. For R Leonis and χ Cygni the meager data are scattering and do not determine mean velocity-curves with sufficient accuracy to allow useful conclusions concerning variation with phase; in fact, the differences between various cycles appear to be greater than the observed variations in any one cycle.

TABLE 2

NORMAL PLACES FOR ABSORPTION-LINE VELOCITIES

Variable	Phase	Velocity	No. Plates
	days	km/sec	
U Orionis 054920	− 3	−21.7	4
	+ 24	−22.3	4
	+ 43	−22.3	3
	+ 73	−17.2	2
R Hydrae 132422	− 56	−10.6	3
	− 22	− 8.9	13
	+ 31	− 6.0	6
	+ 67	−11.0	3
R Cassiopeiae 235350	− 31	+23.2	2
	+ 22	+26.2	8
	+122	+26.4	1

For stars other than those to which reference has been made the determinations of dark-line velocities are not sufficiently extensive to be of much value for the study of changes with phase.

Available data, unfortunately, are inadequate for general conclusions concerning periodic variations in the displacements of the dark lines, and the problem remains in an unsatisfactory state. We do not know with certainty whether or not the results obtained by Joy for *o* Ceti are characteristic of variables with comparable periods. It is clear, however, that the range in velocity is relatively small and that near maximum light—say, from 40 days before maximum to 80 days after—the variations usually do not exceed a very few kilometers per second. This strengthens the previous conclusion[5] that the measured displacements of the dark lines at time of maximum light are reasonably representative of the velocity of the star—in other words, the necessary corrections, if any, are of minor consequence for a study of the galactic motions of the variables.

The cyclic behavior of the spectra of several of the brighter variables merits further observation, preferably with dispersion somewhat higher than that used hitherto. Intensive studies of individual cycles would be particularly valuable.

EMISSION LINES

It is well known that in the spectra of most long-period variables the bright lines have a decided displacement toward the violet relative to the dark lines. This displacement,

[4] Chicago: University of Chicago Press, 1940.

[5] The arguments are summarized in *Spectra of Long-Period Variable Stars*, chap. v.

TABLE 3

MEASURED DISPLACEMENTS OF ABSORPTION AND EMISSION LINES

Star	Desig.	Spect.	Period	A−E
			days	km/sec
S Scl	001032	M6e	366	(+21.)
T And	001726	M4e	281	(+ 5.)
T Cas	001755	M8e	445	+12.2
R And	001838	Se	419	+21.6
U Cas	004047	Se	278	+10.4
U Per	015354	M6e	318	+ 8.9
R Ari	021024	M3e	187	+12.4
W And	021143	M8e	397	+16.1
o Cet	021403	M6e	331	+16.5
R Cet	022000	M4e	167	+10.9
U Cet	022813	M3e	235	+12.4
R Tri	023133	M4e	266	+ 7.1
R Hor	025050	M7e	401	+12.
R Per	032335	M3e	210	+10.9
R Pic	044339	M3e	170	+ 4.
R Aur	050953	M7e	458	+17.4
T Col	051533	M4e	225	+10.
U Aur	053531	M7e	408	+ 8.2
U Ori	054920	M8e	373	+12.8
R Oct	055686	M6e	406	(+15.)
X Mon	065208	M3e	156	+ 7.4
R Gem	070122	Se	370	+15.9
L_2 Pup	071044	M5e	141	+ 4.
V Gem	071713	M4e	275	+11.4
S Gem	073723	M5e	293	(+ 2.4)
R Cnc	081112	M7e	361	+13.0
RT Hya	082405	M6e	252	+ 5.
R Car	092962	M5e	309	+12.
X Hya	093014	M7e	302	+13.8
R LMi	093934	M8e	372	+12.6
R Leo	094211	M8e	313	+13.8
S LMi	094735	M4e	235	+11.5
S Car	100661	K9e	149	+11.
R UMa	103769	M4e	301	(+ 9.3)
Z UMa	115158	M6e	190	+ 5.8
T UMa	123160	M4e	257	+12.2
R Vir	123307	M4e	145	+12.
S UMa	123961	Se	226	+11.8
U Vir	124606	M4e	207	+10.9
V CVn	131546	M5e	192	+ 5.
R Hya	132422	M7e	405	+13.
T Cen	133633	Moe	91	+ 1.
W Hya	134327	M8e	372	+14.8
R CVn	134440	M6e	326	+13.9
R Cen	140959	M4e	(559)	+ 7.
U UMi	141767	M6e	328	+13.0
V Boo	142539	M6e	259	+ 4.6
R Boo	143227	M4e	223	+ 3.
S CrB	151731	M7e	361	+21.
T Nor	153654	M4e	243	+ 8.
R Ser	154615	M7e	357	+16.6
U Her	162119	M7e	406	+16.1
R Dra	163266	M7e	245	+ 9.9
RS Sco	164844	M6e	320	+ 8.
RR Sco	165030	M6e	279	+10.
RY Her	175519	M4e	221	+11.2
T Her	180531	M3e	165	+ 7.9

TABLE 3—*Continued*

Star	Desig.	Spect.	Period	A−E
			days	km/sec
W Lyr	181136	M4e	196	+ 9.
X Oph	183308	M6e	335	+13.4
R Aql	190108	M7e	300	+12.5
T Pav	193972	M(4)e	244	+ 5.
RT Cyg	194048	M2e	190	+ 9.6
χ Cyg	194632	Mpe	407	+15.8
T Aqr	204405	M3e	202	+13.9
X Del	205017	M4e	280	+ 6.7
T Cep	210868	M7e	388	+15.4
W Cyg	213244	M4e	131	− 1.
S Lac	222439	M5e	241	+ 6.2
V Cas	230759	M6e	228	+17.1
R Aqr	233815	M7e+Pec	387	+13.4
R Cas	235350	M7e	430	+16.2
S Phe	235357	M5e	157	(+ 5.)

NOTES TO TABLE 3

T UMa 123160. This star was inadvertently omitted from Figs. 1 and 2.

R Cen 140959. Since the light-curve has a well-marked secondary maximum, the half-period, 279 days, has been used in Fig. 2.

The chief sources of the data are: P. W. Merrill, *Pub. Obs. Univ. Mich.*, **2**, 45, 1916, and *Mt. W. Contr.*, No. 264; *Ap. J.*, **58**, 215, 1923; Leah B. Allen, *Lick Obs. Bull.*, **12**, 71, 1925; A. H. Joy, *Mt. W. Contr.*, No. 311; *Ap. J.*, **63**, 281, 1926 (*o* Ceti); P. W. Merrill and A. H. Joy, *Mt. W. Contr.*, No. 382; *Ap. J.*, **69**, 379, 1929 (R Virginis); A. H. Joy and P. W. Merrill, *Mt. W. Contr.*, No. 559; *Ap. J.*, **85**, 9, 1937 (V Can. Ven.); and P. W. Merrill, unpublished material.

often amounting to 10 or 12 km/sec, must be applied as a correction when stellar radial velocities are determined from the bright lines.

Radial velocities measured both from bright and from dark lines are available for the 72 variables listed in Table 3. The amount of the displacement is correlated with spectral type and with period, although considerable scatter occurs in both relationships (see Figs. 1 and 2). The scatter is probably due partly to error of observation, partly to intrinsic dispersion. In certain stars another cause may enter, namely, the fact that observations of the bright lines were not confined to the same dates as those of the dark lines. It would, of course, be possible to use only those plates on which both bright and dark lines were measured—and this would, in fact, reduce a few of the larger residuals—but it is not at all certain that the data as a whole would thereby be improved. One reason for this is that on practically all the plates well suited for measurement of the dark lines the chief bright lines are overexposed.

The heavy curve in Figure 2 is drawn through a smoothed series of normal places for Me stars. It has the same general shape as the curve previously published,[1] except that the portion corresponding to periods greater than 340 days is flat. The new curve will be used to correct radial velocities of numerous Me variables determined from bright lines alone. This method is considered, on the whole, more satisfactory than a corresponding procedure based on spectral types. The correction-curve for Se variables—based on very few stars—is shown in Figure 2 by the dotted line.

The physical interpretation of the curves is not obvious and will probably remain uncertain until the origin of the bright lines is better understood. The following quantities exhibit positive correlations with one another, although with considerable scatter: (1)

relative displacement of bright lines, (2) intensities of chief bright lines, (3) spectral type, (4) period, and (5) magnitude range.

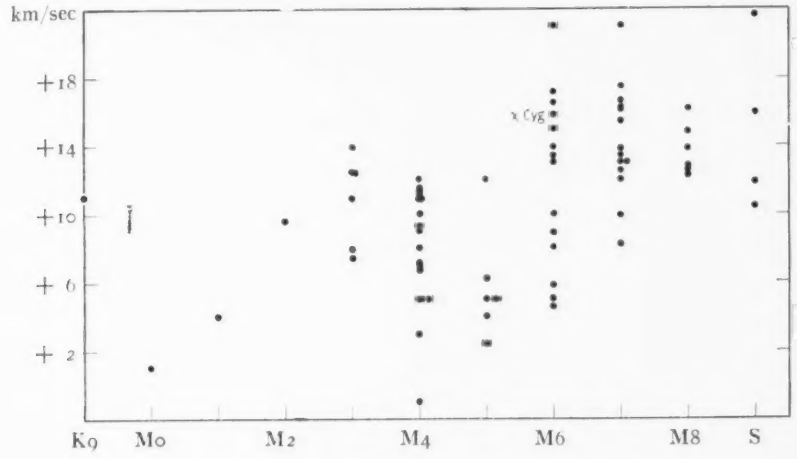

FIG. 1.—Relative displacement of emission lines (A–E) plotted against spectral type

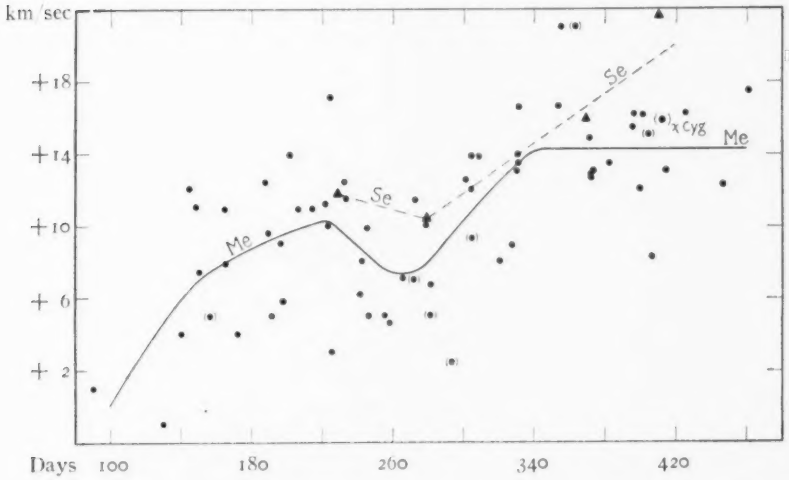

FIG. 2.—Relative displacement of emission lines (A–E) plotted against period of light-variation. Circles indicate variables of spectral type Me; triangles, type Se.

The apparent dip in the curve near 260 days suggests the existence of two series of stars with different displacements, but the spectra do not yield a definite conclusion because the observations are not sufficiently precise or extensive.

CARNEGIE INSTITUTION OF WASHINGTON
MOUNT WILSON OBSERVATORY
November 1940

ABSORPTION SPECTRA OF GASES IN THE EXTREME ULTRAVIOLET*

TOSHIO TAKAMINE AND YOSHIO TANAKA[1]

ABSTRACT

Absorption spectra of *H*, *He*, *Ne*, and *A* in the extreme ultraviolet were photographed by means of a vacuum spectrograph with a concave grating of 20-cm radius at grazing incidence. Lyman continuum, obtained by passing a heavy condensed discharge through a quartz capillary tube, was used as the background. Except for hydrogen, the spectrograph was filled with each of the gases at various pressures. Resonance series of *He*, *Ne*, and *A* were photographed in absorption. In the experiments on hydrogen, dry hydrogen at about 1-mm pressure was kept flowing through the discharge tube. Production of atomic hydrogen by a hot filament of tungsten placed in front of the quartz capillary seemed to help in suppressing the absorption bands of molecular hydrogen; and in that way seven members of the Lyman series of hydrogen were obtained in absorption.

Another interesting feature observed was the transparency of helium for the helium continuum. This was tested by passing a disruptive discharge through the helium tube which served as the source of light for the helium continuum, the spectrograph being filled with helium at various pressures. No marked weakening of the helium continuum was observed even at a fairly high pressure of helium in the spectrograph. This fact is of significance because it proves beyond doubt that the so-called helium continuum is of molecular origin.

INTRODUCTION

Although the emission spectra of most of the simpler gases such as *H* and *He* have been carefully studied, our knowledge of their absorption spectra is rather limited.

It is hardly necessary to mention that almost all the theoretical calculations on the intensity measurements of atomic spectra start from the simplest case of hydrogen, and deal with absorption rather than with emission. Furthermore, the treatment of absorption from the ground state is naturally much simpler than that from an excited state. Hence a study of the absorption spectra of the Lyman series of hydrogen is of no small interest.

It must be admitted at the beginning that at the present stage of our experimental technique any quantitative study of intensity in the extreme ultraviolet is confronted with considerable difficulty. Even a qualitative study is, however, desirable, because to find the conditions under which absorption phenomena actually occur is the first step in the problem.

EXPERIMENTAL ARRANGEMENTS

Source of light.—Lyman continuum supplied the background. For the construction of the quartz capillary and other details the reader is referred to the previous work of one of us.[2] It is true that the use of this source of light is accompanied by various difficulties; it seems, nevertheless, to be the only one giving a continuous spectrum extending below λ 600 A. Two Pyranol capacitors, each having 0.5 μ F, were connected in parallel and were charged by a 10-kw, 170-kv transformer through a mechanical rectifier. The length of each of the two spark gaps in series in the outgoing condenser circuit was varied from 1 to 4 mm, the total gap thus being from 2 to 8 mm.

In actual operation, starting the discharge with a small spark gap served to warm up the capillary. A few hundred flashes were given for each exposure. The quartz capil-

* *Contributions from the Mount Wilson Observatory, Carnegie Institution of Washington*, No. 645.

[1] Both of the Institute of Physical and Chemical Research, Tokyo.

[2] Takamine, Suga, and Kamiyama, *Inst. Phys. and Chem. Research, Sci. Papers*, **33**, 247, 1937.

lary was about 2 cm long and had an inner diameter of 1–3 mm and walls 1 mm thick. A Cenco Hypervac pump was used for evacuation.

The spectrograph.—The very small vacuum-grating spectrograph used in the present experiment was constructed at the Institute of Physical and Chemical Research in Tokyo. A 20-cm concave grating ruled on speculum metal by Dr. J. A. Anderson was mounted at grazing incidence. The Schumann films, prepared by ourselves, were cut into pieces 20 × 2 cm. A curved diaphragm, 19 × 1 cm, which could be moved from outside without affecting the vacuum, allowed two exposures on each film.

On account of the small radius of the grating, the dispersion was very small, ranging from 25 A/mm at λ 500 A to 80 A/mm at λ 8000 A. The drawback of small dispersion was compensated, so to speak, by the enormous brightness of the instrument. The latter advantage is considerable in this kind of experiment where the intensity of the background is by no means high. As a matter of fact, our experience shows that with a 1-m grating the low intensity of the Lyman continuum quite often caused failure to detect the absorption lines. The region covered in one exposure extended from λ 300 A to λ 8500 A, enabling us to photograph the first member of the Lyman series λ 1215 in orders up to the seventh.

RESULTS

Hydrogen.—The fact that a few earlier members belonging to the Lyman series appear at times as absorption lines in the spectra obtained by a quartz capillary discharge has already been recorded by various investigators. Dieke and Hopfield[3] mention in their work on the molecular spectrum of hydrogen that the first member of the Lyman series L1 (λ = 1215 A), appearing as an absorption line, was convenient for use as a wave-length standard. In the photograph by Price and Collins[4] of the extreme ultraviolet absorption spectrum of oxygen we note the line L1 appearing as an absorption line. Takamine, Suga, and Kamiyama[2] have recorded this phenomenon in the study of silicon spectra, and especially the fact that with a small spark gap (low voltage) L1 appears in emission, whereas with increasing spark gap (higher voltage) the line turns into a clear absorption line. In such a case, apparently, an aureole containing atomic hydrogen is formed at the near end of the capillary and acts as an absorbing layer.

To obtain the Lyman series as the chief absorption lines on a perfectly black background is a matter of some experimental difficulty. First, we have to suppress the molecular spectrum of hydrogen, both in emission and in absorption, as much as possible. For this purpose atomic hydrogen supplied by a Wood's tube[5] was tried first. Soon it was found, however, that the use of wet hydrogen for obtaining the so-called "black stage" is to be avoided, because water vapor[6] shows a considerable number of absorption bands in just the region concerned. Thereupon, we tried to freeze out the moisture by making a double-walled Pyrex tube whose outside was kept in contact with liquid air. It was expected that the formation of ice on the inner wall of the inside tube would be of further help in preventing the recombination of the atomic hydrogen, but the method proved ineffective.

The next method we tried was that of thermal dissociation of hydrogen molecules. A coil 10 mm in diameter and 20 mm long, having about 10 turns of 0.75-mm tungsten wire, was placed in the center of a 1-liter flask. The coil was heated to about 2000° C by a current of 30 amp, while a stream of dry hydrogen at 1-mm pressure was kept flowing through the flask. The experimental arrangement is shown in Figure 1.

Flashes of light from the quartz capillary were sent along the axis of the coil. The result thus obtained proved a partial success. A spectrogram obtained in this way is reproduced in Plate XVII, *a;* the magnification is seven fold.

[3] *Phys. Rev.*, **30**, 400, 1927.

[4] *Phys. Rev.*, **48**, 714, 1935.

[5] R. W. Wood, *Proc. R. Soc.*, A, **97**, 455, 1920.

[6] W. C. Price, *J. Chem. Phys.*, **3**, 256, 1935.

As will be seen in Plate XVII, *a*, Lyman-series lines down to the seventh member are present in absorption. Of these, L1 and L2 are strong and sharp, L3 is abnormally broad on account of its blending with a fairly strong absorption band due to molecular hydrogen at λ 973 A, and L4 is seen close to another H_2 absorption band, λ 945 A. The diffuse appearance of the three lines L5, L6, and L7 may again be attributed to their coincidences with the three H_2 absorption bands, λλ 935 A, 930 A, and 925 A.

Strong emission lines due to *O* IV at λ 923 A and λ 921 A unfortunately obliterate the higher members of the Lyman series. Other prominent emission lines seen in Plate XVII, *a* are: *Si* II λ 1206.9, *Si* IV λ 1066.3 A, and the *O* VI doublet λ 1037.6 A, λ 1031.9 A. Most of the absorption lines which appear in Plate XVII, *a*, other than those of the Lyman series, are due to H_2, as we found from the work of Dieke and Hopfield.[3]

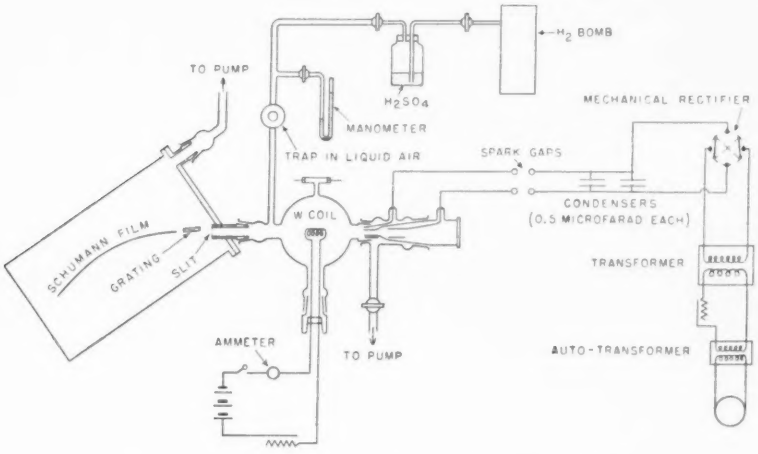

FIG. 1.—Arrangement for hydrogen absorption spectrum

The reason we called the result a partial success is that a check experiment employing the same procedure but without heating the tungsten coil also gave a fairly good spectrogram. However, on comparing the spectrograms taken with and without the heating, it seems safe to say that the heating of the coil helped to make the Lyman absorption spectrum more conspicuous. Improvements on this method, using higher concentration of atomic hydrogen, are to be tried soon.

Rare gases.—In the present experiment, absorption was observed in three rare gases, namely *He*, *Ne*, and *A*. The experimental procedure described in the next paragraph was adopted for them all.

A thin-walled copper tube, about 20 cm long, having an inner diameter of 2 mm, was introduced into the spectrograph with one end near the slit and the other connected to the supply of rare gas through longer tubes. First, we evacuated the entire system; then, keeping the pump going, we opened slightly the stopcock near the reservoir, and the flow started. The speed of the flow was so adjusted by the stopcock that the pressure inside the spectrograph was kept constant at a desired amount during one exposure; in other words, the loss of the rare gas through the slit of the spectrograph into the discharge tube was compensated by the amount flowing in through the narrow copper tube.

Helium.—Pure helium from a tank at 10-atm. pressure was passed through a series of charcoal bulbs immersed in liquid air and through a heated CuO_2 tube for further purification, before entering the spectrograph. Spectrograms showing absorption were taken at various pressures of helium in the spectrograph ranging from a fraction of a milli-

PLATE XVII

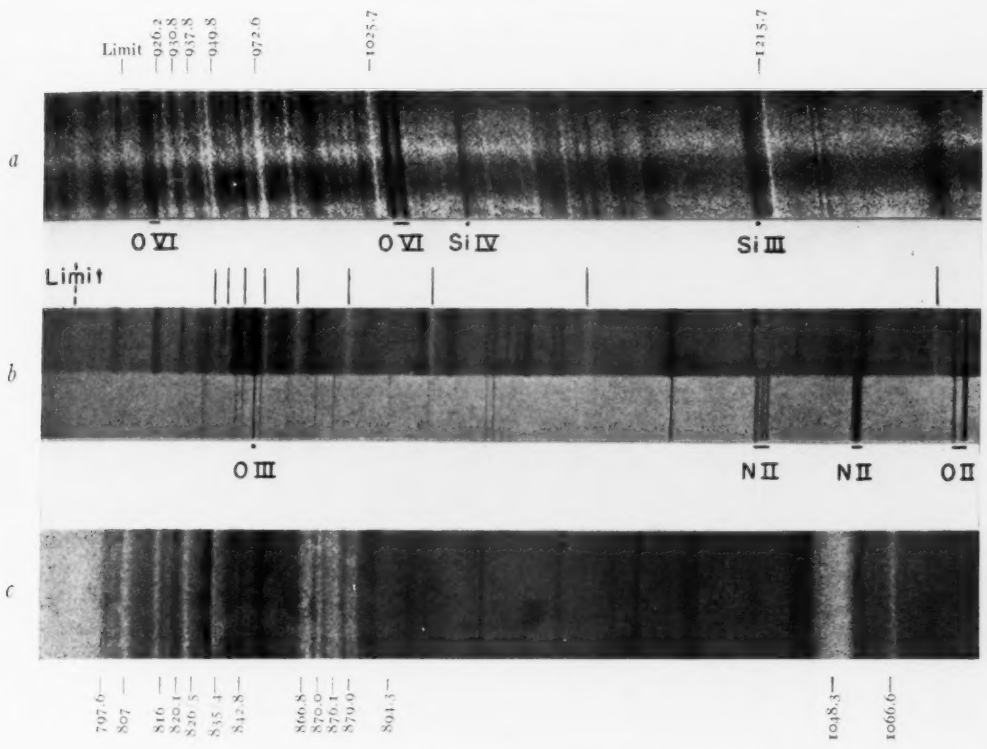

ULTRAVIOLET ABSORPTION SPECTRA OF *H*, *He*, AND *A*

a) Lyman series of hydrogen in absorption. Magnification 9. The *O* IV doublet at λ 922 A is incorrectly marked *O* VI.

b) Helium $1^1S_0 - m^1P_1$ series in absorption. $m = 3$ (λ 537.0 A) to $m = 11$ (λ 506.6 A). Magnification 5.

c) Argon absorption spectrum. Magnification 12.

The wave lengths are given in angstrom units.

UNIV. OF MICH.

meter to several centimeters. Absorption was clearly observed for several members of the resonance series of *He* I ($1\,^1S_0 - m\,^1P_1$). With increasing pressure these absorption lines were broadened quite unsymmetrically, i.e., the edges toward the red remained fixed and fairly sharp, while the violet wing was very markedly extended. In fact, at 14-cm pressure, the wing of the line λ 584 A on the violet side was seen extending about 15 A. It is interesting to note that J. J. Hopfield[7] observed exactly the same feature for this line in emission.

By chance we learned that Dr. R. E. Worley[8] had already obtained an excellent spectrogram of the *He* I lines in absorption at Berkeley in 1939. His photograph, taken with a 3-m grazing-incidence spectrograph, has greater dispersion than ours and shows the series clearly down to the tenth member. It is reproduced in Plate XVII, *b*. The equivalent path length of the absorbing helium column was 30 cm at 1-mm pressure in this case. The details of the experimental arrangement used by Dr. Worley will be described in his article shortly to appear in the *Journal of Scientific Instruments*.

An observation relating to the continuous spectrum of helium seems worthy of mention here. Since the first report by J. J. Hopfield,[9] the emission continuum of helium, ranging from λ 600 A to λ 900 A has been used by many investigators as an excellent background for absorption effects. However, not much seems to be known regarding its origin, although it has been generally accepted as due to helium molecules because it goes hand in hand with the band spectra of helium. This helium continuum is produced, as described by Hopfield, in a disruptive discharge at a pressure of a few millimeters. Under similar conditions the *He* I series occurs strongly in emission. Now an interesting feature is observed when a disruptive discharge in helium is used as the source of light and the spectrograph is filled with helium at a fairly high pressure. We then notice that, whereas the atomic spectrum of helium gradually becomes fainter and finally disappears[10] with increasing pressure of helium in the spectrograph, the intensity of the helium continuum remains practically unaltered. This fact seems to be of significance because it shows very clearly that, as has generally been accepted, the continuous spectrum is of molecular origin. Stated in another way, since the presence of molecular helium in the spectrograph is hardly possible, the molecular radiation suffers no absorption.

Neon.—A liter flask containing pure neon at atmospheric pressure served as the source of neon gas. The experimental procedure was essentially the same as for helium. On account of the limited supply of pure neon, the pressure of neon inside the spectrograph could not be raised so high as with helium; the highest pressure we tried was 4 cm.

The neon lines observed in absorption are listed in Table 1. They all belong to the resonance series as indicated in the table.

A more careful study is clearly needed to bring out the differences in the mode of absorption according to the various series relationships. Here we mention only that, of the two first members of the resonance series, λ 744 and λ 736 A, the line λ 736 A, due to the singlet-to-singlet transition, was absorbed quite strongly and showed considerable unsymmetrical broadening toward the violet at high pressure; whereas the other line, λ 744 A, due to the singlet-to-triplet transition, was absorbed in a far less conspicuous way, without much widening. This feature is quite similar to that previously observed by Takamine and Suga[11] for emission lines.

[7] *Ap. J.*, **72**, 133, 1930.

[8] We are greatly indebted to Dr. Worley for placing his unpublished spectrogram at our disposal.

[9] *Phys. Rev.*, **36**, 784, 1930.

[10] At times the *He* I line λ 584 A was even seen as a shallow absorption strip on the faint extension of helium continuum below λ 600 A serving as background.

[11] *Inst. Phys. and Chem. Research, Sci. Papers*, **29**, 1, 1936.

Argon.—An excellent investigation of the absorption spectrum of argon was published in 1934 by H. Beutler.[12] As our dispersion was much smaller, not much is to be added to his observations, except the fact that we used considerably higher pressures so that the lines λλ 894.3 A ($1\,^1S_0 - 3d_5$), 842.8 A ($1\,^1S_0 - 4d_5$), and 820.1 A ($1\,^1S_0 - 5d_5$) came out in absorption in our experiments. This seems worthy of note because Beutler mentions in his report that the nonappearance of the $1\,^1S_0 - md_5$ lines is rather surprising.

TABLE 1*

NEON ABSORPTION LINES

λ in A	Intensity	Series	Remarks
743.70	1	$1\,^1S_0 - 3\,^3P_1$	
735.89	4	$1\,^1S_0 - 3\,^1P_1$	Considerably widened on the violet side
629.729	2	$1\,^1S_0 - 4\,^3P_1$	
626.819	2	$1\,^1S_0 - 4\,^1P_1$	
619.092	1	$1\,^1S_0 - 3d_5$	Blended
618.668		$1\,^1S_0 - 3d_2$	Blended
615.623	1	$1\,^1S_0 - 3s_1$	
602.712	1	$1\,^1S_0 - 5\,^3P_1$	
600.04		$1\,^1S_0 - 5\,^1P_1$	Covered by *C* II λ 600 group
598.86	1	$1\,^1S_0 - 4d_5$	Blended
598.698		$1\,^1S_0 - 4d_2$	Blended
595.911	1	$1\,^1S_0 - 4s_1$	
591.82	1	$1\,^1S_0 - 6\,^3P_1$	
586.30	1	$1\,^1S_0 - 7\,^3P_1$	

* The wave lengths given in Table 1 are after J. C. Boyce and H. A. Robinson, *J. Opt. Soc.*, **26**, 133, 1936. Our own measurements could be accurate only to 0.5 A.

Unsymmetrical broadening to the violet was observed for the line λ 1048 A by Beutler, who also found a similar phenomenon for the resonance-series lines of *Kr* and *Xe*. A reproduction of the argon absorption spectrum, taken at 40-mm pressure of argon in the spectrograph, is given in Plate XVII, *c*.

In conclusion we wish to express our sincere thanks to Director W. S. Adams for allowing us to work at the Mount Wilson Observatory and to Dr. A. S. King and Dr. J. A. Anderson for many helpful suggestions.

CARNEGIE INSTITUTION OF WASHINGTON
MOUNT WILSON OBSERVATORY
January 1941

[12] *Zs. f. Phys.*, **93**, 177, 1934.

PLANETARY ATMOSPHERES AND WATER-CELL TEMPERATURES

ARTHUR ADEL AND C. O. LAMPLAND

ABSTRACT

One of the most important quantities appearing in the relationship between water-cell transmission W and planetary temperature T is the water-cell transmission of the planetary reflected sunlight. In the absence of information regarding the nature of planetary atmospheres it has been assumed in the past that the sunlight was unmodified in quality by the reflection process. To the extent to which we are now aware of atmospheric composition within the solar system it is shown in this paper, which describes experiments carried out at the Lowell Observatory, that the solar radiation is significantly modified in quality by reflection and absorption.

I. INTRODUCTION

The water cell was first applied in astronomical radiometry twenty-five years ago by W. W. Coblentz;[1] and its use in the measurement of the radiation from planets has provided a simple and ready means of separating, approximately, the reflected solar radiation from the emitted long-wave planetary radiation. If it is assumed that the reflection of sunlight is nonselective, the water cell provides a rapid and certain observational method for determining the presence or absence of planetary radiation. Based on this assumption, the well-known formula[2] for calculating planetary temperatures was derived by Russell and applied by Menzel to the evaluation of water-cell transmission data obtained by Coblentz and Lampland.[3]

As the radiometric observations were extended, it became evident that the water-cell

[1] *Lick. Obs. Bull.* No. 266.

[2]
$$T = T_0 \sqrt[4]{\frac{t'}{t} A \cdot x \frac{\phi(a)}{q\epsilon} \left(\frac{0.76}{W} - 1\right)},$$

where T = the gray-body temperature of that portion of the planet's surface under investigation; $T_0 = 392°\sqrt{R}$, R being the planet's distance from the sun; t' = the terrestrial atmospheric transmission of the planetary reflected sunlight; t = the terrestrial atmospheric transmission of the planetary heat spectrum; A = the albedo of the planet for solar radiation; x = the relative mean apparent surface brightness of the surface element under investigation with respect to that of the entire disk; $\phi(a)$ = the fractional brightness of full phase, which the planet possesses at phase a; $A = p \cdot q$, where q is a function of the manner in which the brightness of the planet varies with phase, and p is the ratio of the radiation reflected at full phase to that emitted by a self-luminous body of the same size and position, which radiates as much energy from each unit of its surface as the planet receives from the sun under normal incidence; ϵ = the emissivity of the gray surface of the planet; W = the water-cell transmission of the energy received from the planet; and 0.76 = the water-cell transmission of direct sunlight, here taken to be the water-cell transmission of the planetary reflected sunlight on the assumption that the reflection process is nonselective.

The determination of planetary temperatures from observations of the water-cell transmission is perhaps the best-known method at the present time. This method, as well as the one employing the ratios of the spectral components, has the advantage that it is not necessary to measure absolute values of the quantities involved. In these methods, as well as in others that may be used, certain factors are as yet imperfectly known, as, for example, the emissivity and the total albedo and the relative albedos. All that can be done under the circumstances is to assign reasonable values to these parameters. Thus far, for example, it is reasonably certain that the emissivities have been assumed sufficiently high to insure that the effective temperatures are likely to be too low instead of too high.

The water cell may well be replaced with a filter, such as quartz of suitable thickness, in cases where the temperature is so low that no appreciable part of the planetary radiation enters the spectral range of transmission of such a filter. This procedure would eliminate the uncertainty of selective action of the planetary surface on the reflected solar radiation.

[3] D. H. Menzel, *Ap. J.*, **58**, 65, 1923.

transmissions were selective in some cases; nor is it surprising that this should be so in view of the presence of the powerful absorption bands in the spectra of the outer planets.[4]

The need for more detailed knowledge of the meaning of water-cell transmissions has been felt for many years in carrying forward the radiometric work of this Observatory. Experiments recently conducted here on the effects of large quantities of methane, ammonia, and carbon dioxide on both the integrated and the dispersed solar radiation provide this knowledge, revealing that the water-cell transmission of planetary reflected solar radiation depends strongly upon the planet in question.

II. EXPERIMENTAL

The gases and vapors, which by their powers of absorption cause the reflected component of planetary radiation to differ from solar radiation in the distribution of relative intensities, are methane and ammonia for the giant planets and carbon dioxide for Venus. Large quantities of these substances are present in the atmospheres of the planets; in consequence, an absorption cell was constructed which would withstand the moderately high pressures represented by large accumulations of gas within the confined space in the laboratory. The absorption cell, constructed of 3-inch, high-pressure steam tubing was 2 meters in length, was fitted with thick glass windows, and was equipped with needle valves and a pressure gauge reading to 300 pounds per square inch.

The thick glass windows of the absorption cell absorb several per cent of the solar radiation in the longer wave lengths; and this effect, as well as the effects of high pressure upon the molecular absorption of solar radiation, will be treated more fully in a later section.

The gases carbon dioxide and methane were introduced at pressures up to 300 pounds per square inch above atmospheric pressure, while the ammonia vapor was examined at various pressures up to 90 pounds per square inch (ammonia liquefies at room temperature when subjected to somewhat higher pressures). The absorption cell was fed by means of a coelostat with aluminized mirrors; and the emergent radiation was incident

[4] "The enormous and rapid changes apparent in the surface markings of Jupiter, as shown by visual observations and more clearly by direct photographs, might lead one to expect interesting things radiometrically. And this happens to be the case. Some of the results are highly interesting. When systematic measures were begun on the planet this past autumn an unexpected result was that the water-cell transmission of parts of the planet in many cases exceeded the water-cell transmission of the directly observed solar radiation by as much as 5–10 per cent. The first and most natural attitude to assume in such an event would be that the observations were in error; and hence checks were sought through as many independent sources as possible in regard to the performance of the apparatus and the manner of making the observations. Other objects, the moon, Venus, and the sun, were observed during the interval covered by the Jupiter measures, and thus far no reasons have been found for not accepting the results as real.

"The high water-cell transmission found for Jupiter led to frequent repetitions of the measures, and, since the added data confirmed previous observations, this apparent difficulty and trouble for the observer stimulated thinking on the problem. The high water-cell transmissions of the planet need not be assumed to be impossible. On the contrary, there appear to be reasonable arguments to offer in support of transmissions for some of the planets higher than observed for the direct solar radiation. A value for the water-cell transmission the same as found for sunlight would imply nonselective reflection or that the albedo is the same for all parts of the spectrum. In puzzling over these unlooked-for results the writer recalled the classic bolometric observations of Langley on the powerful absorption bands of the earth's atmosphere and Slipher's spectrographic observations of the conspicuous atmospheric absorption bands of the outer planets. Except in the case of the earth's atmosphere it is not known to what extent these absorptions invade the invisible domain of the infrared regions of the spectra. The spectrographic observations of the atmospheric absorption, in the deep red, especially, of the outer planets and the extensive bands of absorption in the earth's atmosphere (the more conspicuous of these lie far beyond the reach of the usual spectrographic means) suggest a possible explanation of the high water-cell transmission of Jupiter. If, in the regions of absorption mentioned, additional absorptions are introduced by the atmosphere of Jupiter, the high water-cell transmission of this planet would be explained" (from a paper by C. O. Lampland to the A.A.S. New Haven meeting, Yale University Observatory, December 29–31, 1927).

upon an aluminized condensing mirror, which formed an image of the sun upon the entrance slit of a glass-prism spectrometer containing aluminized mirrors and a thermocouple, whose receiver was coated with evaporated bismuth black. Both the dispersed and the integrated radiations emerging from the cell were analyzed with the spectrometer arrangement; the integrated radiation, by replacing the prism with a pair of plane parallel aluminized mirrors to displace the beam parallel to itself. Like the effects of the thick glass windows and the high pressure of the gas, the effect of the nonuniform reflectivity of the evaporated aluminum surfaces will be discussed later.

The water cell, constructed by the Thermal Syndicate as a single unit of fused quartz, defined a layer of water 1 cm in thickness and was large enough in cross section to be placed in front of the entrance slit of the spectrometer to transmit the entire solar image.

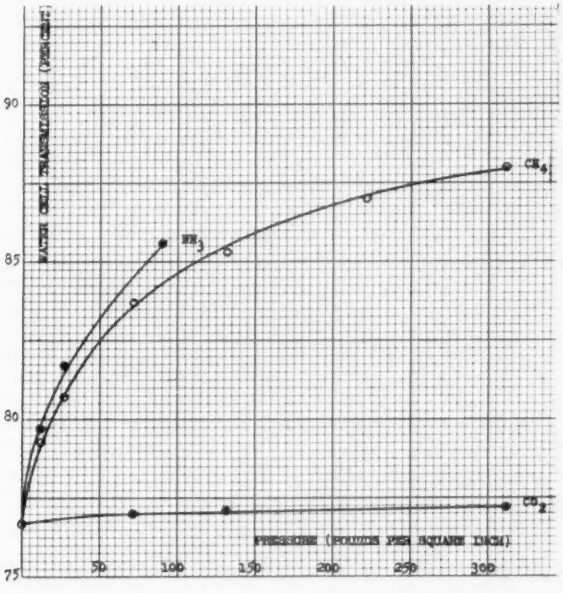

FIG. 1.—The water-cell transmission of solar radiation transmitted by various quantities of the gases ammonia, methane, and carbon dioxide.

The deflections of the galvanometer system in circuit with the thermocouple were recorded.

III. OBSERVATIONS

The observations to be considered here are graphically summarized in Figure 1. These consist of the water-cell transmissions of the integrated radiation emerging from the absorption cell. They have been corrected for the vitreous reflection of the fused-quartz water cell by the reciprocal factor $1/0.93$. The observations were carried out on clear days and with but small variations about a mean small atmospheric water-vapor content. The absorption spectra of the gases corresponding to these water-cell transmissions will be discussed in a future report. However, the curves of Figure 1 may be briefly examined at this time in the light of the spectra of the several molecules concerned. The absorption by the gases is in the form of rotation-vibration bands, and it is therefore largely concentrated on the long wave-length side of the limit of transmission of the water cell (about 1.3 μ). In conjunction with the form of the solar energy-curve this fact explains the convexity of the curves of Figure 1. The weak growth displayed by

the carbon dioxide curve reflects carbon dioxide's weak absorbing nature, even in large amounts, in those regions of the solar spectrum in which reside appreciable quantities of energy. The steep growth of the methane and ammonia curves reflects the vigorous action of these gases on solar radiation of wave lengths greater than 1.3 μ.

The obvious inference to be drawn from Figure 1 is that the water-cell transmission of planetary reflected solar radiation possesses essentially different values for the different planets and that these values will play important roles in future temperature determinations.

IV. DISCUSSION

The forms of the curves in Figure 1 will be modified in a small degree, but their interpretation will not be affected in principle, by the consideration of the following items: (*a*) the reflectivity of evaporated aluminum, (*b*) thick glass windows on the gas absorption cell, and (*c*) the high pressure of the gas during some of the observations.

During the measurements on the integrated radiation, nine first-surface, evaporated aluminum reflections were involved. The reflectivity of evaporated aluminum for one surface is known,[5] while the reflectivity for nine surfaces can be found by raising that for one surface to the ninth power. The effect of the selective reflection upon the measurements is clearly to diminish the water-cell transmission of solar radiation passing through the absorption cell. With the particular water cell used in this experiment the direct transmission of sunlight (no reflections) was observed to be 80 per cent, while with nine aluminized mirrors in the path the transmission was observed to be 72 per cent. It is thus seen that in the absence of the gas absorption cell the nine reflections reduce the water-cell transmission of sunlight by 8 per cent. The magnitude of this effect may also be determined by calculation, through use of the curve of reflectivity of evaporated aluminum, the transmission-curve of the water cell, and the curve of distribution of solar radiation at the earth's surface. The calculation agrees well with the result of the experiment. It is now clear that to compensate for the effects of the selective reflectivity of the evaporated aluminum we should elevate the curves of Figure 1. However, it will be readily realized that the elevation is not uniform along the length of the curve. On the contrary, since it depends so much upon the distribution of the relative intensities in the radiation spectrum concerned, it will grow less as the longer wave-length portion of the solar curve is eradicated, that is, as the amount of gas in the absorption cell is increased. Consequently, while the zero point of the curves for ammonia and methane should be elevated 8 per cent, the end points should be elevated by a somewhat smaller amount. The curve for carbon dioxide, on the other hand, should receive almost uniform elevation along its entire length.

The effect of the thick glass windows on the absorption cell is the enhancement of the water-cell transmission of sunlight by an amount which depends upon the degree of absorption produced by the inclosed gas. Thus, with no gas in the path, the windows on the evacuated cell determine a water-cell transmission of 77 per cent as compared with 72 per cent when the windows are removed. This difference of 5 per cent almost eliminates the decrement induced in the water-cell transmission by the nine aluminum reflections at this end of the curves. The increment brought about by the glass windows is, of course, due to the absorption of the long wave lengths by glass—complete absorption beyond about 2.5 μ and partial absorption at wave lengths shorter than, and near, 2.5 μ. Here again, clearly, as the amount of gas is increased, these are the very regions of the spectrum that will be absorbed by the gas, and the effect of the glass is reduced in proportion to the absorption by gas in the affected wave lengths. The glass increment to the water-cell transmission is consequently lower at those ends of the curves of Figure 1

[5] See e.g., J. Strong, *Procedures in Experimental Physics*, p. 375, Prentice-Hall, New York, 1938. The extension of this curve in the direction of longer wave lengths probably maintains a high level by analogy with the behavior of other evaporated metallic surfaces.

which correspond to the high gas content. The net effect of the aluminum decrement and the glass increment is probably a lowering of the curves by perhaps 3 per cent at the beginning and somewhat less at the end points.

A consequence which is much less easily allowed for is that of pressure on the absorbing gas within the cell. In order to accumulate, within the confines of the laboratory and in the path of the solar radiation, an amount of gas large enough to indicate the trend in the extensive atmospheres of the outer planets and Venus, the methane and carbon dioxide were introduced at pressures of more than 300 pounds per square inch, and the ammonia was introduced at a value near that of the vapor pressure of liquid ammonia at room temperature. The first and principal consequence of increased pressure at constant temperature is the increase of the number of molecules in the path of the radiation. The second result of increased pressure is largely something which no amount of gas at low pressure can produce—namely, an intensification of the perturbative field in the space occupied by the molecules, with a consequent broadening of the energy levels, or, what is the same thing, a broadening of the absorption lines. To illustrate the latter point one may cite the extreme case in which pressure compels the existence of the liquid state, in which case the rotational structure becomes so broad as to provide extensive regions of continuous absorption; for example, the water cell itself absorbs infrared radiation continuously and completely beyond 1.3 μ. It is true that in some degree the transition probability is also enhanced by pressure, that is, the absorption lines are deepened—a result that could be achieved by increased gas content alone. It is clear that the laboratory conditions of the gas, with regard to pressure, are fundamentally different from, for example, the circumstances of the methane and ammonia above the Jovian cloud surface. At the same time it may be pointed out that the excess absorption, at the pressures employed, would appear in the form of additional bands if more gas (approaching the content of the planetary atmospheres) had been used at lower pressures. In this very specialized but pertinent sense of equivalence, therefore, a given amount of gas under high pressure will produce as much absorption as would a higher gas content under low pressure. In this special sense, then, the effects of pressure enable us to approach, in the laboratory, something of the same order of depletion of energy as that which occurs in the longer path lengths of planetary atmospheres. For example, at low pressures and contents—the region of unsaturated absorption—the absorption is proportional to the square root of the pressure and also to the square root of the amount; so that in this range an n-fold change in pressure is equivalent to an n-fold change in path length at the original pressure (as far as the amount of energy absorbed is concerned). At higher pressures and gas contents, where the absorption is more nearly saturated, the absorption depends upon the amount of gas in transcendental fashion, and it depends upon the pressure in a more complex and asymptotic fashion also. Here the "equivalence" is more approximate, and the effects of increased gas content and increased gas pressure are also less noticeable. It is, therefore, likely that the end points of the curves of Figure 1 lie not far from the asymptotes that would be defined by quantities of gas approaching the planetary atmospheric contents.

V. CONCLUSION

As we have seen, the net effect of the aluminum reflectivity and the thick glass windows is a lowering of the end points of the curves of Figure 1 by 2 or 3 per cent, whereas the net effect of the high pressure of the gas is not only to remove this decrement but to elevate the water-cell transmissions to values more nearly corresponding to the extensive envelopes of the outer planets.

The form of the curves in Figure 1 is essentially in accord with expectation. That is to say, in the beginning, when the absorption is quite unsaturated, the absorption should be proportional to the square root of the gas content; and, since the absorption occurs main-

ly at wave lengths beyond the cut of the water cell, one may write, for small amounts of gas,

$$\text{water-cell transmission} = \frac{c_1}{c_2 - k\sqrt{x}},$$

where x is the optical depth. Now $k\sqrt{x} \ll c_2$; that is, the energy removed by the gas from the solar beam is small compared with the total solar energy. We may, therefore, write

$$\text{water-cell transmission} = \frac{c_1}{c_2}\left(1 + \frac{k\sqrt{x}}{c_2}\right).$$

This indicates that the curves should approximate a square-root law in the early stages, which they do. In the stages of higher content, where the absorption follows an exponential behavior, the curves level off as would be expected.

For a planet like Jupiter, whose atmosphere contains both methane and ammonia, it is clear that the water-cell transmission of the Jovian reflected solar radiation will exceed the water-cell transmission of the Saturnian reflected solar radiation (because there is less ammonia vapor in Saturn's atmosphere) by an amount depending upon the extent to which each gas tends to absorb energy left by the other. In Uranus and in Neptune the ammonia vapor appears to have been precipitated from their atmospheres; but the optical depth of the methane penetrated by the solar beam is far greater than in Jupiter and Saturn, probably because of the absence of clouds in the atmospheres of these two more distant and colder planets.

LOWELL OBSERVATORY
FLAGSTAFF, ARIZONA
January 1941

THE IMPORTANCE OF CERTAIN CARBON DIOXIDE BANDS IN THE TEMPERATURE RADIATION FROM VENUS

ARTHUR ADEL

ABSTRACT

There is sufficient carbon dioxide in the earth's atmosphere to absorb completely the fundamental carbon dioxide emissions ν_2 (14.97 μ) and ν_3 (4.27 μ) from the extensive carbon dioxide component of the atmosphere of Venus. It is pointed out, in consequence, that upper-stage bands of the types $\nu_3 \rightarrow (\nu_1, 2\nu_2)$ (near 10 μ) and $(\nu_1, 2\nu_2) \rightarrow \nu_2$ (near 13 μ) determine the quality of the radiation which we receive from the atmosphere of Venus. It is shown that the latter is appreciable in amount and is highly selective in distribution.

The atmosphere of Venus contains an amount of carbon dioxide equivalent to several hundred meters under standard conditions ($T = 273°$ K, $p = 1$ atm.),[1] much of it at temperatures which are probably in excess of 50° C.[2] The infrared emission of carbon dioxide must consequently play an important, and perhaps dominant, role in the radiation from Venus to space. This inference is supported by the radiometric observations of W. W. Coblentz and C. O. Lampland,[3] which show the long wave-length radiation from Venus to be very selective. The active fundamentals ν_2 and ν_3, intensely radiated by Venus, are, of course, absorbed by the 3-meter atmospheres of carbon dioxide (N.T.P.) within our own atmosphere.[4] It is the purpose of the present discussion to specify other carbon dioxide bands which are strongly emitted by Venus and poorly absorbed by the earth's atmosphere and which therefore make the principal contributions to the radiation reaching us from the atmosphere of Venus.

Since the effective temperature of the carbon dioxide–absorbing layer on Venus is in excess of 50° C,[2] we may consider the effective radiating temperature to be in excess of 50° C also. The relative intensities of the carbon dioxide bands emitted by Venus will therefore be defined, wherever the bands or band lines are "black," by the black-body curve for $t \sim 50°$ C. That is to say, with the great amount of carbon dioxide present on Venus certain bands will radiate, in their lines, as fully as would a black body in the same wave lengths and at the same temperature. Such lines will touch the black-body curve mentioned above. Still other carbon dioxide bands will have some of their lines black, while other lines of these bands will fall short.

A black-body curve of the type in question is modified by absorption in the earth's atmosphere[5] to the form shown in Figure 1, where, for convenience in estimating the effect of a change in the adopted temperature, curves have been plotted for $t = 30°$ C and $t = 100°$ C. The existence of carbon dioxide in the earth's atmosphere sufficient completely to absorb the fundamental carbon dioxide emissions ν_2 and ν_3 (centered, respectively, at 14.97 μ and 4.27 μ) is, of course, reflected in these curves. It is clear from Figure 1 that significant contributions to the radiations which reach us from the atmos-

[1] T. Dunham, Jr., *Carnegie Institution of Washington Year-Book*, No. 31, 154, 1932; A. Adel, *Ap. J.*, **85**, 345, 1937.

[2] A. Adel, *Ap. J.*, **86**, 337, 1937; R. Wildt, *Ap. J.*, **91**, 266, 1940.

[3] *Journal of the Franklin Institute*, June and July, 1925, and a series of subsequent observations by C. O. Lampland, as yet unpublished and awaiting more complete analysis based upon recently obtained atmospheric transmissions.

[4] C. O. Lampland, *Pub. A.A.S.*, **9**, 174, 1939.

[5] A. Adel and C. O. Lampland, *Ap. J.*, **91**, 1, 1940, and *ibid.*, p. 481.

phere of Venus will be made only by bands falling between 8 μ and 13.5 μ—that is, mainly by the pair of bands $\nu_3 \rightarrow (\nu_1, 2\nu_2)$ (near 10 μ)[6] and by those members of the bands $(\nu_1, 2\nu_2) \rightarrow \nu_2$, $(\nu_1 + \nu_2, 3\nu_2) \rightarrow (\nu_1, 2\nu_2)$ hereafter referred to as the "ν_2" bands, which are centered on the short wave-length side of 14 μ (near 12 μ and 13 μ).[7] The lo-

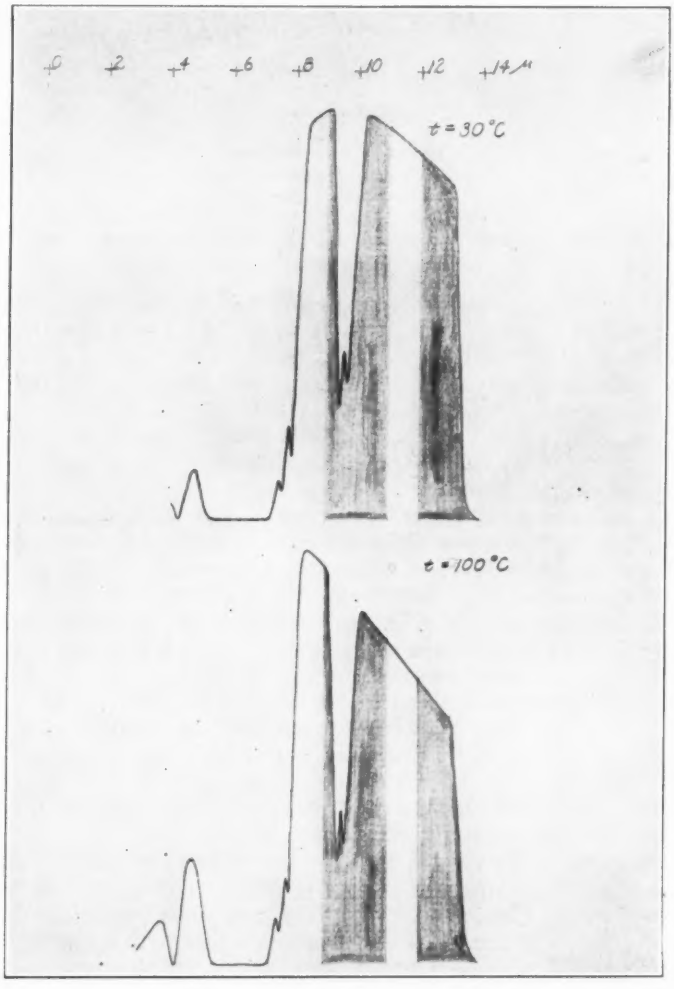

FIG. 1.—Terrestrial atmospheric transmission of energy radiated by the atmosphere of the planet Venus.

cations, but not the relative intensities, of these two sets of bands are shown by the shaded areas of Figure 1. The bands at 10 μ, as observed in the laboratory through about 6-meter atmospheres of carbon dioxide, are shown in Figure 2, which has been taken from a paper by E. F. Barker and A. Adel.[6] The "ν_2" bands differ from the bands at 10 μ in being considerably more intense and in each possessing a strong zero branch, in addition to the P and R branches. The "ν_2" bands may, for the purpose at hand, be

[6] *Phys. Rev.*, **44**, 185, 1933.

[7] *Phys. Rev.*, **41**, 291, 1932.

described as fairly intense. P. E. Martin and E. F. Barker[7] have shown that 25-cm atmospheres of the gas displays considerable absorption in these bands, and there is more than sufficient gas on Venus to make the lines of these bands black—that is, the intensity distribution of fine structure in the "ν_2" Venus emission bands will be defined by points corresponding to the positions of these lines and lying on the black-body curves of Figure 1. There is certainly not enough atmospheric pressure on Venus to accomplish much in the way of broadening the emission lines,[8] and the "ν_2" emission bands will therefore be composed of lines about 1.6 cm^{-1} apart. The bands at 10 μ are not so intense as the "ν_2" bands, some twenty times as much gas being required to develop the former as is required to develop the latter in the laboratory.[6, 7] Even with the large carbon dioxide component of the atmosphere of Venus, many of the lines in these bands

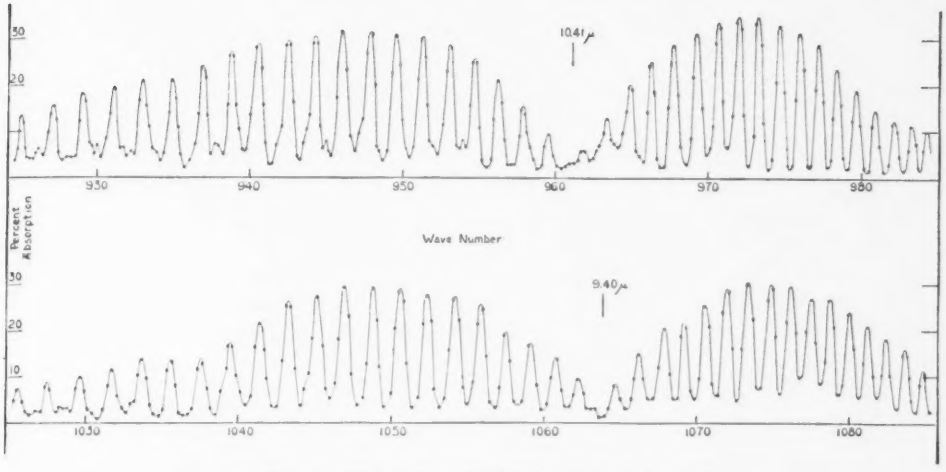

FIG. 2.—The carbon dioxide bands $\nu_3 \rightarrow (\nu_1, 2\nu_2)$

will not be black, though the strongest will be. Lines at the wing extremities, for example, will be about 60 per cent black.[9]

The characteristic radiation from the atmosphere of Venus apparently plays a significant part in the radiation of energy from the planet to space. Any phenomena in the planet's atmosphere which would tend to influence this role are therefore of interest. Now, from an analysis of the conditions on Venus made evident by study of its surface markings, Percival Lowell concluded that the atmosphere of Venus is laden with large particles.[10] More recently, both B. Lyot[11] and B. P. Gerasimovič[12] have arrived at the same conclusion, the former as a result of his measurements and analysis of the polarization of the light from Venus, the latter in consequence of his examination of Müller's photometric observations of Venus. In view of the vigorous atmospheric circulation to be expected on Venus,[10] apropos of the planet's slow rotation and intense heating, it might be expected that the effective level and extent of the layer of large scattering par-

[8] See, e.g., the definition of the lines of the Venus bands $5\nu_3 + (\nu_1, 2\nu_2)$ in W. S. Adams and T. Dunham, Jr., *Pub. A.S.P.*, **44**, 243, 1932.

[9] The intensity calculations were made on the basis of D. M. Dennison's theory of absorption lines (*Phys. Rev.*, **31**, 503, 1928).

[10] *The Evolution of Worlds*, New York, 1909.

[11] Ann. de l'obs. de Paris, sec. de Meudon, **8**, 1, 1929.

[12] *Poulkovo Bull.*, No. 127, 1937.

ticles would vary and that the layer might even be effective in screening more or less of the underlying carbon dioxide, thus preventing the direct passage of the latter's radiation to space. Such blanketing would have more effect upon the weaker bands at 10 μ than upon the stronger "ν_2" bands, and we might expect not only a variable emission from the atmosphere of Venus but also a variable relationship between the amounts radiated in the two sets of bands. Variability of the radiation from Venus has been observed.[13]

The radiation role of the hot, solid surface of Venus is as yet unknown, but in addition to being blanketed by the carbon dioxide it is presumably screened by the layer of large, scattering particles.

In conclusion it is of interest to note that the "ν_2" and 10 μ radiations from heated carbon dioxide convected to the dark side of the planet would provide the type of selective emission which has actually been observed from the unilluminated side of the planet.[3]

LOWELL OBSERVATORY
FLAGSTAFF, ARIZONA
February 1941

[13] C. O. Lampland, *Pub. A.A.S.*, 5, 108, 1927.

ON THE OBSERVABLE RADIATION FROM THE CARBON DIOXIDE IN THE ATMOSPHERE OF VENUS: COMMENTS ON DR. ADEL'S PAPER

C. O. LAMPLAND

The planet Venus still offers to the investigator interesting problems even after many years of prolonged and careful researches devoted to it. It will be necessary to recall here only the great mass of visual and photographic observational data and their interpretations attempted by many with results that are accepted in varying degrees between the wide limits of total disbelief and finality of proof, and the spectrographic investigations which have brought much new information but also leave unsolved some problems for the years to come. In radiation investigations, also, troublesome questions have been encountered, particularly in the interpretations of the spectral distributions and intensities of some of the components of the observed planetary radiation. But the purpose of this brief note is not to review the present status of researches on the planet but to comment on the most recent discussion of the radiant properties of an important constituent of the atmosphere of Venus, one dealing with pertinent new information which should be a useful addition to our knowledge of the planet.

Dr. Adel's paper on the bands of carbon dioxide between 9 μ and 11 μ is of great interest and should prove helpful in dealing with the analysis and interpretation of the observed radiation from the planet. Thus far attention has been given largely to the well-known, powerful, active, fundamental bands of this gas. The interpretation of the net effects, observationally, of these bands as emitters and absorbers in the planet's and the earth's atmosphere should be fairly clear.[1] We need only apply the results of the important infrared investigations of the Astrophysical Observatory of the Smithsonian Institution and others. The earth's atmosphere contains a sufficient amount of carbon dioxide, though the percentage composition is small, to obscure quite completely the radiation of this gas in the planet's atmosphere in the powerful bands mentioned, as far as the radiometer is concerned. This point has been emphasized in connection with the radiometric measurements on the planet now extending over many years.[1] But the bands between 9 μ and 11 μ are quite another matter, as Dr. Adel points out. In this spectral interval the earth's atmosphere does not absorb strongly, except in the ozone band (9.6 μ); and the large amount of carbon dioxide in the atmosphere of Venus, intensely irradiated, should emit considerable energy accessible to detection and measurement with the radiometer. Using transmission screens with cutoff limits near 8 μ and 12 μ, it is possible to isolate the radiation of the carbon dioxide bands here in question, but of course there may also be present the radiation from the surface and from the suspensions of the turbid atmosphere, whatever may be their nature. In many of the observations a considerable percentage of the radiation between 8 μ and 13.5 μ is found between 8 μ and 12 μ; but there are also times when the radiation in this latter spectral interval is practically absent, that is, the two filters mentioned show about the same values, and the explanation of these results is difficult. Perhaps some would simplify the problem by rejecting such divergent results as faulty. But the measurements of this nature extend back over many years, indicating a variability in intensity and spectral quality of the radiation for different parts of the disk,[2] and there appear to be good reasons for

[1] Lampland, *Pub. A.A.S.*, **9**, 174, 1939. [2] *Ibid.*, **5**, 108, 1927; *Pop. Astr.*, **36**, 238, 1928.

accepting the results as real. It is, of course, the investigator's task to ascertain as far as possible the things that are intrinsically planetary and such as are instrumental and observational, and in this he may not always be successful. That the observations are troublesome and difficult to interpret in the state of our present knowledge is not a valid cause to justify their arbitrary rejection, and it will be necessary to seek further for explanations. If there is some variable blanketing layer or veil cutting off the radiation from the carbon dioxide as well as from the true surface (and it would seem that radiation from the heated surface may emerge in the interval 8–12 μ), an obvious question is why this obscuring layer does not of itself radiate? Up to the present time suitable transmission screens have not been available to determine what proportions of the radiation here specially considered may be attributable to the true surface, to the carbon dioxide, and to other constituents of the planet's atmosphere.

LOWELL OBSERVATORY
FLAGSTAFF, ARIZONA
January 28, 1941

THE RECIPROCITY PRINCIPLE IN LUNAR PHOTOMETRY

M. MINNAERT

ABSTRACT

In order to ascertain the exact meaning of the optical reciprocity principle, stated by Helmholtz, some simple idealized experiments are considered. By then applying this principle to the case of a scattering surface, we find a general reciprocity law which is independent of the nature of the surface considered. Definite relations must, therefore, exist between the brightness of two points on the moon, if the lunar surface at these points has identical properties; a photometric test for this identity is thus obtained. From the work of Öpik, Fessenkoff, and Bennett examples are selected in which similar lunar formations are found to have similar surface layers, and other examples in which the surfaces are found to be different. The reciprocity principle restricts the possible forms of the general law of illumination of the lunar surface. Some of the laws thus far proposed are incompatible with it.

The photometric properties of the average lunar surface are at present fairly well known. For more detailed information about the surface features of the moon the photometric investigation of individual points is now required. This work has been initiated by Pickering, Wislicenus-Wirtz, Goetz, Rosenberg, Öpik, Schoenberg, Barabascheff, Fessenkoff, Fessenkoff and Parenago, and Bennett.[1] The measurements by Öpik, by Fessenkoff, and by Bennett are the most important, both because of the precision of the methods used and because of the great number of points investigated.

A detailed photometric investigation of the moon requires (*a*) a comparison between the brightness of different points of the lunar surface at one definite moment and (*b*) a comparison between the same points on different days. Doubtless, observations of the second kind are more uncertain than those of the first, because changes in the atmospheric transmission or in the plate sensitivity may interfere to a certain extent, even if precautions are taken in order to eliminate these influences. This will have to be duly considered in a critical discussion of the results.

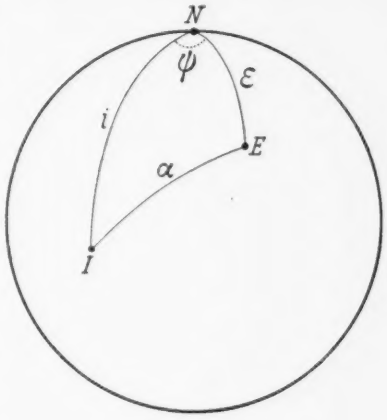

FIG. 1

The ultimate aim must be to determine the characteristic photometric function for each of the typical lunar formations. The surface brightness of a solid body, illuminated by parallel rays from a definite direction and observed from another direction, cannot be expressed by a simple physical law; the formulae thus far proposed are rather empirical and vary from one substance to another. In any case the brightness (i, ϵ, ψ) is a function $H(i, \epsilon, \psi)$ of the angle i between the normal and the incident rays, the angle ϵ between the normal and the direction of observation, and the angle ψ between the azimuth of the incident ray and of the direction of observation (Fig. 1). In most cases, the diffusing properties may be assumed to be symmetrical around the normal, otherwise the azimuth

[1] Pickering, *Selenograph. J.*, 1882; Wislicenus-Wirtz, *A.N.*, **201**, 289, 1915; P. Goetz, *Veröff. Sternwarte Oesterberg, Tübingen*, **1**, No. 2, 1919; H. Rosenberg, *A.N.*, **214**, 137, 1921; Öpik, *Pub. Tartu*, **26**, 3, 1924; E. Schoenberg, Acta Soc. Sc. Fennicae **50**, Nr. 9, 1925; Barabascheff, *Kharkov Pub.*, **1**, 35, 1927; B. Fessenkoff, *Pub. inst. ap. Russie*, **4**, 1, 1928. B. Fessenkoff and Parenago, *Russ. A.J.*, **6**, 279, 1929; A. L. Bennett, *Ap. J.* **88**, 1, 1938.

of the incident ray should be introduced as a fourth co-ordinate. If we consider the surface element under examination as the center of a sphere, the directions of the normal, of the incident light, and of the straight line toward the observer are represented by the points N, I, E; moreover, $i = \widehat{IN}$, $\epsilon = \widehat{EN}$, $\psi = \widehat{INE}$. These are the independent co-ordinates used, for example, by Bennett.

But evidently the spherical triangle INE may also be defined by the co-ordinates i, ϵ, and the phase angle $\alpha = IE$. The use of the angle α as a third co-ordinate instead of ψ has practical advantages: (1) When one of the angles, i or ϵ, is small, a minute change in the position of N, I, or E, leaving the brightness nearly unchanged, often corresponds to a shift of ψ over nearly the entire range from $-180°$ to $+180°$; this is not the case for the angle α; (2) For all points of a lunar photograph α has the same value, while ψ varies from point to point. The majority of the authors have, indeed, used the co-ordinate α.

The complete photometric investigation of one determinate surface element of the moon is made impossible because of two limiting conditions: (*a*) the point I, representing the direction of the incident rays, is always on the same great circle—the "intensity-equator"—and (*b*) the point E, corresponding to the direction of observation, has a fixed position at the center of the lunar disk ($\epsilon = 0$). The effect of the nutations is so small that it may be practically neglected for our purpose. However, it is possible to select a number of points on the surface of the moon, having the same morphological character, of which it may be assumed a priori that they have identical surface layers. From all these points the complete photometric function for this special material may then be derived. There remains only the uncertainty as to whether the points selected have really the same photometric properties.

We shall now show that the limitations due to our position at the surface of the earth may be partly overcome by the application of an optical theorem, namely, the Helmholtz principle of reciprocity.

THE RECIPROCITY PRINCIPLE

Helmholtz has formulated the following theorem:

> Vom Punkte A gehe das Einheitsquantum an Licht von bestimmter Farbe, polarisirt nach einer bestimmten Richtung α, in einer solchen Strahlrichtung aus, dass nach einer Reihe von Spiegelungen und Brechungen schliesslich in B das Quantum x ankomme, und zwar nach einer Richtung β polarisiert. Lassen wir nun von diesem Ziel rückwärts in der umgekehrten Richtung des Endstrahls das Einheitsquantum nach β polarisirten Lichtes, von derselben Farbe ausgehen, so kommt nach allen jenen reciproken und reversibelen Vorgängen, die das Licht erleidet, dasselbe Quantum x also derselbe Bruchtheil nach α polarisirten Lichtes am Ausgangsorte an.[2]

This principle is widely applicable; it applies to reflecting, refracting, absorbing, and scattering media, for each separate wave length and for each plane of polarization. It fails only in the cases of fluorescence or of magnetic rotation. In practice one is immediately confronted with the question whether the principle applies to the total intensity, J, of the light pencil, measured by the energy passing through the entire cross-section, or to the specific intensity, H, passing through each square centimeter of the cross-section.[3] In the case of a radiating surface element, the specific intensity emitted in a given direction is what we call the brightness of this surface element. We shall try to answer this question by imagining some very simple idealized experiments (Fig. 2). We consider an optical system of arbitrary shape, composed of reflecting, refracting, scattering, and absorbing material, inclosed in a hollow vessel which is opaque to radiation except for two minute apertures. These are so small that all the surface elements within the aperture may be considered to emit the same radiation. We imagine one of the holes at

[2] *Theorie der Wärme*, 1, 3, § 42.

[3] In both cases and in all following considerations the energy measurement refers to the radiation contained within the unit of solid angle.

the left side, the other at the right, and we shall write correspondingly at the left or at the right side the intensities relating to each of them. For each experiment and its reciprocal complement both the specific and the total intensities are given in Table 1.

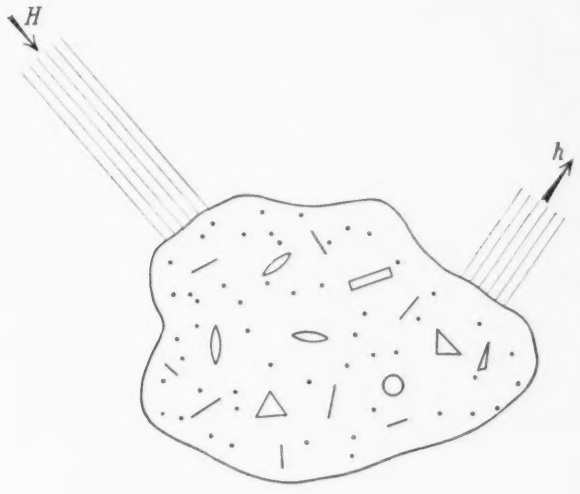

FIG. 2.

TABLE 1

IDEALIZED EXPERIMENTS WITH A DIFFUSING OPTICAL SYSTEM

Experiment	Incident→Escaping		Escaping←Incident	
1	H J	h j	h j	H J
2	$2H$ $2J$	$2h$ $2j$	$2h$ $2j$	$2H$ $2J$
3	H $2J$	$2h$ $2j$	h $2j$	H J
4	H $2J$	$2h$ $2j$	$2h$ $4j$	$2H$ $2J$
5	H J	h $j \cos \vartheta$	$h \cos \vartheta$ $j \cos \vartheta$	H $J \cos \vartheta$
6	H J	h $j \cos \vartheta$	h j	$H \sec \vartheta$ J

Experiment 1.—Both the holes have an area of 1 cm². In this case the specific and the total intensities are equal, and there is no difficulty.

Experiment 2.—Here H, J, h, and j have the same numerical value as in experiment 1; the result is obvious.

Experiment 3.—Now let the left hole have an area of 2 cm², the right one an area of 1 cm². Moreover, assume that the same specific intensity which first was admitted

through the left hole is afterward admitted through the right one. Already, in this very simple case we find that the reciprocity principle is, strictly speaking, not verified, either when it is applied to the specific intensities (upper line) or when it is applied to the total intensities (lower line). It is valid only when we compare the incident specific intensity with the observed total intensity; or when we compare the incident total intensity with the observed specific intensity.

Experiment 4.—Let the left hole again have an area of 2 cm², the right one of 1 cm². We now assume that the same total intensity which first was admitted through the left hole is afterward admitted through the right hole. The conclusion to be drawn from this experiment is the same as for experiment 3.

Experiment 5.—Let us assume that the radiation leaving one of the holes is distributed over the different directions according to the simplest law, i.e., so that the specific intensity is the same in all directions. Let both holes have an area of 1 cm². Let the incident light at the left side be perpendicular to the hole, and let it be observed at the right side under the angle ϑ with the normal. In reversing the experiment, send back the same specific intensity. The conclusion of experiment 3 is again confirmed.

Experiment 6.—Experiment 5 is repeated, but now in the reciprocal experiment the same total energy is sent back. The result is the same. We remark that in experiments 5 and 6 a uniform distribution of the specific intensity over the different directions has been assumed only in order to find out for a very simple case how the reciprocity principle has to be formulated. The applicability of the principle, however, remains quite general.

The curious form of the reciprocity principle which we have found for optical systems presents an interesting analogy with what is known about the principle of Le Chatelier–van 't Hoff in thermodynamics.[4] Here also a reciprocity theorem is valid only when an "intensity parameter" (P, T) is combined with a "quantity parameter" (V, Q). In order to apply the general principle to lunar photometry we shall have to consider the following case. Let radiation of specific intensity H fall upon the left hole under an angle θ with the normal and observe the radiation escaping through the right hole under an angle ϑ. Now try the reciprocal experiment. From the reciprocity principle we conclude that the total intensities, j, j', observed in these two cases will be equal; the observed specific intensities are $h = j/\cos\vartheta$ for the first experiment, $h' = j'/\cos\vartheta'$ for the second. Consequently, $h/h' = \cos\theta/\cos\vartheta$. In these reciprocal experiments, the observed brightnesses are proportional to the cosines of the angles of incidence. We shall give for this theorem an alternative, more direct, derivation which reveals at once its connection with the second principle of thermodynamics.

Experiment 7.—The incident light forms and angle θ with the normal to the diffusing surface, the observed light an angle ϑ; let the two holes have an area of 1 cm.² Consider now the surface element of unit area A, sending the radiation J toward the diffusing system, and the surface element of unit area B, receiving the diffused radiation i; let both of them be perpendicular to the rays of light. In reciprocal experiments we will have: $i/J = i'/J'$. For otherwise, if the two surfaces A, B have initially the same temperature, one of them would receive more heat than it would lose, the case for the other one being reversed. This would contradict the second principle of thermodynamics. In reciprocal experiments the incident radiations must be equal, thus $J = J'$ and $i = i'$. Now the brightness of the diffusing surface is defined as the diffused radiation received by B, divided by the projected area of the diffusing surface; i.e., $h = i/\cos\vartheta$. In the reciprocal experiment the brightness will be $h' = i'/\cos\theta$. Therefore

$$\frac{h}{h'} = \frac{i}{i'}\,\frac{\cos\theta}{\cos\vartheta} = \frac{\cos\theta}{\cos\vartheta}\,.$$

This is precisely the result already obtained.

[4] P. Ehrenfest, *Zs. f. phys. Chem.*, **77**, 227, 1911.

RECIPROCAL EXPERIMENTS WITH DIFFUSING SURFACES

A solid substance of which a diffusing-surface element is investigated may be considered as an optical system, inclosed between opaque walls, in which two coincident holes have been made. The following theorem now is a direct consequence of the reciprocity principle: Let H be the specific intensity of the light, incident under an angle θ, and let h be the brightness of the surface element, observed under an angle ϑ; now try the reciprocal experiment, and let h' again be the brightness observed (the phase angle between the rays of light being kept the same). Then $h/h' = \cos\theta/\cos\vartheta$. This fundamental principle is independent of any assumption about the law according to which the substance diffuses the light; the scattering properties may even be quite asymmetrical with respect to the normal, for example when the surface is covered by minute parallel furrows. It is therefore important for the photometric investigation of any diffusing surface, be it opal glass, the surface layer of a road, or the plains of the moon.

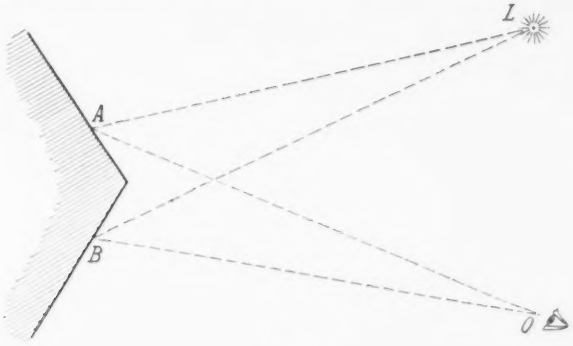

FIG. 3

A very simple way to test the reciprocity principle is indicated in Figure 3. A prism composed of any diffusing substance is illuminated by the lamp L and observed from O. It is now stated that the brightness ratio between A and B is the same for all substances and that it is equal to $\cos\theta/\cos\vartheta$. This principle could be used for photometric standardization just as well as the inverse-square law.

PHOTOMETRIC COMPARISON BETWEEN POINTS OF THE LUNAR SURFACE BY MEANS OF THE RECIPROCITY PRINCIPLE

As a direct consequence of the reciprocity principle it is possible to calculate very simply how the brightness of the individual points of the lunar surface would be altered if the positions of the sun and of the earth were interchanged. Thus, it is possible to "observe" (so to speak) the full moon from all directions on the intensity equator. The calculation to be performed is independent of the physical nature of the surface.

The full importance of the reciprocity principle for the photometry of the moon becomes clear when it is combined with the assumption of symmetry in the scattering properties around the normal. This makes possible an exact photometric comparison between two points of the lunar surface, under definite conditions of illumination and observation. When this comparison shows that the brightness ratio is not as expected, we may conclude with certainty that in the two points investigated the surface properties are not the same. If the ratio is as expected, it may be that the surface material is the same, but certainty can be obtained only in special cases when a series of photometric comparisons under varying conditions is possible. We shall now enumerate the possibilities for photometric comparison, assuming symmetry of the scattering properties around the normal and distinguishing between a simultaneous and a successive comparison (Fig. 4). The effect of the nutations will be neglected.

1. Two arbitrary points of the same latitude may be simultaneously compared for one determinate position of the sun. The comparison between the points P_1 and P_2 is possible when they are situated symmetrically with respect to the earth, E, and the sun, S. We then have:

$$\widehat{EP_1} = \widehat{SP_2}\,; \qquad \widehat{SP_1} = \widehat{EP_2}\,; \qquad \widehat{EP_1S} = \widehat{EP_2S}\,.$$

Thus,

$$\frac{h_1}{h_2} = \frac{\cos \widehat{SP_1}}{\cos \widehat{SP_2}} = \frac{\cos i_1}{\cos i_2}\,.$$

A connection between the several parallels is possible by means of the following consideration.

2. At full moon the points on any circle, concentric with the moon's circumference, may be simultaneously compared. Those points where the surface conditions are identi-

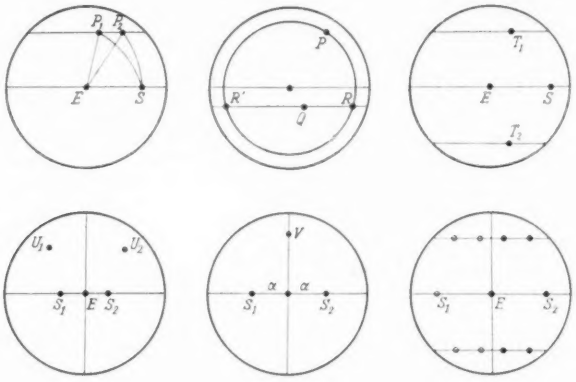

FIG. 4

cal must then be equally bright. By means of the comparisons (1) and (2), two arbitrary points P and Q of the lunar surface may be compared, either directly or in two steps, introducing a third point R or R' (either two or four points R are always available).

3. Two points, T_1, T_2, symmetrical with respect to the equator may be simultaneously compared at all phase angles.

4. Two points, U_1, U_2, symmetrical with respect to the central meridian may be successively compared at all phase angles; if one point is observed at a phase angle $+\alpha$, the other one must be measured at a phase angle $-\alpha$.

5. Points V on the central meridian must have the same brightness at phase angles $+\alpha$ and $-\alpha$. This gives a connection between the photometry of the moon at these two moments, if the scattering properties are assumed to be symmetrical around the normal. Conversely, if the photometric comparison is trustworthy, a test of the symmetry assumption is obtained.

It will be seen that on a lunar photograph any particular point may be directly compared to three other points. If a photograph at phase angle $+\alpha$ and another at phase angle $-\alpha$ are combined, groups of eight points are intercomparable.

APPLICATION OF THE RECIPROCITY PRINCIPLE TO PREVIOUS PHOTOMETRIC MEASUREMENTS

The principles enumerated give a criterion which must be applied before points of the lunar surface can be assumed as identical in surface composition. The use of this cri-

terion will be illustrated by some examples taken from previous work. For reasons given before, we shall make use of simultaneous comparisons only. A systematic survey of all published data is being attempted and will be communicated later if possible.

The points for which measurements are available have not always the exact position required for the application of the reciprocity principle. In order to estimate the influence of these small deviations, the brightness J has been reduced to the value J_0 which would have been found if the angle of incidence had been i_0 instead of i. This reduction has been made according to the illumination law derived by Öpik. From this law, we find, by taking the logarithms and by differentiating,

$$\frac{dJ}{J} = -k \tan i \, di$$

where k is a function of the phase angle, varying from 0 to 0.83 for the continents, from 0 to 0.88 for the Maria.

We shall give examples of good agreement with the reciprocity principle as well as examples of poor agreement; in this last case we must conclude that the points compared have not the same surface composition.

CONSEQUENCES OF THE RECIPROCITY PRINCIPLE FOR THE GENERAL FORM OF THE LAW OF ILLUMINATION OF THE LUNAR SURFACE

Any law giving an exact description of the photometric properties of a solid substance must conform to the reciprocity principle. The laws of Lambert and Lommel[5] satisfy this criterion.

The law of Seeliger,

$$\frac{\cos i}{\mu \cos i + \cos \epsilon},$$

conforms only if the constant μ is equal to 1. For in reciprocal experiments the brightnesses observed will be

$$h = \frac{\cos i}{\mu \cos i + \cos \epsilon} \quad \text{and} \quad h' = \frac{\cos \epsilon}{\mu \cos \epsilon + \cos i}.$$

According to the reciprocity principle, $h/\cos i = h'/\cos \epsilon$. This implies that $\mu = 1$. The law derived by Fessenkoff for the continents is an extension of Seeliger's law and thus cannot be considered as exact, though it may be sufficiently accurate in a restricted region.

Nor is Öpik's law satisfactory. From his paper the impression is obtained that the dependence on i and a has been well determined, while the functional dependence on ϵ is less well established. However, this may be easily determined from the reciprocity principle. For assuming $J = c(\cos i)^k \cdot f(\epsilon)$, we have to satisfy the condition

$$\frac{c(\cos i)^k f(\epsilon)}{\cos i} = \frac{c(\cos \epsilon)^k f(i)}{\cos \epsilon}$$

which is possible only if $f(\epsilon) = (\cos \epsilon)^{k-1}$; so that

$$J = c(\cos i)^k (\cos \epsilon)^{k-1}.$$

This law seems to represent the measurements at least as well as Öpik's formula. In

[5] *Sitzungsber. Akad. München, Math.-phys. Class.*, p. 95, 1887.

particular, the requirement is fulfilled that the brightness should increase with ϵ; for k is always < 1, and therefore $k - 1 < 0$.

TABLE 2

ÖPIK, CONTINENTS

a	Point No.	i	ϵ	J	J_0	cos i_0	$\frac{J_0}{\cos i_0}$	Agreement
84°	27	40°	61°	3.53	3.65	0.829	4.40	good
	37	64	34	2.02	2.11	.485	4.35	
121	25	55	75	2.58	2.81	.656	4.30	good
	35	80	49	0.94	1.22	.259	4.72	
84	15	22	63	2.89	2.92	.948	3.09	poor
	19	65	19	2.61	2.69	.454	5.92	
	36	66	18	2.55	2.67	0.454	5.89	

BENNETT, CRATER BOTTOMS

a	Point No.	i	ϵ	J	J_0	cos i_0	$\frac{J_0}{\cos i_0}$	Agreement
50°	26*i*	67°	17°	15	16.1	0.438	37	good
	44*i*	15	64	39	38.7	.956	41	
26	25*h*	46	21	57	54.2	.656	83	poor
	45*h*	25	49	45	46.1	0.934	49	

The correction of i to i_0 has been made according to Öpik's law for the continents.

FESSENKOFF, MARIA

a	x	y	i	ϵ	J	J_0	cos i_0	$\frac{J_0}{\cos i_0}$	
64°	+650	−046	21°	44°	5.27	5.27	0.934	5.65	Mare Foecunditatis; mean: 6.20
	+683	−195	23	45	5.77	5.74	.934	6.14	
	+742	−169	19	50	6.33	6.37	.934	6.82	
	+716	−104	20	46	5.79	5.77	.934	6.18	
64	+342	−055	45	20	4.86	4.86	.707	6.88	Mare Tranquillitatis; mean: 6.33
	+343	+031	45	20	4.28	4.28	.707	6.05	
	+314	+090	47	19	4.08	4.14	.707	5.85	
	+286	+149	48	19	4.21	4.31	.707	6.10	
	+345	+177	45	23	4.36	4.36	.707	6.17	
	+316	+235	47	23	4.83	4.91	.707	6.95	
64	+308	−139	47	20	5.71	5.80	.707	8.20	Mare Nectaris; mean: 9.35
	+334	−202	46	23	7.36	7.42	.707	10.50	

In deriving exact laws from a more extensive material, the data must be reduced in such a way that the condition of reciprocity is automatically fulfilled.

STERREWACHT "SONNENBORGH"
UTRECHT
August 1940

REYNOLDS' NUMBER FOR EXTRAGALACTIC NEBULAE

F. ZWICKY

ABSTRACT

A program is outlined to analyze the structure and the internal motions of nebulae in terms of the hydrodynamics of models composed of viscous compressible fluids. It is also indicated what types of refinements of the theory may be obtained through the application of statistical mechanics and of particle mechanics.

The first indispensable cornerstone for the hydrodynamic analysis of nebulae is laid through a discussion of the range of Reynolds' number R both for the stellar systems proper and for the systems of interstellar gases which may be present in the form of a matrix of a stellar system. It is shown that in many cases $R \gg 100$, which means that turbulent flows will play a major role in the morphology of nebulae.

A. SUCCESSIVE APPROXIMATIONS IN THE ANALYSIS OF THE STRUCTURE OF NEBULAE

Considerable observational material has been gathered in recent years on the geometrical forms of nebulae and the distribution of luminosity within these forms. Also, some advances have been made in the observational analysis of the velocity distribution in nebulae. It has been suggested in previous papers[1] that the theoretical analysis of the geometrical and dynamical structures of nebulae could in a first approximation be carried out by treating the large-scale motions in nebulae like those in viscous gravitating fluids. This hydrodynamic treatment, combined with some refinements through the use of statistical mechanics, resulted in an understanding of some of the elementary features of the structure of nebulae, such as the characteristic velocity distributions in rotating nebulae and the formation of disklike subdivisions and globular coronae.

The viewpoints sketched in the previous papers[1] suggest the study of the morphology of nebulae along the following lines of successive approximations.

1. One may study hydrodynamic models of nebulae endowed with the proper values for the viscosity η and the compressibility κ of the representative fluid, the internal cohesion of which is the result of the gravitational body forces between the various parts of a nebula. Before the analysis of the representative viscous flow can be at all successfully approached, it is imperative that some insight be gained about the nature of the flows in nebulae. For this purpose a study must be made regarding the range of values which Reynolds' number R may assume in nebulae.[2]

The stability of the laminar state in a rotating compressible fluid depends on the distribution of the moment of momentum and the density as functions of the radius. If the stratification of the fluid corresponds to an "adiabatic" equilibrium, the flow becomes turbulent for a certain value R_t of Reynolds' number R. This critical value R_t will be greater if adiabatic displacements of volumes of the liquid occur which require the transformation of kinetic energy into potential energy (stable stratifications). Conversely, R_t will be the smaller, the more potential energy is transformed into kinetic energy as a result of the convective displacements which occur in the flow (unstable

[1] F. Zwicky, *Ap. J.*, **86**, 217, 1937, and *Phys. Rev.*, **58**, 478, 1940; see also Gunnar Randers, *Ap. J.*, **92**, 235, 1940. In this article Randers has adopted our notions on the viscosity of stellar systems but fails to make the important distinction between laminar, turbulent, and Smoluchowski regions in nebulae.

[2] Since the true nature of turbulence is as yet little known, the question of whether or not the Reynolds number, which characterizes the transition from the laminar flow to the turbulent flow in stellar systems, is of the same order of magnitude as that which characterizes the corresponding transition in terrestrial flows needs to be checked by further observations.

stratifications). Unless the distribution of mass and moment of momentum is extremely stable, it can be assumed that the limiting Reynolds number R_l is of the order of 10 to 1000. A study of Reynolds' number for stellar systems is presented in section B.

2. One may apply the methods of statistical mechanics to nebulae. For stationary nebulae of zero angular momentum the virial theorem, the equipartition principle, and the Boltzmann-Gibbs principle immediately yield important results. Nebulae with angular momenta different from zero present us with new interesting problems seldom touched upon in ordinary statistical mechanics.

3. Certain results of particle mechanics must be introduced in order to arrive at an understanding of the finer details of the structure of nebulae. Particle mechanics is of prime importance for those parts of nebulae in which the mean free paths of the stars become very great. The outlying parts of nebulae—their globular coronae and stellar systems, the total dimensions of which are of the same order as, or smaller than the mean free paths—must here be specially considered. Nebulae of this type, for which I have proposed the term "Smoluchowski system," have become important because of a number of recent discoveries.

B. THE RANGE OF REYNOLDS' NUMBER FOR NEBULAE

Reynolds' number is defined as

$$R = \frac{\rho v D}{\eta}, \tag{1}$$

where ρ, η, and D are the mean density, the mean viscosity, and the total linear dimension of the system, whereas v designates the total range of the deviations in the velocity field of the flow from the velocity field in the stationary state. The importance of Reynolds' number lies in the fact that its magnitude indicates whether the flow is turbulent or laminar.

In discussing the possible values of R, we must consider the following two partial systems of nebulae: (*a*) the stellar system proper; and (*b*) the system of the interstellar gases and dust particles, which fill the interstellar spaces.

For the interstellar gas system Reynolds' number may be calculated immediately, since for a dilute gas the viscosity is

$$\eta = \alpha T^{1/2}, \tag{2}$$

where T is the absolute temperature and α is independent of the density. Introducing numerical values, we obtain, in order of magnitude,

$$\eta = 2 \times 10^{-4} \left(\frac{T}{300}\right)^{1/2} \text{gcm}^{-1}\text{sec}^{-1}, \tag{3}$$

since η for $T = 300^\circ$ is of the order of 2×10^{-4} $\text{gcm}^{-1}\text{sec}^{-1}$. The linear dimensions of nebulae are of the order of $D = 1000$ parsecs $= 3 \times 10^{21}$ cm, or greater. The density of the interstellar gases may vary considerably from case to case. To fix the ideas we shall take $\rho = 10^{-27}$ g/cm^3 as a possible value, while the over-all velocities may vary through the range $0 < v < 500$ km/sec in order of magnitude. With these values we obtain

$$0 < R < 750{,}000 \left(\frac{300}{T}\right)^{1/2}. \tag{4}$$

Since, certainly, $T < 30{,}000^\circ$, we have

$$0 < R < 75{,}000. \tag{5}$$

This means that in most cases, where the stationary state ($R = 0$) has not yet been reached, we shall have $R \gg 100$, and the motions will be turbulent. The motions in the interstellar gases would be laminar in character only if either $v < 1$km/sec or $\rho \ll 10^{-27}$ g/cm^3. This certainly is not the case for the interstellar gases in the Milky Way system, the motions in which are therefore turbulent. The shearing stresses in a turbulent flow are much greater than the shearing stresses in a laminar flow with the same velocity distribution. The transfer of momentum and of moment of momentum, as well as the speed of transformation of kinetic energy of the flow into random (heat) motion of the elementary particles, is also correspondingly larger. This may be of importance not only for the flow of the interstellar gas itself but also for the transfer of momentum and kinetic energy of the stars and clusters of stars to the interstellar gases. Although the characteristic length D for the motion of a star through the interstellar gas may become small enough to make the flow of the gas around the star laminar, this probably is not generally true. A detailed analysis will be necessary to determine the hydrodynamic characteristics of the interstellar gas flow around stars and clusters of stars.

Reynolds' number for the stellar systems proper is far more difficult to determine than that for the system of the interstellar gases. The difficulty lies in the fact that no adequate theoretical analysis of the viscosity of a stellar system is as yet available. We may, however, arrive at a quite satisfactory estimate of the range of values of R by the following indirect procedure. We first re-write Reynolds' number, using some results of the kinetic theory of gases or other tenuous systems composed of a great number of particles or stars. According to this theory, the viscosity of a gas is

$$\eta = \frac{nm\bar{w}\Lambda}{3}, \tag{6}$$

where n is the number of particles per cubic centimeter, m their mass, $\bar{w}$ their average random velocity, and Λ their mean free path. Since the density $\rho = nm$, we obtain for the "dynamic viscosity ν" the relation

$$\nu = \frac{\eta}{\rho} = \frac{\bar{w}\Lambda}{3}, \tag{7}$$

and for Reynolds' number[3]

$$R = \frac{3vD}{\bar{w}\Lambda}. \tag{8}$$

Our task, therefore, is reduced to an estimate of the two dimensionless ratios $v/\bar{w}$ and D/Λ. The first ratio presents no fundamental difficulty, since both v and $\bar{w}$ can, in principle, be observed directly. We repeat that, for nebulae of zero total angular momentum, v is the largest velocity in the velocity field of the hydrodynamic flow with which we approximate the motions in the nebula. When the angular momentum is different from zero we must compare the actual velocity distribution with the velocity distribution in the stationary state of the nebula possessing the same angular momentum. The largest difference between the velocity distribution (constant angular velocity) in the stationary state and the real velocity distribution then represents the value of v. In actual cases the average random velocity of the stars is presumably of the order of $\bar{w} = 10$ km/sec, while v may assume values starting from zero for stationary globular nebulae to about $v = 500$ km/sec, for nebulae of large angular momentum, which devi-

[3] After reading my manuscript, Prof. Theodor von Kármán kindly informed me that expression (8) for Reynolds' number was long ago derived by him in *Abhandl. aus dem aerodynamischen Institut an der techn. Hochschule Aachen*, Heft 4, 25, 1925.

ate much from a stationary state of rotation. We therefore deal with a representative range of values

$$0 < \frac{v}{\bar{w}} < 50 . \tag{9}$$

The second dimensionless ratio D/Λ raises new interesting problems, the solution of which is indispensable if the hydrodynamic analysis is to be at all successfully applied to the large-scale motions in nebulae. In the absence of an adequate theoretical determination of Λ for actual nebulae we must consult the observational data for new clues. We notice that in the case of large values of $v/\bar{w}$ the resulting flow is turbulent ($R > 100$) or laminar ($R < 100$), depending on whether D/Λ is larger or smaller than unity. In addition it would seem, a priori, obvious that the distinction between $\Lambda < D$ and $\Lambda \geqslant D$ must be an important one with regard to the structure of a nebula. Therefore, we first inquire what types of stationary structures we may expect in the two cases.

We should, perhaps, specify here somewhat more closely the meaning in the case of stars of the mean free path Λ. Stars during their travel in stellar systems may change their (vectorial) linear momentum through more or less close encounters and interactions with other stars or groups of stars or through the action of the average gravitational field due to the wholesale distribution of matter in the nebula or through the close interaction with gas and dust clouds through which the star moves. The mean free path Λ may then be defined as the distance Λ through which the three components of the linear momentum change their magnitude, on the average, by a given factor, say about $1/e$.

In the case $\Lambda \geqslant D$, the contribution of all close encounters with other gravitating bodies to the change of momentum of a star is negligible. Were it not for the total average gravitational field of the nebula, the star would change its momentum inappreciably and in the majority of cases would escape from the nebula. Obviously, the distribution of matter in such a nebula can never reach a Boltzmann stationary state, since a distribution in which the central regions of low potential energy are favored places of condensation can result only when a sufficiently great number of close encounters is available. For $\Lambda \cong D$, on the contrary, the peripheral regions of a nebula are favored because the velocity of individual stars will be the smallest in regions of high gravitational potential and the stars, on the average, will spend longer periods of time in those regions rather than in the central parts of (algebraically) low gravitational potential where the average velocities are higher. It should also be mentioned that Λ, as we have defined it, depends strongly on the velocity of each individual star, increasing with the velocity.

Smoluchowski was the first to investigate temperature jumps, slip regions, and other kinetic properties of gases in which the mean free paths become comparable with the dimensions of the containers. I therefore suggested that nebulae for which $\Lambda \geqslant D$ be called "Smoluchowski systems." In addition to systems for which $\Lambda \sim D$, the considerations sketched apply to the far outlying tenuous regions, globular coronae, extensions, etc., of all nebulae. There exist, however, significant differences between nebulae which are pure Smoluchowski systems and the outlying regions of nebulae which possess heavy central condensations. In the latter cases, the gravitational field in the outlying parts will often be very closely proportional to $1/r^2$, where r is the distance from the center, with the result that any star which is undisturbed by close encounters will individually preserve a constant angular momentum. In a pure Smoluchowski system which lacks heavy central condensation the average gravitational potential may be a complicated function of the spatial co-ordinates resulting in corresponding complications of the paths of the individual stars.

Through recent discoveries Smoluchowski systems have come into greater promi-

nence than previously. The Sculptor and Fornax systems, discovered by the staff of the Harvard College Observatory, are presumably systems of this type. They do not possess any central condensation and exhibit a smooth distribution of stars which puts them into the class of stationary Smoluchowski systems. On the other hand, the Leo system and the Sextans system recently found on Mount Palomar represent nonstationary Smoluchowski systems with no central condensations but with large and irregular fluctuations in the star density over their various parts.

In the case of pure Smoluchowski systems the hydrodynamic approach is obviously of little use, and statistical mechanical considerations based on the results of particle mechanics must be introduced to analyze the problem of the most probable distribution of mass and kinetic energy in such systems.

For $\Lambda < D$ a Boltzmann stationary distribution of mass and kinetic energy will be established the more rapidly, the smaller the ratio Λ/D. From this theoretical basis in combination with certain observations we may now arrive at an estimate of the smallest values of Λ/D which actually occur in extragalactic stellar systems. The following observations may be used:

a) As long as the observed mass distribution as a function of the distance r from the nucleus of a nebula coincides with that predicted by the Boltzmann distribution theorem, we must have $\Lambda(r)/D < 1$. For instance, as long as the radial distribution of mass is approximately that of an isothermal gravitational gas sphere, the mean free path is considerably smaller than D. For every nebula there exists a critical radius r_c, for which the transfer of kinetic energy into potential energy $m\Phi$ of a star of mass m, or vice versa, over one mean free path becomes considerable. The value of r_c is determined by the relation

$$\frac{\overline{w^2}}{2} = \Phi(r_c + \Lambda) - \Phi(r_c) . \tag{10}$$

Since the mass distribution in a nebula cannot be observed directly, it would be necessary to make some assumption about the relation between luminosity and mass before one could apply the criterion just mentioned to the determination of Λ/D. This would be an unsatisfactory procedure, and we therefore propose to make use of the following dynamic criterion exclusively.

b) As long as $\Lambda \ll D$ in a nebula of nonvanishing angular momentum, the hydrodynamic analysis, as well as Boltzmann's principle, demand that in a stationary state the angular velocity ω as a function of r be a constant. Vice versa, if $\omega(r) = \text{const.}$ between $r = 0$ and $r = r_c$, we may conclude that $\Lambda(r)/D < 1$ between the stated limits of r. From direct observations we know that in many nebulae $\omega(r) = \text{const.}$ for $r < r_c$, where the surface brightness $L(r_c)$ is about equal to $L(0)/1000$. In these cases there can hardly be any doubt that $\rho(r_c)$ is at least smaller than $\rho(0)/100$. Since Λ is inversely proportional to ρ, we conclude that at the center of a nebula of the type described, we have for stars,

$$\frac{\Lambda}{D} < 0.01 . \tag{11}$$

The combination of equations (8), (9), and (11) results in the following estimate for the range of Reynolds' number, for extragalactic stellar systems,

$$0 < R < 15{,}000 . \tag{12}$$

The lower limit is applicable for stationary, nonrotating, globular nebulae; and the upper limit is, in order of magnitude, equal to Reynolds' number, which characterizes

the turbulent motion in the center of very dense and dynamically very disturbed systems.

In another place[1] we have already shown how the threefold subdivision of nebulae into turbulent, laminar, and Smoluchowski regions leads to interesting and unexpected results regarding the geometrical structure and the velocity distribution in nebulae of nonvanishing angular momentum.

With the determination of the range of Reynolds' number, the first necessary cornerstone is laid for the analysis of the motion of nebulae in terms of models of gravitating viscous fluids. Although such an analysis may go a long way in explaining structural and dynamic features of nebulae, it must be emphasized again that a still more adequate analysis must also introduce the notion of compressibility in order to account for the variation in time and space of the density in nebulae, which is a result of the combined action of gravitational forces and inertial forces (D'Alembert forces). It is at once clear that the latter types of forces must play a considerable role, since disturbances of the internal structure of nebulae caused by encounters are to a great extent characterized by internal pulsations, in addition to differential rotation, as has been discussed previously.[1]

Finally, it should be mentioned that the consideration sketched here may also be extended in some measure to the analysis of the structure of clusters of nebulae. In analogy to the two types of nebulae characterized by $\Lambda < D$ and $\Lambda \geqslant D$, there exist also clusters of nebulae of the Boltzmann statistical type and of the Smoluchowski type. The Virgo cluster and the two Fornax groups presumably represent examples of the second type, while the Coma cluster is the most characteristic example of the first type.

My sincere thanks are due to Professor Theodor von Kármán, with whom I had many discussions on the hydrodynamics of nebulae.

California Institute of Technology
Pasadena, California

THE DISTANCES AND LUMINOSITIES OF THREE NOVAE

DEAN B. McLAUGHLIN

ABSTRACT

The residual radial velocities of interstellar calcium lines in the spectra of v356 Aquilae, Nova Monocerotis 1939, and Nova Ophiuchi 1919 are interpreted as being due to the galactic-rotation effect. On the assumption of a uniform distribution of calcium along the line of sight, the following distances, r, and absolute magnitudes, M (corrected for absorption), are derived: v356 Aql, $r = 1700$ pc, $M = -5.5$; Nova Mon 1939, $r = 1300$ pc, $M = -6.8$; Nova Oph 1919, $r = 3100$ pc, $M = -6.6$.

In 1932 H. Spencer Jones[1] pointed out that the anomalous velocity of the interstellar calcium lines in the spectrum of Nova Ophiuchi 1919 could be explained by the effect of galactic rotation. On the reasonable assumption that the distance of the nova is twice that of the effective calcium (or in other words, that the calcium is uniformly distributed along the line of sight) he calculated a distance for that nova of 3400 parsecs and an absolute magnitude of -5.5. Sanford[2] gave a rough estimate of distance for Nova Monocerotis 1939, based upon the same method, as "slightly greater than 1000 parsecs."

It is proposed to determine the distances and luminosities of these two novae, and in addition v356 Aquilae, by means of the galactic-rotation effect. In the calculation we shall adopt the following constants. For the solar motion,

$$\text{apex, } \alpha = 271^\circ\ ; \qquad \delta = +28^\circ\ , \qquad \text{velocity} = 19.6 \text{ km/sec}\ ;$$

for the galactic rotation,

$$\text{longitude of center } (l_0) = 324^\circ,$$

$$\text{Oort constant} \qquad A = 0.016 \text{ km/sec/parsec}\ ;$$

and

$$\text{absorption of light in space} = 0.5 \text{ mag/kpc}.$$

The effective distance of the absorbing calcium atoms is given by

$$\bar{r}_c = \frac{V_r}{A \sin 2(l - l_0)}\ ,$$

where V_r is the residual radial velocity of the interstellar lines, that is, the observed velocity corrected for the solar motion; and l is the galactic longitude of the star. Then for uniform distribution of calcium we have the distance of the nova

$$r_N = 2\bar{r}_c\ .$$

The results of these calculations, with all other essential data relating to the three novae, are collected in Table 2.

[1] *Observatory*, **55**, 252, 1932.

[2] *Pub. A.S.P.*, **52**, 35, 1940.

NOVA V356 AQUILAE 1936

The writer[3] found an anomalous velocity of +1 km/sec for the *Ca* II lines in this nova. This result was based on two Michigan plates which were somewhat underexposed and were taken with a wide slit. During a recent visit to the Mount Wilson Observatory the writer measured five good spectrograms of this nova. The velocities of the interstellar lines are given in Table 1.

The apparent magnitude at principal maximum was not observed. At the time that the maximum was due (as judged from abundant testimony of other novae), there was a ten-day interruption in the observations.[4] The writer[5] estimated conservatively that the maximum was 6.8 mag. The brightest *observed* maximum occurred two months later and was nearly as bright, 7.0 mag. Since then, examination of the Mount Wilson spectro-

TABLE 1

INTERSTELLAR CALCIUM VELOCITIES OF V356 AQUILAE

Mt. Wilson Plate No.	Date (1936)	Velocities in Km/Sec	
		K	H
V 1583	Sept. 22	.....	−6.
V 1588	27	−5.5	+0.5
V 1593	28	−9.	−6.
γ 21068*	Oct. 4	+6.	−2.
V 1608	5	+2.5	−7.5
Means	.....	−2.6	−4.4
Mean of H and K	.....	−3.5±1.3	

* Short camera, velocities given half-weight.

grams indicates that during the time the nova was of magnitude 8.0–8.4 (omitting observations at the second maximum of light, about October 4) the spectrum was of a type characteristic of a slow nova at 2.5 mag. below maximum. This would indicate a maximum of 5.7 mag., but conservatively we may adopt 6.4 mag. as a mean of estimates based on the character of the light-curve and of the spectrum. From the galactic-rotation effect we then derive a distance of 1700 parsecs and an absolute magnitude (corrected for absorption of light in space) of −5.5.

NOVA MONOCEROTIS 1939

Sanford[6] determined the velocity of the interstellar lines as +27 km/sec. The writer measured the same spectrogram and obtained an identical result. This nova was discovered long after maximum; its greatest brilliance undoubtedly occurred when it was above the horizon only in daylight. The writer has compared the Mount Wilson spectrograms with those of other novae. According to the normal behavior, the spectrum on December 26 and January 17 corresponds to a decline of 5.4 mag. and 5.9 mag., respectively, from maximum. The observed apparent magnitudes[7] were 9.6 and probably 10.0 or slightly fainter. Hence the calculated magnitude at maximum was 4.2. Erring on the side of conservatism, we adopt 4.5 mag. for purposes of calculation. Thus, we obtain a distance of 1300 parsecs and a corrected absolute magnitude of −6.8.

[3] *Pub. A.A.S.*, **9**, 12, 1937.

[4] *Pop. Astr.*, **45**, 219, 1937.

[5] *Ibid.*, **47**, 539, 1939.

[6] *Loc. cit.*

[7] Whipple, *Harvard Bull.*, No. 912, 1940.

NOVA OPHIUCHI 1919

The Lick[8] and Mount Wilson[9] velocities of the interstellar lines are in exact accordance—i.e., +6 km/sec. In this case the principal maximum was apparently observed as 7.4 mag. A second and equal maximum of light occurred nearly two months later, and it was at that second maximum that the spectrographic observations were obtained. The calculated distance is 3100 parsecs, and the absolute magnitude, −6.6.

DISCUSSION

The data and results are collected in Table 2. The probable errors depend chiefly upon the uncertainties of the measured velocities, but allowance has been made for the contribution by the probable errors of the constants of galactic rotation.

TABLE 2

COLLECTED DATA AND CALCULATED DISTANCES AND LUMINOSITIES OF THREE NOVAE

	v356 Aql	N Mon 1939	N Oph 1919
Right ascension (1900)	19^h12^m2	6^h38^m8	18^h09^m5
Declination (1900)	$+1°33'$	$-1°55'$	$+11°35'$
Galactic longitude (l)	$5°$	$181°$	$7°$
Galactic latitude (b)	$-6°$	$-1°$	$+12°$
Velocity of interstellar *Ca* II (km/sec)	−3.5	+27	+6
Correction for solar motion	+16.7	−17	+18.7
Residual *Ca* II velocity	+13.2	+10	+24.7
Distance of nova in parsecs	1700±200	1300±350	3100±400
Apparent magnitude at maximum	6.4*	4.5*	7.4
Absolute magnitude at maximum, uncorrected	−4.7±0.5	−6.1±0.8	−5.0±0.5
Correction for space absorption	−0.8	−0.7	−1.6
Corrected absolute magnitude at maximum	−5.5±0.5	−6.8±0.8	−6.6±0.5

* Apparent magnitudes inferred from light-curve and spectrum.

The luminosities which have been derived by this method are in good agreement with those which have been determined for typical novae by other investigators by means of several different methods. Sanford gives a smaller distance, 800 parsecs, for Nova Monocerotis, based upon the equivalent widths of interstellar H and K. It would be of considerable interest to have determinations of distances by that method for v356 Aquilae and Nova Ophiuchi 1919.

The use of different constants for the solar motion or the galactic rotation would not materially alter the results. Thus, for v356 Aquilae, using $A = 0.014$, $l_0 = 333°$ (Berman), we obtain a corrected absolute magnitude of −6.3. If, on the other hand, we use $A = 0.0185$, $l_0 = 324°$ (Joy), the absolute magnitude becomes −5.1. A roughly similar range is obtained by increasing or decreasing the residual velocity by 2 km/sec.

It should be pointed out that the estimates of apparent magnitude at maximum for v356 Aquilae and Nova Monocerotis depend upon an extensive intercomparison and correlation of the spectra of novae, studied in conjunction with the light-curves.[10]

The writer is indebted to Dr. Walter S. Adams, director of the Mount Wilson Observatory, for the privilege of using the spectrograms of novae at that observatory.

THE OBSERVATORY
UNIVERSITY OF MICHIGAN
February 6, 1941

[8] *Pub. Lick Obs.*, **14**, 16, 1920. [9] *Ap. J.*, **51**, 121, 1920. [10] Unpublished.

THE 1914 SHELL SPECTRUM OF ζ TAURI

RALPH B. BALDWIN

ABSTRACT

The spectrum of ζ Tauri is characterized by numerous sharp absorption lines produced in an outer shell of gas. In 1914 these shell lines were very strong. This paper presents an analysis of the 1914 spectrum and compares it to the weaker shell spectra of 1921 and 1926. Lines of *H*, *He* I, *C* II, *O* I, *O* III, *Mg* I, *Mg* II, *Al* I, *Si* II, *Ca* II, *Ti* II, *Cr* II, *Fe* II, *Fe* III, and *Ni* II were identified.

In 1914, ζ Tauri exhibited an extremely complex spectrum in which rotationally broadened absorption lines, sharp absorption lines, and broad double emission lines were concurrently present. This paper gives an analysis of the sharp shell spectrum and compares it with shell spectra of 1921 and 1926 when the lines were much weaker.

The shell spectrum cannot be classified on the Draper scale as it presents certain features of type B, such as *He* I lines (those arising from metastable levels), and some of type A, such as the numerous enhanced metallic lines. The *Mg* I lines give evidence of rather low excitation. It is probable that the shell is divided into layers with different excitation conditions. Both *O* I and *O* III seem to be present, although *O* II was not found. The identification of *O* III may be due merely to chance coincidences, but the *O* I lines seem to be correctly identified. The *Fe* II lines were especially numerous, and a few of the stronger *Fe* III lines were observed.

The four *He* I lines in the photographic region which arise from metastable levels are all present as sharp lines. Numerous other *He* I lines were found, but without exception they were broad and diffuse and were undoubtedly produced below the shell, in the true reversing layer. On the other hand, the *Si* II lines, λλ 3854, 3856, 3863, 4128, and 4131, and *Mg* II 4481 were rather prominent. Hence the dilution of photospheric radiation was not sufficient to depopulate greatly the lower energy-levels of these lines. The *Mg* I triplet lines, λλ 3829, 3832, and 3838, were strong and of normal relative intensities.

Struve and Wurm[1] have analyzed the spectra of several shell stars, including ζ Tauri in the 1937 shell stage, and have concluded that the strengths of the *He* I lines can be explained by assuming a dilution factor of $W = 0.01$, i.e., the radius of the shell equals five times the radius of the photosphere. The spectrum in 1937 appears to have been very similar to that of 1914 except that the *Si* II and *Mg* II lines were weaker than in 1914, and the *He* I lines stronger, as far as can be judged from reproductions of the spectra. Hence the dilution of radiation may not have been quite as large in 1914 as in 1937.

This is the second of a series of papers dealing with the shell spectra of the small and peculiar group of B stars which show composite spectra. The first paper was on γ Cassiopeiae in the 1940 shell stage and has already appeared.[2] Other stars which will be similarly treated are HR 8731, β Monocerotis, ϕ Persei, ϵ Capricorni, and Pleione.

The spectra of ζ Tauri were very kindly loaned for this study by the Observatory of the University of Michigan.

[1] *Ap. J.*, **88**, 84, 1938.

[2] *Ap. J.*, **93**, 333, 1941.

PLATE XVIII

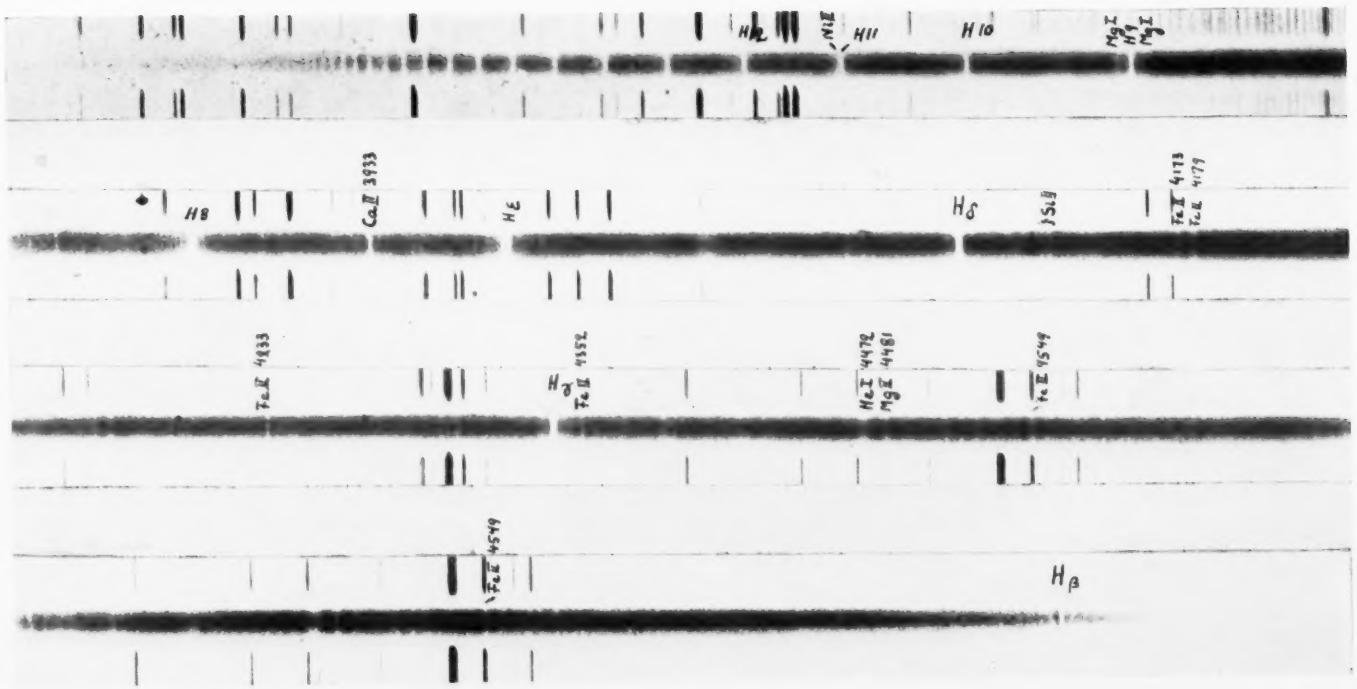

THE SPECTRUM OF ζ TAURI IN 1914

UNIV. OF MICH.

Measured (I.A.)	Int (1)	Int (2)	Int (3)	Identification		Notes
3608.56	0					
13.57	0			HeI	3.64 (3)	
37.19	0					
42.77	0					
43.58	1					
59.44	0			H33	9.42 (-)	a
				TiII	9.76(60)	c
60.38	0			H32	0.28 (-)	
61.24	1			H31	1.22 (-)	
62.25	2			TiII	2.24(40)	c
				H30	2.26 (-)	a
63.49	3			H29	3.40 (-)	
64.81	4	2		H28	4.68 (-)	
66.15	5	2		H27	6.10 (-)	
67.80	5	2		H26	7.68 (-)	Hω
69.55	6	2		H25	9.47 (-)	Hψ
70.88	0					
71.45	7	2		H24	1.48 (-)	Hχ
73.00	0					
73.89	7	2		H23	3.76 (-)	Hϕ
75.24	1	0				
76.35	8	2		H22	6.36 (-)	Hυ
77.92	1			CrII	7.70 (2)	b
					7.86(4r)	a
					7.93 (2)	c
78.82	0					
79.46	9	2		H21	9.36 (-)	Hτ
80.70	0					
81.60	2	1				
82.82	10	3		H20	2.81 (-)	Hσ
85.48	1			TiII	5.20(250)	
86.81	10	3		H19	6.83 (-)	Hρ
88.51	2			γ Cassiopeiae		
89.47	1					
91.53	11	4		H18	1.56 (-)	Hπ
94.55	1	1				
95.94	0			OIII	5.37 (4)	
97.07	12	5		H17	7.15 (-)	Hο
98.44	0			CrII	8.02 (3)	b
				OIII	8.70 (5)	b
99.20	0					
3700.13	2	2				
01.56	0					
02.31	0			OIII	2.75 (5)	
03.03	3			?		a
				OIII	3.37 (5)	c
03.92	13	5		H16	3.86 (-)	Hξ
06.34	1			TiII	6.22(20)	
07.77	0			OIII	7.24 (6)	
10.69	1					
11.84	14	6		H15	1.97 (-)	Hν,a
				FeII	1.97 (1)	c
13.38	1			CrII	2.94 (6)	
15.55	2			CrII	3.98 (2)	c
				OIII	5.08 (6)	b
				CrII	5.18 (2)	b
18.65	1					
21.47	1			TiII	1.64(15)	
22.01	15	8	2	H14	1.94 (-)	Hμ
25.72	2	2		?		a
				FeII	5.30 (3)	b
					5.90(?2)	c
27.45	0			FeII	7.03 (p)	a
				CrII	7.37 (1)	c
29.07	0					
30.29	1					
31.44	1					
34.40	16	9	3	H13	4.37 (-)	Hλ
36.17	0			CrII	5.59 (p)	
38.00	0			CrII	8.36 (2)	
41.73	0			TiII	1.65(50)	

Measured (I.A.)	Int (1)	Int (2)	Int (3)	Identification		Notes
3743.80	0					
45.88	0			?		a
				FeII	6.56 (p)	c
47.37	1	1		FeII	7.50(?2)	
48.81	3	0	2	TiII	8.00(10)	c
				FeII	8.49 (8)	a
				CrII	8.68 (1)	c
50.13	17	10	4	H12	0.15 (1)	HK
51.76	0					
52.72	0					
53.32	1					
54.41	0			OIII	4.67 (7)	b
				FeII	5.56 (4)	b
				CrII	5.58 (2)	c
57.41	0			OIII	7.21 (5)	b
				TiII	7.69(30)	a
59.52	3	0		TiII	9.30(200)	a
				FeII	9.46 (6)	b
				OIII	9.87 (9)	c
61.60	3	0		TiII	1.32(200)	a
					1.88(15)	d
62.80	1			FeII	2.89 (5)	
64.24	2			?		a
				FeII	4.12 (1)	b
65.83	0					
66.80	0			CrII	6.67 (p)	
67.51	0			CrII	7.23 ( )	
69.49	6	2		NiII	9.46 (5)	
70.63	18	12	5	H11	0.63 (2)	Hι
72.30	0					
74.10	1			?		a
				OIII	4.00 (6)	b
				TiII	4.65 (2)	c
78.32	0					
80.12	0					
83.47	2	1		FeII	3.35 (4)	
92.40	1			γ Cassiopeiae		
95.40	2	1				
97.82	19	13	6	H10	7.90 (3)	Hθ
3801.49	1					
03.50	1			?		a
				FeII	3.04 (0)	c
08.77	0					
10.09	1					
11.58	1					
13.05	0			TiII	3.40 (2)	e
14.14	2	1		FeII	4.12 (4)	a
				TiII	4.60 (4)	c
15.73	0					
16.74	1					
22.58	1			FeII	1.97 (p)	c
					2.74 (3)	a
23.76	0					
25.02	1			FeII	4.91 (4)	
26.20	0					
27.44	0			FeII	7.08 (4)	a
					7.69 (p)	c
28.40	1			?		a
				FeII	8.86(?2)	b
29.50	3	0	0	MgI	9.37(40)	
30.57	1			γ Cassiopeiae		
31.74	2					
32.49	4	0	1	MgI	2.31(80)	
35.32	20	15	8	H9	5.39 (4)	Hη
37.27	0					
38.39	4	1	1	MgI	8.30(100)	
39.83	2					
41.75	1			?		a
				FeII	1.35(-1)	c
43.77	0					
45.48	0			γ Cassiopeiae		b
				FeII	6.29 (1)	b

Measured (I.A)	Int (1)	Int (2)	Int (3)	Identification		Notes
3847.56	1					
49.65	4	2	2	NiII	9.54 (1)	a
				?		b
52.07	0					
53.70	1	0		SiII	3.67 (3)	
55.26	0			FeII	5.13 (0)	
56.15	5	3	2	SiII	6.03 (8)	
58.16	0					
59.70	2			γ Cassiopeiae		
60.84	0			FeII	0.11 (p)	c
					0.92 (3)	a
62.52	4	2	1	SiII	2.60 (6)	
64.08	0			FeII	3.41 (1)	c
					3.95 (1)	a
65.70	1			CrII	5.65 (1)	
72.90	0					
74.86	0					
76.15	0			CII	6.19 (4)	a
					6.41 (2)	c
84.74	1					
88.85	23	17	12	HeI	8.65(10)	b
				H8	9.05 (5)	Hζ,a
91.82	0					
93.91	1					
95.31	1					
96.87	0					
98.43	1					
3900.30	1			TiII	0.54(70)	
02.69	1			γ Cassiopeiae?		
04.04	0			γ Cassiopeiae		
05.38	2			?		a
				CrII	5.66 (2)	b
06.35	4	3	1	?		b?
				FeII	6.04 (5)	a
13.53	2			TiII	3.47(60)	
14.25	0			FeII	4.48 (2)	
15.29	1					
20.88	0			CII	0.68 (8)	
23.66	0					
24.90	1					
27.48	0			γ Cassiopeiae		
30.55	0			FeII	0.31 (8)	
31.57	0			γ Cassiopeiae?		
32.70	1			γ Cassiopeiae		
33.76	7	4	2	CaII	3.68(40OR)	K
34.99	0			Interstellar?		K
36.14	3	0	0	FeII	5.94 (6)	
37.28	0					
38.58	4	1	2	FeII	8.29 (2)	b
					8.97 (4)	a
				?		b
40.59	0					
42.56	1					
44.25	0			AlI	4.02(10R)	
45.01	0			CrII	5.11 (1)	c
				FeII	5.23 (1)	a
47.50	4	2	2	OI	7.33(10)	a
					7.51 (7)	b
					7.61 (4)	c
48.99	1					
52.69	1					
55.10	1			γ Cassiopeiae?		
56.35	0					
58.20	1					
59.30	1					
61.48	2	0	1	FeII	0.90 (3)	a
				AlI	1.54(10R)	c
				OIII	1.59 (8)	b
62.80	0					
64.64	3	2	2	FeII	4.12 (1)	d
				HeI	4.73 (4)	a

Measured (I.A.)	Int (1)	Int (2)	Int (3)	Identification		Notes
3967.44	2					
68.62	6	1	1	CaII	8.49(350R)	H
69.99	21	16	10	H7	0.08 (6)	Hε
74.07	1			FeII	4.16 (3)	b
				? (broad)		a
75.15	0			FeII	5.03 (2)	
76.54	0					
79.39	0			CrII	9.51 (2)	b
				? (broad)		b
81.06	0			?		b
				FeII	1.62(-1)	b
88.93	0					
92.03	1					
93.83	0					
4002.34	2			FeII	2.07 (2)	b
					2.55 (3)	a
12.30	2			TiII	2.39 (4)	b
				FeII	2.47 (1)	b
13.65	0					
15.45	1			NiII	5.48 (1)	
18.98	1			FeII	8.47 (p)	d
20.66	0					
23.01	1					
27.09	1					
28.15	2			TiII	8.35 (7)	
32.95	2			FeII	2.95 (3)	
35.99	2					
37.93	1			?		a
				CrII	8.04 (2)	b
40.70	1					
42.23	1					
44.30	1					
46.64	0					
48.89	1			FeII	8.83 (3)	
53.03	0					
54.91	1			γ Cassiopeiae?		
57.32	1			FeII	7.46 (2)	
63.44	0					
67.12	4	2	0	NiII	7.04 (6)	
70.11	1			FeII	9.88 (1)	a
					0.05 (0)	b
71.69	2			γ Cassiopeiae		
73.59	1					
76.92	1			FeII	7.16(?3)	
78.57	1			γ Cassiopeiae		
80.59	0					
82.40	2			?		a
				FeII	2.59 (1)	c
86.28	0			γ Cassiopeiae?		b
				CrII	6.13 (0)	b
88.67	1			?		a
				FeII	8.76 (p)	b
92.14	1			γ Cassiopeiae		
94.10	0					
95.93	0					
99.11	2					
4101.62	23	17	13	H6	1.75 (7)	Hδ
05.49	1					
06.71	0					
09.69	0					
11.53	2			CrII	1.00 (2)	b
				FeII	1.90 (1)	a
14.69	1					
16.53	1					
18.45	1					
20.23	1					
22.88	1			FeII	2.64 (4)	
24.73	1			FeII	4.79 (1)	
26.67	1					
28.43	5	1	0	SiII	8.05 (8)	b
				FeII	8.74 (3)	b

Measured (I.A.)	Int (1)	Int (2)	Int (3)	Identification		Notes
4130.10	0					
30.95	5	2	0	SiII	0.88(10)	
33.21	1					
35.34	0					
36.66	1					
38.71	0			FeII	8.36(ON)	
40.27	1					
41.60	2			γ Cassiopeiae		
45.76	1			CrII	5.81 (3)	
47.23	1					
48.54	0					
52.19	1					
56.64	1					
57.95	0					
59.13	0					
63.54	0			TiII	3.66(40)	
66.68	1			?		a
				FeII	6.70(tr)	b
69.00	1			FeII	8.66 (p)	
71.68	0			TiII	1.91(30)	
73.40	4	2	0	FeII	3.45 (8)	
76.35	0					
78.10	3	1		?		a
				FeII	7.70 (1)	b
79.01	5	2	0	FeII	8.86 (8)	a
				CrII	9.32 (2)	c
84.17	1					
86.45	0			γ Cassiopeiae		
88.29	1					
91.44	0					
94.62	0					
96.24	1					
99.40	1					
4205.77	0					
08.50	0					
11.74	0					
19.16	1					
30.36	1					
31.89	1					
33.25	7	3	0	FeII	3.17(11)	
36.48	3	1				
39.34	1					
42.42	1			CrII	2.38 (5)	
49.03	1			γ Cassiopeiae		
53.87	0					
58.24	0			FeII	8.16 (3)	
60.83	1					
62.40	1			CrII	1.94 (1)	
64.65	1					
67.40	0			CII	7.02 (8)	b
					7.27(10)	a
73.63	0			FeII	3.32 (3)	
76.06	1			?		a
				CrII	5.56 (0)	c
78.54	1			FeII	8.13 (1)	
80.02	1					
82.39	2	1				
84.14	1			CrII	4.23 (2)	
86.33	1			?		b
				FeII	6.31 (1)	a
88.22	0			TiII	7.89 (2)	e
90.91	0			TiII	0.23(50)	
92.61	0					
94.30	0			TiII	4.05(40)	b
					4.15(40)	b
95.93	1					
96.71	1			FeII	6.57 (6)	
99.85	2			TiII	0.06(60)	
4301.33	0			TiII	1.93(15)	
03.25	4	2	2	FeII	3.17 (8)	
05.49	1					
07.68	3	1	1	TiII	7.91(40)	
08.99	0					
10.21	0					
11.94	1			TiII	2.88(35)	b
				?		b
14.61	3			FeII	4.29 (4)	a
					4.32 (1)	c
				TiII	4.98(40)	b
17.57	1					
20.51	1			?		a
				TiII	0.96 (1)	d
23.94	1					
26.03	2					
27.55	0					
29.39	2					
31.13	1			FeII	1.53 (3)	
33.44	1					
36.81	4			TiII	7.93(50)	f
40.27	22	18	14	H5	0.48 (8)	Hγ
44.17	1			TiII	4.29 (2)	e,g
46.70	1					
48.51	1					
49.98	0					
51.80	5	1	1	FeII	1.76 (9)	
54.68	1			FeII	4.36 (2)	
57.60	2	0	0	FeII	7.57 (4)	
58.91	0					
60.31	0					
63.77	1					
68.77	2	1	0	OI	8.30(10)	a
				FeII	9.40 (2)	b
72.93	1			FeIII	2.41(20)	
74.66	0					
76.90	0					
79.82	0			OIII	9.55(3n)	
85.37	4	1	0	FeII	4.32 (1)	c
					5.38 (7)	a
87.27	0					
95.52	2			TiII	5.04(60)	b
				FeIII	5.78 (6)	b
98.14	0			γ Cassiopeiae		
99.82	1			TiII	9.78(35)	
4401.68	0			γ Cassiopeiae		
03.71	1					
11.58	1			TiII	1.08(15)	
14.20	0			FeII	3.60 (1)	
17.00	3	0	0	FeII	6.82 (7)	a
				TiII	7.72(40)	b
20.10	1			FeIII	9.59(10)	
22.50	1					
25.28	0					
27.25	2			γ Cassiopeiae		
30.71	0			FeIII	0.97 (7)	
34.68	1			γ Cassiopeiae		
43.46	1			TiII	3.81(50)	
48.22	0					
50.29	0			TiII	0.49(10)	
51.74	3			FeII	1.54 (4)	
54.56	0			FeII	5.26 (2)	
56.17	1			γ Cassiopeiae		a
				TiII	6.64(tr)	e
61.98	1			?		a
				FeII	1.43(-1)	d
68.61	2			TiII	8.50(50)	
71.83	4			FeII	2.92 (2)	d,h
78.43	1					
81.10	4			MgII	1.14(100)	
					1.34	
84.67	1					
88.82	2	0	0	TiII	8.33(15)	d
				FeII	9.18 (4)	a

Measured (I.A.)	Int (1)	Int (2)	Int (3)	Identification		Notes
4491.46	1	0	0	FeII	1.40 (5)	
92.60	0					
95.67	1					
97.58	0					
99.50	0			FeII	9.71 (0)	
4501.29	0			TiII	1.28(40)	
03.13	1			γ Cassiopeiae		
08.49	4	0	0	FeII	8.28 (8)	
11.91	1			γ Cassiopeiae		
15.37	4	0	0	FeII	5.34 (7)	
19.99	2	0	0	FeII	0.22 (7)	
22.37	3	0	0	FeII	2.63 (9)	
24.85	1					
27.32	1					
31.96	0					
34.45	2			TiII	3.97(30)	b
				FeII	4.17 (2)	b
38.78	1					
41.51	1			FeII	1.52 (4)	
44.93	0					
49.33	6	2	1	FeII	9.21 (4)	b
					9.47(10)	a
				TiII	9.62(60)	b
					9.64(60)	b
52.54	0					
55.59	3	0	0	CrII	4.99 (3)	b
				FeII	5.89 (8)	a
58.91	1			CrII	8.65(20)	
63.66	0			TiII	3.77(30)	
66.42	0			CrII	5.78 (2)	
69.32	0					
72.01	1			TiII	1.98(50)	
76.04	2	0	0	FeII	6.33 (4)	
79.98	0			FeII	0.06 (3)	
83.75	5	1	1	FeII	2.84 (3)	c
					3.83(11)	a
86.53	0					
88.40	1			CrII	8.21(15)	
92.88	1			?		a
				CrII	2.06 (2)	c
96.24	1			?		a
				FeII	5.69(-2)	c
98.86	0			FeII	8.53 (1)	
4600.94	1			?		a
				FeII	1.38 (p)	c
05.88	0					
07.51	1					
10.65	0					
13.61	0					
15.56	0					
18.73	0			CrII	8.79(10)	
20.04	0			FeII	0.51 (3)	
24.23	1			CrII	4.57 (2)	
25.64	0			FeII	5.91 (1)	
29.40	4	0	0	FeII	9.34 (7)	
34.98	2			CrII	4.08(10)	b
				FeII	5.35 (5)	a
38.70	0					
42.05	0					
45.03	1					
50.09	0					
53.98	0					
56.20	0			FeII	6.97 (1)	
57.81	0					
63.15	0			FeII	3.70 (0)	
66.95	0			FeII	6.75 (2)	
73.94	1					
77.96	0					
80.92	0					
84.08	0					
91.50	0					
95.84	0					

Measured (I.A.)	Int (1)	Int (2)	Int (3)	Identification		Notes
4697.33	1			FeII	9.32(tr)	
4700.31	1					
03.61	0					
08.27	0			TiII	8.67(tr)	c
				FeII	8.97(73)	a
09.83	0					
11.55	1					
17.47	1					
26.98	2					
31.52	1			FeII	1.44 (3)	
42.20	0					
45.69	0					
48.48	0					
52.65	0					
56.42	0					
58.62	1					
65.22	0					
68.94	1					
73.13	2					
77.48	1					
82.29	1					
85.82	1					
88.07	1					
91.75	1					
94.95	0					
97.39	0					
4802.64	0					
04.99	2			TiII	5.10 (2)	
12.94	1			?		a
				CrII	2.36 (2)	b
18.13	1			?		a
				FeII	8.23 (p)	b
20.46	0					
24.54	1			CrII	4.14(10)	
31.85	0					
34.91	1					
40.10	2			?		a
				FeII	9.98 (p)	c
44.45	0					
48.20	1			CrII	8.25 (8)	
61.28	15	12	8	Hδ	1.34 (9)	Hδ
64.98	1			CrII	4.32 (3)	i
75.58	1					
86.04	0					
89.29	1					
92.81	0					
96.20	2	1	0			
99.55	1					
4903.28	0					
07.03	1					
12.94	1			FeII	3.37 (1)	
23.96	6	4	4	FeII	3.93(12)	
30.34	1					
34.76	1					
39.06	1					
42.31	0					
44.50	1					
47.16	1					
54.45	1			FeII	3.98 (C)	
57.94	1					
64.21	1					
68.84	0			OI	7.40 (4)	b
					7.86 (6)	a
					8.76 (5)	a
78.05	1					
81.73	1					
90.55	1			FeII	0.59 (1)	
96.44	2					
99.38	1					
5005.95	1					
13.53	4	3	1	HeI	5.68 (6)	j
18.05	4	4	3	FeII	8.43(12)	

Notes to Table I

(1) October 2-11, 1914
(2) January 8, 1921
(3) February 15-19, 1926
a Principal contributor
b Strong component
c Weak component
d Trace
e Identification inadequate or doubtful
f Blended with violet absorption wing of broad Hγ
g Blended with red absorption wing of broad Hγ
h Major contributor is broad HeI 4472
i Confused with Hβ structure
j Confused with FeII 5018 structure

DEARBORN UNIVERSITY
NORTHWESTERN UNIVERSITY
January 31, 1941

INTERCOMPARISON OF VARIOUS SPECTRAL CLASSIFICATIONS OF FAINT STARS

ALEXANDER N. VYSSOTSKY

ABSTRACT

The comparisons involve 8500 stars from the seventh to the thirteenth magnitude; of these, 5500 have been classified at the McCormick Observatory especially for this purpose. The results are summarized in Tables 1 and 2 and in Figures 1, 2, and 3. In general it may be said that all systems of classification agree at Ao, with the exception of faint Potsdam stars; in other classes corrections must be applied to convert the spectral classification from one system to another (Table 2). As far as can be determined, there is no magnitude error in the *Henry Draper Extension* (Nos. 1, 2, and 5), the Bergedorf, Mount Wilson, and McCormick classifications. Potsdam is also free from magnitude error for classes later than F8. A marked difference is found between the systems of the *Henry Draper Catalogue* and the *Henry Draper Extension* (Nos. 1, 2, and 5) in the later spectral classes.

It is shown that corrections derived from a single regression-curve will always overcorrect, unless the accidental errors in the standard system are unusually small.

In order to furnish spectra for the proper-motion programs in progress at the Leander McCormick Observatory, over 300 plates have thus far been obtained with the 10-inch Cooke prismatic camera. As each spectral plate covers 80 square degrees, it is usually possible to obtain more than one proper-motion region on a plate; in addition, about 70 of the Kapteyn Selected Areas are wholly or partly included. In a few cases when spectra for the Selected Areas had already been published in the *Bergedorfer Spektral-Durchmusterung*, some of their stars were classified on our plates in order to determine the limiting magnitude of our plates taken under average conditions. This turned out to be about $12^{m}.0$ photographic. Incidentally, it was found that the McCormick classification differed appreciably from that of Bergedorf. Similarly, from a plate which overlapped the *Henry Draper Extension* (HDE) No. 5, it appeared that a systematic difference also existed between the McCormick and the HDE classifications but in the opposite sense to that found in connection with Bergedorf.

Thus, it appeared desirable to investigate the matter in detail, adequate material being already in hand for a representative comparison with the *Spektral-Durchmusterung* of Bergedorf (zones $+75°$, $+60°$, and $+45°$) and of Potsdam (zone $-15°$). But since the plan for the spectroscopic program had purposely excluded the large areas covered by the HDE Nos. 1, 2, and 5, there was not enough material for a satisfactory comparison with the HDE. Consequently, special plates were taken for this purpose, and still others were taken specially for a comparison with the *Henry Draper Catalogue* (HDC) itself. In this connection, as will be described later, various devices were used to insure that the appearance of brighter stars should be similar to that of eleventh-magnitude stars on our regular program plates. Throughout the comparisons care was taken that the McCormick spectra should be representative, plates of average quality being used and stars situated in all parts of the plates being classified. Furthermore, the McCormick classifications were made entirely without previous reference to any published spectra.

In order that the study might be more nearly complete, comparisons of the Bergedorf system with HDE and with the Mount Wilson spectra in the Selected Areas are included; also, a rediscussion of the comparison of the Potsdam system with the Harvard classification published by Mrs. Payne-Gaposchkin has been made possible by the use of manuscript material which she most kindly put at the author's disposal.

Finally, the material of the McCormick-Bergedorf and the HDE-Bergedorf comparisons has been examined to find whether there are any systematic differences in the

classifications of McCormick or HDE corresponding to the "d" and "g" characterizations of the Bergedorf spectra.

OBSERVATIONAL TECHNIQUE

A 7° objective prism mounted in front of the 10-inch Cooke triplet ($F = 1:4.5$) gives a dispersion of 2.7 mm between $H\beta$ and $H\epsilon$. Since the color-curve of the triplet is rather steep, it is necessary to obtain two photographs of each region, one focused on $H\gamma$ and the G band and the other focused on the H and K lines. The spectra are widened by means of a micrometer screw which shifts the plateholder in right ascension; a shift of 0.01 mm every 12 minutes during a total exposure of 120 minutes gives satisfactory plates focused on the G band, whereas the plates focused on the H and K lines are obtained by a shift of 0.01 mm every 18 minutes during a total exposure of 108 minutes. The number of shifts varies somewhat, fewer shifts at longer intervals being used for declinations south of the equator and more shifts north of +60°.[1] The telescope is guided throughout the exposure by means of a 5-inch guiding telescope.

Cramer Hi-Speed Special plates were used, developed with Eastman DK 20 (previously with the fine-grain developer recommended by W. W. Morgan[2]). The particular advantage of the Hi-Speed Special emulsion for this work is its relatively small reciprocity-law failure;[3] at the same time the grain is sufficiently fine for classifying spectra of small dispersion. Each plate covers 9°.7 in right ascension and 11°.9 in declination, the region of satisfactory definition being 8° by 10°. The scale of the plates is 1 mm = 178″.

CRITERIA FOR SPECTRAL CLASSIFICATION

The criteria adopted were to some extent imposed by the color-curve of the instrument and its resolving-power. They were arrived at by comparing spectra in the region around $\alpha = 17^h0$, $\delta = 0°$, with the HDC classification. In this part of the sky the limits of the HDC are fainter than the average, since Miss Cannon here used plates of shorter dispersion. In fact, the dispersion on these "B" plates is not very different from that on the "MF" plates used for the HDE classification, but the spectra are widened much more on the B plates.

B0 Hydrogen lines very narrow, invisible on underexposed spectra; the spectrum to the violet of λ 3900 is strong*
B2 *H* lines narrow, barely visible on underexposed spectra; violet end strong
B5 *H* lines well pronounced but narrow; violet end strong
B8 *H* lines strong but narrow
A0 *H* lines strong and broad; K line either absent or just suspected
A2 *H* lines the same as in A0; K line well visible
A5 K line strong but weaker than (H + $H\epsilon$)
F0 K = (H + $H\epsilon$); no G band; *H* lines rather strong
F2 *a*) K ≥ (H + $H\epsilon$); G band faint but visible; *H* lines strong
b) K ≥ (H + $H\epsilon$); G band invisible; *H* lines weak
F5 G band well pronounced but weaker than $H\gamma$
F8 G band = $H\gamma$
G0 G band stronger than $H\gamma$; in very faint spectra the G band is just suspected and only the H and K lines are prominent

* This is true even in the case of B stars which are known to be heavily reddened, such as HD 168607 and 168625, whose color excess is greater than 1 mag., according to Popper and Seyfert (*Pub. A.S.P.*, **52**, 401, 1940). In other words, in spite of space reddening, the ratio of the intensity of the continuous spectrum at λ 3800 to that at λ 4000 is markedly greater than for A and F stars, which are affected to the violet of λ 3900 by the confluence of the wings of the *H* lines. Furthermore, owing to the low contrast of the developed plates, even the reddening along the whole course of the spectrum is not very conspicuous.

[1] This is necessitated by the effects of differential refraction on the guiding, since the plate covers some 10° in declination and the guiding star is 4½° north of the center of the region.

[2] *Ap. J.*, **83**, 254, 1936.

[3] G. Z. Dimitroff, *Harvard Circ.*, No. 430, p. 13, 1938.

G5 G band strong; $H\gamma$ very faint or absent; intensity of the spectrum on both sides of the G band is about the same
K0 Owing to unresolved absorption lines, the portion of the spectrum to the violet of the G band is noticeably less intense than that to the red of it (Lindblad's "break at the G band")
K2 The break at the G band is pronounced; λ 4227 well visible; frequently numerous lines are visible between $H\gamma$ and $H\delta$
K5 The break at the G band is very pronounced; λ 4227 is prominent
M0 The head of the first *TiO* band at λ 4950 is just visible
M2 The first band is strong; the second band head at λ 4760 is weak but certain
M5 The band head at λ 4585 is well visible
M8 All three bands are intense, making the spectrum appear of fairly uniform intensity all the way from $H\beta$ to $H\delta$; for very faint stars only the heads of the bands appear

It is seen that the McCormick criteria are descriptive and thus differ essentially from the criteria of numerical line ratios used in the Potsdam system and to a lesser extent in the Bergedorf system. The criteria for classes A2 and later combine those of the HDC and of Stockholm; for classes earlier than A2 our criteria are essentially those established at Upsala[4] and result in a luminosity classification rather than a temperature classification.

Of necessity, since more than one criterion is used, there are spectra in which the criteria are inconsistent. Thus, a spectrum in which the break at the G band is just noticeable but the *Ca* I line λ 4227 is prominent, is classified as K0 in spite of the *Ca* I line, since that line is more sensitive to absolute magnitude than is the break. Such peculiarities are duly noted in the proper-motion catalogue.

METHOD OF COMPARISON

In order to obtain the systematic differences between any two given sets of spectra, the observed differences expressed in tenths of a spectral class were grouped to form two regression-curves in the usual manner. The necessity of using both regression-curves arises from three reasons: (1) the fact that the accidental dispersion in all of the sets considered here is of about the same order, the average difference being about a quarter of a spectral class; (2) the uneven distribution of stellar frequencies along the spectral sequence and its rather abrupt limits at both ends; and (3) variations in the number of discrete steps used, from one system to another. Thus, the problem of intercomparison of spectral systems is essentially different from an intercomparison of systems of stellar magnitudes, in which (1) the standard system of magnitudes is usually of higher accuracy than the one to be compared with it; (2) the groups at each end, which are affected by selection, may be discarded, since the scale difference is usually linear; and (3) it is possible to formulate a fairly precise definition of the quantity measured.[5]

The true relation between any two systems may be found by drawing a curve midway between the two regression-curves, provided the accidental errors are the same in the two systems. Although this is not exactly the case, still, as is shown later, the accidental errors are probably never sufficiently different to make the midway curve differ very much from the true relation. In many cases it is quite obvious that the two regression-curves lead to contradictory results when used separately, especially where the natural frequency of the stars is at a minimum between two maxima (class F) and near the beginning and end of the sequence. Thus, from the regression of HDC on McCormick we have

$$(F2.0)_{McC} = (F3.5)_{HDC},$$

[4] *Trans. I.A.U.*, **5**, 181, 1935.

[5] Cf. "The System of the HDCDM Magnitudes," *Ap. J.*, **83**, 216, 1936.

but the regression of McCormick on HDC gives

$$(F2.0)_{HDC} = (F3.0)_{McC} .$$

Obviously, the true systematic difference between HDC and McCormick at this point is much less than a tenth of a spectral class.

Stars which have not been classified to the nearest subclass and certain stars whose classification is qualified with a colon have been omitted from the comparison. Again, the cases in which the difference in classification is more than one and one-half spectral classes have been regarded as mistakes of some sort and have been excluded. These cases are listed individually in the Appendix.

The results of the comparisons are summarized in Figures 1 and 2. The data used for the various curves are described in the succeeding sections; here it will suffice to describe their general form. The dotted curve is the regression of the system represented by the abscissae on the system represented by the ordinates; the dashed curve is the other regression. A 45°-line has also been indicated in every case. Points involving less than three stars have been omitted; points of low weight (from three to five stars) are connected to their neighbors by dots or dashes spaced at greater distances than ordinary. In general, for the regressions on McCormick and Harvard the means are derived for each separate subclass, whereas, for the regressions on Bergedorf and Potsdam the subclasses are grouped to center approximately around 0, 2, 5, and 8; thus: 0; 1, 2, 3; 4, 5, 6; 7, 8, 9. Exceptions occur when the material is meager. The exact position of each group mean is plotted; thus, if G1 and G2 are infrequent compared with G3, the mean may be at G2.6 instead of at G2.0. In deriving numerical means, Ma, Mb, and Mc are taken as equal to M1, M5, and M8, respectively. Of necessity, the dotted curve is always below the dashed curve at the lower end of the correlation and above it at the upper end. Frequently, also, the curves cross one another three times instead of once, because of the minimum in the frequency distribution at class F. In general, the smaller the accidental errors, the closer together the two regression-curves will lie.

In Figure 2 are given the corresponding midway curves which show very nearly the true relationships between the systems. A 45°-line is also given in every case. The curve marked "Predicted" is an indirect comparison found by eliminating McCormick between the last curve of the first row and the first curve of the second row. The fact that the predicted curve agrees so closely with the direct comparison to its right is an indication of the reliability of the procedure.

ACCIDENTAL AND SAMPLING ERRORS

For each subclass of each regression the mean accidental difference was computed after the systematic correction for that particular subclass had been applied. The factor $\sqrt{n/(n-1)}$ was then applied to correct for the limited size of the group, n being the number of stars in the subclass. The resulting values for the regressions represented by dotted lines in Figure 1 are tabulated in Table 1. No item is given when the number of stars in the subgroup is 5 or less or when two or more subgroups are combined because of meager data. The quantities which appear in italics are based on 25 or more stars; thus, the probable error of any of these is not more than 10 per cent of its value, whereas the probable error of any of the items in ordinary type is between 10 and 20 per cent of its value. The weighted mean for the entire regression is tabulated opposite the "dotted regression." The following line gives the corresponding quantity, similarly computed from the dashed regression-curve. Since in nearly every case in Figure 1 the angle which the dashed curve makes with the x axis is greater than the angle which the dotted curve makes with the y-axis, the corresponding accidental differences computed from the dashed curve are usually larger than the others. The weighted mean from both re-

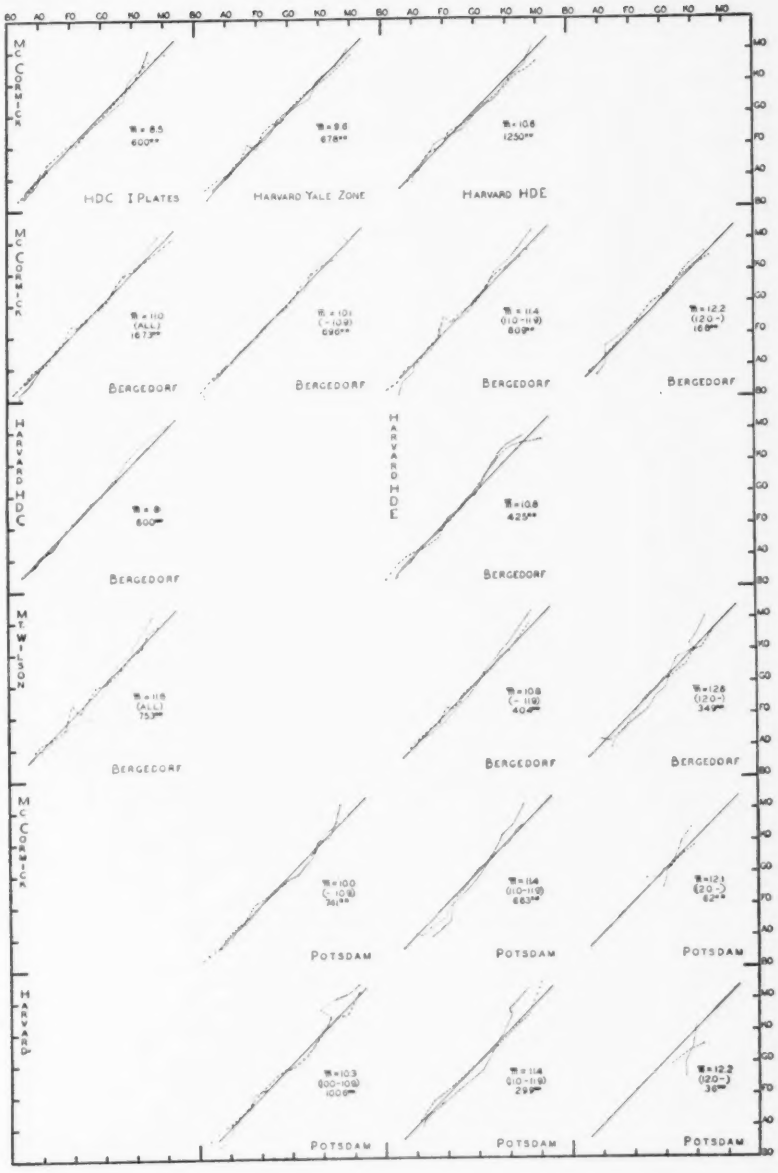
B0 A0 F0 G0 K0 M0
MCCORMICK
HDC I PLATES
HARVARD YALE ZONE
HARVARD HDE
BERGEDORF
HARVARD HDC
MT WILSON
POTSDAM
HARVARD

FIG. 1

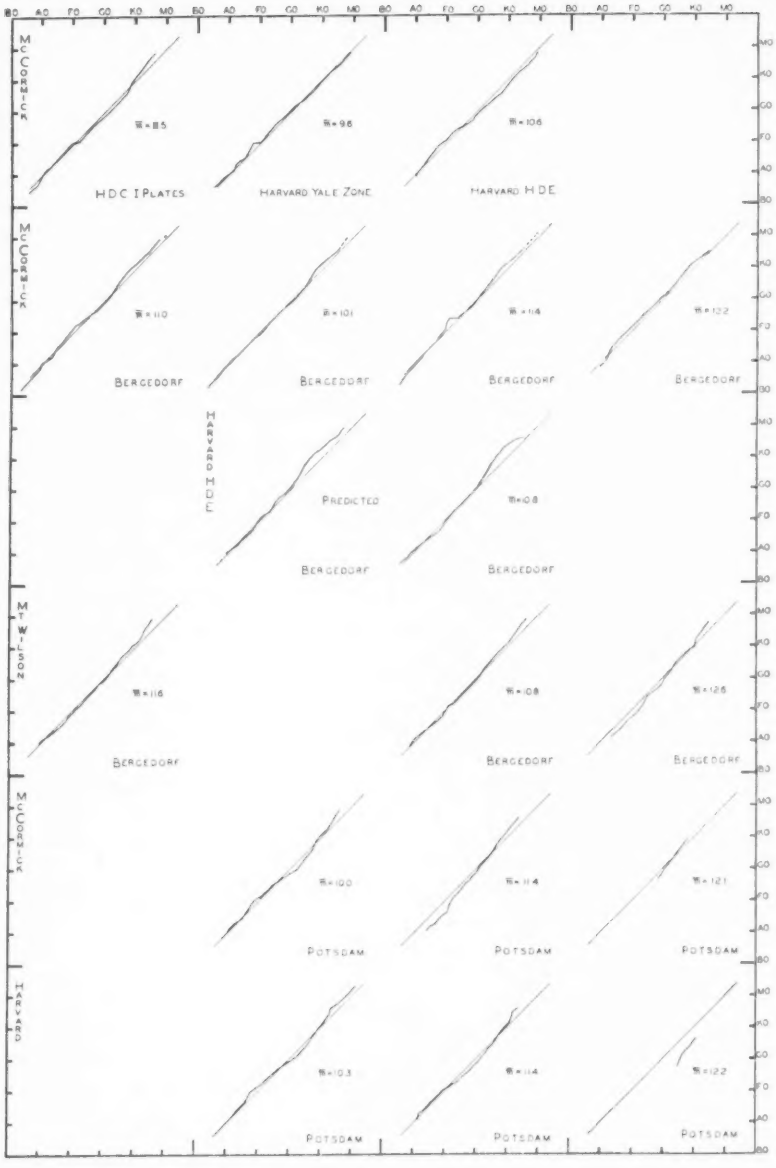
B0 A0 F0 G0 K0 M0
M CORNISH
HDC I PLATES
HARVARD YALE ZONE
HARVARD HDE
BERGEDORF
PREDICTED
M WILSON
POTSDAM
HARVARD

FIG. 2

gressions appears in the next to the last line, and below it is its probable error computed from the number of stars involved. The quantity in the next to the last line gives the best idea of the combined accidental errors of the two systems compared.

As was to be expected, the comparisons indicate a distinct increase in accidental error toward the faintest stars visible on the plates. The accidental errors of each system might now be derived by combining the data of a three-way comparison, such as HDE,

TABLE 1

MEAN ACCIDENTAL DIFFERENCES (CORRECTED)

	McCormick v. HDC	McCormick v. HYZ	McCormick v. HDE	McCormick v. Bergedorf			HDE v. Bergedorf	Mt. Wilson v. Bergedorf		McCormick v. Potsdam			Harvard v. Potsdam		
Average pg. mag.	8.5	9.6	10.6	10.1	11.4	12.2	10.8	10.8	12.6	10.0	11.4	12.1	10.3	11.4	12.2
No. of stars*	600	678	565	531	640	160	425	404	349	683	574	62	1006	299	36
B2	.....	.....	.....	1.7	.....	.....	.....	.....	.....	.....	.....	.....	.....	.....	.....
B3	.....	.....	.....	.....	.....	.....	3.0	.....	.....	.....	.....	.....	.....	.....	.....
B5	2.2	.....	.....	1.1	2.6	.....	2.0	.....	.....	.....	.....	.....	.....	.....	.....
B8	0.7	1.9	1.5	1.5	1.7	.....	3.7	2.5	.....	0.8	.....	.....	2.2	.....	.....
B9	.....	.....	.....	.....	.....	.....	1.2	.....	.....	.....	.....	.....	1.3	.....	.....
A0	0.7	1.6	1.2	1.1	1.4	2.2	1.3	1.4	2.2	2.0	3.8	.....	0.6	2.6	.....
A2	1.1	1.1	1.4	2.0	2.5	.....	1.8	1.9	1.6	2.3	5.0	.....	2.4	2.3	.....
A3	.....	.....	1.3	.....	.....	.....	3.5	.....	.....	.....	.....	.....	2.6	.....	.....
A5	3.4	3.2	2.6	2.7	3.6	.....	3.4	3.0	.....	3.5	2.6	.....	3.2	.....	.....
A7	.....	.....	.....	.....	.....	.....	4.1	.....	.....	.....	.....	.....	2.4	.....	.....
A8	.....	.....	.....	.....	.....	.....	.....	4.0	5.4	.....	.....	.....	.....	.....	.....
F0	3.2	3.5	3.9	3.6	4.0	.....	4.0	.....	3.6	2.7	2.9	.....	3.6	.....	.....
F2	3.9	3.0	3.9	2.4	3.2	.....	4.5	4.0	5.2	2.8	3.1	.....	3.8	.....	.....
F5	3.4	2.6	2.7	1.9	2.8	.....	3.6	3.2	3.7	3.2	2.9	.....	4.3	4.6	.....
F8	2.5	3.0	2.5	1.6	2.4	2.7	2.2	2.1	1.6	2.2	2.5	.....	4.1	4.5	.....
G0	3.7	2.6	3.1	2.2	2.4	3.3	3.9	2.0	2.4	2.7	3.1	.....	4.7	3.1	.....
G2	.....	.....	.....	.....	.....	.....	.....	3.3	2.6	.....	.....	.....	.....	.....	.....
G5	3.1	3.5	3.8	1.7	2.5	3.1	2.2	2.3	3.2	2.1	2.9	.....	3.0	3.0	.....
G8	.....	.....	.....	.....	.....	.....	.....	2.6	2.9	.....	.....	.....	.....	.....	.....
K0	2.1	2.7	2.3	2.1	2.4	3.0	2.4	2.3	3.2	1.7	2.7	.....	1.7	1.8	.....
K2	1.5	2.0	2.5	2.2	2.7	3.4	3.1	2.4	4.2	1.7	3.1	.....	1.9	2.3	.....
K5	2.0	3.2	2.2	1.7	2.3	2.0	3.2	2.2	3.1	1.0	2.4	.....	2.5	3.1	.....
K7	.....	.....	.....	.....	.....	.....	4.2	.....	.....	.....	.....	.....	2.6	3.0	.....
M	1.5	2.1	1.6	.....	4.4	.....	.....	3.1	2.0	1.5	3.0	.....	2.5	2.8	.....
All—Dotted regression	2.1	2.5	2.5	1.9	2.5	3.0	2.6	2.6	2.8	2.3	3.0	2.8	2.7	3.1	4.1
Dashed regression	2.3	2.5	2.4	2.1	2.6	3.3	2.7	3.0	3.6	2.5	3.6	3.4	2.8	3.8	5.3
Both regressions	2.2	2.5	2.4	2.0	2.6	3.1	2.7	2.8	3.2	2.4	3.3	3.1	2.8	3.4	4.7
Probable error	±0.05	±0.05	±0.05	±0.04	±0.05	±0.12	±0.07	±0.08	±0.09	±0.05	±0.07	±0.20	±0.05	±0.10	±0.40

* In certain cases additional material was added to the comparison after this computation had been completed; this accounts for the discrepancies as to the number of stars between Figure 1 and Table 1.

McCormick, and Bergedorf.[6] However, this cannot be rigorously carried through, since the McCormick plates taken for the comparison with HDE were exposed for only one-half as long as the run-of-the-mill plates used in the comparison with Bergedorf. Hence the McCormick error is somewhat larger for a star of magnitude 11.0 in the comparison with HDE than in the comparison with Bergedorf. Similarly, the limiting magnitude on the McCormick plates used in the comparison with Potsdam is slightly brighter than on those used in the comparison with Bergedorf, because of the greater zenith distance

[6] Cf. Butler and Thackerey, *M.N.*, **100**, 450, 1940.

of the Potsdam regions. Furthermore, the average accidental error depends upon the relative frequencies of various spectral classes, since in most of the systems examined the accidental error in the classification of A stars is decidedly smaller than the average. In this connection it is interesting to note that in nearly every case the accidental error in the classification of F stars is decidedly larger than the average; however, since the relative frequency of F stars is always small, the effect on the average is not important.

In order to avoid sampling errors, care was taken wherever possible to choose a number of samples representatively distributed as to galactic latitude, etc. As the classification of short dispersion spectra may be considerably affected by the position on the plate, the contrast of the plate, the focus, seeing, and guiding, it is of importance to know just how large the sampling error may be. For this purpose the McCormick-Bergedorf and the McCormick-Potsdam comparisons are well suited, the first being composed of seven samples and the second of eight. In each of the samples, mean systematic differences were formed for each spectral subgroup. The maximum variation of these values in the regressions of Bergedorf on McCormick is given in the upper line of the following tabulation (omitting groups with 5 stars or less); the corresponding quantities in the regressions of Potsdam on McCormick are given in the lower line.

B5	B8	A0	A2	A5	F0	F2	F5	F8	G0	G5	K0	K2	K5
3.1	1.2	0.6	1.1	3.4	5.2	6.8	3.1	1.4	2.6	2.8	5.0	3.7	2.7
	6.0	2.4	2.4	2.1	4.6	4.6	2.7	1.5	3.9	3.4	2.1	5.1	4.1

In nearly every case in the McCormick-Bergedorf comparison these variations are larger than would be expected in sampling a thoroughly mixed assemblage; this indicates that there is a real variation in classification from region to region either at McCormick or Bergedorf. Likewise, in the McCormick-Potsdam comparison, the variations in B8, A0, and A2 are decidedly larger than would be expected, but the material does not indicate the certain existence of a sampling error in the later classes. However, the most important point is that no marked dependence of the classification on galactic latitude appears in either comparison, as far as can be judged. It is believed that, in general, the material presented in this paper should be fairly free from sampling error because of the diversity of the samples chosen; however, in the case of the comparisons involving Potsdam stars of twelfth magnitude it was impossible to choose the samples satisfactorily, and consequently it is not surprising to find inconsistent results.

McCORMICK VERSUS HARVARD

A comparison of the spectral classification used in HDC with the classification of fainter stars on long-exposure plates presents difficulties. The HDC stars brighter than 8.0 are badly overexposed on the regular McCormick plates; on the other hand, much shorter exposures result in spectral images of somewhat different appearance as to the relative contrast at different wave lengths and as to definition; again, the use of a small diaphragm in front of the lens is open to the objection that it changes the definition and the color-curve of the lens. In order to avoid these difficulties, it seemed simplest to make the comparison with the fainter stars which are to be found in the published zone catalogues of the Yale Observatory. In doing this it was assumed (but later found to be erroneous) that these would be on the same system as the HDC. Three samples at representative galactic latitudes were chosen from the zone $+25^\circ$ to $+30^\circ$,[7] at right ascensions 2^h, 7^h, and 10^h; and 640 stars between the eighth and tenth photographic magnitudes were classified on the regular McCormick plates. As the possibility remained that the McCormick classification of this material was not the same as that of the fainter McCormick stars, an attempt was made to secure additional plates exposed so as to approximate the appearance of the spectra of fainter stars. For this purpose one pair of

[7] *Trans. Astr. Obs. of Yale University*, **9**, 1933.

plates was obtained with exposures of 20 minutes, instead of the standard 2 hours; and a second pair was taken with the standard exposure time, through a diaphragm consisting of twenty-four holes, each with a diameter of 0.75 inches. While the second method preserved the original color-curve and relative contrast, the definition was not so good as the average because of the diffraction pattern. Altogether 635 stars between magnitudes 7 and 9.5 have been classified on these plates with reduced exposure.

A study of the whole material indicates that the stars of the zone which were classified in the HDC are on a different system from those classified especially for the zone catalogue. This was not immediately established, since the effect might well have been due to a magnitude error in the McCormick classification. The latter possibility is ruled out, however, by the fact that the HDC stars classified on the plates with reduced exposure yield substantially the same curves as those classified on the normally exposed plates. Since the HDC stars on the plates with reduced exposure appear considerably fainter than the supplementary stars on the normal plates, it follows that the discrepancy must be between the system of the HDC stars and that of the supplementary stars for the Yale zones (hereafter designated as HYZ stars). Accordingly, the material for the HDC and HYZ stars has been discussed separately.

Before there was any thought of making an intercomparison of systems by means of the McCormick plates, it was necessary to find the magnitude limit to which our classification would be reliable. For this purpose, as mentioned previously, a few comparisons were made with Bergedorf; and, for comparison with HDE No. 5,[8] whose limiting magnitude is brighter, a pair of plates of 1-hour exposure was obtained. Subsequently, a second pair of like exposure was secured for a comparison with HDE No. 1.[9] As there is no difference between the two comparisons and as there is no apparent dependence on magnitude, the entire material for the HDE comparison involving 1250 stars has been combined for the subsequent discussion.

The diagrams in the first row of Figure 2 illustrate the relations between the McCormick and the HDC, HYZ, and HDE systems. It is seen that the curves are rather similar up to G5 but that, from that point on, the McCormick spectra are classified later than those in HDC and earlier than in HDE, whereas they agree almost precisely with those in HYZ. This might be attributed to a variation in the McCormick system with magnitude, in spite of the precautions taken, were it not for independent evidence that the variation is in the Harvard systems. Thus, (*a*) the comparison of McCormick with Bergedorf in the second row of Figure 2 shows no dependence on the magnitude in the late spectral classes; (*b*) the regressions of Bergedorf on HDC and HDE, given by the dotted curves in the third row of Figure 1, indicate a variation in the Harvard systems much like that found in the McCormick comparison; and (*c*) a similar variation between HDC and HDE No. 1 has been found by Schalén.[10] All these comparisons with HDC involve Harvard "I" plates, which were used in the northern hemisphere.[11]

However, with the existing material it is impossible to form any definite conclusions concerning the system of HYZ. The samples for the comparison with McCormick, which were all chosen from the zone $+25°$ to $+30°$, indicate that the HYZ system lies between HDC and HDE. On the other hand, Schalén[10] and Vanas,[12] from a comparison with the zone $+50°$ to $+60°$,[13] find that HYZ deviates from HDC even more than does HDE No. 1. The spectra for this zone were published as HDE Nos. 3 and 4; but they are not, of necessity, on the same system with the spectra of HDE Nos. 1, 2, and 5, for which uniform instrumental equipment was used throughout. Apparently, much more material is needed. In this connection it is interesting to note that in the comparisons of

[8] *Harvard Ann.*, **100**, 61, 1931.

[9] *Harvard Ann.*, **100**, 1, 1925.

[10] *Medd. Upsala*, No. 55, p. 9, 1931.

[11] Cf. Introduction to *Henry Draper Catalogue* volumes.

[12] *Upsala Ann.*, **1**, No. 1, 45, 1939.

[13] *Harvard Ann.*, **100**, 38 and 51, 1928.

McCormick and Harvard with Potsdam given in the last two rows of Figure 2, we have an indication that the McCormick system is very close to the Harvard system in the $-40°$ to $-50°$ zone, as far as tenth-magnitude stars are concerned; the fainter groups are affected by sampling errors, as is explained in the sections dealing with Potsdam.

Columns 1 and 2 of Table 2 give the adopted differences of McCormick versus HDC and HDE, read from the curves of Figure 2. Also, a "predicted" comparison between HDC and HDE has been derived, and the adopted differences given in column 3 of the table.

McCORMICK VERSUS BERGEDORF

Seven samples have been classified as shown in the accompanying table.[14] In all the samples the limiting magnitude of the Bergedorf material is considerably fainter than

Selected Area	Declination	Galactic Latitude	Bergedorf Observer	No. of Stars Classified
5	$+75°$	$+42°$	Sn	162
8	$+60$	-3	Sn	307
11	$+60$	$+27$	Wa	178
19	$+60$	-1	St	339
23	$+45$	-7	Sn	370
33	$+45$	$+68$	Wa	130
38	$+45$	$+18$	Sn	187
Total				1673

that of the McCormick material; on the average, it is at least a magnitude fainter. This enables us to form a very fair idea of the relative accuracy of the faintest McCormick spectra and their systematic tendencies. It is seen from the second row of Figure 2 that the three magnitude classes agree at Ao and from Go on. There is some tendency for the McCormick classification of the faintest F stars to be late, as compared with the brighter ones; and in the middle group there is a hump at Fo which depends on 11 stars. Since the curves bear such a close resemblance to one another in other respects, they have been combined into the mean curve given at the left. Column 4 of Table 2 gives the adopted differences of McCormick versus Bergedorf.

HARVARD VERSUS BERGEDORF

The relation of the Bergedorf system to HDC has been treated on page E 11 of Volume 1 of the *Bergedorfer Spektral-Durchmusterung*. There are three scatter diagrams, one for each of the Bergedorf observers; also, there are tabulated data for a regression-curve of Bergedorf on HDC for each observer. The corresponding curve for Wachmann has been plotted as a dotted curve in the third row of Figure 1. Unfortunately, no data are available for the corresponding dashed curve; however, the dotted curve, together with the dotted curve in the diagram to its right, serves to give us an approximation to an indirect comparison of HDC and HDE; this has already been referred to in a previous section.

The comparison of Bergedorf with HDE is obtained from an overlap between Wachmann's Milky Way Field No. 2[15] and HDE No. 5; in all, the two catalogues have 425 stars in common. An inspection of the curves shows a considerable systematic difference between the two systems, beginning at G5. The possibility that such large differences

[14] *Bergedorfer Spektral-Durchmusterung*, **1**, 1935; **2**, 1938.

[15] *Spektral-Durchmusterung von Milchstrassenfeldern*, **1**, 23, 1939.

result from a rather large sampling error was tested by deriving a predicted relation from a combination of the McCormick versus HDE curve with the McCormick versus Bergedorf curve. This indirect comparison, plotted in Figure 2, confirms the direct comparison surprisingly well. Since the curve of the indirect comparison is based on many more stars from more samples, the two curves have been combined with equal weight in deriving the differences tabulated in column 5 of Table 2.

MOUNT WILSON VERSUS BERGEDORF

Humason has classified over 4000 faint stars in the first 115 of Kapteyn's Selected Areas,[16] using a slitless spectrograph with the 60-inch reflector. The dispersion of his spectra is three and a half times that of the Bergedorf spectra, so that the general appearance must differ considerably. This makes a comparison of the two systems of particular importance.[17] Humason has already published a comparison[18] based on the 438 stars in the first 19 areas; consequently, the comparisons given in Figures 1 and 2 have been based on the more recently available material in the $+45°$ zone. In these 24 areas 750 stars are available. The diagrams in Figures 1 and 2 agree very well with the scatter diagram published by Humason, as do also the values of the accidental errors. An inspection of the curves corresponding to the two magnitude groups in Figure 2 brings out the important fact that beyond F5 there is no evidence of a difference in classification depending upon magnitude. Farlier than F5 there does seem to be a moderate difference; but in view of the fact that the two regression-curves for the fainter group in Figure 1 lie so far apart, it cannot be regarded as well established. Consequently, the material has been combined into the curve at the left, the corresponding differences being given in column 6 of Table 2.

McCORMICK VERSUS POTSDAM

Of the 91 Selected Areas classified at Potsdam, only those in the $-15°$ zone are accessible for observation at McCormick.[19] Accordingly, out of eleven overlaps on the McCormick plates, the eight in the accompanying list were chosen, everything available in low latitudes being included. Becker, who classified the spectra in this zone, remarks that on the plate for S.A. 123 the images are not sharp and that the plate for S.A. 133 is heavily fogged.

Selected Area	Galactic Latitude	No. of Stars Classified
123	0°	135
124	+13	164
126	+35	283
127	+42	194
129	+47	80
133	+12	175
137	−40	200
139	−66	235
Total		1467

[16] *Mt. Wilson Contr.*, No. 458, p. 171, 1932; *Ap. J.*, **76**, 224, 1932.

[17] Incidentally, it also accounts for the rather large accidental differences in the comparison shown in Table 1.

[18] *Mt. Wilson Contr.*, No. 560, p. 9, 1937; *Ap. J.*, **85**, 14, 1937.

[19] *Pub. Ap. Obs. Potsdam*, **28**, No. 2, 1938.

An inspection of the curves in Figures 1 and 2 indicates that the three magnitude groups agree very well from Go on. Earlier than F2 there is marked disagreement. The material for this part of the fainter curve consists of 80 stars from the three low-latitude areas. In one of these areas, No. 123, the Potsdam material was below par; in this area Becker has frequently assigned to class F stars which are clearly of class A on the McCormick plates. In the other two areas such cases occur less frequently, but they persist in area No. 124 among stars fainter than $11^m.0$. This is not surprising in view of Becker's statement that the H and K lines are frequently not visible on his spectra fainter than $11^m.0$ or $11^m.5$, so that his classification of the early-type stars rests entirely on the hydrogen lines.[20] Here we have a confirmation of the deduction by Mrs. Payne-Gaposchkin[21] that the negative color indices of Becker's faint F stars in S.A. No. 193 must be due to a confusion of B and F spectra by Becker. Since the *TiO* bands are not visible on the Potsdam plates,[22] their classification of M stars differs considerably from the McCormick classification. Whereas McCormick lists 24 of the 1467 stars as Mo or later, Potsdam lists only 3 stars. In column 7 of Table 2 the differences tabulated are derived from the stars brighter than $11^m.0$.

HARVARD VERSUS POTSDAM

The data used for the comparisons of Harvard and Potsdam is part of the material discussed by Mrs. Payne-Gaposchkin elsewhere.[21] She has very graciously suggested that her original working-sheets might be used for a rediscussion of the material in a manner similar to the other comparisons in this paper. There were 3100 stars included in her discussion, half of which were brighter than the tenth magnitude. Since we are here concerned chiefly with fainter stars, we have used only the stars fainter than $9^m.9$ in the $-40°$ to $-50°$ zone of the Cape Observatory (unpublished), together with those whose spectra are given on Henry Draper charts in *Harvard Annals*, **105**. Consequently, the total number of stars is reduced to 1341.

The first two curves in Figure 2 show great similarity, but the curve for the faintest group, involving 36 stars, is decidedly discordant. However, this is probably due to a sampling error rather than to a magnitude error, for all the stars in the third group were in Selected Areas 168 and 169, whose Harvard classification occurs in the single region published in *Harvard Annals*, **105**. An analysis of the brighter stars of this region shows that they, too, deviate greatly from the mean of all stars in the same sense as the fainter stars. The figures tabulated in column 7 of Table 2 are taken from the midway curve for the 1006 stars in the brightest group.

GIANT AND DWARF CRITERIA

In the McCormick-Bergedorf comparison there are 548 stars of Bergedorf type Go or later for which the Bergedorf observers have included a designation concerning the giant or dwarf character. This constitutes 69 per cent of all the stars of these spectral classes and should be a sufficient number to determine whether any difference in the McCormick classification corresponds to the difference between, say, a gKo and a dKo on the Bergedorf system. The material was divided into sixteen groups, as shown in the accompanying tabulation. For each group the mean Bergedorf class ($\overline{C}_B$), as well as the mean McCormick class ($\overline{C}_M$), was found. The regression of McCormick on Bergedorf for all stars gave the McCormick class ($\overline{C}_{BM}$), which would, normally, correspond to C_B. The difference between $\overline{C}_M$ and $\overline{C}_{BM}$ is tabulated; the plus sign indicates that McCormick classifies the particular group later than the average, and the minus sign indicates the

[20] *Pub. Ap. Obs. Potsdam*, **27**, No. 2, 6, 1930.

[21] *Ap. J.*, **90**, 321, 1939.

[22] *Pub. Ap. Obs. Potsdam*, **27**, No. 1, 16, 1929.

opposite. The number of stars in each group is given in parentheses. The results are rather unexpected and are difficult to interpret. For instance, it would appear that the McCormick classification of a Bergedorf dG2 would be 3.8 subclasses earlier than the McCormick classification of a Bergedorf d: G2 (there being only 9 stars which are characterized by d:: in the group of 44). The probable error of this difference, as formally computed, is 0.4, or only about one-tenth of the difference.

Bergedorf Class	d Stars	d: and d:: Stars	g Stars	g: and g:: Stars
Go-4	−0.9 (58)	+2.9 (44)	+1.9:: (5)	+2.7 (24)
G5-9	−1.4 (78)	+0.8 (71)	+1.5 (21)	+0.4 (49)
Ko-4	−0.8 (55)	+0.9 (41)	+0.1 (26)	+0.9 (31)
K5-9	+0.3 (17)	−1.6 (8)	−2.9:: (3)	−1.0 (17)
Total	(208)	(164)	(55)	(121)

A similar analysis was attempted with the material of the HDE-Bergedorf comparison. Here the number of late-type stars (Go and later) is only 130, and the proportion with giant-dwarf designation is smaller. Hence the grouping is slightly different from that used before. There is perhaps some similarity between the two tables.

Bergedorf Class	d Stars	g, g:, and g:: Stars
Go-4	−1.3 (15)	.....
G5-9	+1.2 (25)	+1.7 (14)

It has not been possible to discuss the "d" and "g" designations of the Potsdam catalogue, since very few stars in the −15° zone are characterized with these symbols.[23]

CONVERSION OF SPECTRA TO ANOTHER SYSTEM

Table 2 gives readings from the midway curves, which may be used to convert the spectral classification from one system to another. It may be objected that a midway curve does not give the average spectrum in system Y corresponding to a given spectrum in system X; that the correct curve for such a purpose is the regression of Y on X, the dashed curve. However, the dashed curve is not satisfactory for our purpose, since it will tend to overcorrect, on account of the errors in system X. This will be obvious from the following example. Suppose a large portion of the sky is photographed twice with the same prismatic camera. For each region one plate is marked "A" and the other is marked "B," it being left entirely to chance which plate receives which designation. Then all the plates are classified independently by one observer, the classifications from the A plates being entered in the A catalogue and those from the B plates being entered in the B catalogue. Subsequently an investigator who is ignorant of the history of the two catalogues decides to convert all spectra in the B catalogue to the system of the A catalogue. Following the above reasoning, he would derive the regression of A on B and apply corresponding corrections to the B spectra, although they were already on the same system as A, by definition! Furthermore, for the faintest stars he would derive larger corrections at the ends of the sequence (and at class F) than for stars a magnitude brighter. This follows since the faintest stars have the largest accidental errors, which

[23] In this connection see reference 21 and also D. Hoffleit, *Ap. J.*, **90**, 621, 1939.

TABLE 2

ADOPTED SYSTEMATIC DIFFERENCES

(Unit: One-tenth of a Spectral Class)

	(1) McC v. HDC		(2) McC v. HDE		(3) HDE v. HDC		(4) McC v. BSD		(5) HDE v. BSD		(6) MtW v. BSD		(7) McC v. PSD		(8) Harvard v. PSD	
	a	*b*	*a*	*b*	*a*	*b*	*a*	*b*	*a*	*b*	*a*	*b*	*a*	*b*	*a*	*b*
B2	.....	.....	.....	.....	.....	.....	+1.3:	.....	.....	.....	.....	.....	.....	.....	.....	.....
B5	+1.0:	−1.0:	.....	.....	.....	.....	+1.0	−0.9	−1.0:	+1.1:	.....	.....	.....	.....	.....	.....
B8	+0.8	−1.4	+1.2	.....	.....	.....	+0.4	−0.5	−0.7	+0.8	.....	.....	−0.2	+0.1	+0.3	−0.3
A0	0.0	0.0	+0.3	−0.7	−0.2	+0.3	−0.2	+0.2	−0.4	+0.4	−0.2	+0.3	0.0	0.0	0.0	0.0
A2	−0.2	+0.1	−0.2	+0.2	0.0	0.0	+0.3	−0.3	+0.1	−0.1	0.0	0.0	−0.5	+0.6	0.0	0.0
A5	−0.3:	+0.3:	−0.7	+0.8	+0.5:	−0.6:	−0.2	+0.2	+0.7	−0.6	+1.2:	−1.0:	+0.3:	−0.3:	−0.3:	+0.3:
A8	−0.4:	+0.4:	−1.4	+1.3	+0.6:	−0.6:	−0.6	+0.8	+0.6:	−1.0:	+0.8:	−1.2:	−0.7:	+1.0:	−0.9:	+2.0:
F0	−0.5:	+0.3:	−1.1	+0.8	+1.0:	−0.7:	−1.0:	+1.3:	0.0:	0.0:	+0.8:	−0.8:	−1.2:	+1.1:	−2.0:	+1.3:
F2	+0.5:	−0.7:	−1.0	+1.0	+1.3:	−1.3:	−1.5	+0.9	+0.1:	−0.1:	+0.8:	−0.5:	−0.6	+0.5	−1.1:	+0.8:
F5	+0.6:	−0.7:	+0.5	−0.3	+0.4:	−0.6:	−0.3	+0.3	−0.2	+0.4	+0.7:	−0.7:	−0.2	+0.2	−0.8:	+0.7:
F8	+0.8	−0.7	+1.0	−1.2	0.0	0.0	+0.5	−0.3	−0.3	+0.3	+0.8	−0.8	+0.9	−0.7	0.0	0.0
G0	+1.0:	−1.0:	+1.0	−1.0	0.0:	0.0:	+0.4	−0.4	−0.3	+0.3	+0.5	−0.6	+2.2	−1.3	+1.3	−0.8
G2	+1.2	−1.1	+1.5	−1.0	0.0:	0.0:	+0.2	−0.2	−0.8	+1.2	+0.1	−0.1	+2.0	−2.2	+1.8	−1.5
G5	+1.2	−1.2	+2.2	−1.7	−0.5:	+0.6:	−0.8	+1.1	−1.9	+3.2	−0.6	+0.6	+1.3	−1.6	+1.4	−1.7
G8	+0.2	−0.5	+1.8	−2.2	−1.2	+1.6	−1.8	+2.2	−3.2	+3.9	−1.0	+0.8	0.0	0.0	+0.4	−0.7
K0	−0.7	+0.8	+1.4	−1.7	−1.7	+2.1	−2.5	+1.6	−3.7	+3.4	−1.0:	+1.0:	−0.5	+0.6	−0.2	+0.3
K2	−1.0	+1.3	+1.4	−1.3	−2.1	+3.0	−1.5	+1.3	−3.6	+3.0	−0.8:	+1.4:	−0.4	+0.5	−0.5	+0.7
K5	−1.8	+2.6	+2.2	−1.7	−3.0	+3.8	−1.0	+1.0	−3.1	+1.9	−2.2:	+3.0:	−1.3	+2.4	−1.7	+2.5
K8	−2.5	.....	+1.2	−1.8	−3.8	.....	−1.5:	+2.0:	−2.8	.....	−3.0:	.....	−2.6	.....	−2.2:	+1.8:
M0	.....	.....	.....	.....	.....	.....	−2.0:	.....	.....	.....	.....	.....	.....	.....	−1.8:	+1.8:
M2	.....	.....	.....	.....	.....	.....	.....	.....	.....	.....	.....	.....	.....	.....	−1.8:	.....

Col. 1. HDC "I" plates.
Col. 2. HDE Nos. 1 and 5.
Col. 3. Indirect comparison derived from columns 1 and 2.
Col. 4. Zones +75°, +60°, and +45°.
Col. 5. Mean between direct comparison of Milchstrassenfeld No. 2 with HDE No. 5 and the indirect comparison derived from columns 2 and 4.
Col. 6. Zone +45°.
Col. 7. Stars brighter than eleventh magnitude in zone −15°.
Col. 8. Stars from magnitude 10.0 to 10.9 in zone −45°.

necessarily makes the two regression-curves lie farther apart at the ends (and at class F) than curves for stars with smaller accidental errors. Thus, he would discover a spurious magnitude error. What the investigator should do, if he is intent upon applying some sort of correction, is to apply to *both A and B* corrections which are $1/\sqrt{2}$ of the size of the ones he found in his regression. These would be of the same nature as the corrections which parallax observers apply to a series of trigonometric parallaxes before discussing them statistically. Just as the corrections to parallaxes eliminate negative parallaxes, so the corrections to spectra would reduce the observed frequencies of B, F, and M stars relative to A, G, and K stars. Since such corrections are not even in use for the HDC, it seems to be an extra refinement to worry about them for those stars whose accidental errors are not very much larger, particularly since the ends of the regression-curves are always the portions which are most poorly determined because of paucity of stars.

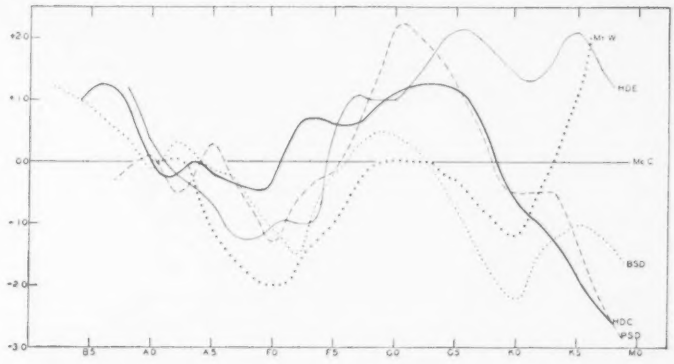

FIG. 3.—Correction to be applied to the McCormick classification to convert it to another system

The items in Table 2 whose probable errors are 0.1 and 0.2 are given in italics; those with probable errors 0.3 and 0.4 are in regular type; items with still larger errors are designated with a colon. Each of the errors has been formally computed from the number of stars in the subclass and the accidental errors for that subclass. However, it should be noted that the figures in Table 2 are read from the midway curves, which, of necessity, smooth out some of the irregularities of the regression-curves. Hence the actual errors are not so large as those indicated in the table.

In order to convert McCormick to HDC, we enter with the McCormick class as argument and find the correction under *a* in column 1. To convert HDC to McCormick, we enter with the HDC class as argument and find the correction under *b* in column 1. A similar procedure is to be followed in other conversions.

CONCLUSION

Figure 3 gives a comparison of the relations of the McCormick system to the various other systems, as derived from the midway curves. In the case of Mount Wilson the relation has been predicted by eliminating Bergedorf between the first curve in the second row of Figure 2 and the first curve in the fourth row. Obviously, it would be much more desirable to relate all the systems to HDC; however, because of the difficulties in the comparison of a system of classification for bright stars and a system for faint stars, this procedure with the present material would not be so reliable as that leading to Figure 3.

One of the important results of the investigation is that most of the systems investigated are apparently free from magnitude error, provided we treat HDC and HDE (Nos. 1, 2, and 5) as separate systems. Failure to discriminate between the spectra classified on Harvard B, MF, and A plates would perhaps account for the difficulties encountered by Jennings[24] when he found unexpected space densities for K3–M stars with increasing distance.

Our results have also an immediate bearing upon the normal relation between the spectra and color indices of faint stars. Clearly, such a relation should include an explicit statement as to the system of spectral classification used.

I am greatly indebted to Dr. Emma T. R. Williams, who contributed largely to the statistical discussion in this paper and suggested several important additions. My sincere appreciation is due to Dr. Cecilia Payne-Gaposchkin, who very kindly put at my disposal her manuscript material on the comparison of the Harvard and Potsdam classifications and who discussed certain aspects of the problem with me; I also wish to thank Mrs. Margaret Walton Mayall for furnishing information as to the type of plates used in classifying the Yale zones.

APPENDIX

The following list includes all the cases encountered in which authorities differ by more than one and a half spectral classes. These stars were omitted in the formation of means for the regression-curves. It is evident from an examination of the list that the cases are not, by any means, due chiefly to clerical errors. This is indicated by the high relative frequency of cases of confusion between B and F stars. In each case involving McCormick, the identification and classification were reviewed, and instances representing recognizable errors at McCormick were eliminated. A comparison of the number of cases in the list with the total number of stars classified in the sample indicates that misclassification is considerably more frequent in low latitudes than in high.

[24] *Harvard Circ.*, No. 438, p. 4, 1940.

Yale Zone +25° to +30°		McC Sp.
No.	Sp.	
5100	Ko	Fo
9493	Ao	K2
9663	Go	Ao
9764	A2	G5

HDE Nos. 1 and 5		McC Sp.
No.	Sp.	
227769	B	Go
228207	F2	B5
228457	Mo	F5
257466	F5	K5
262226	B8	Go

Bergedorf			McC Sp.
S.A.	No.	Sp.	
8	429	F3p	B5
	614	G2	B5
	618	F5	Bo
	762	F5	B8
	1205	F2p	B2
	1283	F4	B2
	1306	Fo	B2
	1348	F8	B5
11	574	G5	M8
19	493	Ao	Go
	563	F2:	B5
	730	F5p	B2
	982	B5	Go
	1061	A1	G5
	1085	G3	Bo
	1884	Go	B5
	1918	F5	B5
	1956	G3	B2
23	1910	G2	Ao
38	700	A6	G5

Bergedorf Milchstrassenfeld No. 2		HDE No. 5 Sp.
No.	Sp.	
170	F4	Bo
386	Fo	K5
405	Fop	Bo
510	A9	G5
627	Ma	Ao
824	Ao	Ko
964	B5	F5
1082	F6	B8
1234	B8p	Go
1929	A5:	K2
2619	F4	Ko

Bergedorf			Mt. W. Sp.
S.A.	No.	Sp.	
20	1276	Fo	B2
33	331	A2	G2
39	1197	K4	A9
40	792	F7p	B1
	1810	F5	B5
	1851	G8	A4

Potsdam			McC Sp.
S.A.	No.	Sp.	
123	120	Bo	cF5
	142	F6	Ao
	149	F7	Ao
	174	F6	Ao
124	143	F8	Ao
	153	F6	Ao
	278	F6	Ao
	279	G2	B5
	280	G4	Mo
	305	F9	B5
126	3	G6	M5
	280	G4	M5
127	193	G3	M2
133	86	F9	M2
	376	F9	K5
	392	F7	Ao
139	301	F5	K2

Potsdam			Harvard Sp.
S.A.	No.	Sp.	
168	304	Ko	F2
169	28	F2	Ko
170	724	A3	K5
171	351	Ko	Fo
	468	F1	K2
	568	G6	Ao
172	229	F6	B2
	518	Fo	B3
	589	G3	Ao
	1133	F4	B5
	1348	F2	K2
	1632	Go	Ao
173	220	Go	A2
174	274	G7	Fo
175	144	Go	A3
179	694	G4	Mb
180	163	G5	B8
	382	F2	B
	1083	Fo	B3

Leander McCormick Observatory
University of Virginia
February 1941

THE LIGHT-CURVE OF THE ECLIPSING VARIABLE 29 CANIS MAJORIS*

CARL K. SEYFERT

ABSTRACT

A new photographic light-curve has been obtained of the eclipsing variable 29 Canis Majoris. One hundred and fifty observations of two or three exposures each were obtained with a 6-inch telescope at the McDonald Observatory during the years 1939 and 1940. Certain anomalies in the form of the light-curve are mentioned. Three solutions were made for the ellipticity and eclipse of the components.

The star 29 Canis Majoris (HD 57060; $m_{vis} = 4.90$; spectrum, 07sfk; $\alpha = 7^h14^m5$; $\delta = -24°23'$ [1900]) was found to have a variable radial velocity by E. B. Frost[1] in 1906. Spectroscopic orbits have been published by W. E. Harper,[2] J. A. Pearce,[3] Luyten and Ebbighausen,[4] and O. Struve and F. Sherman.[5] S. Gaposchkin[6] first observed the light variation and published photometric orbital elements of 29 Canis Majoris. Elvey and Rudnick[7] have observed this star with the photoelectric cell at the McDonald Observatory. Certain anomalies in their light-curve have led the writer to undertake a new determination of the light-curve.

The observations were obtained with the 6-inch UV telescope (focal length 32 inches) at the McDonald Observatory during the years 1939 and 1940. The exposures (30–60 sec each) were made mostly on Eastman 40 plates at a setting approximately 7 mm out of focus. This procedure produced extrafocal star images 1.2 mm in diameter, having exceptionally uniform disks. By means of a tube sensitometer a standardization exposure of exactly the same length as the stellar exposure was impressed on each plate while the plates were still cold from the outside air. The apertures of the tube sensitometer were diaphragmed down to produce images of the same size as those of the star images. The sensitometer exposure on each plate was used to establish the magnitude scale of the plate, so that the measures of the variable and comparison star could be converted into magnitude differences. This procedure, similar to one adopted many years ago by J. A. Parkhurst[8] with the same telescope, was repeatedly tested by means of exposures on the North Polar Sequence. No differences between the magnitude scales obtained directly from the polar stars and from the sensitometer exposures could be detected. As an added precaution the standardization exposures were placed on the sky fog of the plate, whether the fog was visible or not. Tests proved that any appreciable sky fog increased the errors of measurement noticeably, and therefore measures from plates with noticeable fog were not used.

Only one star—30τ Canis Majoris (HD 57061)—could be used as comparison star, in order that large distance corrections might be avoided. 30τ Canis Majoris, situated only 24′ from the variable and with almost exactly the same color and spectral type, makes an almost ideal comparison star for this purpose. Unfortunately, it is 0.5–0.9 mag. brighter than 29 Canis Majoris—a circumstance more than offset by its proximity in

* *Contributions from the McDonald Observatory, University of Texas*, No. 32.

[1] *Ap. J.*, **23**, 265, 1906.

[2] *Pub. Dom. Obs.*, **4**, 115, 1917.

[3] *Pub. Dom. Ap. Obs.*, **6**, 49, 1932.

[4] *Ap. J.*, **82**, 246, 1935.

[5] *Ap. J.*, **93**, 84, 1941.

[6] *Harvard Bull.*, No. 902, p. 17, 1936.

[7] A preliminary solution was announced by them in *Ap. J.*, **88**, 503, 1938.

[8] *Ap. J.*, **36**, 169, 1912.

color, spectrum, and space to the variable. Gaposchkin did not use 30τ Canis Majoris as a comparison star in his investigation because it is located in the middle of a cluster of stars. These cluster stars are completely invisible on my plates and hence do not affect the measures.

A special series of plates was taken in an attempt to examine the comparison star for variability. The results are negative but are somewhat inconclusive because of the lack of close comparison stars. However, the observations show that, if 30τ Canis Majoris is variable, the amplitude of its variation is certainly less than 0.10 mag. and probably less than 0.06 mag.

All the plates taken for this investigation were measured in the null-type photometer[9] of the McDonald Observatory. A circular diaphragm was used, which produced an image

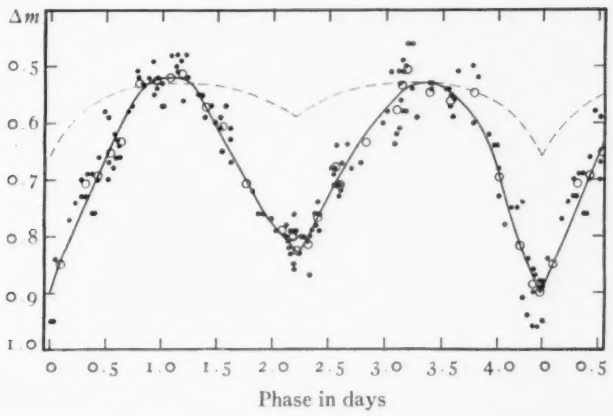

FIG. 1.—The light-curve of 29 Canis Majoris. The filled circles represent individual observations; the large open circles represent normal points (five observations each); the full line is the observed light-curve; the broken line is the observed curve corrected for ellipticity of the components.

with a diameter approximately 75 per cent of that of the star and of the standardization images, and the measures were reduced to magnitude differences by means of the sensitometer exposures.

One hundred and fifty observations were used, each consisting of the mean measure from two or three separate exposures taken on the same plate. A plot of the observations against phase is given in Figure 1. The phases were computed with Harper's value of the period (4.3934 days) and with primary minima occurring at JD 2424982.207+PE. Thirty normal points were computed by forming groups of five observations each. These normal points are listed in Table 1 and are indicated by open circles in Figure 1, together with the best mean light-curve that could be fitted to the normal points (full line in Fig. 1). The mean error of a single observation as determined from the scatter about the mean light-curve is ±0.034 mag.

An examination of Figure 1 shows that the slopes of the curve defining the principal minimum (phase zero) are very nearly equal (i.e., the principal minimum is symmetrical). The secondary minimum, however, seems to show definite asymmetry in that the fall to minimum is less steep than the rise. The rising branch of the secondary minimum seems to show a break at about phase 2.75 days. Unfortunately, because of the lack of observations at this point, the character of the break cannot be defined specifically, but it may be due to the changing character of the emission lines in the spectrum of the primary as

[9] *Ap. J.*, **91**, 117, 1940.

described by Struve.[5] The light-curves obtained both by Gaposchkin[6] and by Elvey and Rudnick[7] indicate similar asymmetries.

The present light-curve indicates little or no eccentricity of the orbit of 29 Canis Majoris—a result in agreement with the Elvey-Rudnick and the Gaposchkin light-curves of the same star, but contradictory to the spectroscopic data, which yield for the eccentricity 0.16 (Harper), 0.15 (Luyten and Ebbighausen), and 0.06 (Struve). Struve's values of e and ω, together with a probable value of i (65°), lead to a predicted displacement of one minimum with respect to the other of 0.12 day. In view of the small size of this displacement and of the difficulty of detecting it, considering the asymmetry in the secondary minimum, the present solution has been made with e assumed to be zero. Furthermore, since both components are very hot stars, reflection effects and a darkened solution have been omitted. The present solution treats only the ellipticity and the eclipse of the components.

TABLE 1

NORMAL POINTS (FIVE OBSERVATIONS EACH) FOR 29 CANIS MAJORIS

No.	Mean Phase	29 Can. Maj.−30τ Can. Maj.	No.	Mean Phase	29 Can. Maj.−30τ Can. Maj.
1	0^{d}096	0^{m}850	16	2^{d}318	0^{m}814
2	0.310	.708	17	2.399	.766
3	0.422	.692	18	2.546	.680
4	0.540	.652	19	2.590	.708
5	0.624	.634	20	2.824	.634
6	0.796	.530	21	3.094	.578
7	0.952	.526	22	3.143	.534
8	1.070	.520	23	3.196	.508
9	1.187	.512	24	3.398	.546
10	1.398	.572	25	3.574	.562
11	1.550	.606	26	3.791	.548
12	1.765	.708	27	4.006	.694
13	2.085	.790	28	4.202	.818
14	2.164	.798	29	4.310	.886
15	2.214	0.826	30	4.374	0.900

From the observed light-curve it can be seen that the eclipses are partial and that the depths of primary and secondary minima are 0.37 and 0.30 mag., respectively. Independent solutions for the primary and secondary minima agreed sufficiently well to make a combined solution practicable. Consequently, the primary and secondary minima were combined in the usual manner and three solutions were obtained according to the method of H. N. Russell.[10] Since Struve's plates do not show the secondary spectrum, it is assumed that $L_1 \geqslant 2.5L_2$, indicating that the ratio of the two radii (k) must be $\leqslant 0.9$ (solution 1, Table 2). On the other hand, k must be $\geqslant 0.343$, the limiting case for α, the percentage of eclipse, being equal to 1.0 (total grazing eclipse, solution 2). One intermediate case ($k = 0.7$) was used in solution 3. All the solutions listed in Table 2 were made after the light-curve had been "rectified" for ellipticity of the components, by using a constant $z = 0.36$ (the observed curve, corrected for ellipticity, is indicated by the broken line in Fig. 1). Although other ellipticity constants were tried, this value of z fitted the observations best.

An examination of the place where primary minimum falls on the radial velocity-curve of the brighter component shows that the star eclipsed at principal minimum is the brighter of the two. This indicates that the brighter star also has the greater surface

[10] *Ap. J.*, **35**, 315, 1912; **36**, 54, 1912.

brightness. Consequently, since the ratio of brightness is $\geqslant 2.5$ in intensity and the ratio of surface brightness is 2.1, the star eclipsed at principal minimum must be the larger of the two.

Since Struve finds no evidence of a secondary spectrum, the solution must remain indeterminate within the ranges given above. In addition, only minimum values of the masses can be derived from the combination of spectrographic and photometric elements. Struve's observations lead to a mass function

$$f = \frac{(a_1 \sin i)^3}{P^2} = 4.57 ,$$

in agreement with Harper's value. If in the expression for the mass function we adopt a

TABLE 2

PHOTOMETRIC ELEMENTS OF 29 CANIS MAJORIS

		Primary Minimum (JD 2424982.207) Period (4.3934 Days)		
		Solution 1	Solution 2	Solution 3
Ratio of radii	k	0.9	0.343	0.7
Amount of eclipse	a_0	0.189	1.000	0.278
Loss of light at primary minimum	$1-\lambda_2$	0.111	0.111	0.111
Loss of light at secondary minimum	$1-\lambda_1$	0.052	0.052	0.052
Light of larger star	L_1	0.725	0.948	0.813
Light of smaller star	L_2	0.275	0.052	0.187
Ratio of surface brightness	J_1/J_2	2.13	2.13	2.13
Inclination of orbit	i	62°.1	73°.6	69°.5
Semimajor axis of larger star	a_1	0.426	0.536	0.373
Semimajor axis of smaller star	b_1	0.313	0.419	0.286
Semiminor axis of larger star	a_2	0.383	0.184	0.262
Semiminor axis of smaller star	b_2	0.282	0.144	0.201
Eccentricity of meridian section	ϵ	0.680	0.625	0.641
Eccentricity of orbit (assumed)	e	0.0	0.0	0.0
Ellipticity constant	z	0.36	0.36	0.36

probable value of sin $i = 0.9$ and assume m_1/m_2 equal to unity, we obtain the minimum values

$$m_1 = m_2 = 25 \odot .$$

If m_1/m_2 is much greater than unity, the mass of the system increases greatly. If, for example, we adopt solution 1 ($k = 0.9$) and assume that the masses are proportional to the photographic luminosities, we obtain

$$m_1 = 232 \odot \qquad \text{and} \qquad m_2 = 88 \odot .$$

Solution 2 or solution 3 of this paper would lead to even greater masses. These extremely large masses are not considered probable, hence it seems likely that the ratio of the masses of the components of 29 Canis Majoris must be smaller than would be predicted from the slope of the mass-luminosity relation for very luminous stars.

McDONALD OBSERVATORY
December 1940

THE SPECTRUM OF THE SHELL OF PLEIONE*

OTTO STRUVE AND P. SWINGS

ABSTRACT

The absorption spectrum of the shell of Pleione, which made its appearance in 1938, has a radial velocity of +10.3 km/sec. It shows sharp cores of the Balmer lines as far as H_{31}. *Mg* II 4481 and *Si* II 4128, 4131 are weak, probably because of the dilution of the exciting radiation. The lines of *Ni* II, *Fe* II, and *Cr* II are relatively strong; those of *Ti* II and *Mn* II are very weak; *Fe* I, *Mg* I, and *Sr* II are present. The lines of *Fe* II give an excitation temperature of about 17,000°. The ionization is greater than in the shell of 17 Leporis, but not all intensities are accounted for by the ionization theory.

The dilution factor is of the order of 0.1. From the state of ionization the electron pressure, estimated to be of the order of 0.5 bar in 17 Leporis, is probably appreciably higher in Pleione. Geometrical considerations suggest a value of $P_e = 0.1$ bar. The shells of stars like Pleione are not unlike the reversing layers of normal supergiants. But the stars inside these shells belong to the main sequence. The shells form a spectral sequence which runs parallel to the normal stellar sequence from the early B's to the late A's. The ionization of the shells is lower than that of the corresponding stars.

1. Pleione (28 Tauri = BS 1180, $\alpha = 3^h43^m2$, $\delta = +23°50'$ [1900]) is a member of the Pleiades cluster. Its Harvard spectral type is B8p, and its visual apparent magnitude is 5.18. The proper motion ($\Delta\alpha = +0''.016$ and $\Delta\delta = -0''.049$) and the radial velocity (+10 km/sec) agree with those of other cluster members. Adopting for the Pleiades a parallax of $0''.006$, or a distance of 170 parsecs, the visual absolute magnitude of Pleione is −1.0. It, therefore, belongs to the main sequence, as do the other early-type members of the Pleiades. It is reasonable to suppose that the radiation of Pleione resembles that of a black body; then if its color index is −0.05, we compute for the radius

$$\log_{10} R = 0.82I - 0.20M_v + 0.51 = 0.7$$

$$R = 5R_\odot$$

2. From December 28, 1888, when the first spectrographic observation[1] was secured at Harvard, until February 2, 1903, when H. W. Jung recorded the presence of double reversals of the hydrogen lines, emission features were prominent in the spectrum of Pleione. In November and December, 1905, E. B. Frost[2] noticed at the Yerkes Observatory that all emission lines had disappeared. Between 1905 and 1924 numerous spectrograms taken at the Yerkes Observatory show strong absorption lines of *H*, with marked Stark-effect wings and with a pronounced rounding-off at the centers of the contours, suggestive of rapid axial rotation. The usual *He* I lines λ 4472, λ 4026, etc., were exceedingly broad and shallow, indicating an equatorial line-of-sight component of the rotational velocity of about 300 km/sec. The line *Mg* II 4481 was so weak and broad that its existence could not be definitely established. Our spectrograms, with their relatively high dispersion of 30 A/mm, are not suitable for determining the spectral class of this object.

In October, 1938, McLaughlin[3] and Orren Mohler[4] independently announced the reappearance of emission lines in Pleione. McLaughlin also discovered narrow absorption cores in the *H* lines, as far as $H\eta$, and a large number of weak, narrow lines of *Fe* II,

* *Contributions from the McDonald Observatory, University of Texas*, No. 33.

[1] A description of the spectral changes was given by R. H. Curtiss, *Pub. Obs. U. of Michigan*, **3**, 19, 1923.

[2] *Ap. J.*, **23**, 268, 1906. [3] *Ap. J.*, **88**, 622, 1938. [4] *Ap. J.*, **88**, 623, 1938.

Ti II, *Sc* II, *Cr* II, *Ni* II, and perhaps *V* II. He states that *He* I 3819 was conspicuous and was wider than the metallic lines. The lines of *Si* II and *Mg* II 4481 were possibly wider than those of the metals.

3. From photoelectric observations made at Harvard in 1935, 1936, and 1937, Calder[5] believes that the brightness of Pleione had gradually decreased by about one-sixth of a magnitude, and more recently E. G. Williams[6] finds a reddening corresponding to an increase in the color index of 0.08 mag.

4. The following spectrographic observations have been secured at the Yerkes and McDonald Observatories:

1938	Dec. 16	$1^h\ 8^m$	U.T. at Yerkes	λλ 3900–5000	disp. 30 A/mm at λ 4500
1940	Sept. 13	9 7	U.T. at Yerkes	λλ 3900–5000	disp. 30 A/mm at λ 4500
1940	Nov. 3	11 22	U.T. at Yerkes	λλ 3900–5000	disp. 30 A/mm at λ 4500
1940	Nov. 12	9 45	U.T. at McDonald	λλ 3100–4900	disp. 40 A/mm at λ 3933
1940	Dec. 8	0 37	U.T. at Yerkes	λλ 3900–5000	disp. 30 A/mm at λ 4500
1941	Jan. 7	4 20	U.T. at McDonald	λλ 6000–6600	disp. 180 A/mm at *Hα*
1941	Jan. 7	5 2	U.T. at McDonald	λλ 3100–4900	disp. 40 A/mm at λ 3900

During the last two years the general appearance of the spectrum has remained the same. The metallic lines are strong and fairly sharp. The sharp absorption cores of *H* are strong and are visible to H_{31}. It is clear that the correlation between the number of Balmer absorption lines and absolute magnitude, which exists among normal stars,[7] breaks down completely in the case of Pleione. We are evidently concerned not with a normal reversing layer but with a tenuous shell at a considerable distance from the reversing layer. Several other objects of this class are known, but in no other case have we any reliable information concerning the absolute magnitude and the radius of the star.

5. The radial velocity of the shell of Pleione is found to be +10.3 km/sec. This agrees closely with the value of 10.0 ± 1.3 km/sec found from measurements of the broad lines[8] prior to the origin of the shell. The sharp cores of *H* and the narrow lines of *Cr* II, *Ti* II, *Ni* II and *Fe* II give substantially the same velocity. The shell does not expand, as it does in 17 Leporis or P Cygni, but remains stationary, as in γ Cassiopeiae.

6. We proceed with a detailed description of the spectrum. The shell may best be compared with α Cygni (cA2) and 4 Lacertae (cB8)—both normal supergiants. Most of the metallic lines and the cores of the hydrogen lines are much weaker in Pleione than in α Cygni.

H.—Hβ shows a weak double emission line, with the violet component slightly the stronger. *Hα* is a fairly strong double emission line. The sharp absorption cores are superposed over broad wings which resemble those observed prior to 1938. They may now be slightly narrower, but in any case weakening of the underlying B8 spectrum by the continuous spectrum of the shell is in this case negligible. Small-dispersion spectrograms by Morgan and Miss Sherman bring out the broad wings conspicuously. The discontinuity in the energy distribution near the Balmer limit is much less conspicuous than in α Cygni. It is less abrupt and resembles that observed in main-sequence stars. This phenomenon is caused by the broad wings of the underlying hydrogen lines.

He I.—The broad lines of the B8 star, λλ 4472, 4026 (2^3P-n^3D), 4388 (2^1P-n^1D), etc., are heavily blended with metallic lines. The same is true of λ 3820 (2^3P-6^3D). Our spectrograms show no clear indication of any of the sharp lines which arise from

[5] *Harvard Obs. Ann.*, **105**, 453, 1937.

[6] *Observatory*, **62**, 301, 1939.

[7] Unsöld and Struve, *Ap. J.*, **91**, 365, 1940.

[8] J. H. Moore, *Pub. Lick Obs.*, **18**, 28, 1932 (star HD 23862).

metastable levels and which are observed in the shells of ζ Tauri, φ Persei, γ Cassiopeiae, etc. The excitation temperature must be too low to produce sufficient populations in levels whose excitation potentials are of the order of 20 volts.

Mg II.—The line λ 4481 is present, and its estimated rotational broadening is about 150 km/sec—one-half of the broadening shown by the normal B8 lines. This line is too weak in comparison with the lines of *Fe* II, etc., but it is now stronger than it was prior to 1938. The enhancement after 1938 is a phenomenon not heretofore recorded. It is probable that the line is produced in relatively low layers of the shell. This effect suggests stratification in the shell.

Si II.—The lines λ 4128, λ 4131 ($3^2D-4^2F^0$) are very weak and broad. They originate from ordinary levels, and the dilution of radiation in the shell accounts for this effect. The lines $\lambda\lambda$ 3854, 3856, 3863 ($sp^2\ ^2D-4^2P^0$) are also very weak. Although the level $sp^2\ ^2D$ is not metastable, the transition probability from it to the ground level 3^2P^0 should be smaller than that from 3^2D to 3^2P^0. The fact that dilution in Pleione and also in 17 Leporis tends to weaken the violet group of *Si* II lines cannot be reconciled if the corresponding transition probability is more than about 100 times smaller than that of $3^2D \rightarrow 3^2P^0$. It is difficult from the existing evidence on *Mg* II and *Si* II to estimate the dilution factor. The fact that *Mg* II 4481 is present in the lower layers suggests roughly that $W = 0.1$ and $r = 1.5R$, where R is the radius of the star. We note that if this shell were opaque for continuous radiation and if the effective temperature were the same as that of the B8 star the apparent magnitude would have increased by 1.0 mag. The observations have shown a very small decrease.

Fe II.—All strong lines are present, and nearly all come from metastable levels. There seems to be a pronounced excitation effect, which cannot be explained by differences in the curves of growth of α Cygni and Pleione:

λ 3468	$c^2G_{3\frac{1}{2}}-z^2G^0_{3\frac{1}{2}}$	E.P. 4.1 volts	strong in Pleione
λ 3493	$c^2G_{4\frac{1}{2}}-z^2G^0_{4\frac{1}{2}}$	E.P. 4.1 volts	strong in Pleione
λ 3296	$a^4D_{1\frac{1}{2}}-z^6D^0_{1\frac{1}{2}}$	E.P. 1.1 volts	weak in Pleione

Other lines show the same behavior. If we assume for α Cygni $T' = 8000°$, we find the excitation temperature of Pleione from

$$\log \frac{n_{rs}}{n'_{rs}} - \log \frac{n_{rt}}{n'_{rt}} = 5040\ (E_{rs} - E_{rt}) \left(\frac{1}{T'} - \frac{1}{T} \right).$$

The left side of the equation is estimated to be about log 10. Hence $T = 17{,}000°$, which is in sufficient agreement with the spectral type of the exciting star. The result is of low precision, but the important thing here is to ascertain that the excitation conditions in shells are in accord with the theory of dilution and that no hitherto unknown effects appreciably influence the populations of the various levels.

Lines of *Fe* II which start from ordinary levels are rather weak but are probably present:

λ 3906	$c^2F_{2\frac{1}{2}}-x^4G^0_{3\frac{1}{2}}$	E.P. 5.5 volts	present in Pleione
λ 4003	$d^2D_{2\frac{1}{2}}-x^2F^0_{3\frac{1}{2}}$	E.P. 5.9 volts	blended with *Fe* II
			$b^4P_{1\frac{1}{2}}-z^4P^0_{1\frac{1}{2}}$, fairly strong

It is not yet known on theoretical grounds whether these lines should be weakened when the dilution factor is of the order of 0.1. Although the lower levels, c^2F and d^2D, are not metastable, they can combine only with several odd quartet and sextet levels,

which lie within about 1 volt from these two even levels.[9] The corresponding probabilities are undoubtedly rather low, so that it should not surprise us that the lines are actually present. Their weakness in 17 Leporis[10] may well be due to the low excitation temperature of the star.

Ti II.—The lines of *Ti* II are greatly weakened with respect to α Cygni, and there is an indication that low-level lines—like λ 3388 ($a^4F_{3\frac{1}{2}}-z^4G^o_{3\frac{1}{2}}$), E.P. = 0.0 v.—are weakened more than high-level lines—like λ 4172 ($b^2F_{2\frac{1}{2}}-x^2D^o_{1\frac{1}{2}}$), E.P. = 2.6 v. It is certain that the low-level lines are relatively much weaker than in 17 Leporis,[11] where they are probably enhanced with respect to α Cygni. All lines come from metastable levels.

Cr II.—All lines come from metastable levels and are relatively strong. There is no definite indication of the excitation effect.

Fe I.—Several lines, such as λλ 4404 ($a^3F_3-z^5G^o_4$), 4071, 4045 ($a^3F-y^3F^o$) are present but are weak. All arise from metastable levels.

Ca I.—λ 4227 is absent.

Ca II.—H and K ($4^2S-4^2P^o$) are strong and sharp. These lines were absent prior to 1938. λ 3706 and λ 3737 ($4^2P^o-5^2S$) are present. The former is blended with a faint line of *Ti* II, which is weakened in Pleione; the latter is blended with a strong line of *Fe* I, which may be serious. Unless the indentification of λ 3706 with *Ca* II is erroneous, its occurrence as a sharp line in Pleione is definitely contrary to the theory of dilution: level $4^2P^o_{\frac{1}{2}}$ is the upper level of *Ca* H. The B8 star is relatively deficient in radiation falling in the wing of Hε, and the corresponding depopulation of state $4^2P_{\frac{1}{2}}$ should be conspicuous. There is no explanation for the anomaly.

Sc II.—λ 4246 and λ 4375 are fairly strong but are much weaker than in 17 Leporis.

Sr II.—The ultimate lines λ 4078, λ 4215 are present but are weak.

Ni II.—These lines are greatly enhanced in Pleione.

Mg I.—The lines λ 3832, λ 3838 ($3^3P^o-3^3D$) are present. Although state $3^3P^o_1$ is not metastable, the transition probability $3^3P^o_1 \rightarrow 3^1S_0$ is small, and the occurrence of λ 3832 is not surprising.

V II.—All strong lines are present. A relatively strong line, otherwise unaccounted for, at λ 4529.05 may belong to *V* II 4528.51 ($a^3D_3-z^3F^o_4$), in which case the spectrum would be even more enhanced in Pleione than *Ni* II. The line λ 4005.7 ($a^3G_5-z^3G^o_5$) is also relatively strong, but λ 3545, λ 3557 ($a^3F-z^3D^o_2$), though present, are not as greatly enhanced as are the lines of *Ni* II. It is more probable that λ 4529.05 is an unidentified line.

Mn II.—All lines are greatly weakened in Pleione.

S II.—An otherwise unidentified line at λ 4250.4 is probably not *S* II 4249.94 (as in α Cygni), and several other relatively strong lines of *S* II, λ 4162, λ 4153, show rather unsatisfactory coincidences. The fact that these lines originate from normal levels renders the identification doubtful.

A strong, sharp line was observed at λ 3748.5, in the immediate vicinity of H_{12}. This line is present in α Cygni, but Struve and Wyse found only relatively unimportant contributors to the line. It is probably a strong line of *Fe* II observed by Dobbie at λ 3748.49.

7. The results of the preceding section may be summarized by listing the elements in the order of decreasing intensity ratio: Pleione/α Cygni (Table 1).

It is instructive to compare this table with a similar table for 17 Leporis.[12] The weakness of *Si* II and *Mg* II in both stars is accounted for by dilution. The great weakening in Pleione of *Ti* II and *Mn* II and the relative strengthening of *Ni* II and *Fe* II, show that the state of ionization of the shell in Pleione is higher than in 17 Leporis. But the place

[9] Dobbie, *Ann. Sol. Phys. Obs. Cambridge*, **5**, Part 1, 8, 1938.

[10] *Ap. J.*, **90**, 732, 1939.

[11] *Ibid.*, p. 730.

[12] *Ibid.*, p. 734.

of *V* II is not consistent with the change of ionization, and the presence of *Fe* I and *Sr* II is abnormal.

TABLE 1

Element	*Ni* II	*Fe* II	*Fe* II	*Cr* II	*Sc* II	*V* II	*Mg* I
I.P.	18.2	16.5	16.5	16.6	12.8	14.7	7.6
Average E.P.	3	4	1	2–3	0–0.3	1	2.7
Element	*Fe* I	*Sr* II	*Ti* II	*Mn* II	*Si* II	*Mg* II	.....
I.P.	7.8	11.0	13.6	15.7	16.3	15.0	.....
Average E.P.	0–1	0	1	1.8	7–10	9	.....

The material is quite insufficient to determine the ionization. But we can at least compute the quantity

$$\log \frac{n_{r+1}}{n_r} + \log \frac{P_e}{W} = -I_r \frac{5040}{T} + \tfrac{5}{2} \log T - 0.48 + \log \frac{2u_{r+1}}{u_r}$$

for several typical elements, such as *Ni* II and *Mn* II. We shall disregard the partition functions.

TABLE 2

Star	17 Leporis	Pleione
T	10,000°	17,000°
I_r (*Ni* II)	18.2 volts	18.2 volts
I_t (*Mn* II)	15.7 volts	15.7 volts
$\left(\log \frac{n_{t+1}}{n_r} + \log \frac{P_e}{W}\right)_{Mn\ II}$	+1.61	+5.44
$\left(\log \frac{n_{t+1}}{n_t} + \log \frac{P_e}{W}\right)_{Ni\ II}$	+0.36	+4.70

In order that the ionization be not excessive we must assume that in 17 Leporis P_e/W is of the order of 10 bar. Since[13] $0.01 < W < 0.1$, we find, approximately, $P_e = 0.5$ bar, or $n_e = P_e/kT = 3 \times 10^{11}$. This is very similar to the electron density of the solar chromosphere. In the case of Pleione the higher temperature gives rise to a much higher degree of ionization. If $P_e = 0.5$ and $W = 0.1$, we have

$$\left(\log \frac{n_{r+1}}{n_r}\right)_{Mn\ II} = +4.7$$

and

$$\left(\log \frac{n_{r+1}}{n_r}\right)_{Ni\ II} = +4.0 .$$

[13] *Ibid.*, p. 727.

The ionization is so strong that it is difficult to understand how any lines of *Ni* II or *Mn* II can remain in sight. Adopting a third ionization potential of 30 volts, we find that

$$\log \frac{n_{r+2}}{n_{r+1}} = +0.5 ,$$

so that lines of the doubly ionized ions should be observed. We certainly have no strong lines of *Fe* III, and it is extremely doubtful that the ionization is anything like as high as our computations have suggested. Perhaps the exciting temperature of Pleione is lower than $T = 17{,}000°$, and perhaps the electron temperature T_e is not equal to T, as we had tacitly assumed. Even so, it is difficult to see how the density of the shell of Pleione can fail to exceed that of 17 Leporis by a factor of 10, at least. Perhaps we can speak of the former as a dwarf shell and of the latter as a giant shell. Another possible source of error is in our estimate of W. If for Pleione $W < 0.01$, then the third ionization would be relatively unimportant, and a reasonable adjustment of pressure and dilution would satisfy the observations.

There remains the question of whether a pressure of the order of $P_e = 0.5$ bar is consistent with the geometrical dimensions of the shells. Because of the width of *Mg* II 4481 it is probable that the shell has an appreciable thickness. In the case of Pleione the average radius of the shell is about $r = 1.5R = 7.5R_\odot$. The metallic lines in Pleione are approximately of the same intensity as in a main-sequence star of corresponding spectral type. This suggests that the numbers of atoms and electrons per square centimeter are also the same in the shell and in such a reversing layer. Computation then shows that the pressures are roughly in the ratio

$$\frac{\text{pressure of reversing layer}}{\text{pressure of shell}} = 10^3 .$$

The average pressure in the reversing layer of a normal main-sequence star is about 100 bar. Hence, geometrical considerations lead to a pressure in the shell of 0.1 bar, which is in sufficient agreement with the value suggested by the state of ionization.

The order of magnitude of P_e in shells, and their thicknesses, suggests structures which resemble the reversing layers of supergiant stars. For a red giant[14] the geometrical extent of the atmosphere is roughly two thousand times greater than that of the sun, or about 6×10^{10} cm $\sim 1R_\odot$. The pressures, on the other hand, are in the ratio of about 100 : 1, so that $P_e = 1$ bar in the giant. These considerations are crude and do not clarify individual differences such as those between Pleione and 17 Leporis. But they serve to give us a picture of a typical shell surrounding a main-sequence star.

It is significant that all known absorption shells form a more or less uniform spectral sequence, which runs parallel to the usual sequence, with the shell nearly always showing a lower degree of ionization than the exciting star. There is no obvious theoretical reason for this phenomenon; the chromosphere of the sun shows that the outer layers of a stellar atmosphere may well be highly ionized. But the chromosphere has not enough matter in it to be comparable to the shells of Pleione or 17 Leporis. The existence of a spectral sequence of shells means that the average pressures of the shells are of the same order or that they vary in a regular manner with the spectral type of the exciting star. Our comparison of Pleione and 17 Leporis suggests a ratio in pressure of at least 10, but we do not know whether or not this is a general effect.

A rather remarkable fact is the absence of any pronounced effects, in any of the shells

[14] Unsöld, *Physik der Sternatmosphären*, p. 147, Berlin, 1938.

thus far observed, which may be attributed to departures of stellar energy-curves from black-body curves. Departures produced by continuous *H* absorption, similar to those discussed by Pannekoek,[15] should alter the ionization and the excitation of various atoms whose potentials lie on different sides of λ 911.

Another interesting circumstance is the pronounced tendency of shells to form around main-sequence stars of classes B3–B5. There is a close relationship between ordinary Be stars and stars surrounded by absorbing shells.

The question might be asked: What will happen to a star if the shell becomes very dense. We know that such shells exist and that there are all gradations, from shells which are almost transparent to continuous radiation to shells which are completely opaque. If the density of a shell is great, the continuous absorption must also be great, and the dilution must be negligible. If such a shell does not expand, the star will be a giant or a supergiant. But why some shells expand while others do not is not known. Nor have we the slightest idea how a stationary shell may be formed without a visible outburst of light.

YERKES OBSERVATORY
AND
MCDONALD OBSERVATORY
December 1940

[15] *Ap. J.*, **84**, 488, 1936.

THE VISUAL SPECTRUM OF PLEIONE*

JESSE L. GREENSTEIN

ABSTRACT

The spectrum of Pleione has been compared with that of α Cygni in the visual region. The shell lines are dominantly of *Fe* II, *Mg* I, and *Na* I; they show almost no systematic velocity displacement. Lines arising from nonmetastable levels are weakened; for example, *Si* II is extremely shallow and broad. The dilution, however, is only moderate.

The visual region of the spectrum of Pleione, 28 Tauri, has been investigated on plates taken with the grating spectrograph attached to the 40-inch refractor of the Yerkes Observatory. The dispersion is 27 A/mm. Agfa Super Pan Press films were used; the plates were taken on September 15 and 16 and on October 3, 1940. No certain traces of the original, rotationally broadened lines can be seen. *Hα* is a strong emission line, about 8 A wide without underlying wings. The radial velocity before the outburst was given as $+10\pm1$ km/sec. The present shell spectrum gives the essentially identical velocity of $+7\pm2$ km/sec.

The sharp *Fe* II lines dominate the spectrum in the visual region. They match the lines of α Cygni almost precisely in relative and, I believe, in absolute intensities. Their mean displacement corresponds to a velocity of +7 km/sec. The *Na* I lines are definitely less sharp than in α Cygni; their velocities are +16 km/sec. The *Si* II lines are extremely shallow and broad; their measured velocities of −4 km/sec are subject to considerable uncertainty. The central reversal of *Hα* is strong and broad and cuts well below the continuum; the velocity obtained is +17 km/sec. The violet and red emission components are of equal intensity.

The spectroscopic behavior of the different elements with respect to dilution of radiation is essentially as expected. A detailed comparison of the intensities of the lines in Pleione with those in α Cygni has been made, and a résumé of the observed effects is given below. Since there are few lines of *Ti* II, *Cr* II, *Ni* II, and *Mn* II in this region, it was not possible to study the level of ionization in the shell. I shall therefore neglect possible differences of ionization.

Fe II.—Some sixteen good lines are found to be the same in the two stars. All these lines originate from metastable levels, with excitation potentials up to 4 volts. The excitation temperature is not lower than in α Cygni.

Si II.—All lines are weakened; λ 5041 and λ 5056 are absent, λ 5979 is weak, and λ 6347 and λ 6371 are extremely shallow. In α Cygni the latter are by far the strongest in the spectrum; they have total absorptions of the order of 1.2 A and their profiles on microphotometer tracings have an estimated width of 4 A. In Pleione, however, the lines have total absorptions of about 0.5 A; their total width is at least 6 A. (These estimates are uncertain because of the shallowness of the lines.) There is no doubt that the population of the nonmetastable, excited levels of *Si* II is less than normal by a factor of at least 5. Since the lines of *Si* II were not visible before the outburst, those now seen must originate at some depth in an extended nebulous envelope, at a point where the dilution is not large.

Mg I.—The presence of *Mg* I is of some interest in such a high-temperature shell, just as its presence in α Cygni is somewhat anomalous. Since neutral sodium appears in Pleione and in the B5 spectrum of β Lyrae,[1] *Mg* I may be expected. The effects of dilu-

* *Contributions from the McDonald Observatory, University of Texas*, No. 33.

[1] Greenstein and Page; *Ap. J.*, **93**, 128, 1941.

tion for *Mg* I are found to be similar to those observed in Pleione[2] and 17 Leporis[3] in the lines λλ 3828, 3829, and 3832. These lines arise from the same lower levels as do the lines λλ 5167, 5173, and 5184. The line λ 5173, $3^3P_1^0 - 4^3S_1$, should be relatively weakened if the dilution is high, since it is connected by an intersystem line to the ground level. The line λ 5173 is, in fact, seen and does not appear to be appreciably weaker than in α Cygni; it behaves like λ 5184, which arises from a metastable level. Either the dilution is not large, or the line is produced deeper down in the nebulous envelope, like *Si* II. If the latter were true, the line might be expected to be so shallow and weak, like *Si* II, that it might disappear. Struve and Swings[2] have shown that the dilution is actually not large.

O I.—At λ 6156 and λ 6158 a pair of *O* I lines is found in α Cygni. The lines are very weak but are present in Pleione. The lines arise from the state 3^5P which communicates with a lower $^5S^0$ state; the latter is metastable, and the lines at λ 3948 might be of interest. They are weak ($I = 1$) but unblended in α Cygni.[4]

S II, Mg II, and P II.—The lines of these elements arise from nonmetastable levels and are not found with certainty in Pleione. The *S* II lines are visible in α Cygni, and *S* II is a strong feature of the visual spectrum[1] of β Lyrae.

Certain unidentifiable lines have been found. A line near λ 5226.7 is apparently stronger than in α Cygni. In the latter it is a blend of *Fe* I and *Ti* II; its enhancement in Pleione must arise from an unidentified component. There is a strong, unidentified line in υ Sagittarii[5] at λ 5227.3. Another unidentified line strengthened in Pleione is λ 5371.3; it is also present in υ Sagittarii, where it is tentatively identified as *Al* II and *N* I—an identification which cannot apply to Pleione. A diffuse line at λ 5527.7 may be partly identified as *Mg* I. Again, this identification is unsatisfactory, since λ 5528.4 of *Mg* I arises from $3^1P_1^0$, which is nonmetastable. Near λ 5876 of *He* I a peculiar phenomenon was observed. On one plate two sharp lines (λ 5875.0 and λ 5877.0) were found; on two other plates only a diffuse feature at λ 5876.7 was seen. The line, or group of lines, is enhanced with respect to α Cygni. This behavior is rather surprising, in view of the nonmetastability and high excitation potential of the 2^3P levels. The line λ 5016, arising from the metastable level, 2^1S, was not seen.

YERKES OBSERVATORY
March 1940

[2] Struve and Swings, *Ap. J.*, **93**, 446, 1941.

[3] Struve and Roach, *Ap. J.*, **90**, 732, 1939.

[4] Struve, *Ap. J.*, **90**, 699, 1939.

[5] J. L. Greenstein, unpublished.

THE EMISSION LINES IN THE SPECTRA OF B 1985 AND WY GEMINORUM*

P. SWINGS AND O. STRUVE

ABSTRACT

The spectra of B 1985 and WY Gem show numerous emission lines in the ultraviolet region. These have been identified with [*Fe* II], *Fe* II, [*Cr* II], and *Cr* II. The permitted lines of *Fe* II and *Cr* II are relatively much stronger in B 1985 than in WY Gem. Lines of high excitation potential are relatively weaker in the stars than in the laboratory. The strength of forbidden [*Fe* II] in the shells of these stars suggests that the lifetimes of the metastable levels are considerably shorter than those of metastable levels of [*O* I], [*N* II], [*S* II], etc.

These two objects[1] are known to possess strong emission lines of ionized iron, both permitted and forbidden, and some of their characteristics have been recently discussed by the authors.[2] In WY Gem the forbidden lines of [*Fe* II] are considerably stronger than the permitted *Fe* II lines of the photographic region, whereas, in B 1985, the relative intensities of *Fe* II and [*Fe* II] are about the same as in η Carinae. Each of the two objects consists of an M-type star and of a hot companion approximately of type B3e. The authors have devoted several recent papers to the discussion of binaries of similar type, such as Z And, TC Br, AX Per, CI Cyg, α Sco, etc.; the present note is concerned with the bright lines not previously discussed. The observational material consists of (*a*) spectrograms on Eastman Process emulsion, extending from λ 3900 to λ 4900, taken with the glass spectrograph of the McDonald Observatory (dispersion 26 A/mm at $H\gamma$)[3] and (*b*) spectrograms taken in the ultraviolet region from λ 3100 to λ 3450 (dispersion 57 A/mm at λ 3220).

Besides bright H and K lines which are weakly present in B 1985, the material shows the following emissions: (1) permitted and forbidden lines of *Fe* II; (2) permitted and forbidden lines of *Cr* II; and (3) a forbidden line of *S* II.

IONIZED IRON

A. PERMITTED LINES

In the photographic region all the strong *Fe* II lines arise from excited levels between 5.3 and 5.6 volts, their lower levels lying between 2.6 and 2.9 volts. The photographic region is, therefore, not suitable for a discussion of the behavior of bright lines arising from widely separated excited levels. The situation is quite different in the region λλ 3130–3425, which contains strong *Fe* II lines arising from excited levels ranging from 4.8 volts (z^6D^0) to 8.6 volts (y^2F^0). Many *Fe* II lines have been observed in B 1985 and WY Gem in that region, and the results are summarized in Table 1, in which the lines have been classified according to increasing potential of the upper level.

This table clearly illustrates the effect of the excitation potential. A line of laboratory intensity 10 gives a stellar line of estimated intensity 5 when the excited level is around

* *Contributions from the McDonald Observatory, University of Texas*, No. 34.

[1] Boss 1985 = HD 60414–60415; −14°1971; α (1900) 7^h29^m2; δ (1900) − 14°18′; m = 5.2. WY Geminorum = HD 42474; +23°1243; α (1900) 6^h05^m8; δ (1900) +23°14′; m = 7.4 − 7.9.

[2] *Ap. J.*, **91**, 546, 1940.

[3] The spectrum of α Orionis was used for comparison, this spectrum being very similar to the late-type component of the two objects investigated.

5 volts and a stellar intensity of only 1 when the excitation potential is around 8 volts. The intensities are, thus, quite different from those which we should expect if the re-

TABLE 1

PERMITTED LINES OF *Fe* II OBSERVED IN EMISSION BETWEEN λ 3130 AND λ 3425 IN B 1985

TRANSITIONS		LABORATORY		INTENSITY IN B1985	REMARKS
		λ	Intensity		
$a^4D-z^6D^o$	$3\frac{1}{2}-3\frac{1}{2}$	3255.88	8	3	
(1.1 v.) (4.8 v.)	$3\frac{1}{2}-4\frac{1}{2}$	3277.35	9	4	
	$2\frac{1}{2}-2\frac{1}{2}$	3281.29	7	3	
	$1\frac{1}{2}-\frac{1}{2}$	3285.42	3	0	
	$1\frac{1}{2}-1\frac{1}{2}$	3295.81	6	1	
	$2\frac{1}{2}-3\frac{1}{2}$	3302.86	4	2	1
	$\frac{1}{2}-\frac{1}{2}$	3303.47	4		
$a^4P-z^4D^o$	$2\frac{1}{2}-1\frac{1}{2}$	3166.67	4	1–0	
(1.7 v.) (5.5 v.)	$1\frac{1}{2}-\frac{1}{2}$	3170.34	6	1–0	
	$1\frac{1}{2}-1\frac{1}{2}$	3186.74	11	3–4	2
	$\frac{1}{2}-\frac{1}{2}$	3193.81	11	5	
	$\frac{1}{2}-1\frac{1}{2}$	3210.45	10	4	
	$1\frac{1}{2}-2\frac{1}{2}$	3213.31	13	5	
	$2\frac{1}{2}-3\frac{1}{2}$	3227.73	13	6	
$a^4P-z^4F^o$	$2\frac{1}{2}-2\frac{1}{2}$	3163.09	5	3	3
(1.7 v.) (5.5 v.)	$1\frac{1}{2}-2\frac{1}{2}$	3183.11	8	4	
	$2\frac{1}{2}-3\frac{1}{2}$	3196.07	10	5	
$a^2P-z^4P^o$	$1\frac{1}{2}-\frac{1}{2}$	3416.02	5	0–1	
(2.3 v.) (5.8 v.)					
$b^2G-z^4H^o$	$3\frac{1}{2}-3\frac{1}{2}$	3289.35	7	1–0	3
(3.8 v.) (7.5 v.)					
$b^2F-z^2D^o$	$2\frac{1}{2}-1\frac{1}{2}$	3297.89	5	0	
(3.9 v.) (7.6 v.)					
$b^4D-y^4F^o$	$3\frac{1}{2}-4\frac{1}{2}$	3259.05	10	0–1	
(3.9 v.) (7.7 v.)					
$b^2G-z^2G^o$	$3\frac{1}{2}-3\frac{1}{2}$	3167.85	11	1	
(3.8 v.) (7.7 v.)					
$b^4D-x^4D^o$	$2\frac{1}{2}-2\frac{1}{2}$	3135.36	9	0–1	
(3.9 v.) (7.8 v.)	$3\frac{1}{2}-3\frac{1}{2}$	3177.53	10	1	
$c^2G-y^2G^o$	$3\frac{1}{2}-3\frac{1}{2}$	3162.80	8	3	4
(4.1 v.) (8.0 v.)	$4\frac{1}{2}-4\frac{1}{2}$	3187.29	8	3–4	4
$c^2D-y^2F^o$	$2\frac{1}{2}-2\frac{1}{2}$	3175.08	4	0–1	3
(4.7 v.) (8.6 v.)	$1\frac{1}{2}-2\frac{1}{2}$	3180.16	7	1–2	3

1. Possibly weakly blended.
2. Major contribution of a blend.
3. Blend.
4. Minor contribution of a blend.

combination process were predominant. A behavior of the observed type would be obtained in the case of excitation by electron collisions.

B. FORBIDDEN LINES

Besides the new forbidden transitions given in our previous paper,[2] among which the most prominent is a^4F-b^4D, the present material provides the following information. In the photographic region two faint emission lines have been observed at λ 4114.4 and λ 4249.1; they may be identified as $a^4F_{4½}-b^2H_{5½}$ (λ pred. = 4114.5) and $a^4D_{3½}-b^4D_{3½}$ (λ pred. = 4249.1). In the far ultraviolet region we shall consider four forbidden multiplets (Table 2).

The forbidden transition $a^6D_{4½}-b^4D_{3½}$ gives probably the major contribution to the stellar line; there is a permitted *Fe* II line at 3175.08 (lab. int. 4), but it arises from the very high level y^2F^0 at 8.6 volts; and, according to Table 1, it should not have any appreciable intensity in B 1985. The identification of $a^6D_{3½}-b^4D_{2½}$ is doubtful because of the discrepancy in wave length and because of the high stellar intensity. These results supersede our previous work on the same multiplet; in our first paper[2] the stellar line

TABLE 2

FORBIDDEN LINES OF *Fe* II IN THE ULTRAVIOLET REGION OF B 1985 AND WY GEM

Transition		λ Pred.	λ in B1985	Intensity in B1985	Remarks
a^6D-b^4D	$4\frac{1}{2}-3\frac{1}{2}$	3175.28	3175.3	0–1	Slightly blended
	$3\frac{1}{2}-2\frac{1}{2}$	3224.54	3223.7	2	Doubtful identification
a^6D-b^2F	$3\frac{1}{2}-2\frac{1}{2}$	3181.05	3180.6	1–2	Blended
a^6D-b^2G	$4\frac{1}{2}-4\frac{1}{2}$	3289.76	3289.2	1–0	Minor contribution
a^4F-c^2G	$4\frac{1}{2}-4\frac{1}{2}$	3164.26	3163.1	4n	Partial contribution in blend
	$3\frac{1}{2}-3\frac{1}{2}$	3217.51	3217.7	1–0	

λ 3290 had been attributed to a^6D-b^4D, but it is presumably due to a permitted *Fe* II line.

The transition $a^6D_{3½}-b^2F_{2½}$ (from doublet to sextet) is possibly the major contributor to the stellar line λ 3180.6 (int. 1–2). There is an *Fe* II line of intensity 7 at λ 3180.16, but it again arises from the high level y^2F^0 at 8.6 volts and should not produce a stellar intensity of 1–2; the identity remains uncertain.

The line $a^6D_{4½}-b^2G_{4½}$ gives only a minor contribution to a blend. In a^4F-c^2G, the transition $3\frac{1}{2}-3\frac{1}{2}$ appears to give the complete identification, whereas the line $4\frac{1}{2}-4\frac{1}{2}$ gives only a partial contribution to the observed stellar line. The present information with regard to [*Fe* II] is summarized in Figure 1.

IONIZED CHROMIUM

In the ultraviolet region several permitted *Cr* II lines are observed in emission. The observations are summarized in Table 3.

A fairly strong, bright line measured in both objects at λ 3993.10 may be attributed to [*Cr* II], $a^6S_{2½}-b^4D_{3½}$, as has been mentioned previously;[2] the excitation potential of b^4D is 3.1 volts.

IONIZED SULPHUR

A bright line has been measured in both objects at λ 4068.56. This is the strongest component of the transauroral pair of [*S* II] (exc. pot. 3.0 v.). In WY Gem a line had been measured by Redman[4] at λ 4068.8 and attributed tentatively to [*Fe* II]. The attribution to [*S* II] is now beyond any doubt.

[4] *Pub. Dom. Ap. Obs., Victoria*, **6**, 34, 1931; *M.N.*, **92**, 118, 1932.

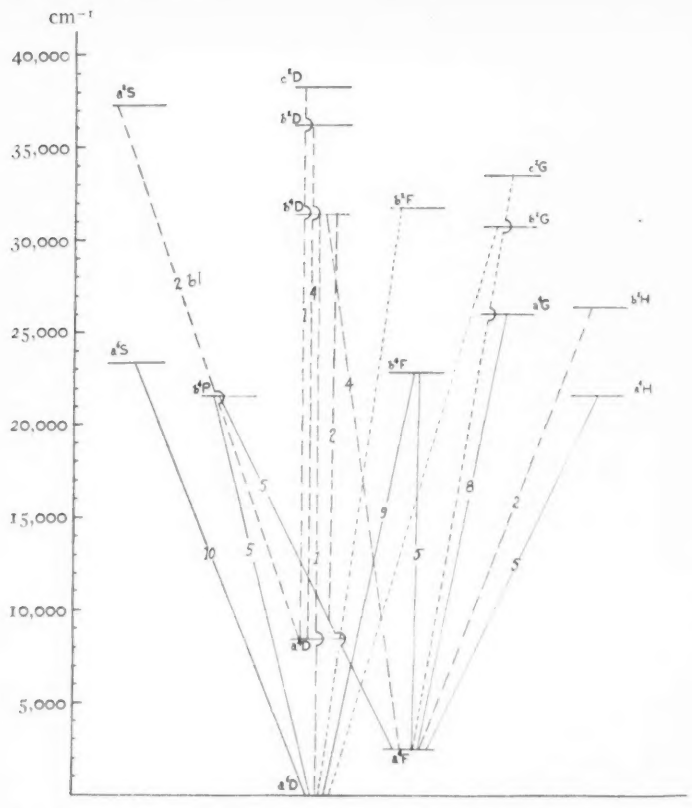

FIG. 1.—Forbidden lines of *Fe* II observed in B 1985 and WY Gem. *Full drawn lines:* forbidden transitions observed previously in other stars; *dashed lines:* new observed lines; and *dotted lines:* transitions probably present.

TABLE 3

PERMITTED LINES OF *Cr* II OBSERVED IN EMISSION IN B 1985

TRANSITIONS		LABORATORY		INTENSITY IN B 1985
		λ	Intensity	
$a^4D-z^4P^o$	$1\frac{1}{2}-1\frac{1}{2}$	3403.35	15	0–1
(2.4 v.) (6.1 v.)	$3\frac{1}{2}-2\frac{1}{2}$	3408.78	20	1–2
	$2\frac{1}{2}-1\frac{1}{2}$	3422.76	20	2
$a^4D-y^4P^o$	$3\frac{1}{2}-2\frac{1}{2}$	3368.06	20	0–1
(2.4 v.) (6.1 v.)				
$a^4D-z^4F^o$	$1\frac{1}{2}-2\frac{1}{2}$	3120.37	15	0–1n
(2.4 v.) (6.4 v.)	$2\frac{1}{2}-3\frac{1}{2}$	3125.00	20	0–1
	$3\frac{1}{2}-4\frac{1}{2}$	3132.06	20	1

The simultaneous presence of [*Fe* II] and of transauroral [*S* II] in the emitting atmospheres of B 1985 and WY Gem is very interesting. They also appear simultaneously in several other stars: η Carinae, HD 45677, VV Cephei, MWC 17, +11°4673 at certain stages. This should be related to the fact that in certain objects (e.g., MWC 17 and +11°4673) [*Fe* II] and [*N* II] appear together. It also happens that [*Fe* II] and [*O* I] are observed in the same bright-line star (e.g., MWC 17, HD 45677, and certain stages of novae).

REMARKS ON THE TRANSITION PROBABILITIES OF THE [*Fe* II] LINES

The simultaneous appearance of the forbidden lines of [*Fe* II] and of other elements throws some light upon the problem of the transition probabilities of the [*Fe* II] lines. We consider here the probabilities of transitions between various terms of the $3d^64s$ and $3d^7$ configurations; no computed probabilities are as yet available for such a complex case.

The intensity I of a forbidden line of frequency ν is given by

$$I = \frac{NA_1h\nu}{B + C + A_1 + A_2 + \ldots .}$$

where N is the number of atoms arriving per second in the upper state; $A_1, A_2, \ldots .$ are the probabilities of line emissions; B is the probability of removal from the upper level by a collision either of the first kind (gain of energy) or of the second kind (loss of energy); and C is the probability of removal by absorption If A is much greater than B and C (the normal case in nebulae), we have

$$I = \frac{Nh\nu}{1 + \frac{A_2}{A_1} + \ldots .} .$$

In the extreme case where $B + C$ is much greater than $A_1 + A_2 + \ldots .$, we have

$$I = \frac{NA_1h\nu}{B + C} .$$

In the intermediate cases of shells all factors should be considered.

We know that [*Fe* II] has never been observed in any planetary nebula, even if the excitation is low enough. For example, in BD+30°3639, [*Fe* II] is absent, whereas [*O* II] and [*N* II] are strong; in IC 418, [*O* II] is also very strong and [*O* III] is weaker; in neither case does [*Fe* II] appear. This is true for all planetaries even when [*O* I] is present. This absence may be attributed to one of two causes: the relatively low abundance of iron compared to the lighter elements or the distribution of electronic excitation among many levels. From the observation in nebulae of [*Fe* VII] and [*Fe* VI], which have only a small number of metastable levels and for which the transition probabilities are known,[5] it appears that iron must be less abundant than sulphur (by a factor of the order of 10), nitrogen, and oxygen (by a factor of 100).[6] Within the range of electron kinetic energy between 1.6 and 4.8 volts, *Fe* II possesses 50 sublevels, from $a^4P_{2\frac{1}{2}}$ (1.66 v.) to $c^2D_{1\frac{1}{2}}$ (4.72 v.), into which the Fe^+ atoms may be brought by collisions; the average distance between two sublevels is only about 0.06 volt. But, on the other hand, the collisional cross-section for a collision of the first kind between an electron and an atom is large when the kinetic energy of the elec-

[5] S. Pasternack, *Ap. J.*, **92**, 129, 1940.

[6] Bowen and Wyse, *Lick Obs. Bull.*, **19**, No. 495, 1939.

tron is only slightly above that necessary to bring the atoms to a higher level; for electrons of higher velocity the collisional cross-section falls off rapidly. The presence of a large number of sublevels will thus increase the exciting efficiency of the collisions with electrons, and it is by no means certain that the populations of the *Fe* II levels will be much reduced, in comparison with atoms with few low levels, such as *S* II, *N* II, or others. A more definite statement is at present impossible because the collisional cross-section is very sensitive to the structures of the colliding particles and to the relative velocities. Under nebular conditions the effects of de-excitation by collisions of the first or the second kind and by absorptions are unimportant. The only major factor is the number of atoms arriving per second in the excited states.

Thus, the absence of [*Fe* II] in nebulae suggests that under nebular conditions the combined effect of lower abundance and of the larger number of metastable states reduces considerably the intensity of the [*Fe* II] lines as compared to [*O* I], [*N* II], and [*S* II].

The observations show that the situation is quite different in the emitting layers of stars, such as B 1985, WY Gem, η Carinae, and others. In these shells the electron pressure is much higher than in most nebulae, as is shown by the predominance of the transitions of auroral type. The de-excitation of certain excited states by collisions or absorptions is no longer negligible.

The proximity of the metastable and ordinary excited levels of *Fe* II would tend to increase their de-excitation by collisions or absorptions, compared to [*O* I], [*N* II], or [*S* II], in which the ordinary levels lie rather high above the metastable states. Hence, unless we assume very peculiar abundances, we are tempted to seek the explanation for the strength of the [*Fe* II] lines in relatively high probabilities of these forbidden transitions.

In a nebula of low excitation, the lines of [*Fe* II] are much weaker than the lines of [*N* II] and [*S* II] by a factor of the order of 100. On the contrary, in certain stellar shells, despite the unfavorable conditions of de-excitation by collisions or absorptions, the [*Fe* II] lines are stronger than [*N* II] or [*S* II]. The transition probabilities for the auroral or transauroral lines are 2.2 sec^{-1} for [*O* I]; 2.2 sec^{-1} for [*N* II]; and 0.32 and 0.13 sec^{-1} for [*S* II]. The excitation potentials of [*S* II] and [*Fe* II] are practically the same. It is difficult to estimate how much of this phenomenon is due to ionization effects and how much to the transition probabilities. But it appears safe to assume that the strongest lines of [*Fe* II] have a transition probability appreciably higher than the forbidden lines of [*O* I], [*N* II], and [*S* II], the ratio being of the order of 100. A similar result would be obtained for configuration $3d^5$ of [*Cr* II].

McDonald Observatory
January 1941

STUDIES OF FAINT B-TYPE STARS*

CARL K. SEYFERT AND DANIEL M. POPPER

ABSTRACT

Magnitudes, color indices, spectral types, and radial velocities have been determined for 118 B-type stars, mostly between photographic magnitudes 9.0 and 11.0. A solution for galactic rotation, with $A = 17.5$ km/sec/kpc, yields a mean distance of the stars of 1.9 kiloparsecs, and a K term of -4.4 km/sec.

From the observed increase with color excess of the difference between apparent distance modulus and true distance modulus, the latter evaluated from the radial velocities, we find the ratio

$$\frac{\text{total photographic absorption}}{\text{color excess}} = 3.2 ,$$

where the color excesses are on the International System. The following values of absolute photovisual magnitudes are found from the radial velocities, apparent magnitudes, and total absorptions:

cB.....	-4.6	Bo.....	-4.4
O.....	-3.9	B2.....	-2.8

The correlation of color excess with apparent distance modulus is much better than the correlation with true modulus.

This investigation is based upon observations of radial velocities, magnitudes, colors, and spectral classes of 118 B-type stars between photographic magnitudes 8.2 and 11.6. Since the rotation of the galaxy is now an established fact and the constants defining the rotation have been determined within rather narrow limits, these additional observations of a relatively small number of B stars can contribute little to the study of the dynamics of our own system. Since faint B stars are distant and their peculiar motions are small, it is entirely feasible, even with such limited data, to determine their absolute magnitudes from a study of the reflection of the rotation of the galaxy on their radial velocities. This problem is, of course, complicated by the presence of absorption in the Milky Way plane, which reduces the apparent brightnesses of the stars. An approximate value of the absorption can be determined for each star from a consideration of the observed color of the star relative to the color of stars of similar type which are unaffected by absorption. Hence, with distances established through an analysis of the velocities and apparent magnitudes corrected for absorption, the absolute magnitudes of the B stars under consideration can be evaluated.

THE MATERIAL

The stars selected for study were chosen mainly from the *Henry Draper Catalogue and Extension*,[1] the *Bergedorfer Spektral-Durchmusterung*,[2] and the *Potsdamer Spektral-Durchmusterung*.[3] Only stars listed as fainter than 9.0 pg. mag. were chosen, in order to avoid duplicating material being obtained at the Victoria Observatory. Furthermore, stars listed as brighter than $10^{m}5$ of spectral class Oe–B5 between declinations 0° and $-23°$, included in the *Henry Draper Catalogue*, were avoided to prevent overlapping Dr. Neubauer's current investigation at the Lick Observatory of stars in that zone. We

* *Contributions from the McDonald Observatory, University of Texas*, No. 35.

[1] *Harvard Ann.*, Vols. **91–100**, 1918–1936.

[2] *Hamburger Sternwarte in Bergedorf*, 1935 and 1938.

[3] *Potsdam Pub.*, Nos. 90, 91, and 92, 1931–1938.

chose stars which had been listed in the catalogues as being between types Oe and B_5. In addition a number of stars listed as B, without any subgroup classification, were observed. An attempt was made to observe only the fainter of the later-type stars, B_4–B_5.

For the stars included in the present investigation, spectrograms have been obtained with the Cassegrain spectrograph[4] of the 82-inch McDonald reflector. The spectrograph, as we have used it, employs two glass prisms and is equipped with an f/2 Schmidt camera of 180-mm focal length, which combination produces a dispersion of 76 A/mm at $H\gamma$. In general, Agfa Superpan Press film was used, though some spectrograms were obtained on Agfa Superplenachrome Press film. The films were developed for 8 minutes in D-11 developer at 65° F.

It is desirable to use plates rather than film for radial-velocity work. Since the radius of curvature of the field of the f/2 Schmidt camera is about 6 inches, however, it is not suited to the use of plates if good definition is to be obtained over an appreciable wavelength range. Precautions were taken to reduce the effects of humidity and temperature changes. The spectrograph is thermostatically controlled; the films were clamped between metal plates over their full length and half their width by a strong spring; the comparison spectrum was exposed both near the beginning and near the end of each stellar exposure; care was taken in processing, that the temperatures of developer, rinse water, and fixing baths be within 5° F of one another.

The undesirable effects that might be expected from the use of film are (1) irregular distortion of the film and (2) systematic creeping of the film during exposure. That (1) is not large may be seen qualitatively from the smoothness of the reduction-curves used in radial-velocity determinations. To test (2) qualitatively, all exposures longer than 2 hours were examined carefully, and in no case did the definition of the comparison spectrum appear less sharp than on short exposures.

Objective tests of distortion and creeping were also made. The iron arc was exposed through that portion of the slit ordinarily occupied by the stellar image. After an interval of several hours the iron-arc comparison was exposed in the usual way. Eleven such exposures were made with an average interval of 6 hours between the two parts, corresponding to the exposure time on a star of about 11.6 mag. For control, exposures were made with only a few seconds' interval between the two parts. These controls were processed with the test exposures.

All the exposures were measured and reduced in the same manner as the stellar spectrograms, except that the displacements were expressed in microns (μ) rather than in kilometers per second. From the control exposures it was found that the probable error of the position of a single line is 0.8 μ. This is made up of errors of setting, errors in drawing the reduction-curves, and distortion of the films. Unfortunately, we have no data for the determination of an analogous quantity based upon measures of glass plates. The probable error of the position of a single line on the exposures with several hours between parts is 1.2 μ. This value includes systematic displacements. On these test exposures a systematic shift of the whole film between parts of the exposure as large as 2.5 μ may be experienced (average shift 1.2 μ for test exposures and 0.3 μ for control exposures); and systematic shifts of one end of the film with respect to the other as large as 3 μ may be found, though the shift was as large as 2 μ in only three cases. A slight dependence of these shifts upon time interval is present. Since on all stellar spectrograms the comparison spectrum was exposed both near the beginning and near the end of the stellar exposure, there is no reason to expect systematic effects of the order of the displacements found in the tests.

MAGNITUDES AND COLORS

For all but 25 of the stars included in this investigation photographic magnitudes on the International System were determined by means of plates taken with the 3-inch

[4] A description of this instrument may be found in *McDonald Obs. Contr.*, No. 1, p. 74, 1940.

Ross photographic camera (focal length 21 inches) and the 6-inch UV telescope (focal length 32 inches). The zero point and scale of each plate were determined by comparisons with stars of the North Polar Sequence. Photographic magnitudes of 17 stars for which no Ross or UV plates were available were taken from the *Bergedorfer Spektral-Durchmusterung* and were adopted after applying to them a correction of $+0^{m}.1$ to reduce them to the system of this investigation. Finally, for 8 stars it was necessary to obtain rough photographic magnitudes from the strength of the continuum in the photographic region of the spectrum as a function of time and conditions of exposure.

The color of each star on the International System (i.e., $m_{pg}-m_{pv}$) was determined by one or more of the following methods: (*a*) from photovisual magnitudes obtained with the 3-inch Ross photovisual camera used with a yellow filter over the objective; (*b*) from photovisual magnitudes obtained with the 6-inch UV telescope with a yellow filter placed between the objective and the photographic emulsion; (*c*) from measures of the spectrograms themselves, concerning which more will be said below; and (*d*) from the reduction to the International System of photoelectric colors determined by Stebbins, Huffer, and Whitford.[5] The photovisual magnitudes mentioned in (*a*) and (*b*) were determined by means of comparisons with stars of the North Polar Sequence, and the colors were obtained by combining the photovisual magnitudes so determined with the photographic magnitudes mentioned in the preceding paragraph.

Colors obtained from measures of the spectrograms (method [*c*]) were determined in the following manner. Each spectrogram was measured in four different wave-length regions by means of a null-type photometer built by Seyfert.[6] The photometer was equipped with a slit which produced an image on the emulsion 0.6 mm long and 0.1 mm wide. Measures with this slit in the photometer gave a determination of the integrated intensity, on an arbitrary scale and zero point, at the following wave lengths:

λλ	λ̄
4160–4202	4181
4282–4325	4303
5233–5326	5279
5500–5615	5557

The calibrations for intensities on each night were effected by means of exposures made with a tube sensitometer. The zero point of the color scale was established each night by means of a spectrogram of a B-type star for which Stebbins, Huffer, and Whitford[5] have determined the color with a photoelectric cell, henceforth referred to as the "standard star." Measures in the photometer at the wave lengths noted above were made on the standard-star spectrogram together with measures of the exposures on the sensitometric strips, making it possible to reduce the measures of the spectrograms of a star of unknown color to intensities. The measures at the two blue wave-length regions were combined to give a mean intensity measure in the blue, and a similar procedure was used for the two measures in the photovisual region of each spectrogram. The mean effective wave lengths of the measures of color from the spectrograms are

$$\lambda_{pg} = 4240\ \text{A}$$

and

$$\lambda_{pv} = 5420\ \text{A}\,.$$

The ratio, on a magnitude scale, of the mean intensities at the two mean wave lengths produced a color, on a scale close to that of the International System, for each star for

[5] *Ap. J.*, **91**, 20, 1940.

[6] This instrument is described in *Ap. J.*, **91**, 117, 1940.

which a suitable spectrogram was available.[7] Corrections for differential extinction were applied.

In order to establish a color scale, three sets of spectrograms of ten B-type stars of widely different color, for which Stebbins, Huffer, and Whitford have determined colors with the photoelectric cell, were obtained and measured as described above. The photoelectric colors, reduced to the International System by means of material kindly furnished us in advance of publication by Dr. W. W. Morgan, were then used to bring our spectral colors to the International Scale. Finally, it should be mentioned that when it was considered that atmospheric refraction might appreciably affect the measures of colors from the spectrograms (i.e., at zenith distances greater than 45° or greater than 30° in good seeing) the spectrograph was turned at such an angle as to make the slit perpendicular to the horizon, so that the atmospheric spectrum was oriented along the length of the slit.

A check on the accuracy of the colors determined from the spectrograms is afforded by means of comparisons of the colors so determined with the colors independently determined from the Ross and UV cameras. For 87 stars for which colors have been determined with the Ross cameras and from the spectrograms, the mean difference, $C.I._{Ross} - C.I._{Spectra}$, is $-0^m.01$ (average difference without regard to sign, $\pm 0^m.17$). For 37 stars for which colors have been determined both with the UV camera and from the spectrograms, the average difference is $C.I._{UV} - C.I._{Spectra} = +0^m.11$ (average difference without regard to sign, $\pm 0^m.15$). A preliminary investigation leads us to believe that most of this latter difference is due to an unknown source of error in the photographic magnitudes determined with the UV camera, and therefore a correction of $-0^m.11$ has been applied to the photographic magnitudes, and hence to the colors, obtained with the UV camera.

From the internal agreement between measures we find

p.e. of one color determined with the Ross cameras = ±0.10,
p.e. of one color determined with the UV camera = ±0.11,
p.e. of one color determined from two spectrograms = ±0.08.

Since the color of each star in the table of observations, part I, is determined, on the average, from 2.5 different sources (counting a mean color from 2 spectrograms as one source), the p.e. of a final color in part I of the table is $\pm 0^m.06$. The p.e. of a color of part II of the table is $\pm 0^m.07$.

RADIAL VELOCITIES

The spectrograms were measured in the customary manner. Measures were recorded to 0.001 mm, which corresponds to about 4.5 km/sec. Only in a small percentage of cases were lines measured of a wave length greater than λ 4500. Hydrogen and helium lines contribute the preponderance of the weight for most stars. Though the K line was measured whenever possible, it was never combined with the other lines in forming the mean velocity. The wave lengths used for the stellar lines, as well as those used for the iron-arc comparison spectrum, are the laboratory values. The velocities were reduced to the sun by Van Biesbroeck's graphical method.[8] The probable errors of the measures and the agreement between measures of two or more spectrograms of the same star are indicated in the table of observations.

In order to reduce our velocities to the system of Moore's catalogue,[9] 58 spectrograms of 23 B-type stars considered to have constant velocity were measured. The differences —Catalogue *minus* measure—were weighted according to the probable errors of the

[7] Only spectrograms exposed on Agfa Superpan Press film were used in this manner for the determinations of colors.

[8] *Ap. J.*, **64**, 258, 1926.

[9] *Lick Obs. Pub.*, Vol. **18**, 1932.

measures and of the catalogue values. The resulting correction, which was applied to all our measured velocities, is -2.1 ± 0.8 km/sec. The probable error is disappointingly large and leaves the correction somewhat uncertain.

The question of variability of the radial velocity of a star cannot be decided with finality on the basis of 2 spectrograms. If the difference of the measured velocities of a star from any 2 spectrograms exceeded five times the larger probable error of measurement, the fact has been indicated by the comment, "velocity variable?" in the notes in the table of observations. Thirteen per cent of our stars with 2 or more spectrograms fall into this category. Plaskett and Pearce have estimated[10] that about 30 per cent of the B-type stars are spectroscopic binaries.

SPECTRAL CLASSIFICATION

The spectra were classified according to the system of E. G. Williams.[11] For the O-type stars H. H. Plaskett's paper[12] was consulted. One hundred spectrograms of 35 stars served as standards. Williams' classifications differ in some of the subdivisions from those of Victoria.[13] Whenever the discussion of our material requires conversion from one system to the other, we have used the following correspondence:

Williams.....	B0	B1	B2	B3	B4	B5	B6	B7	B8
Victoria.....	O9.5	B1	B2	B2.6	B3	B4	B5.4	B7	B8

The correspondence is none too well determined and appears to depend systematically on line character from B3 to B6. We have preferred to use Williams' system because his criteria are well defined; he has given a list of accurately evaluated standard stars; all subdivisions are used; and systematic effects depending on luminosity and line character are ostensibly avoided.

As Williams emphasizes, the primary criteria for spectral classification should be ratios of line intensities. His Figures 1 and 5 show, however, that absolute intensities are of considerable assistance, particularly for types O8 to B2. For types B2 and later, the fundamental criterion must be the ratio *H*/*He*. *Mg* II 4481 appears to be a considerably better criterion of luminosity than of spectral type. The type adopted was decided upon by simultaneous examination of all spectrograms of a star. In order to obtain an evaluation of the accidental uncertainty of these types, classifications were made from the individual spectrograms independently. The average difference of these latter estimates from the adopted classification was one-half of a subclass. This is an upper limit to the accidental uncertainty of classification, except for stars with very poor lines, since in its determination full weight was given to poorly exposed spectrograms and to those of stars with poor lines. Stars with particularly diffuse lines are indicated by the symbol *n* in the table of observations. Spectral types for these stars are somewhat less certain than for the others. When the type is only a rough estimate, the subclass is inclosed in parentheses.

In the luminosity classification we have not made use of an "intermediate" class, as has Williams, and have employed the symbol *c* rather than *g* for highly luminous stars. A few stars have been called c^-, and a few, considered to be slightly brighter than the main sequence, have been indicated by the comment "luminous?" in the footnotes to the table. The fundamental criterion of luminosity in spectral types B2 and later is the

[10] *Pub. Dom. Ap. Obs., Victoria*, Vol. 5, No. 2, 1931.

[11] *Ap. J.*, **83**, 109, 1936.

[12] *Pub. Dom. Ap. Obs., Victoria*, Vol. 1, No. 30, 1922.

[13] *Pub. Dom. Ap. Obs., Victoria*, Vol. 5, No. 1, 1931.

intensity of the hydrogen lines. For types B4 and later a c star is easily distinguished from a main-sequence star. For these types the strength of *Mg* II 4481 is an aid to luminosity classification. For types B2 and B3 it is more difficult to detect the wings of the hydrogen lines on spectrograms of such low dispersion as ours, and hence the luminosity classification is more difficult. For these types, as well as for types B1 and B4, the ratio of the helium lines, λλ 3964 and 4026, has been found to be a fairly reliable criterion. The line λ 3964 is enhanced in the spectra of c stars. Since the lower energy-level of this line is metastable, we should expect the line to be enhanced in the spectra of stars with extended atmospheres, such as those of the supergiant stars.[14]

It is nearly impossible for us to make a luminosity classification for types earlier than B2 on the basis of hydrogen-line intensities. Hence, we must use the strengthening of lines other than hydrogen and helium in the supergiant stars. Even this criterion is of little assistance in types Bo and earlier. Thus, on the basis of the stellar spectra alone, it appears to us that the supergiant branch merges with the main sequence near type Bo. This point is brought out again in the discussion of the observational data. Since all our stars are distant, it is considered inadvisable to employ color excess or interstellar K-line intensity as an indication of luminosity.

THE TABLE OF OBSERVATIONS

The table of observations is divided into two parts. In part I are listed data for the 96 stars for which we have obtained 2, or in a few cases, 3 spectrograms. Part II contains data for 22 additional stars for which we have obtained only 1 spectrogram. Nearly all the stars of part II have poor lines.

The first column of the table gives the designation of the star. In most cases this is the *Henry Draper Catalogue* number. Numbers larger than 225300 are to be found in the *Henry Draper Extension* (*Harvard Ann.*, Vol. **100**). If the designation is hyphenated, the star is listed by Selected Area and number in the Area, as taken from the *Bergedorfer Spektral-Durchmusterung* (northern declinations) or from the *Postdamer Spektral-Durchmusterung* (southern declinations). A few stars, listed by BD number, are to be found in *Yale Transactions*, Volume **11** or **12**. The 1900 positions were taken from these same sources. Galactic co-ordinates (fourth and fifth columns) were interpolated from the Lund Observatory table.

The photographic magnitude (sixth column), if listed to two decimals, was obtained from Ross plates or from UV plates. If only one decimal is given, without colon, the Bergedorf magnitude, increased by 0.1 mag., is listed. The magnitudes of a few stars were estimated from the densities of the spectrograms combined with the exposure times. These magnitudes are given to one decimal, followed by a colon. The determinations of color index and spectral type (seventh and eighth columns) have already been discussed.

The radial velocities in the ninth and tenth columns are the weighted means of the measures, decreased by 2.1 km/sec. The two letters following the stellar velocities have the following significance. The small letters designate the root means of the squares of the individual probable errors of measurement of the 2 or 3 spectrograms, computed from the agreement between the various lines measured. The capital letters designate the probable errors of the mean velocities given in the table, computed from the agreement between the two or three measures. Their meaning is as follows:

a and A	.....	0 to ± 4.1	km/sec
b	B	± 4.1	8.0
c	C	8.1	12.0
d	D	12.1	16.0
e	E	±16.1	±20.0
f	F	>±20.0	

[14] Struve and Wurm, *Ap. J.*, **88**, 105, 1938.

If the capital letter is omitted, only one or none of the spectrograms of the star yielded a radial velocity.

For the K-line velocities the capital letter has the same meaning as for the stellar velocities. The italicized letter in the next column serves as an indication of the intensity of the K line according to eye estimates. The scale of intensities, established by comparison with the K line on spectrograms of standard stars for which intensities have been measured by Williams,[15] is roughly as follows:

a	>0.7	equivalent angstroms
b	0.6–0.7	
c	0.4–0.5	
d	0.3	
e	<0.3	
None	Too weak to be visible; probably weaker than 0.15 equivalent angstroms	

The word "weak" indicates that the spectrograms are too poorly exposed to show the K line.

An *R* in the last column refers to a remark in the notes at the end of the table.

DISCUSSION

The data presented here are for a relatively small number of B-type stars, not well distributed along the Milky Way. Seventy per cent of the stars lie between longitudes 40° and 150°. We hope that more observations will be added in the future. A few tentative conclusions, however, may be drawn now from the material.

Solutions for $A\bar{r}$ and for K in the galactic-rotation formula,

$$\rho \equiv V + V_{\odot} \cos \lambda = A\bar{r} \sin 2(l - l_0) \cos^2 b + K ,$$

were carried out separately for stellar and for interstellar velocities. V is the observed radial velocity. The solar-motion term, $V_{\odot} \cos \lambda$, where $V_{\odot}$ is the solar velocity and λ is the angular distance, star to apex, was obtained from the chart of Pearce and Hill.[16] The longitude of the center of rotation, l_0, was taken to be 325°. The mean distance of the stars is given by $\bar{r}$. Second-order terms were neglected. We included in the solutions only velocities of classes A, B, and C, i.e., with probable errors less than 12.1 km/sec. They were assigned weights 4, 3, and 2, respectively. For each solution we formed nine normal points, combining velocities for stars 180° apart in longitude. The values obtained from these solutions are as follows:

Solution	No. of Stars	$A\bar{r}$	K
Stellar	67	34.3±1.5(p.e.) km/sec	−4.4±1.0(p.e.) km/sec
Interstellar	68	16.6±2.6	−3.6±1.8

Thus, if A is 17.5 km/sec/kpc,[17] the stars observed by us are at a mean distance $\bar{r}$ of 1.9 kiloparsecs. The K term has the same sign as that found by Trumpler[18] for galactic clusters and mentioned by him for other distant objects.

[15] *Ap. J.*, **79**, 280, 1934.

[16] *Pub. Dom. Ap. Obs., Victoria*, Vol. **6**, No. 4, 1931.

[17] R. E. Wilson, *Ap. J.*, **92**, 170, 1940.

[18] *Ap. J.*, **91**, 186, 1940.

TABLE 1

OBSERVATIONS OF B STARS

STAR	α 1900	δ 1900	l	b	m_{pg}	C.I.	SPEC.	STAR VEL.	K LINE		REMARKS
									Vel.	Int.	
	Part I										
236589....	0^h52^m1	+55° 53′	92	− 6	8.90	−0.11	B0.5	− 53bB	−38A	*c*	
8-1482....	0 52.1	+61 24	91	0	9.4	+ .35	cB2	− 30bA	−12D	*c*	
8-1128....	1 1.8	+60 1	93	− 2	10.16	− .01	B1.5	+ 6bA	−31B	*b*	
236644....	1 5.3	+57 4	93	− 5	9.61	− .20	B3	− 70cD	−34A	*b*	R
236664....	1 7.4	+58 35	94	− 3	9.98	− .15	B4n	—f	−32:	*d*	
236683....	1 11.0	+58 22	94	− 3	9.80	− .15	B2	− 34bB	−45B	*b*	R
236827....	1 35.1	+59 5	97	− 2	9.49	+ .01	B3.5	− 42bA	−17A	*d*	
232534....	1 42.2	+50 38	100	−10	9.54	− .19:	B(3)neα	−105cD	− 3B	*d*	
236896....	1 45.9	+59 58	98	− 1	9.86	+ .01	B5	− 47bA	−26B	*c*	
236917....	1 52.3	+55 39	100	− 5	9.83	− .09	B4neα	− 22bB	−45B	*d*	
236954....	2 5.5	+58 43	101	− 1	9.68	+ .35	c⁻B2.5	− 49bA	−29B	*d*	R
236960....	2 17.7	+58 47	102	− 1	9.88:	+ .29:	B1	− 45bA	0B	*d*	
236963....	2 20.9	+56 11	104	− 3	9.36	− .20	cB2.5	− 36bA	−13B	*c*	
236971....	2 28.4	+57 3	104	− 2	9.63	+ .23	B1	− 51bA	− 4B	*c*	
236995....	2 37.6	+58 7	105	− 1	8.82	+ .21	cB6	− 51bA	−28A	*a*	R
237011....	2 43.9	+60 9	105	+ 2	10.44	+ .19	B1.5	− 40cC	− 9A	*d*	
237019....	2 45.7	+60 3	105	+ 2	9.04	+ .01	O7	− 68cB	−22C	*e*	
9-911.....	2 53.4	+60 12	106	+ 2	10.53	+ .33	B1n	+ 10cF	−22B	*e*	R
9-1612....	3 0.4	+61 1	106	+ 3	10.8	+ .43	B(6)neα	—f	+ 8	*d*	
237153....	3 26.6	+58 19	110	+ 4	9.97	+ .70	c⁻B3	− 39bA	−47A	*d*	
237174....	3 38.3	+57 12	112	+ 3	9.26	− .12	B3	− 13bA	− 7A	*d*	
23-1640...	3 46.2	+45 17	121	− 5	10.9	+ .09	B8	− 2eD	−20C	*d*	
237213....	3 56.5	+55 44	115	+ 3	8.97	+ .32	cB3	+ 13aA	−14A	*b*	
232932....	4 10.1	+50 42	120	+ 1	9.33	− .06	B5	− 9bB	+10F	*e*	
232947....	4 17.6	+53 11	119	+ 4	9.59	+ .23	B0	− 44cC	−21A	*c*	
232971....	4 23.7	+53 36	120	+ 5	9.49	+ .07	B5neβ	− 37e	0	*e*	R
24-1035...	4 31.7	+46 33	126	+ 1	10.7	+ .08:	B4.5	− 31cF	−14A	*e*	R
24-554....	4 39.2	+44 3	128	0	10.6	+ .14	B2e	− 13bC	−10B	*c*	R
24-211....	4 42.1	+43 35	129	0	10.9	− .21	B4	− 12bD	− 2	*d*	R
24-986....	4 47.8	+45 53	128	+ 3	11.2	+ .10:	B(4)neγ	− 46eB	−26B	*c*	R
24-738....	4 48.1	+44 47	129	+ 2	10.8	+ .15	B4	− 1bA	+ 4A	*e*	
243035....	5 16.9	+33 28	141	0	10.76	− .14	B0	− 12fE	+41A	*e*	
243070....	5 17.1	+33 29	141	0	10.94:	− .10:	B1.5	− 10cB	+11A	*b*	
25-459....	5 28.5	+44 13	133	+ 8	10.6	+ .02	B7	− 22cA	−10A	*c*	
245967....	5 33.7	+34 3	143	+ 3	10.46:	+ .17:	B3	+ 9bC	− 4	*e*	
248890....	5 48.0	+31 8	147	+ 4	10.35:	− .16:	B3.5	− 10dB	+11B	*d*	
248903....	5 48.1	+31 9	147	+ 4	9.40	− .21	B3	0bD	−23A	*e*	R
249179....	5 49.6	+28 46	149	− 3	9.71	− .12	B(5)neβ	+ 34dE	+22	*d*	
250289....	5 55.0	+23 20	154	+ 2	8.60:	+ .30	c⁻B4	+ 14bC	+ 8A	*c*	R
253214....	6 6.4	+20 7	158	+ 2	9.5:	+ .08	B4neβ	− 7dC	+ 1A	*d*	R
254755....	6 12.5	+22 43	157	+ 5	9.2:	+ .36:	O9	+ 3bB	−10A	*d*	R
265134....	6 45.9	+13 44	168	+ 8	8.85	− .25	O9n	+ 23bD	+10B	*c*	R
123-501...	7 11.2	−15 3	197	0	10.38	− .03	B7	+ 52cE	+37A	*d*	
123-548...	7 11.6	−14 37	197	0	10.47	− .24:	B5.5	+ 65cC	+30E	*e*	
123-822...	7 13.7	−15 27	198	0	8.60	−0.11	c⁻B3	+ 66cB	+46A	*c*	

TABLE 1—*Continued*

Star	α 1900	δ 1900	l	b	m_{pg}	C.I.	Spec.	Star Vel.	K Line		Remarks
									Vel.	Int.	
123-1778	7^h21^m6	−14°53′	198	+ 2	9.00	−0.03	cB1.5	+ 82aA	+47A	*c*	
65886	7 55.8	−25 48	211	+ 3	9.22	− .20	B4	+ 42eF	+47	*b*	
172-905	8 37.8	−44 55	232	− 1	8.39	+ .01	cB1.5	+ 33bC	−12	*d*	
172-1789	8 46.8	−45 10	233	0	8.69	− .01	B1n	+ 6fF	0A	*d*	
172-1822	8 47.2	−45 11	233	0	9.43	− .10	B2	− 19bA	− 5E	*d*	
172-1864	8 47.8	−45 18	233	0	8.78	− .07	Bc.5	+ 26cE	+16	*e*	R
172-2000	8 49.9	−45 40	234	0	9.10	+ .33	B1	+ 17dA	Weak		
233622	9 14.7	+50 31	135	+45	9.2:	− .26	B3.5n	+ 26cD	None		
123884	14 5.1	−17 31	297	+40	9.2:	− .10:	cB6	+ 5aB	−14A	*e*	R
148989	16 26.7	−48 40	303	− 2	8.92	− .05	cB1	− 40dC	Weak		
152386	16 47.9	−44 50	309	− 2	8.21	− .10	O8f	− 17cA	−13A	*c*	R
−18°4365	16 52.4	−19 4	330	+13	9.2:	− .30	B1	+ 19bB	−34A	*e*	
154313	16 59.6	−42 12	312	− 2	9.22	+ .22	O8	− 29bA	−50	*c*	
155134	17 4.6	−41 40	313	− 3	8.93	+ .01	B2	− 18aA	−20A	*e*	
155336	17 5.8	−32 58	320	+ 2	9.24	− .23	B2	− 1bB	−16A	*c*	R
164019	17 54.0	−28 36	330	− 4	8.93	+ .01	O9	− 31bA	− 3B	*d*	
134-292	18 4.9	−16 44	341	0	9.25	− .16	B1.5	− 23bA	− 8A	*c*	
−19°4955	18 12.2	−19 10	340	− 3	10.0:	+ .63	cB1.5	+ 6bA	−25	*c*	R
−12°4982	18 12.6	−12 13	346	0	9.55	+ .57	Bo	+ 24bA	− 2	*d*	
168941	18 17.2	−27 0	333	− 8	8.93	− .27	O9.5	+110bC	−14A	*e*	
230211	18 52.9	+14 16	14	+ 4	9.93	+ .17	B4eδ	− 3bA	+ 5A	*d*	
231285	19 18.9	+15 1	18	− 1	10.3:	+ .35	Bo.5n	− 14cC	+ 1A	*b*	
231616	19 25.9	+18 3	21	− 1	10.8:	+ .44	B3	+ 13bC	−26A	*e*	
226868	19 54.6	+34 56	39	+ 2	9.35	+ .35	Bo	− 12bA	−24B	*d*	
226951	19 55.5	+35 51	39	+ 2	8.91	− .06	Bo.5	− 8bC	−10B	*e*	R
227018	19 56.1	+35 2	39	+ 2	9.05	+ .11	O6	+ 41bB	− 12C	*c*	
227245	19 58.6	+35 24	40	+ 2	9.93	+ .26	O8	− 13bA	− 4A	*d*	
227424	20 0.2	+33 17	38	0	10.12	− .11	B3.5n	− 44cF	+30B	*d*	R
227728	20 3.2	+37 44	42	+ 2	9.70	− .11	B2	− 18bA	−30A	*c*	
227960	20 5.4	+35 45	40	0	9.17	− .12	O8.5	− 8bB	−16A	*c*	
228053	20 6.3	+36 24	41	+ 1	8.84	+ .09	cB1	+ 7bA	−11A	*c*	
228199	20 7.7	+36 12	41	+ 1	8.74	+ .05	Bo.5	+ 4bA	−20A	*d*	
235350	20 42.2	+50 50	57	+ 5	9.21	+ .10	B2.5	− 18bA	− 6C	*e*	
239626	21 15.0	+59 41	67	+ 7	9.74	+ .35	Bo.5	− 20bB	−22A	*e*	
41-2761	21 50.7	+46 21	62	− 6	10.7	− .16	B3	− 50cC	−17B	*b*	
235673	21 54.0	+52 20	66	− 2	9.05	+ .07	O7.5	− 42cB	−23A	*c*	
239812	21 54.4	+59 33	70	+ 4	10.21	− .12	B8	+ 18eD	+33:	*e*	
239828	21 58.1	+59 1	70	+ 3	9.98	+ .44	cB4	− 42bB	−40C	*b*	
239923	22 15.8	+58 27	72	+ 2	9.41	+ .45	cB4	− 40bE	−13C	*d*	R
235807	22 17.4	+55 3	70	− 2	9.47	− .10	B1	−118cE	−23B	*c*	R
239989	22 28.3	+60 10	74	+ 2	10.09	+ .08	B3.5	− 37bA	−33A	*e*	
235874	22 28.9	+50 42	70	− 6	9.18	− .22	B3.5	− 56cA	−23B	*c*	
235989	22 49.3	+52 6	73	− 6	9.16	− .25:	B(4)n	− 85cE	−33B	*c*	
240165	22 58 0	+56 39	76	− 3	10.31	+ .18:	Bon	− 84eE	Weak		
236044	23 2.6	+54 12	76	− 5	9.30	− .01:	Bo	− 37bB	−18D	*b*	
19-315	23 10.1	+59 3	79	− 1	11.0	+ .27	B1	− 66cA	−39B	*b*	
19-363	23 11.7	+59 48	79	0	11.3	+ .21	B1.5	− 75cA	−18A	*d*	
19-1778	23 18.5	+61 35	80	+ 1	11.1	+ .43	O7	− 76dC	−17:	*b*	
19-1233	23 21.6	+60 10	80	0	11.30	+ .35	B3.5	− 25bA	−26B	*c*	
240319	23 26.9	+58 33	80	− 2	10.41	+ .27	B4	− 50cD	+ 5B	*e*	
240458	23 52.5	+55 18	83	− 6	9.34	+0.03	B4neα	− 20dF	−24B	*c*	

TABLE 1—*Continued*

Star	α 1900	δ 1900	*l*	*b*	m_{pg}	C.I.	Spec.	Star Vel.	K Line Vel.	K Line Int.	Remarks
	Part II										
8-1162	1h 2m9	+60° 6′	93	− 2	9.28	+0.25	B1n	− 34f	−19	*d*	
8-1717	1 8.1	+61 10	93	− 1	11.6	− .02:	B5n	− 7c	−52:	*c*	
8-736	1 10.2	+59 40	94	− 2	11.1	+ .24	B3n	+ 4f	−36	*e*	
237007	2 42.8	+59 59	105	+ 2	9.45	− .20	B2	− 96d	− 1	*e*	
24-491	4 33.8	+44 20	128	− 1	11.3	+ .23:	Bn	—f	Weak		R
24-1094	4 39.9	+46 2	127	+ 2	11.5	+ .47:	B5neβ	− 22f	−30	*e*	
123-96	7 7.7	−14 18	196	− 1	10.17	+ .11	Bneβ	—f	+47	*d*	
123-414	7 10.6	−15 10	197	− 1	9.95	+ .14	Bneγ	+ 28f	+29	*e*	
123-778	7 13.3	−15 54	198	0	10.68	+ .14	B4	+ 6d	+24	*d*	
147756	16 18.6	−45 19	305	+ 2	8.17	− .30	B(4)nea	− 9e	−18	*e*	
153295	16 53.4	−42 10	312	− 1	9.13	+ .12	Bneγ	+ 7c	Weak		
162718	17 47.3	−24 45	332	− 1	9.11	+ .50	Bneγ	− 13f	+20	*e*	R
163667	17 52.2	−31 47	327	− 5	8.61	− .02	B1.5n	+ 15f	−54	*e*	
166056	18 3.8	−24 8	335	− 4	9.18	− .10	B3	+ 44a	Weak		
227173	19 58.0	+35 16	40	+ 2	10.95	+ .06:	B4.5n	− 28d	−49	*e*	
227611	20 2.0	+35 37	40	+ 1	8.58	− .13	Bneδ	− 24f	− 1:	*c*	R
227991	20 5.8	+37 31	42	+ 1	10.09	+ .07	B8	− 43a	−19	*d*	
228256	20 8.4	+39 43	45	+ 3	10.34	+ .07:	Bneβ	—f	−36:	*c*	
228279	20 8.6	+37 17	43	+ 1	10.28	+ .07	B4n	+ 10d	−12	*e*	
239758	21 41.6	+58 36	68	+ 4	9.30	− .14	B5nea	+ 11f	−11	*d*	
239772	21 45.1	+58 31	69	+ 4	9.93	− .22	B8n	—f	None?		
240372	23 38.4	+58 26	82	− 3	9.79:	+0.80:	B7	− 44c	Weak		

REMARKS

236644 Velocity variable? Two spectra visible

236683 Luminous?

236954 Three exposures

236995 K line partly stellar?

9-911 Velocity variable?

232971 MWC 85

24-1035 Velocity variable?

24-554 Velocity variable? All the hydrogen lines visible on our spectrograms, i.e., to $H\zeta$, inclusive, show emission lines superposed on broad absorptions

24-211 Velocity variable?

24-986 Three exposures

248903 Velocity variable?

250289 Velocity variable?

253214 MWC 135

254755 Velocity variable? Three exposures

265134 Lines poorer than class b probable errors would indicate; three exposures

172-1864 Two spectra visible? Velocity variable?

123884 K line mostly stellar? This star appears to be approximately 3 kiloparsecs from the galactic plane

152386 The following lines are in emission: *Hα*, *Hβ*, *He* II 4686, *N* III 4640, 4634, 4097 (4103 not strong enough to be verified), *Si* IV 4088, 4116

155336 Luminous?

−19°4955 *C* II 4267 much stronger than in any other star observed. Three exposures

226951 Two spectra visible? Velocity variable? Three exposures

227424 Velocity variable?

239923 Velocity variable?

235807 Velocity variable?

24-491 *Hα* weak emission?

162718 MWC 273

227611 MWC 327

It is readily seen in the table of observations that the color indices of the stars, and consequently their color excesses, lie within a large range of values. Because of this fact we are able to obtain empirically a provisional value for the important ratio

$$\frac{\text{total photographic absorption}}{\text{color excess}} \equiv \frac{A_{pg}}{E} \equiv \chi .$$

The color excess E is defined as the observed color index *minus* the normal color index for the spectral type. A_{pg} can be evaluated by determining the differences of the apparent distance moduli, $m - M$, and the true distance moduli,

$$m_0 - M = -5(1 - \log r) ,$$

where the distances r are evaluated from the radial velocities. Photographic magnitudes are used throughout.

By definition,

$$m_0 = m - A_{pg} = m - \chi E . \tag{1}$$

Then, for a small range in E we may write

$$\overline{m - M} + 5(1 - \overline{\log r}) = \chi \bar{E} . \tag{2}$$

It is not necessary to assume that $m - M$ is constant over each interval of E. Instead, for each star we write,

$$M = \bar{M}_{B2} + \Delta M ,$$

and assign values of ΔM as a function of spectral type. Then equation (2) may be written in the form,

$$\bar{M}_{B2} + \chi \bar{E} = \overline{m - \Delta M} + 5(1 - \log \bar{r}) . \tag{3}$$

If this equation is written for several intervals of E, it may be solved for $\bar{M}_{B2}$ and χ. We have chosen B2 so that positive and negative values of ΔM would approximately balance each other. The average distance $\bar{r}$ for each group of stars in a given range of values of E is found from the galactic-rotation terms in the radial velocities, where we assume $A = 17.5$ km/sec/kpc. The method is similar to that employed by Greenstein[19] to obtain values of $\bar{M}$. We have neglected the correction term $5(\log \bar{r} - \overline{\log r})$, since our dispersion in distances is not large. The correction, evaluated for several groupings of stars, was found never to exceed +0.1 mag. and hence can be neglected. Its effect would be to cause our computed luminosities to be slightly too high.

Before solving equation (3) we must discuss the values of E and of ΔM. Supergiants and O-type stars are omitted, mainly because of uncertainties in the ΔM.

Normal color indices on the International System of the B-type stars were kindly supplied to us in advance of publication by Dr. W. W. Morgan. They were determined by reducing graphically Bottlinger's photoelectric colors to King's system and then reducing King's system to the International System, with the zero point taken as −0.14 for A0 stars. These values are listed herewith. The system of spectral types is that of Williams, which, as mentioned earlier, differs somewhat from the Victoria classification. Un-

[19] *Proc. Nat. Acad. Sci.*, **26**, 259, 1940.

fortunately, we have no data at hand to determine the dependence of normal color index on luminosity, on line character, or on the presence or absence of emission lines.

Type.....	Bo	B2	B4	B6	B8
Color index....	−0.66	−0.60	−0.49	−0.41	−0.33

According to Morgan, considerable uncertainty exists in these values.

Values of $\Delta M = M - \bar{M}_{B_2}$ have been obtained from various sources.[20] The values depend on assumed corrections for interstellar absorption. Errors in these corrections should not greatly affect the value of χ. Two scales of ΔM were used.

Type.....	Bo	B2	B4	B6	B8
ΔM, scale A.....	−1.5	0	+0.7	+1.5	+2.3
ΔM, scale B.....	−1.1	0	+0.6	+1.3	+2.0

Stars of types later than B5 play very little part in the solution.

In forming values of $\overline{m - \Delta m} + 5(1 - \log \bar{r})$, values of ρ determined from interstellar lines were multiplied by two and given half-weight. Weights were also assigned according to the reliability of the observed color indices and spectral types; according to the probable errors of the radial velocities as in the solution for galactic rotation; and according to the size of the coefficient, $\sin 2(l - l_0) \cos^2 b$, stars with values smaller than 0.4 being omitted. Mean values of E, ranging from +0.35 to +1.04, were used for 8 groups of stars. The solutions yielded the following values:

$\bar{M}_{B_2}$	χ	Solution	
−3.6±0.5(p.e.)....	3.4±0.35(p.e.)	K term=0	A scale of ΔM
−3.3 0.5.....	3.1 0.35	K term=−5 km/sec, stellar velocities only	A scale of ΔM
−3.4±0.5.....	3.0±0.35	K term=0	B scale of ΔM

We shall adopt the values

$$\bar{M}_{B_2} = -3.4 \quad \text{and} \quad \chi = 3.2, \text{ photographic.}$$

The corresponding photovisual values are

$$\bar{M}_{B_2} = -2.8 \quad \text{and} \quad \chi = 2.2,$$

since, by definition, $\chi_{pg} - \chi_{pv} = 1$ if the colors are measured in the same effective wave lengths in which the absorptions are determined.

It may be mentioned that the value of the ratio χ found here does not differ greatly from the value 2.9 found by Aller and Trumpler[21] on the International System. Their result is based on the observations of C. E. Smith for a region in the great dark lane in Aquila. Very few B stars entered into their determination.

[20] Stebbins, Huffer, and Whitford, *op. cit.*; Greenstein, *op. cit.*; Wilson, *op. cit.*

[21] *Pub. A.S.P.*, **51**, 339, 1939.

Our value of χ is not greatly dependent on the values of normal color indices used, since the mean spectral type does not vary greatly with mean E. If we use a scale of normal color indices with Bo = −0.34, B4 = −0.28, and B8 = −0.18, we find χ = 3.1, photographic. The zero point of the absolute-magnitude scale, on the other hand, is more critically affected. The corresponding value is $\bar{M}_{B_2} = -2.5$, photographic. In this solution the mean value of E ranges from +0.12 to +0.71.

If the law of interstellar absorption has the form

$$\Delta m_\lambda = a + b\lambda^{-n},$$

and if we use λ 4250 and λ 5400 for the photographic and photovisual effective wave lengths, respectively, then the value $\chi = 3.2$ leads to the value

$$n = 1.6.$$

Stebbins, Huffer, and Whitford, among others, have shown that between wave lengths 4500 A and 9000 A, interstellar absorption follows the λ^{-1} law. The λ^{-1} law requires a value of $\chi = 4.6$, which does not appear to be admitted by our observations. Spectrophotometric observations are needed for wave lengths shorter than λ 4500, to help settle the problem.

Having obtained χ, we are now in a position to determine values of $\bar{M}$ for the c stars and for the O-type stars, according to the method employed by Greenstein[19] and outlined in the introduction to this paper. The normal color index of the O-type stars was taken to be −0.66, while the c stars were assumed to have the same normal colors as main-sequence stars. We have also solved for $\bar{M}_{Bo}$, since the value of ΔM is most uncertain for this type, and for $\bar{M}_{Be}$. Weights were assigned as in the solution for χ and $\bar{M}_{B_2}$. The K term was assumed to be zero. The only effect of a negative value of K would be to reduce slightly the value of $\bar{M}$ for the c stars. The values obtained are as follows:

Mean Type	No. of Velocities	$\bar{M}_{pg}$
cB2.8	21	−5.1±0.3(p.e.)
O8	15	−4.6 0.5
Bo.2	16	−5.0 0.4
B3.8e	11	−2.8±0.6

From our meager data on the Be stars no evidence of a systematic difference of luminosity dependent on the existence of emission lines appears to be present.

The absolute magnitudes suggested by this discussion are presented,[22] together with determinations by other writers,[23] in Table 2. The greatest discrepancy between our results and those of others exists in the case of the c stars. In the work of previous investigators the c stars have been the reddest stars, and the discrepancy may reflect an overcorrection by others for space absorption. It may reflect, on the other hand, the inability of the present writers to classify stars correctly according to luminosity. This latter difficulty

[22] The use of the more contracted scale of normal color indices mentioned on p. 473, with $\chi = 3.1$, leads to values of photographic magnitudes 0.9 mag. fainter, on the average, than those listed here, and photovisual magnitudes 0.7 mag. fainter. It is evident, therefore, that the choice of normal colors is a critical one.

[23] Wilson's value of $\bar{M}_c$ was kindly supplied to us in advance of publication.

has been mentioned in the section on "Spectral Classification." No value of χ can increase the difference $\bar{M}_{Bo} - \bar{M}_c$ for our stars. We are not in a position to discuss the variation of $\bar{M}_c$ with spectral type.

Stebbins, Huffer, and Whitford[24] have found no evidence of a regular increase of color excess with distance. This is also true of our observations, though the range of distance modulus represented here is rather small, the dispersion in $m_0 - M$ being ± 0.5 mag. There is, however, a very good correlation of E with the *apparent* modulus $m - M$, the correlation coefficient being about 0.7. A random selection of 160 of Stebbins' stars likewise gives a correlation coefficient of Stebbins' E_1 against $m - M$ of 0.8. If all the stars were at the same distance, the correlation of E with $m - M$ would be perfect. The effect of a scatter in the distances is merely to decrease the correlation.

TABLE 2

Type	$\bar{M}_{pg}$	$\bar{M}_{pv}$	Wilson	Stebbins	Greenstein
			$\bar{M}_{pv}$	$\bar{M}_{pv}$	$\bar{M}_{pv}$
cB	−5.1	−4.6	−5.3	−5.5	−6.3
O	4.6	3.9	.....	4.5	4.4
Bo	5.1	4.4	.....	4.0	4.6
B2	3.4	2.8	.....	−3.0	−3.3
B4e	−2.8	−2.3	.....	.....	.....

Since the mean color excess of our stars is 0.64 mag. and the mean distance is about 2 kiloparsecs, the average coefficient of color excess is about 0.3 mag. per kiloparsec, and of photographic absorption about 1.0 mag. per kiloparsec. No great significance is attached to these values.

It is interesting to notice the influence on color excess of apparent irregularities in the distribution of stars as revealed by the photographs of Barnard and of Ross. Of our stars with E less than 0.4, excluding the 2 at latitudes 40° and 45°, 14 are in regions of normal appearance, while 6 are in bright clouds. Two might be suspected of involvement with inconspicuous, small-scale dark areas. Of the stars with E greater than 0.9, 5 are in approximately normal regions, 2 are in bright clouds, 2 are in emission nebulosities, 5 are in conspicuous, large-scale dark areas, and 6 are in small-scale "holes" of dark nebulosity.[25] These general conclusions are similar to those of Stebbins.

We are indebted to the other members of the staff of the McDonald Observatory for assistance with some of the observations.

McDonald Observatory
January 1940

[24] *Ap. J.*, **92**, 193, 1940.

[25] The existence of the two very red B stars near M 17, announced by us in *Pub. A.S.P.*, **52**, 401, 1940, had previously been noted by O'Keefe, *Pub. A.A.S.*, **10**, 25, 1940.

UNIV. OF MICH.

PLATE XIX

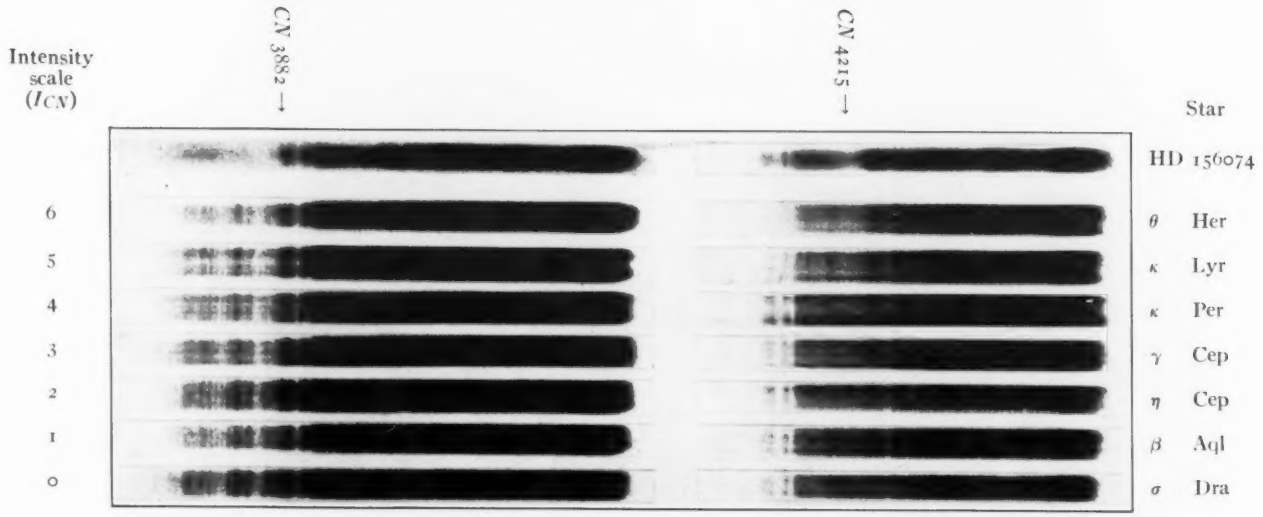

STANDARD STARS DEFINING THE SCALE OF *CN* INTENSITY

The bands extend to the violet (*left*) of the indicated heads. The Ro star HD 156074 is added at the top to indicate the much greater intensity of the bands in even the earliest of these stars.

THE EXTENSION TO THE SUPERGIANTS OF THE CYANOGEN CRITERION OF STELLAR LUMINOSITY

PHILIP C. KEENAN

ABSTRACT

The behavior of *CN* in stars of accurately known spectral types and absolute magnitudes has been studied by combining intensity estimates of the bands at λ 3882 and λ 4215. When plotted against spectral type, the observed band intensities show progressively earlier maxima in going from dwarfs to supergiants. The usual equations of dissociative equilibrium can be extended successfully to the atmospheres of the supergiants to account for the observations.

The absolute maximum in *CN* intensity is reached near type K1 by stars with visual absolute magnitudes in the neighborhood of −2. For types G4–K1 the luminosity effects in the bands are strong enough to allow good spectroscopic absolute magnitudes to be determined from their intensities. G-type stars of high luminosity are easily detected, even with very low dispersion, by picking out spectra with intense *CN* bands; and in this way discovery surveys can be extended to faint apparent magnitudes.

In 1922 Lindblad[1] showed that the bands of *CN* are powerful criteria of luminosity in stars of type G. The especial usefulness of these bands is due to their considerable width, which allows them to be detected in spectra of such low dispersion that most of the atomic lines are invisible. In particular, measured total intensities of the band system extending some 70 A to the violet of the principal head at λ 4215 were correlated with luminosity and spectral type by Lindblad and his co-workers at Upsala and Stockholm.[2] Their observations show a greater apparent scatter than should be expected from the considerable precision of their measures. This may be due in part to the fact, brought out by W. Iwanowska,[3] that enhanced atomic lines contribute largely to the observed intensities in some stars, particularly the later supergiants. A similar scatter has been common to the data of others who have investigated the bands and this has limited the practical use of the *CN* criterion in the separation of giants and dwarfs,[4] although Miss Iwanowska was able to demonstrate that in the early G's the strength of the λ 4215 band in the supergiants is even greater than in giants of corresponding type.

THE OBSERVATIONS

The present study was planned to obtain data improved in two respects: (1) intensities of both the λ 4215 and λ 3882 bands were observed and combined to form a mean, and (2) observations were limited to stars for which both spectral type and absolute magnitude were well determined.

The instrument used was a small slitless spectrograph, with optical parts designed by Professor Ross, which was adapted to the Yerkes 24-inch reflector by Dr. Greenstein and Mr. Ridell. The spectra were taken on Agfa Super Plenachrome Press films and had a mean dispersion of 425 A/mm between $H\beta$ and $H\epsilon$.

On this small scale it was found possible to estimate band intensities as easily as one ordinarily estimates line intensities when working with higher dispersions. All estimates were made by direct comparison with a set of spectra of standard stars arranged in order of *CN* strength. These standards are reproduced in Plate XIX, where the intensity scale

[1] *Ap. J.*, **55**, 85, 1922.

[2] References to earlier work will be found in the comprehensive discussion by Lindblad and Stenquist, *Stockholm Iakt.*, **11**, No. 12, 1934.

[3] *Stockholm Iakt.*, **12**, No. 5, 1936, and *Wilno Obs. Bull.*, No. 18, 1937.

[4] C. Schalén, *Upsala Medd.*, No. 55, 1932; F. Becker, *Potsdam Pub.*, No. 27, 1930, No. 28, 1938; Becker and Kohlschütter, *Bonn. Veröff.*, No. 27, 1933; D. Hoffleit, *Ap. J.*, **90**, 621, 1939.

TABLE 1

INTENSITY OF *CN* BANDS IN BRIGHT STARS

Star	α 1900	δ 1900	m_v	Spectrum	Lum. Class	I_{CN}
Sun (from spectrum of Vesta)				G4	V	0.5
ϵ And	0^h33^m	+28°.8	4.52	G4	III–IV	1.5
δ And	34	+30.3	3.49	K3	III	3.2
α Cas	35	+56.0	2.2–2.8	K1	II–III	4.5
η Cas	43	+57.3	3.64	F9	V	0
η And	52	+22.9	4.62	G9	III	2.7
μ Cas	1 02	+54.4	5.26	G6	V	0
φ Cas	14	+57.7	5.25	F0	I*a*	0
ψ Cas	19	+67.6	4.96	K1	III	3.0
χ Cas	27	+58.7	4.88	K2	III	2.7
51 And	32	+48.1	3.77	K3	III	2.5
HD 9900	34	+57.7	5.74	K1	I–II	4.5
S 497	36	+42.1	5.10	G2	V	0
107 Pis	37	+19.8	5.32	K1	V	0.7
S 525	41	+63.4	5.74	K0	V	1.0
δ Tri	2 11	+33.8	5.07	G0	V	0
14 Per	38	+43.9	5.58	G0	I	0.5
η Per	43	+55.5	3.93	K2	I	2.2
τ Per	47	+52.4	4.06	G0	II	0.2
κ Per	3 03	+44.5	4.00	G9	III	4.0
κ Cet	14	+ 3.0	4.96	G4	V	0.1
o Tau	19	+ 8.7	3.80	G4	II–III	2.2
σ Per	24	+47.6	4.55	K3	III	1.5
S 1037	28	+17.5	6.39	K1	IV	0.7
ϵ Eri	28	− 9.8	3.81	K1+	V	0.2
δ Eri	38	−10.1	3.72	K1	IV	2.0
ι Aur	4 50	+33.0	2.90	K3	II	2.0
β Cam	55	+60.3	4.22	F8	I*b*	3.0
λ Aur	5 12	+40.0	4.85	G1	V	0
β Lep	24	−20.8	2.96	G4	II	1.2
δ Aur	51	+54.3	3.88	G7	III	3.0
46 ψ' Aur	6 17	+49.3	5.10	K4	I	0.5
ϵ Gem	38	+25.2	3.18	G8	I	4.0
ω Gem	56	+24.4	5.21	.....	.....	2.7
ι Gem	7 20	+28.0	3.89	K0	III	2.7
κ Gem	38	+24.6	3.68	G9	III	2.5
β Gem	39	+28.3	1.21	K0+	III	3.0
ω Cnc	55	+25.7	5.88	K1	II–III	4.8
ζ Mon	8 04	− 2.7	4.41	G3	I	1.2
β Cnc	11	+ 9.5	3.76	K4	III	1.0
o UMa	22	+61.0	3.47	G5	II–III	2.5
δ Cnc	39	+18.5	4.17	K1	III	3.7
ϵ Leo	9 40	+24.2	3.12	G5	I–II	1.7
43 β Com	13 07	+28.4	4.32	F9	V	0
η Boo	50	+18.9	2.80	G0	IV	0
ρ Boo	14 28	+30.8	3.78	K2	III	2.2
ξ Boo	47	+19.5	4.64	G6+	V	0
β Boo	58	+40.8	3.63	G7	III	2.0
δ Boo	15 11	+33.7	3.54	G7	III–IV	1.0
ι Dra	23	+59.3	3.47	K1	III	3.0
θ Dra	16 00	+58.8	4.11	F8	III	0
ζ Her	38	+31.8	3.00	G1	IV	0
η Her	39	+39.1	3.61	G6	III	2.2
σ Oph	17 22	+ 4.2	4.44	K2	II	2.7
β Dra	28	+52.4	2.99	G2	I	1.5
μ Her	43	+27.8	3.48	G5	IV	1.0
ξ Dra	52	+56.9	3.90	K2	III	2.5
θ Her	53	+37.3	3.99	K1	II	5.5

TABLE 1—*Continued*

Star	α 1900	δ 1900	m_v	Spectrum	Lum. Class	I_{CN}
70 Oph A	18^h00^m	+ 2°5	4.3	Ko+	V	0
S 5454	06	+38.5	6.40	K2	V	0
η Ser	16	− 2.9	3.42	K1	IV	1.2
κ Lyr	16	+36.0	4.34	K2	II–III	5.0
δ Dra	19 13	+67.5	3.24	G9	III	2.7
κ Cyg	15	+53.2	3.98	G6	III	2.7
31 Aql	20	+11.7	5.23	Ko	IV	1.2
σ Dra	33	+69.5	4.78	G9	V	0.2
γ Aql	42	+10.4	2.80	K3	II	1.7
η Aql	47	+ 0.8	3.7–4.3	Gop	Cepheid	0.5:
ε Dra	49	+70.0	3.99	G7	IV	0.5
β Aql	50	+ 6.2	3.90	Ko	IV–V	1.0
γ Sge	54	+19.2	3.71	K5	III	0.7
η Cep	20 43	+61.5	3.59	Ko	IV	2.0
ξ Cyg	21 01	+43.5	3.92	K3+	I	1.2:
63 Cyg	03	+47.2	4.88	K4	II	1.7
ζ Cyg	09	+29.8	3.40	G9	II	3.5
1 Peg	17	+19.4	4.24	Ko+	III	3.5:
ζ Cap	21	−22.9	3.86	G4	I	3.0
β Aqr	26	− 6.0	3.07	Go	I	0.5
ρ Cyg	30	+45.2	4.22	G9	III–IV	1.2
ε Peg	39	+ 9.4	2.54	K1	I	2.7
9 Peg	40	+16.9	4.52	G5	I	4.2
α Aqr	22 01	− 0.8	3.19	G1	I	1.5
ζ Cep	07	+57.7	3.62	K1	I	2.5
24 Cep	08	+71.9	4.99	G7	III	3.0
HR 8485	10	+39.2	4.64	K3	III	1.7
1 Lac	12	+37.2	4.22	K2	III	2.5:
35 Peg	23	+ 4.2	4.93	Ko+	IV–V	1.7
η Peg	38	+29.7	3.10	G4	III	0.7
λ Peg	42	+11.7	4.31	Ko	II–III	4.0
μ Peg	45	+24.1	3.67	G7	III	2.7
ι Cep	46	+65.7	3.68	Ko	III	2.7
51 Peg	53	+20.2	5.59	G7	V	0.2
π Cep	23 05	+74.8	4.56	G2	III	0
S 7259	08	+56.6	5.65	K3	V	0.5
γ Pis	12	+ 2.7	3.85	G5	III	2.2
υ Peg	20	+22.9	4.57	F8	III	0
λ And	33	+45.9	4.00	G6+	IV	1.0
γ Cep	35	+77.1	3.42	K2	IV	3.0
ψ And	41	+45.9	5.09	G3	I	1.6
τ Cas	42	+58.1	5.09	K1	III	3.0
ρ Cas	49	+56.9	4.4–5.1	F8	Ia	0

defined by the spectra is shown on the left. Each scale division represents roughly 0^m1 central absorption in the λ 4215 band. In the stars of lowest *CN* intensity the λ 3882 band appears first, and its strength can be conveniently estimated by comparison with the deep absorption feature due to a blending of strong metallic lines in the neighborhood of λ 3825. The rate of increase of the λ 3882 band is at first rapid but is not so marked in the upper part of the scale, where the λ 4215 band is just becoming prominent. By using the two bands together we have an extended sensitive scale which makes possible the rapid estimation of *CN* intensities.

The program stars are listed in Table 1, in which the last three columns contain, respectively, the Yerkes spectral type,[5] the luminosity class, and the mean cyanogen in-

[5] The classification is on the system of the Yerkes "Atlas of Stellar Spectra," to be published shortly.

tensity. This last quantity, I_{CN}, is compared with the Stockholm cyanogen equivalent, c_v, in Figure 1, for the stars measured on both systems; c_v is essentially the central depth of the λ 4215 band expressed in magnitudes, and the values plotted in the diagram are direct means of the five principal catalogues of Stockholm and Upsala observations.[6] For stars earlier than K3 and belonging to luminosity classes II–V the correlation is good, while for the supergiants (class I) and the few stars of later type (unplotted) the *CN*

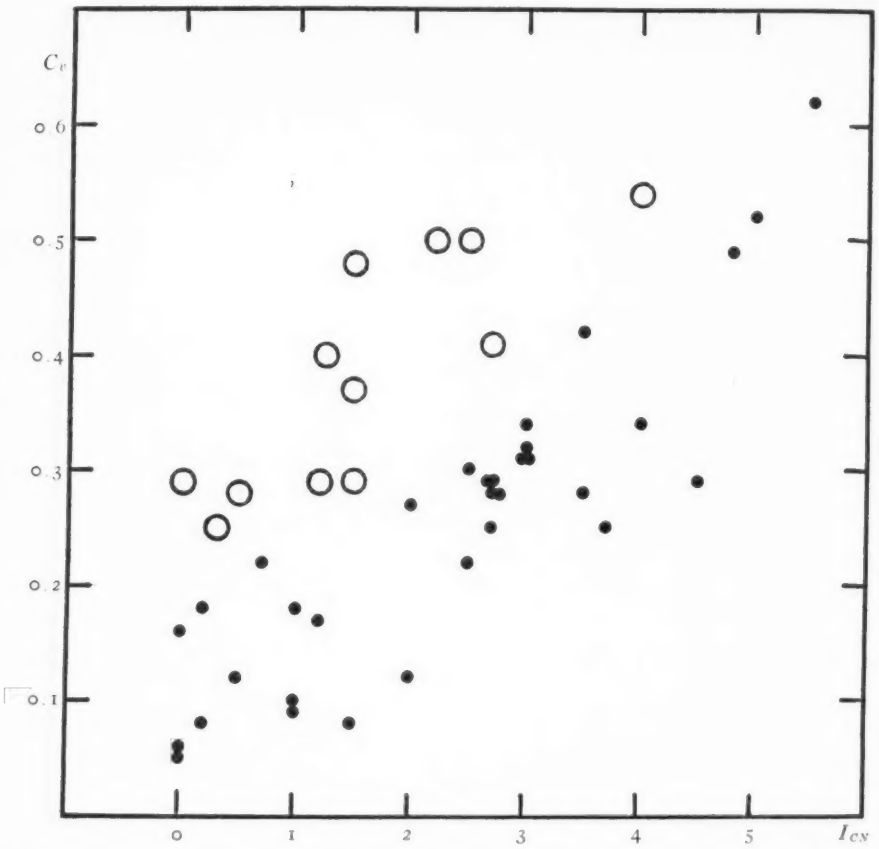

FIG. 1.—Comparison of Yerkes cyanogen intensities (I_{CN}) with Stockholm cyanogen equivalents (c_v). Dots represent luminosity classes II–V for types F8–K2. Supergiants of all types are shown by large open circles.

strength is measured as relatively less at Yerkes, which indicates that at least part of the influence of the atomic lines has been eliminated in the observations made here. This appears to be due largely to the fact that intensities of weak, broad absorption markings can be estimated better by visual examination of the negatives than on microphotometer tracings, where the uncertainty in drawing the background of the continuous spectrum can introduce large systematic errors. However, it should be pointed out that the internal accuracy of the Stockholm cyanogen equivalents is quite high. The mean error of an entry as computed from the differences of the values from the catalogues taken in pairs

[6] The data of the first four catalogues are taken from the tables given by Lindblad and Stenquist, after removal of the reduction to a common spectral type, while the measures of Miss Iwanowska have been added without corrections.

is $\pm 0^{m}056$. For the values of I_{CN} in Table 1 we have $\sigma = \pm 0.45$; hence, the accidental errors in the two systems are of the same order of magnitude.

The variation of *CN* intensity with spectral type is shown for dwarfs, giants, and supergiants in the lower part of Figure 2. Stars of intermediate luminosity have been ex-

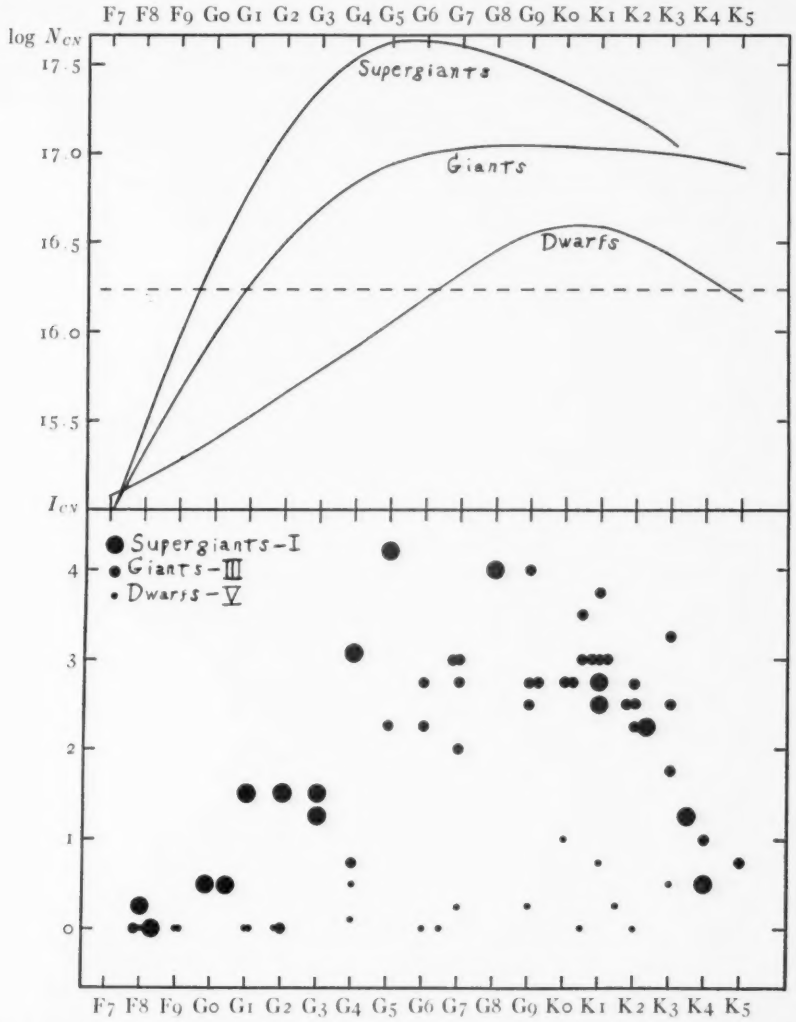

FIG. 2.—Cyanogen intensity as a function of spectral type. *Lower section:* observed intensities; *upper section:* computed numbers of *CN* molecules.

cluded from this diagram as completely as possible in order to bring out the differences between the main groups. In addition to the usual separation between giants and dwarfs the earlier maximum (G6) of the supergiants is striking. For types later than K1 they have actually less cyanogen strength than the giants.

INTENSITY-CURVES FROM DISSOCIATION THEORY

The observational differences are sufficiently clear cut to justify a comparison with the predictions of the dissociation theory. For this purpose curves for the logarithms of the

numbers of *CN* molecules in stars of the types and luminosities covered by the observations were computed on the basis of the reduction of luminosity classes to absolute magnitudes previously published[7] and the effective temperature scale given in Table 2.[8] The temperatures for the supergiants were derived from the scale for the giants and a table of intrinsic colors for the stars of the two luminosity classes.[9] In computing the values of the surface gravity, g, the formulation of the mass-luminosity law by Russell and Moore[10] was employed. It is interesting to note that g now comes out even more nearly constant than before for the main sequence; between F7 and K5 no significant variation is indicated. In the case of the supergiants there is evidence that the equation of hydrostatic

TABLE 2

EFFECTIVE TEMPERATURE, SURFACE GRAVITY, AND PHOTOSPHERIC PRESSURES

TYPE	DWARFS				GIANTS				SUPERGIANTS			
	T_e	log g	log P_e*	log p_g†	T_e	log g	log P_e	log p_g	T_e	log g	log P_e	log p_g
F7.....	6330°	4.56	1.77	5.13	6080°	3.13	+1.00	4.30	5820°	1.41	+0.25	3.28
F8.....	6260	4.56	1.72	5.16	5840	3.06	+0.95	4.30	5420	1.27	−0.10	3.28
G0.....	6080	4.54	1.62	5.20	5400	2.89	+0.61	4.33	4930	0.93	−0.42	3.28
G2.....	5880	4.54	1.55	5.23	5060	2.77	+0.46	4.35	4550	0.76	−0.57	3.28
G4.....	5650	4.53	1.45	5.26	4800	2.68	+0.35	4.35	4200	0.65	−0.75	3.32
G6.....	5420	4.52	1.32	5.31	4590	2.65	+0.28	4.36	3920	0.54	−0.85	3.43
G8.....	5180	4.52	1.24	5.35	4400	2.61	+0.19	4.40	3690	0.43	−0.99	3.53
K0.....	4950	4.53	1.14	5.41	4250	2.52	+0.09	4.41	3530	0.34	−1.06	3.55
K2.....	4670	4.57	1.08	5.47	3980	2.29	−0.08	4.45	3390	0.18	−1.16	3.55
K3.....	4460	4.57	1.02	5.51	3850	2.10	−0.19	4.45	(3300)	0.07	−1.23	3.54
K5.....	4040	4.52	0.98	5.85	3600	1.71	−0.36	4.44	.....	.....	.....	.....

* P_e = electron pressure in dynes/cm². † P_g = gas pressure in dynes/cm².

equilibrium can be used to describe the pressure gradient only if a value of g lower than the gravitational one is inserted.[11] For these stars the table gives

$$g_{\text{apparent}} = \tfrac{1}{2} g_{\text{gravitational}} ,$$

which was used in the computations, although it may well be that lower values for both giants and supergiants will eventually prove necessary. The tabulated electron pressures are based upon Wildt's table of opacities,[12] which estends only to $T_e = 4200°$; for lower temperatures it was necessary to extrapolate the pressures.

The composition adopted (Table 3) is not greatly different from the original Russell mixture. Some observations[13] have indicated that the abundance of *O*, *N*, and *C* should be lowered by a factor of 10; but such a change shifts the maxima of the computed num-

[7] *Ap. J.*, **91**, 506, Table 3, 1940.

[8] For dwarfs and giants the scale given by Kuiper (*Ap. J.*, **88**, 429, 1938) was modified to accord with type G4 for the sun.

[9] I am indebted to Dr. Morgan for his reduction of Bottlinger's photoelectric color indices to the International System. These were the data used in constructing the table.

[10] *The Masses of the Stars*, p. 112, "Astrophysical Mono.," University of Chicago Press, 1940.

[11] Pannekoek, *B.A.N.*, **8**, No. 301, 175, 1937; Christie and Wilson, *Ap. J.*, **81**, 453, 1935; Menzel, *Harvard Circ.*, No. 417, 1936; Roach, *Ap. J.*, **93**, 1, 1941; Kuiper, Struve, and Strömgren, *Ap. J.*, **86**, 591, 1937.

[12] *Ap. J.*, **90**, 611, 1939. The method of computation of P_e was the usual one (cf. Unsöld, *Physik der Sternatmosphären*, chap. vii) except that within each atmosphere the expression $\bar{\kappa} = CP$ was assumed.

[13] Menzel, *Pop. Astr.*, **47**, 137, 1939; and Unsöld, *Verh. d. deutsch. phys. Ges.*, in press.

bers of molecules so far toward later types that it could be reconciled with the *CN* observations only if the heat of dissociation, D_0, of *CO* is much higher than the value of 10^{v}.3 adopted. It is the formation of *CO* which determines the maximum of *CN;* hence an error in $D_0(CN)$, taken here as 6^{v}0, is not serious; but the existing uncertainty in $D_0(CO)$ may be one electron volt or more;[14] and not until the physical chemists reach better agreement on this point will the stellar data on *CN* allow reliable conclusions as to abundances.

The predicted curves are shown in the upper section of Figure 2. The several uncertain factors in the computations permit only qualitative comparisons at present;[15] but, if the broken line is taken to indicate approximately the number of molecules necessary for marginal appearance of the bands, the variations in the observed intensities are satisfactorily represented. The agreement is particularly striking for the supergiants where

TABLE 3*

(θ = Relative number of atoms per unit volume)

Elements	θ	$\Sigma\theta$	Ionization Potential
H	0.80		
O	.0080	0.8108	13.5 volts
N	.0020		
C	.0008		
He	.18653	.18903	25.5
Ne	0.0025		
Fe, Si, Mg, Ni, etc.		.00015	7.8
Al, Ca, Na, etc.		0.00002	6.1

* An important recent paper by B. Strömgren (*Festschrift für Elis Strömgren*, p. 218, Copenhagen, 1940) indicates a hydrogen/metal ratio of 10,000 for the sun, or slightly less than twice the ratio used here. The agreement is close enough for the purposes of this investigation.

departures from thermal equilibrium might have been expected to cause trouble. The fact that the curve for the supergiants is too high by about 0.3 in the logarithms with respect to the other two probably means that in these stars there is considerable additional opacity due to sources not yet taken into account.

CYANOGEN BANDS AS LUMINOSITY CRITERIA

In Figure 3, I_{CN} is plotted as a function of luminosity class for several groups of spectral types. The importance of separating the spectral subdivisions is shown by the rapid but consistent variation in the luminosity effects; in fact, much of the apparent scatter in the earlier observations was a scatter in the spectral types available. The luminosity effect increases rapidly through type G until at K0 the curves show a definite maximum, the greatest cyanogen strength being reached near K1 by bright giants with visual absolute magnitudes in the neighborhood of -2. For later types the bands become too weak to show marked luminosity effects.

With the help of these calibration-curves band intensities can be used to determine spectroscopic absolute magnitudes for classes G4–K1 with an accuracy equal to that of the best ratios of atomic lines as estimated on spectra of much higher dispersion. How-

[14] Herzberg, *Molecular Spectra and Molecular Structure*, Table 36, 1939; White, *J. Chem. Phys.*, **8**, 459, 1940.

[15] For giants and dwarfs the curves do not differ essentially from the original ones derived by Russell (*Ap. J.*, **79**, 317, 1934). For later work cf. Nicolet, *Mém. Inst. d'astrophysique*, Liége, **9**, No. 204, 1937, and Ledoux, *Mém. Inst. d'astrophysique*, **9**, No. 212, 1937. The first application of dissociation theory to the supergiants appears to have been made by Fujita, *Japanese J. Astron. and Geophys.*, **13**, 21, 1935; **17**, 17, 1939.

ever, their usefulness for this purpose is limited by the necessary condition that the spectral types be well determined, requiring in turn spectrograms whose scale is not less than about 200 A/mm.

On the other hand, spectra of very small scale can be used alone for the discovery of G-type supergiants. If all stars with $I_{CN} \geqslant 4$ in Figure 3 are selected, it is at once evident

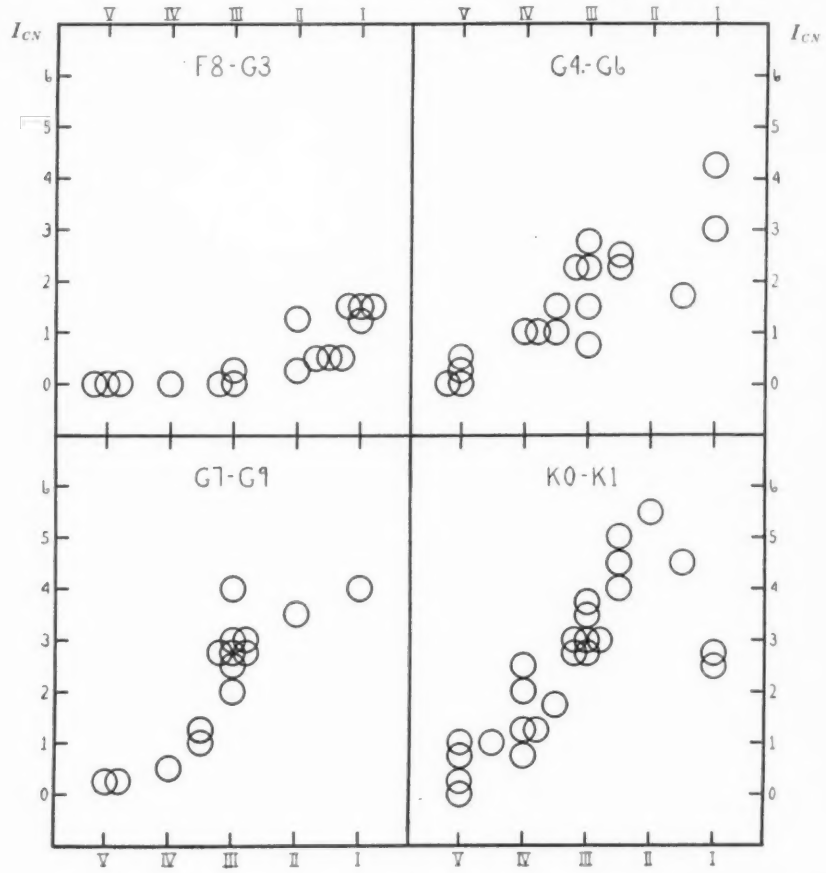

FIG. 3.—Luminosity effects in the *CN* bands. The abscissae are the following luminosity classes:

Supergiants	I	Subgiants	IV
Bright giants	II	Dwarfs	V
Giants	III		

that they form a group with high mean luminosity. Stars with bands of this strength are easily picked out on slightly widened spectra taken with objective prisms, and in this way observing lists may be built up for detailed investigations of the absolutely bright stars. If they are later observed for radial velocity with spectrographs of greater dispersion, the separation of supergiants from bright giants can be carried out. Several supergiants have already been detected here with the 24-inch reflector, in spite of the small field, and with fast Schmidt cameras discovery surveys could readily be extended to the twelfth visual magnitude.

YERKES OBSERVATORY
January 1941

RADIATION PRESSURE IN THE CONVECTIVE STELLAR MODEL

LOUIS R. HENRICH

ABSTRACT

The investigation of the effect of radiation pressure in the point-source model requires a study of the effect of radiation pressure in the convective model. The equations of state and of equilibrium are, therefore, derived for the wholly convective model with radiation pressure. Tables obtained by integrating these equations for various values of the ratio of the radiation pressure to the gas pressure at the center are given. A relation is also obtained between the mass, the mean molecular weight, and the central value of the ratio of the radiation pressure to the gas pressure.

Since in the limiting case of vanishing radiation pressure the model reduces to the convective polytrope, it is possible to consider the actual density distribution with small amounts of radiation pressure as a perturbation of the polytropic case. The necessary first-order equation is obtained and integrated.

1. *Introduction.*—The effect of radiation pressure in the equation of hydrostatic equilibrium of a star is generally neglected in current discussions of stellar structure. This provides a fair approximation for stars of about the solar mass, as it can be shown[1] quite generally that for these stars the ratio $(1 - \beta_c)$ of the radiation pressure to the total pressure at the center must necessarily be less than about 5 per cent. On the other hand, in masses somewhat larger than that of the sun the radiation pressure will begin to contribute appreciably to the total pressure. In a general way we may expect this to require quite significant corrections to those models in which the radiation pressure is neglected. Thus, it is known that in the luminosity formula derived, for instance, on the standard model[2] the ratio β of the gas pressure to the total pressure occurs with a fairly high power.

Now, according to our present ideas on the mechanism of energy generation in stars, the energy generation is expected to be so highly concentrated toward the center that a good approximation is provided by the point-source model. All stars, therefore, must be expected to have convective cores. When radiation pressure is neglected, the convective cores are polytropic regions of index $n = 3/2$. However, if radiation pressure cannot be neglected, we can no longer use a polytropic representation of the core. Thus, a first step in the analysis of stellar models with allowance for radiation pressure is the study of wholly convective stars. In this paper, therefore, we shall restrict ourselves to the study of these convective configurations. In a later paper we shall consider the problem of fitting envelopes to such convective cores and thus establish a theoretical relation among the mass, the luminosity, the radius, and the mean molecular weight which is valid for all masses.

2. *The equation of state.*—The equation of convective equilibrium between the total pressure, P, and the density, ρ, can be expressed in the form[3]

$$\frac{dP}{P} = \Gamma_1 \frac{d\rho}{\rho}, \tag{1}$$

where the adiabatic exponent, Γ_1, is given by

$$\Gamma_1 = \beta + \frac{(4 - 3\beta)^2(\gamma - 1)}{\beta + 12(\gamma - 1)(1 - \beta)}. \tag{2}$$

[1] S. Chandrasekhar, *An Introduction to the Study of Stellar Structure*, p. 75, Chicago, 1939.

[2] *Ibid.*, p. 233. [3] *Ibid.*, p. 56.

In equation (2) β is the ratio of the gas pressure to the total pressure and γ is the ratio of specific heats, neglecting radiation pressure. Since the light elements, like hydrogen and helium, are highly abundant in stellar interiors, we can assume that $\gamma = 5/3$. Then

$$\Gamma_1 = \frac{32 - 24\beta - 3\beta^2}{3(8 - 7\beta)} . \tag{3}$$

On the other hand, we have the general relation

$$P = \left[\left(\frac{k}{\mu H}\right)^4 \frac{3}{a} \frac{1 - \beta}{\beta^4}\right]^{1/3} \rho^{4/3} , \tag{4}$$

where k is the Boltzmann constant, μ is the mean molecular weight which is assumed to be constant, H is the mass of the proton, and a is the Stefan-Boltzmann constant. Differentiating equation (4) logarithmically, we have

$$\frac{dP}{P} = -\frac{4 - 3\beta}{3(1 - \beta)} \frac{d\beta}{\beta} + \frac{4}{3} \frac{d\rho}{\rho} . \tag{5}$$

Eliminating $d\rho/\rho$ between equations (1) and (5) and using equation (3) for Γ_1 we find

$$\frac{dP}{P}\left\{1 - \frac{4}{3} \frac{3(8 - 7\beta)}{32 - 24\beta - 3\beta^2}\right\} = -\frac{4 - 3\beta}{3(1 - \beta)} \frac{d\beta}{\beta} , \tag{6}$$

or

$$\frac{dP}{P} = -\frac{32 - 24\beta - 3\beta^2}{3\beta^2(1 - \beta)} d\beta . \tag{7}$$

The foregoing equation can be integrated to give

$$P = \text{constant } e^{32/3\beta} \beta^{-8/3}(1 - \beta)^{5/3} . \tag{8}$$

Let y denote the ratio of the radiation to the gas pressure, so that

$$y = \frac{1 - \beta}{\beta} ; \qquad \beta = \frac{1}{1 + y} ; \qquad 1 - \beta = \frac{y}{1 + y} . \tag{9}$$

In terms of y, equation (8) becomes

$$P = \text{constant } e^{32y/3} y^{5/3}(1 + y) . \tag{10}$$

According to equation (4) we have

$$\rho = \text{constant } \left(\frac{\beta^4}{1 - \beta}\right)^{1/4} P^{3/4} = \text{constant } \frac{1}{y^{1/4}(1 + y)^{3/4}} P^{3/4} , \tag{11}$$

or, substituting for P from equation (10), we have

$$\rho = \text{constant } e^{8y} y . \tag{12}$$

Since the gas pressure is given by

$$\beta P = \frac{k}{\mu H}\,\rho T\,, \tag{13}$$

we can express T in the form

$$T = \frac{\mu H}{k}\,\frac{1}{1+y}\,\frac{P}{\rho}\,. \tag{14}$$

Then, according to equations (10) and (12), we have

$$T = \text{constant}\; e^{8y/3}\, y^{2/3}\,. \tag{15}$$

We have thus expressed P, ρ, and T in terms of the single parameter y. In terms of the values of these quantities at the center of the configuration we have

$$\left.\begin{aligned} P &= P_c e^{32(y-y_c)/3}\left(\frac{y}{y_c}\right)^{5/3}\left(\frac{1+y}{1+y_c}\right),\\ \rho &= \rho_c e^{8(y-y_c)}\left(\frac{y}{y_c}\right),\\ T &= T_c e^{8(y-y_c)/3}\left(\frac{y}{y_c}\right)^{2/3}, \end{aligned}\right\} \tag{16}$$

which are our fundamental equations.

In addition, the values of the constants in equations (16) may be fixed in terms of any two of the four constants. Thus, let us choose ρ_c and T_c to be the values of the density and temperature at the center of the configuration. Then the value of y_c will be determined by the equation

$$y_c = \frac{a}{3}\,\frac{\mu H}{k}\,\frac{T_c^3}{\rho_c}\,. \tag{17}$$

This equation follows from the definition of y.

Using equation (13), the first equation of (16) can be written alternatively as

$$P = \frac{k}{\mu H}\,\rho_c T_c e^{32(y-y_c)/3}\left(\frac{y}{y_c}\right)^{5/3}(1+y)\,. \tag{18}$$

If we let

$$P = P_c e^{-32y_c/3}\, y_c^{-5/3}(1+y_c)^{-1}\Pi\,; \qquad T = T_c e^{-8y_c/3} y_c^{-2/3}\Theta\,, \tag{19}$$

where

$$\Pi = e^{32y/3} y^{5/3}(1+y)\,; \qquad \Theta = e^{8y/3} y^{2/3}\,, \tag{20}$$

we obtain expressions for the variation of pressure and temperature which do not involve y_c.

3. *The equation of hydrostatic equilibrium.*—For a spherically symmetric distribution of matter the usual form for the equation is

$$\frac{1}{r^2}\frac{d}{dr}\left(\frac{r^2}{\rho}\frac{dP}{dr}\right) = -4\pi G\rho\,, \tag{21}$$

where r is the radius and G is the gravitational constant. This may be re-written in the present case in terms of the variables y and r. Using the expression for ρ as given by equations (16) and for P as given by equation (18), we have

$$\left.\begin{aligned}
\frac{1}{\rho}\frac{dP}{dr} &= \frac{k}{\mu H}T_c e^{-8y_c/3}y_c^{-2/3}e^{-8y}y^{-1}\frac{d}{dr}\{e^{32y/3}y^{5/3}(1+y)\}\,,\\
&= \frac{k}{\mu H}T_c\frac{e^{-8y_c/3}}{y_c^{2/3}}\frac{e^{-8y}}{y}\{e^{32y/3}[\tfrac{3}{8}^2y^{5/3}(1+y)+\tfrac{5}{3}y^{2/3}(1+y)+y^{5/3}]\}\frac{dy}{dr}\,,\\
&= \frac{k}{\mu H}T_c\frac{e^{-8y_c/3}}{y_c^{2/3}}\{e^{8y/3}[\tfrac{3}{8}^2y^{5/3}+\tfrac{4}{8}^0y^{2/3}+\tfrac{5}{3}y^{-1/3}]\}\frac{dy}{dr}\,,\\
&= \frac{k}{\mu H}T_c\frac{e^{-8y_c/3}}{y_c^{2/3}}\{e^{8y/3}[4(\tfrac{8}{3}y^{5/3}+\tfrac{5}{3}y^{2/3})+\tfrac{5}{2}(\tfrac{8}{3}y^{2/3}+\tfrac{3}{3}y^{-1/3})]\}\frac{dy}{dr}\,,\\
&= \frac{k}{\mu H}T_c\frac{e^{-8y_c/3}}{y_c^{2/3}}\frac{d}{dr}\{e^{8y/3}y^{2/3}(4y+\tfrac{5}{2})\}\,.
\end{aligned}\right\} \tag{22}$$

If we now let

$$F = e^{8(y-y_c)/3}\left(\frac{y}{y_c}\right)^{2/3}(1+\tfrac{8}{5}y) \tag{23}$$

and

$$\sigma = e^{8(y-y_c)}\left(\frac{y}{y_c}\right), \tag{24}$$

then equation (21) becomes[4]

$$\frac{1}{r^2}\frac{d}{dr}\left(r^2\frac{dF}{dr}\right) = -\frac{8\pi G}{5}\frac{\mu H}{k}\frac{\rho_c}{T_c}\sigma\,. \tag{25}$$

Now introduce the variable, ξ, defined by

$$r = a\xi\,; \qquad a^2 = \frac{5k}{8\pi G\mu H}\frac{T_c}{\rho_c}\,; \tag{26}$$

then equation (25) becomes

$$\frac{1}{\xi^2}\frac{d}{d\xi}\left(\xi^2\frac{dF}{d\xi}\right) = -\sigma\,. \tag{27}$$

[4] This equation is essentially the same as that given by J. Wasiutynski in *M.N.*, **100**, 364, 1940. (There appears to be a typographical error in his equation 4.) Since the present writer was not aware of any place in which the complete equations were derived, it seemed useful to set down the derivations.

On examining equations (23) and (24), it appears that for very small values of the quantity y_c the only significant terms in the expressions for F and σ are $(y/y_c)^{2/3}$ and (y/y_c), respectively. Thus, as y_c approaches zero, equation (27) approaches the Lane-Emden equation of index $n = 3/2$. As the quantity y_c becomes very large, the dominant terms in the expressions for F and σ are $e^{8(y-y_c)/3}$ and $e^{8(y-y_c)}$, respectively. So for increasing values of y_c, equation (27) approaches the Lane-Emden equation of index $n = 3$.

We now have both F and σ expressed parametrically in terms of the quantities y and y_c. For purposes of actually integrating equation (27) it would be convenient to eliminate y from the relation between F and σ. This elimination cannot be carried out analytically. However, the elimination can be effected numerically by tabulating σ as a function of F. Since both F and σ involve y_c, this would strictly mean a tabulation with two parameters in the form $\sigma(F, y_c)$. However, y_c occurs in this relation in a simple way so that we can eliminate it from the tabulation. To do this we shall introduce Z and ζ instead of F and σ, defined as follows:

$$F = e^{-8y_c/3} y_c^{-2/3} Z \; ; \qquad \sigma = e^{-8y_c} y_c^{-1} \zeta \; , \tag{28}$$

where

$$Z = e^{8y/3} y^{2/3} (1 + \tfrac{8}{5} y) \; ; \qquad \zeta = e^{8y} y \; . \tag{29}$$

Further, let

$$\xi = a_1 \eta \; ; \qquad a_1 = e^{8y_c/3} y_c^{1/6} \; . \tag{30}$$

In terms of these variables equation (27) becomes

$$\frac{1}{\eta^2} \frac{d}{d\eta} \left(\eta^2 \frac{dZ}{d\eta} \right) = -\zeta \; , \tag{31}$$

in which form the explicit occurrence of y_c has been eliminated.

The following relation between the derivatives in the two different sets of variables may be noted:

$$\frac{dF}{d\xi} = \frac{e^{-8y_c/3} y_c^{-2/3}}{e^{8y_c/3} y_c^{1/6}} \frac{dZ}{d\eta} = \frac{a_1}{\zeta_c} \frac{dZ}{d\eta} \; , \tag{32}$$

where ζ_c is the value of ζ at the center of the configuration.

4. *The mass relation and other relations.*—We have the following equation for the mass

$$M(y_c) = \int_0^R 4\pi \rho r^2 dr = 4\pi a^3 \rho_c \int_0^{\xi_1} \sigma \xi^2 d\xi \; , \tag{33}$$

or

$$M(y_c) = 4\pi a^3 \rho_c \left(-\xi^2 \frac{dF}{d\xi} \right)_{\xi_1} \; , \tag{34}$$

where R is the total radius of the star and the bracketed quantity is evaluated at the boundary, where ξ takes the value ξ_1. In terms of the Z, η variables this relation is

$$M(y_c) = \frac{4\pi a^3 a_1^3 \rho_c}{\zeta_c} \left(-\eta^2 \frac{dZ}{d\eta} \right)_{\eta_1} \; . \tag{35}$$

According to equations (26) and (17) the quantity $a^3\rho_c$ in equation (34) is given by

$$a^3\rho_c = \left(\frac{5k}{8\pi G\mu H}\right)^{3/2}\left(\frac{T_c}{\rho_c}\right)^{3/2}\rho_c = \left(\frac{5k}{8\pi G\mu H}\right)^{3/2}\left(\frac{3k}{a\mu H}\,y_c\right)^{1/2}. \tag{36}$$

The mass relation (34) then becomes

$$M(y_c) = C\left(\frac{5}{2}\right)^{3/2}\frac{1}{\mu^2}\,y_c^{1/2}\left(-\xi^2\frac{dF}{d\xi}\right)_{\xi_1}, \tag{37}$$

where we have put

$$C = 4\pi\left(\frac{1}{4\pi G}\right)^{3/2}\left(\frac{3}{a}\right)^{1/2}\left(\frac{k}{H}\right)^2. \tag{38}$$

Inserting numerical values for the various physical constants we find $M(y_c)$ in solar masses to be

$$\frac{M(y_c)}{\odot} = 4.420\,\frac{1}{\mu^2}\,y_c^{1/2}\left(-\xi^2\frac{dF}{d\xi}\right)_{\xi_1}. \tag{39}$$

We may also obtain limiting expressions for the mass by considering the two limiting polytropes $n = 3/2$ and $n = 3$. We have[5]

$$M(n) = 4\pi\left[\frac{(n+1)K}{4\pi G}\right]^{3/2}\rho_c^{(3-n)/2n}\left(-\xi^2\frac{d\theta_n}{d\xi}\right)_{\xi_1}, \tag{40}$$

where θ_n is the solution of the Lane-Emden equation with index n, and K is defined by the relation

$$P = K\rho^{1+1/n}. \tag{41}$$

Using equation (4) we may express K in terms of β_c and ρ_c as follows:

$$K = \left[\left(\frac{k}{\mu H}\right)^4\frac{3}{a}\,\frac{1-\beta_c}{\beta_c^4}\right]^{1/3}\rho_c^{(n-3)/3n}. \tag{42}$$

Then, substituting in equation (40), we have

$$M(n) = C(n+1)^{3/2}\,\frac{1}{\mu^2}\left(\frac{1-\beta_c}{\beta_c^4}\right)^{1/2}\left(-\xi^2\frac{d\theta_n}{d\xi}\right)_{\xi_1}, \tag{43}$$

or in terms of y_c we have

$$M(n) = C(n+1)^{3/2}\,\frac{1}{\mu^2}\,y_c^{1/2}(1+y_c)^{3/2}\left(-\xi^2\frac{d\theta_n}{d\xi}\right)_{\xi_1}. \tag{44}$$

With $n = 3/2$ and 3, respectively, the foregoing equation gives the limiting forms of equation (39) for the cases $y_c = 0$ and $y_c = \infty$. Then

$$\frac{M(n=\frac{3}{2})}{\odot} = 12.00\,\frac{1}{\mu^2}\,y_c^{1/2}(1+y_c)^{3/2}, \tag{45}$$

[5] Chandrasekhar, *op. cit.*, p. 97.

and

$$\frac{M(n=3)}{\odot} = 18.05\,\frac{1}{\mu^2}\,y_c^{1/2}(1+y_c)^{3/2}\,. \tag{46}$$

The ratio of the central to the mean density is easily seen to be

$$\frac{\rho_c}{\bar{\rho}} = \frac{1}{3}\left(\frac{-\xi}{\frac{dF}{d\xi}}\right)_{\xi_1}\,. \tag{47}$$

From equation (26) we can further obtain a relation between the quantity y_c, the central temperature, and the radius of the configuration. We have

$$T_c = \frac{8\pi G\mu H}{5k}\,\frac{a^3\rho_c\xi_1}{a\xi_1}\,. \tag{48}$$

Using equation (36), we find

$$T_c = \left(\frac{5}{8\pi G}\,\frac{3}{a}\right)^{1/2}\frac{k}{\mu H}\,\frac{y_c^{1/2}\xi_1}{R}\,. \tag{49}$$

When this is combined with equation (37), we have

$$T_c = Q(y_c)\,\frac{1}{1+y_c}\,\frac{\mu H}{k}\,\frac{GM(y_c)}{R}\,, \tag{50}$$

where

$$Q(y_c) = \frac{2}{5}\,\frac{1+y_c}{\left(-\xi\,\frac{dF}{d\xi}\right)_{\xi_1}}\,. \tag{51}$$

For the two limiting polytropes there is a similar relation in which

$$Q(n) = \frac{1}{(n+1)\left(-\xi\,\frac{d\theta_n}{d\xi}\right)_{\xi_1}}\,. \tag{52}$$

We also see that the quantities

$$\left(\frac{5}{2}\,\frac{1}{1+y_c}\right)^{1/2}\xi_1\,; \qquad \left(\frac{5}{2}\,\frac{1}{1+y_c}\right)^{1/2}\left(-\frac{dF}{d\xi}\right)_{\xi_1} \tag{53}$$

lie, respectively, between the values of the quantities

$$(n+1)^{1/2}\xi_1(n)\,; \qquad (n+1)^{1/2}\left(-\frac{d\theta_n}{d\xi}\right)_{\xi_1} \tag{54}$$

for the two limiting polytropes.

5. *Integration of the equations and results.*—We have seen in equations (16) how the physical structure of the wholly convective configurations are uniquely determined in terms of y_c. A one-parametric series of integrations of the final equation will therefore suffice to determine the properties of these configurations. The integration was started in each case by using a series expansion for Z and ζ, as follows:

$$Z = Z_c + Z_2\eta^2 + Z_4\eta^4 + \dots , \tag{55}$$

and

$$\zeta(Z) = \zeta(Z_c) + (Z - Z_c)\left(\frac{d\zeta}{dZ}\right)_{Z_c} + \frac{(Z - Z_c)^2}{2!}\left(\frac{d^2\zeta}{dZ^2}\right)_{Z_c} + \dots . \tag{56}$$

Substituting these series in the differential equation (31) and comparing coefficients, we find

$$\left.\begin{aligned} Z = Z_c - \tfrac{1}{6}\zeta_c\eta^2 + {}_1\tfrac{1}{20}(\zeta_c\zeta_c')\eta^4 - \frac{1}{7!}(\zeta_c\zeta_c'^2 + \tfrac{5}{3}\zeta_c^2\zeta_c'')\eta^6 \\ + \frac{1}{9!}(\zeta_c\zeta_c'^3 + {}^{2\,6}_{3}\zeta_c^2\zeta_c'\zeta_c'' + {}^{3\,5}_{9}\zeta_c^3\zeta_c''')\eta^8 + \dots , \end{aligned}\right\} \tag{57}$$

where the primes denote differentiation with respect to Z. If $\zeta = Z^n$, it is seen that this relation reduces to the ordinary starting series for the Lane-Emden equation of index n.

TABLE 1

CONSTANTS OF THE CONFIGURATIONS

Model	$\frac{\xi_1}{(1+y_c)^{1/2}}$	$\frac{\left(-\frac{dF}{d\xi}\right)_{\xi_1}}{(1+y_c)^{1/2}}$	$\frac{M}{\odot}\mu^2$	$\frac{\rho_c}{\bar{\rho}}$	Q
$n = 3/2$	3.654*	0.2033†	.....	5.99	0.538
$y_c = 0.01$	3.681	.2019	1.23	6.08	.538
$y_c = 0.10$	3.914	.1889	4.67	6.91	.541
$y_c = 0.25$	4.260	.1693	9.49	8.39	.555
$y_c = 0.5$	4.738	.1449	18.68	10.90	.582
$y_c = 1.0$	5.446	.1165	43.2	15.58	.630
$y_c = 2.0$	6.311	.0918	118.7	22.93	.691
$n = 3$	8.724*	0.0537†	.....	54.18	0.854

* $= [\frac{2}{3}(n+1)]^{1/2}\xi_1(n)$. † $= [\frac{2}{3}(n+1)]^{1/2}(-d\theta_n/d\xi)_{\xi_1}$.

The values of Z, Π, Θ, ζ, and α_1 are given in Table 9 as functions of y. The value of ζ as a function of Z is given in Table 10. This latter table was used in performing all the integrations except the one for $y_c = 2.0$. The results of the integrations are given in Tables 3–8, where η, Z, $dZ/d\eta$, and ζ are tabulated for each step of the integration. In the case of $y_c = 2.0$, Table 10 was not used since the values of Z and ζ became too large. A separate table was developed for this case, the integration giving ξ, F, $dF/d\xi$, σ, and y. Integrations have been performed for $y_c = 0.01$, 0.10, 0.25, 0.5, 1.0, 2.0.

The more important quantities characterizing the configurations are collected in Table 1. The values for the limiting polytropes $n = 3/2$ and 3 are also given.

TABLE 2 PERTURBING FUNCTION

ξ	f_1	σ_1	ξ	f_2	σ_2
0.0	1.60000	0.00000	1.9	1.54837	0.38095
0.1	1.60000	.00000	2.0	1.53388	.41845
0.2	1.60000	.00013	2.1	1.51678	.45253
0.3	1.60000	.00066	2.2	1.49692	.48222
0.4	1.59999	.00203	2.3	1.47417	.50667
0.5	1.59997	.00484	2.4	1.44847	.52519
0.6	1.59991	.00971	2.5	1.41979	.53723
0.7	1.59979	.01731	2.6	1.38815	.54240
0.8	1.59953	.02825	2.7	1.35364	.54046
0.9	1.59908	.04305	2.8	1.31639	.53129
1.0	1.59833	.06207	2.9	1.27658	.51486
1.1	1.59714	.08547	3.0	1.23446	.49118
1.2	1.59536	.11320	3.1	1.19031	.46019
1.3	1.59280	.14500	3.2	1.14447	.42169
1.4	1.58925	.18036	3.3	1.09732	.37500
1.5	1.58449	.21858	3.4	1.04932	.31848
1.6	1.57827	.25880	3.5	1.00099	.24766
1.7	1.57034	.30000	3.6	0.95296	0.14587
1.8	1.56045	0.34109			

TABLE 3 $\eta_1 = 7.7603$ $y_c = 0.01$

η	Z	$-dZ/d\eta$	ζ	η	Z	$-dZ/d\eta$	ζ
0.0	0.048433	0.0000000	0.0108329	4.0	0.026038	0.0085341	0.0042294
0.2	.048361	.0007212	.0108083	4.2	.024334	.0085069	.0038185
0.4	.048145	.0014365	.0107349	4.4	.022638	.0084421	.0034244
0.6	.047787	.0021402	.0106136	4.6	.020959	.0083427	.0030488
0.8	.047290	.0028266	.0104460	4.8	.019303	.0082118	.0026933
1.0	.046658	.0034903	.0102342	5.0	.017676	.0080524	.0023588
1.2	.045896	.0041264	.0099809	5.2	.016084	.0078680	.0020464
1.4	.045009	.0047303	.0096892	5.4	.014530	.0076616	.0017564
1.6	.044006	.0052978	.0093626	5.6	.013020	.0074366	.0014892
1.8	.042893	.0058253	.0090051	5.8	.011557	.0071960	.0012449
2.0	.041679	.0063099	.0086207	6.0	.010143	.0069430	.0010232
2.2	.040372	.0067489	.0082137	6.2	.008780	.0066805	.0008238
2.4	.038982	.0071407	.0077884	6.4	.007471	.0064115	.0006464
2.6	.037519	.0074837	.0073494	6.6	.006216	.0061385	.0004905
2.8	.035992	.0077776	.0069008	6.8	.005016	.0058644	.0003554
3.0	.034411	.0080219	.0064469	7.0	.003870	.0055916	.0002409
3.2	.032787	.0082174	.0059917	7.2	.002779	.0053226	.0001466
3.4	.031128	.0083647	.0055390	7.4	.001741	.0050596	.0000726
3.6	.029444	.0084654	.0050923	7.6	.000754	.0048056	.0000209
3.8	0.027745	0.0085211	0.0046548	η_1	0.000000	0.0046101	0.0000000

TABLE 4 $\eta_i = 4.6153$ $y_c = 0.1$

η	Z	$-dZ/d\eta$	ζ	η	Z	$-dZ/d\eta$	ζ
0.0	0.326290	0.000000	0.222554	2.4	0.167696	0.096512	0.074742
.1	.325919	.007410	.222129	2.5	.158078	.095795	.068006
.2	.324809	.014769	.220861	2.6	.148546	.094795	.061592
.3	.322968	.022027	.218763	2.7	.139128	.093537	.055510
.4	.320409	.029136	.215860	2.8	.129847	.092048	.049770
.5	.317148	.036048	.212188	2.9	.120725	.090350	.044375
.6	.313207	.042721	.207789	3.0	.111783	.088468	.039327
.7	.308613	.049113	.202713	3.1	.103037	.086427	.034625
.8	.303395	.055187	.197015	3.2	.094502	.084249	.030262
0.9	.297587	.060912	.190759	3.3	.086191	.081956	.026235
1.0	.291225	.066259	.184011	3.4	.078114	.079569	.022533
1.1	.284349	.071204	.176838	3.5	.070280	.077108	.019147
1.2	.276999	.075729	.169312	3.6	.062694	.074592	.016068
1.3	.269218	.079819	.161503	3.7	.055362	.072039	.013284
1.4	.261050	.083467	.153481	3.8	.048287	.069466	.010783
1.5	.252539	.086667	.145315	3.9	.041469	.066889	.008555
1.6	.243731	.089419	.137070	4.0	.034909	.064322	.006589
1.7	.234670	.091728	.128808	4.1	.028604	.061779	.004874
1.8	.225400	.093601	.120587	4.2	.022552	.059274	.003405
1.9	.215964	.095050	.112460	4.3	.016748	.056819	.002175
2.0	.206404	.096088	.104476	4.4	.011186	.054427	.001185
2.1	.196760	.096733	.096677	4.5	.005860	.052113	.000449
2.2	.187070	.097005	.089101	4.6	.000760	.049892	.000021
2.3	0.177370	0.096924	0.081780	η_i	0.000000	0.049561	0.000000

TABLE 5 $\eta_i = 3.0806$ $y_c = 0.25$

η	Z	$-dZ/d\eta$	ζ	η	Z	$-dZ/d\eta$	ζ
0.0	1.08214	0.00000	1.84726	1.6	0.52842	0.47811	0.50836
.1	1.07907	.06138	1.83755	1.7	.48110	.46768	.43178
.2	1.06990	.12161	1.80876	1.8	.43497	.45460	.36279
.3	1.05482	.17956	1.76187	1.9	.39026	.43938	.30131
.4	1.03410	.23424	1.69845	2.0	.34715	.42251	.24704
.5	1.00811	.28474	1.62056	2.1	.30579	.40443	.19963
.6	0.97732	.33034	1.53063	2.2	.26629	.38553	.15861
.7	.94223	.37049	1.43129	2.3	.22870	.36616	.12349
.8	.90341	.40480	1.32528	2.4	.19306	.34664	.09376
0.9	.86147	.43311	1.21527	2.5	.15937	.32722	.06890
1.0	.81699	.45539	1.10378	2.6	.12761	.30813	.04842
1.1	.77059	.47178	0.99309	2.7	.09773	.28956	.03189
1.2	.72282	.48256	.88517	2.8	.06967	.27166	.01889
1.3	.67425	.48810	.78163	2.9	.04337	.25457	.00916
1.4	.62536	.48886	.68375	3.0	.01873	.23842	.00257
1.5	0.57662	0.48535	0.59246	η_i	0.00000	0.22617	0.00000

TABLE 6 $\eta_1 = 1.7171$ $y_c = 0.5$

η	Z	$-dZ/d\eta$	ζ	η	Z	$-dZ/d\eta$	ζ
0.00	4.30175	0.0000	27.2991	0.90	1.92080	3.3538	5.4792
.05	4.29039	0.4535	27.1519	0.95	1.75569	3.2484	4.6067
.10	4.25655	0.8983	26.7157	1.00	1.59615	3.1317	3.8379
.15	4.20085	1.3259	26.0064	1.05	1.44265	3.0068	3.1663
.20	4.12437	1.7287	25.0491	1.10	1.29556	2.8765	2.5847
.25	4.02851	2.1001	23.8765	1.15	1.15506	2.7430	2.0852
.30	3.91498	2.4347	22.5271	1.20	1.02127	2.6086	1.6598
.35	3.78572	2.7286	21.0421	1.25	0.89419	2.4748	1.3007
.40	3.64284	2.9791	19.4641	1.30	.77376	2.3431	1.0005
.45	3.48855	3.1853	17.8339	1.35	.65983	2.2147	0.7521
.50	3.32505	3.3471	16.1899	1.40	.55222	2.0905	.5491
.55	3.15455	3.4660	14.5658	1.45	.45070	1.9712	.3857
.60	2.97913	3.5442	12.9902	1.50	.35502	1.8573	.2566
.65	2.80076	3.5847	11.4863	1.55	.26487	1.7493	.1572
.70	2.62123	3.5911	10.0715	1.60	.17999	1.6474	.0837
.75	2.44215	3.5672	8.7580	1.65	.10003	1.5518	.0331
.80	2.26495	3.5170	7.5533	1.70	.02470	1.4627	.0039
0.85	2.09082	3.4446	6.4604	η_1	0.00000	1.4338	0.0000

TABLE 7 $\eta_1 = 0.53516$ $y_c = 1.0$

η	Z	$-dZ/d\eta$	ζ	η	Z	$-dZ/d\eta$	ζ
0.00	37.4190	0.000	2980.96	0.28	14.9985	90.363	385.86
.01	37.3693	9.919	2971.95	.29	14.1080	87.725	337.50
.02	37.2210	19.729	2945.13	.30	13.2442	85.022	294.05
.03	36.9755	29.328	2901.05	.31	12.4077	82.278	255.16
.04	36.6355	38.615	2840.65	.32	11.5987	79.516	220.47
.05	36.2045	47.497	2765.14	.33	10.8174	76.754	189.65
.06	35.6871	55.894	2676.04	.34	10.0636	74.010	162.35
.07	35.0885	63.734	2575.04	.35	9.3371	71.298	138.26
.08	34.4145	70.958	2464.00	.36	8.6374	68.631	117.08
.09	33.6715	77.522	2344.86	.37	7.9643	66.017	98.53
.10	32.8664	83.393	2219.58	.38	7.3169	63.467	82.35
.11	32.0061	88.552	2090.08	.39	6.6947	60.986	68.30
.12	31.0977	92.993	1958.20	.40	6.0969	58.579	56.14
.13	30.1486	96.722	1825.65	.41	5.5228	56.252	45.69
.14	29.1656	99.753	1693.99	.42	4.9716	54.006	36.75
.15	28.1558	102.110	1564.59	.43	4.4424	51.844	29.16
.16	27.1255	103.827	1438.63	.44	3.9345	49.767	22.76
.17	26.0812	104.940	1317.11	.45	3.4468	47.775	17.41
.18	25.0286	105.492	1200.80	.46	2.9787	45.868	12.99
.19	23.9731	105.529	1090.32	.47	2.5292	44.046	9.39
.20	22.9196	105.098	986.08	.48	2.0975	42.307	6.50
.21	21.8726	104.247	888.38	.49	1.6828	40.650	4.25
.22	20.8359	103.024	797.33	.50	1.2842	39.073	2.54
.23	19.8132	101.477	712.97	.51	0.9011	37.574	1.32
.24	18.8073	99.650	635.20	.52	0.5325	36.152	0.52
.25	17.8209	97.587	563.86	0.53	0.1778	34.803	0.08
.26	16.8562	95.327	498.71	η_1	0.0000	34.135	0.00
0.27	15.9149	92.907	439.49				

TABLE 8 $\xi_1 = 10.9308$ $y_c = 2.0$

ξ	F	$-dF/d\xi$	σ	y
0.00	4.20000	0.00000	1.00000	2.00000
0.25	4.18960	.08302	0.99379	1.99927
0.50	4.15864	.16420	.97543	1.99707
0.75	4.10780	.24178	.94574	1.99344
1.00	4.03818	.31421	.90598	1.98839
1.25	3.95124	.38018	.85778	1.98196
1.50	3.84872	.43868	.80299	1.97420
1.75	3.73257	.48905	.74356	1.96516
2.00	3.60490	.53094	.68142	1.95490
2.25	3.46781	.56432	.61833	1.94349
2.50	3.32343	.58942	.55587	1.93099
2.75	3.17376	.60667	.49534	1.91746
3.00	3.02070	.61671	.43777	1.90296
3.25	2.86595	.62024	.38390	1.88756
3.50	2.71105	.61808	.33422	1.87132
3.75	2.55731	.61103	.28898	1.85428
4.00	2.40587	.59989	.24826	1.83650
4.25	2.25765	.58543	.21197	1.81801
4.50	2.11338	.56835	.17992	1.79885
4.75	1.97363	.54929	.15187	1.77904
5.00	1.83885	.52882	.12748	1.75860
5.25	1.70930	.50742	.10643	1.73755
5.50	1.58518	.48551	.08837	1.71587
5.75	1.46656	.46343	.07296	1.69357
6.00	1.35346	.44148	.05990	1.67061
6.25	1.24579	.41987	.04888	1.64697
6.50	1.14348	.39879	.03963	1.62261
6.75	1.04634	.37837	.03190	1.59744
7.00	0.95423	.35871	.02548	1.57141
7.25	.86692	.33988	.02018	1.54440
7.50	.78421	.32193	.01582	1.51629
7.75	.70588	.30487	.01226	1.48690
8.00	.63170	.28872	.00938	1.45603
8.25	.56144	.27347	.00706	1.42341
8.50	.49489	.25910	.00522	1.38868
8.75	.43182	.24559	.00377	1.35138
9.00	.37203	.23291	.00264	1.31086
9.25	.31530	.22102	.00179	1.26623
9.50	.26146	.20990	.00115	1.21616
9.75	.21029	.19949	.00069	1.15855
10.00	.16166	.18977	.00038	1.08990
10.25	.11536	.18069	.00017	1.00342
10.50	.07126	.17221	.00006	0.88338
10.75	.02920	.16430	.00001	0.67310
ξ_1	0.00000	0.15891	0.00000	0.00000

TABLE 9

y	Z	Π	θ	ζ	α_1
0.02	0.080204	0.0018605	0.077717	0.023470	0.549542
.04	.138454	.0074547	.130126	.055085	.650631
.06	.197121	.0184859	.179854	.096964	.734253
.08	.259230	.0376564	.229814	.151718	.812515
.10	.326290	.0688610	.281284	.222554	.889498
.12	.399366	.1176026	.335039	.313404	0.967174
.14	.479369	.191572	.391641	.429080	1.046706
.16	.567155	.301431	.451557	.575462	1.128892
.18	.663578	.461865	.515201	.759725	1.21434
.20	.769516	0.692989	.582967	0.990606	1.30355
.22	0.885886	1.022214	.655241	1.27874	1.39698
.24	1.013659	1.48674	.732413	1.63703	1.49503
.26	1.15387	2.13683	.814879	2.08116	1.59811
.28	1.30762	3.04018	.903050	2.63013	1.70660
.30	1.47609	4.28767	0.997355	3.30695	1.82091
.32	1.66054	6.00089	1.098242	4.13946	1.94144
.34	1.86235	8.34214	1.206182	5.16131	2.06859
.36	2.08296	11.52747	1.321674	6.41314	2.20279
.38	2.32395	15.8438	1.44524	7.94399	2.34449
.40	2.58701	21.6713	1.57744	9.81301	2.49416
.42	2.87395	29.5128	1.71887	12.09146	2.65227
.44	3.18672	40.0319	1.87014	14.8651	2.81934
.46	3.52741	54.1029	2.03192	18.2373	2.99590
.48	3.89828	72.8761	2.20491	22.3322	3.18252
.50	4.30175	97.8615	2.38986	27.2991	3.37977
.52	4.74041	131.040	2.58756	33.3172	3.58830
.54	5.21706	175.003	2.79885	40.6019	3.80875
.56	5.73469	233.144	3.02463	49.4114	4.04183
.58	6.29653	309.889	3.26583	60.0557	4.28825
.60	6.90602	411.014	3.52348	72.9063	4.54880
.62	7.56689	544.046	3.79864	88.4082	4.82428
.64	8.28310	718.777	4.09244	107.0946	5.11555
.66	9.05894	947.941	4.40610	129.6041	5.42353
.68	9.89898	1248.07	4.74089	156.7007	5.74917
.70	10.80814	1640.63	5.09818	189.298	6.09349
.72	11.7917	2153.43	5.47941	228.491	6.45755
.74	12.8553	2822.50	5.88612	275.585	6.84247
.76	14.0050	3694.45	6.31993	332.142	7.24946
.78	15.2473	4829.56	6.78259	400.030	7.67977
.80	16.5891	6305.73	7.27592	481.476	8.13473
.82	18.0380	8223.50	7.80189	579.143	8.61575
.84	19.6018	10712.61	8.36256	696.207	9.12430
.86	21.2893	13940.3	8.96013	836.459	9.66196
.88	23.1094	18122.0	9.59694	1004.421	10.23037
.90	25.0722	23535.2	10.27547	1205.49	10.83130
.92	27.1879	30536.8	10.99835	1446.09	11.4666
.94	29.4680	39585.9	11.7684	1733.89	12.1382
.96	31.9245	51272.4	12.5885	2078.04	12.8481
0.98	34.5702	66354.0	13.4619	2489.40	13.5986
1.00	37.4190	85803.4	14.3919	2980.96	14.3919
0.01	0.048433	0.0005216	0.047670	0.010833	0.476703
0.25	1.082142	1.78482	0.772959	1.84726	1.54592
2.00	$1.38093 \cdot 10^3$	$8.76510 \cdot 10^9$	$3.28794 \cdot 10^2$	$8.88611 \cdot 10^6$	$2.32492 \cdot 10^2$

TABLE 10

Z	y	ζ	Z	y	ζ
0.001	0.000031616	0.000031624	0.05	0.01045865	0.01137137
.002	.000089392	.000089456	.06	.01348626	.01502269
.003	.000164144	.000164359	.07	.01665630	.01903042
.004	.000252574	.000253084	.08	.01993232	.02337813
.005	.000352756	.000353753	.09	.02328539	.02805339
.006	.000463382	.000465103	.10	.02669235	.03304650
.007	.000583479	.000586209	.11	.03013452	.03834973
.008	.000712288	.000716358	.12	.03359686	.04395681
.009	.000849188	.000854977	.13	.03706719	.04986252
.010	.000993663	.001001593	.14	.04053567	.05606253
.011	.001145267	.001155809	.15	.04399438	.06255316
.012	.001303617	.001317283	.16	.04743691	.06933125
.013	.001468370	.001485721	.17	.05085814	.07639408
.014	.001639223	.001660861	.18	.05425399	.08373930
.015	.001815902	.001842474	.19	.05762121	.09136482
.016	.001998156	.002030353	.20	.06095730	.09926887
.017	.002185758	.002224314	.21	.06426027	.1074498
.018	.002378496	.002424188	.22	.06752866	.1159062
.019	.002576176	.002629820	.23	.07076137	.1246368
.020	.002778615	.002841072	.24	.07395764	.1336405
.021	.002985642	.003057813	.25	.07711696	.1429163
.022	.003197100	.003279927	.26	.08023908	.1524632
.023	.003412837	.003507300	.27	.08332388	.1622805
.024	.003632710	.003739832	.28	.08637141	.1723673
.025	.003856587	.003977427	.29	.08938184	.1827232
.026	.004084336	.004219995	.30	.09235544	.1933473
.027	.004315845	.004467459	.31	.09529256	.2042393
.028	.004550979	.004719724	.32	.09819362	.2153986
.029	.004789645	.004976732	.33	.1010591	.2268248
.030	.005031729	.005238408	.34	.1038895	.2385176
.031	.005277131	.005504685	.35	.1066853	.2504764
.032	.005525753	.005775505	.36	.1094471	.2627012
.033	.005777501	.006050804	.37	.1121754	.2751915
.034	.006032285	.006330532	.38	.1148709	.2879471
.035	.006290017	.006614630	.39	.1175342	.3009678
.036	.006550613	.006903051	.40	.1201659	.3142536
.037	.006813992	.007195746	.41	.1227665	.3278038
.038	.007080075	.007492670	.42	.1253366	.3416188
.039	.007348788	.007793778	.43	.1278769	.3556982
0.040	0.007620057	0.008099030	0.44	0.1303879	0.3700420

TABLE 10 - Continued

Z	y	ζ	Z	y	ζ
0.45	0.1328702	0.3846499	4	0.4852027	23.53369
.46	.1353244	.3995222	5	.5310969	37.18720
.47	.1377510	.4146585	6	.5696482	54.29591
.48	.1401506	.4300590	7	.6029444	75.01028
.49	.1425238	.4457236	8	.6322850	99.47089
.50	.1448710	.4616521	9	.6585353	127.8101
.6	.1670260	.6354650	10	.6823018	160.1533
.7	.1870903	.8357373	11	.7040266	196.6202
.8	.2054231	1.062582	12	.7240421	237.3251
0.9	.2223031	1.316151	13	.7426047	282.3779
1.0	.2379487	1.596621	14	.7599168	331.8847
1.1	.2525332	1.904184	15	.7761405	385.9478
1.2	.2661962	2.239041	16	.7914082	444.6662
1.3	.2790512	2.601400	17	.8058292	508.1366
1.4	.2911922	2.991471	18	.8194949	576.4522
1.5	.3026973	3.409468	19	.8324825	649.7042
1.6	.3136325	3.855601	20	.8448579	727.9817
1.7	.3240541	4.330086	21	.8566775	811.3713
1.8	.3340100	4.833134	22	.8679903	899.9579
1.9	.3435418	5.364956	23	.8788393	993.8249
2.0	.3526858	5.925760	24	.8892618	1093.053
2.1	.3614737	6.515756	25	.8992908	1197.723
2.2	.3699332	7.135148	26	.9089558	1307.913
2.3	.3780892	7.784140	27	.9182829	1423.699
2.4	.3859636	8.462937	28	.9272955	1545.158
2.5	.3935759	9.171732	29	.9360146	1672.363
2.6	.4009439	9.910728	30	.9444592	1805.388
2.7	.4080835	10.68012	31	.9526464	1944.305
2.8	.4150088	11.48010	32	.9605918	2089.184
2.9	.4217331	12.31086	33	.9683098	2240.098
3.0	.4282681	13.17260	34	.9758130	2397.112
3.1	.4346246	14.06549	35	.9831136	2560.297
3.2	.4408126	14.98972	36	.9902224	2729.718
3.3	.4468410	15.94549	37	.9971495	2905.443
3.4	.4527184	16.93296	38	1.003904	3087.538
3.5	0.4584523	17.95232	39	1.010495	3276.063
			40	1.016930	3471.089

Figure 1 illustrates the density distribution for the various cases integrated and also the density distribution for the two limiting polytropes. In Figure 2 the logarithm of the product of the mass, in units of the solar mass, times the square of the mean molecular weight is plotted against the logarithm of y_c. It is seen that this curve lies between the two limiting curves given by equations (45) and (46).

6. *Perturbation theory for small values of* y_c.—It has been indicated that in the limiting case of vanishing radiation pressure the model considered here reduces simply to the polytrope with index $n = 3/2$. Consequently, it would seem likely that the density

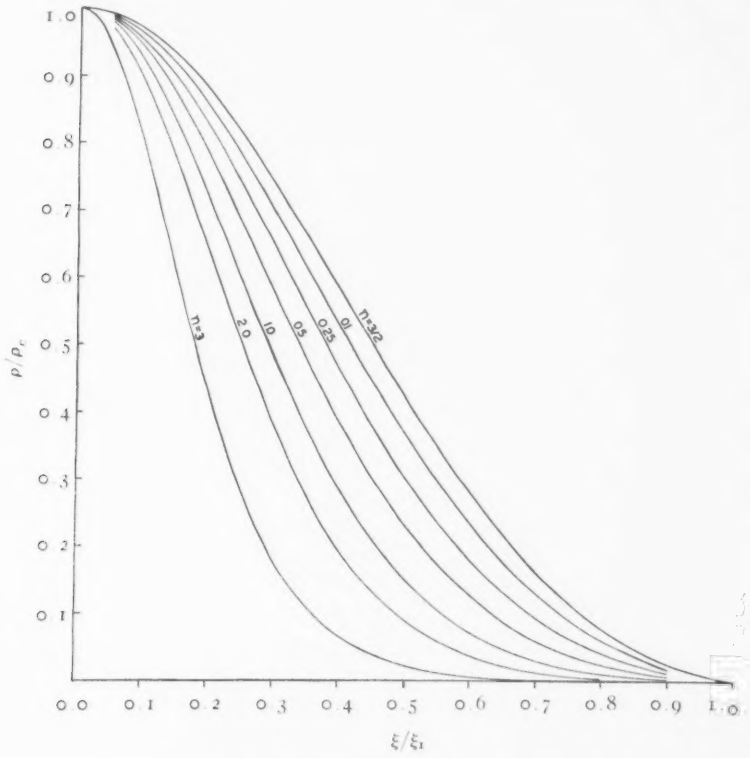

FIG. 1.—The density distribution in the convective model with radiation pressure. Each curve is labeled with the central value of the ratio of the radiation pressure to the gas pressure (y_c). The two limiting curves are the solutions of the Lane-Emden equation with index $n = \frac{3}{2}$ and $n = 3$, respectively.

distribution in stars of small mass might be represented quite accurately by considering the extent to which the density distribution in these stars deviated from the distribution in the limiting polytrope. It would, therefore, be of interest to consider the effect of radiation pressure as a perturbation of the polytrope of index $n = 3/2$. Such a calculation would probably be sufficient for the treatment of the majority of stars.

We shall, therefore, seek a solution of the differential equation of the following form

$$F = \theta_{3/2} + y_c f_1 ; \qquad (58)$$

and

$$\sigma = \theta_{3/2}^{3/2} + y_c\sigma_1 , \tag{59}$$

where $\theta_{3/2}$ denotes the Lane-Emden function of index $n = 3/2$, while f_1 and σ_1 are first-order terms for the potential and density, respectively. We shall restrict ourselves to

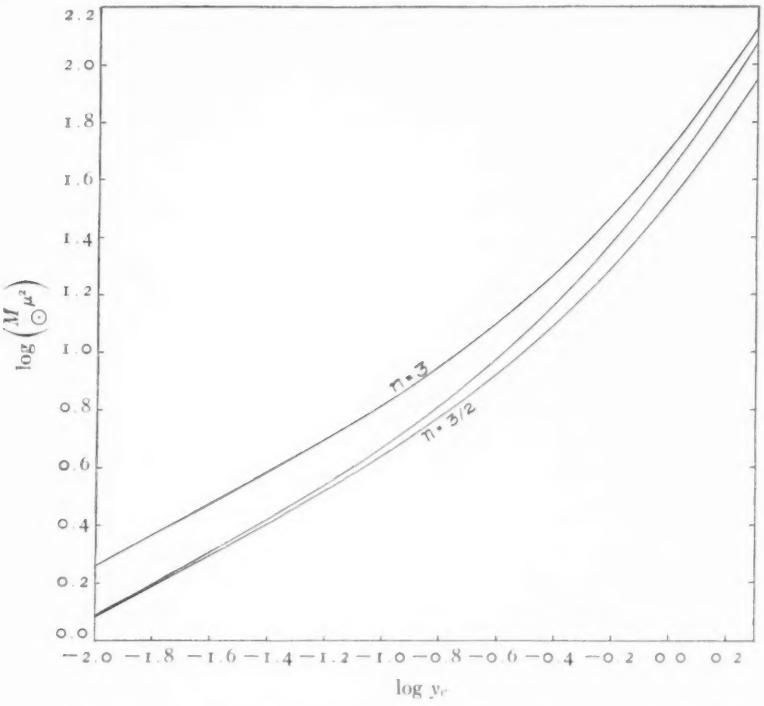

FIG. 2.—The mass as a function of y_c. The central curve is for the convective model with radiation pressure. The asymptotes are for the polytropes of index $n = \frac{3}{2}$ and $n = 3$, respectively.

terms of the first order and neglect the higher-order terms. Using equations (23) and (24) we find

$$\left.\begin{aligned} F &= \left(\frac{y}{y_c}\right)^{2/3}(1 + \tfrac{6}{10}y - \tfrac{8}{3}y_c + \dots .) , \\ \sigma &= \left(\frac{y}{y_c}\right)(1 + 8[y - y_c] + \dots .) , \end{aligned}\right\} \tag{60}$$

or, eliminating y between the foregoing equations, we find

$$\sigma = F^{3/2} + y_c(\tfrac{8}{5}F^3 - 4F^{3/2}) + \dots . \tag{61}$$

Expanding F in terms of $\theta_{3/2}$ and f_1, according to equation (58), and retaining only the first-order terms, we have

$$\sigma = \theta_{3/2}^{3/2} + y_c(\tfrac{3}{2}\theta_{3/2}^{1/2}f_1 - 4\theta_{3/2}^{3/2} + \tfrac{8}{5}\theta_{3/2}^{3}) , \tag{62}$$

so that

$$\sigma_1 = \tfrac{3}{2}\theta_{3/2}^{1/2} f_1 - 4\theta_{3/2}^{3/2} + \tfrac{8}{5}\theta_{3/2}^{3} . \tag{63}$$

On substituting equations (58) and (59) in the differential equation (27) and eliminating the terms which represent merely the solution of the Lane-Emden equation, we obtain

$$\frac{1}{\xi^2}\frac{d}{d\xi}\left(\xi^2 \frac{df_1}{d\xi}\right) = -\tfrac{3}{2}\theta_{3/2}^{1/2} f_1 + 4\theta_{3/2}^{3/2} - \tfrac{8}{5}\theta_{3/2}^{3} . \tag{64}$$

Actually, this relation is not valid near the boundary. For it was necessary to expand the quantity $F^{3/2}$ as a binomial series in which $\theta_{3/2}$ was taken as the larger term. Since $\theta_{3/2}$ approaches zero at the boundary, this condition is not fulfilled for all values of the radius. But for sufficiently small values of y_c the errors are not appreciable except in the immediate neighborhood of the boundary.

The results of the integration of equation (64) are given in Table 2. Using this, a comparison was made with the exact integration for $y_c = 0.01$. This showed that up to 97 per cent of the radius this method gave the quantity σ with an error of less than two units in the fourth decimal place. On the other hand, a comparison with the integration for $y_c = 0.1$ indicated that this perturbation theory would probably not be useful for values of $y_c \geqslant 0.03$.

We may finally note here that this perturbation theory can be used in connection with the complete point-source model to obtain the first-order corrections introduced by radiation pressure in the mass-luminosity relation obtained, for instance, on the basis of the Cowling model.

I am greatly indebted to Dr. S. Chandrasekhar for suggesting this investigation and for many helpful discussions.

YERKES OBSERVATORY
February 1941

NOTES

THE RESONANCE BANDS OF THE *NH* MOLECULE IN SPECTRA OF CLASS R

ABSTRACT

The ultraviolet resonance bands of *NH* have been identified in the spectra of R-type stars, photographed at the McDonald Observatory with dispersions of 120 A/mm and 60 A/mm. The intensities of these bands have been compared with those of C_2, *CN*, and *CH*. The large scattering of these intensities suggests considerable differences in the relative abundances of *H*, *C*, and *N*.

The spectra of several of the brighter carbon stars of class R have been photographed with a quartz spectrograph attached to the 82-inch reflector of the McDonald Observatory. Two different cameras were used, giving dispersions of 120 A/mm and 60 A/mm, respectively, at λ 3300. The spectrograms extend as far as λ 3250, the limit imposed by the transparency of the glass optics of the collimator, and show a wealth of hitherto unobserved detail; the dispersion is much higher than that used by Shane[1] in his survey of ultraviolet R spectra. With a few exceptions, to be stated presently, practically all absorption features below λ 3900 were identified with atomic lines of *Fe* I, *Ni* I, and *Ti* II. In view of the great strength of the D lines observed by Shane in some N stars,[2] a careful search was made on all spectrograms for the second member of the principal series of sodium (λλ 3302–3303), but its presence could not be acertained. Perhaps the sodium doublet is masked by what looks like the head, at λ 3301, of an absorption band degraded toward the red. There is a similar head at λ 3289, degraded toward the violet, which makes the region between λ 3301 and λ 3289 stand out against a fainter continuous background. This appears to be a characteristic feature of all the R stars that have been investigated. No reasonable identification of these two heads can be suggested at present.

The most interesting find is the resonance bands ($^3\Pi \rightarrow {}^3\Sigma$ system) of the molecule *NH* at λ 3360 (0 − 0) and λ 3370 (1 − 1). These were known to exist in the spectrum of the sun,[3] and of Arcturus.[4] They also had been suspected of occurring in the spectra of several R stars,[5] but this identification remained doubtful on account of the exceedingly low dispersion used and the ensuing possibility of blending with the *CN* band at λ 3360.1 (2 − 0).

Fortunately, the *CN* band is strongly degraded toward the shorter wave lengths and hence does not interfere with the (1 − 1)-band λ 3370 of *NH*. Moreover, the $^3\Pi \rightarrow {}^3\Sigma$ system of *NH* consists of singularly symmetrical and narrow bands—a peculiarity that is fully understood and can be explained in terms of the shape of the potential curves of the electronic states involved. On the McDonald spectrograms the two *NH* bands look like a pair of very broad and hazy atomic lines, about 5 A in width. Hence it is inherently improbable that the appearance of the narrow *NH* band λ 3360 would be greatly affected by the cyanogen band, which would extend from λ 3360 toward shorter wave lengths over a range of about 50 A (as judged by the extension of the [0 − 0] and

[1] *Lick Obs. Bull.*, **13**, 123, 1928.

[2] *Ibid.*, **10**, 79, 1920.

[3] A. Fowler and C. C. L. Gregory, *Phil. Trans.*, A, **218**, 351, 1919.

[4] R. W. Shaw, *Ap. J.*, **83**, 225, 1936.

[5] R. Wildt, *Ap. J.*, **84**, 303, 1936.

[1 − 1] bands of cyanogen). In fact, the intrinsic strength of the (2 − 0)-band, λ 3360, should be considerably smaller than that of the (1 − 0)-band, λ 3590, which is plainly visible in all R spectra.

The only faint indication of the *CN* absorption from λ 3360 toward shorter wave lengths is found, among the spectra investigated, in that of HD 79319, in which the cyanogen bands reach the maximum strength observed, according to Table 1. The

TABLE 1

STELLAR SPECTRA OF CLASS R

STAR	m_{vis}	SPECTRUM	BAND INTENSITIES				REMARKS
			C_2	CN	NH	CH	
HD 113801	8.7	K5p	1	2	3	1	HD: transition type between K and Ro
BD−19°3634							
HD 76846	9.2	Ro	2	3	2	2	
BD+34°1929							
HD 100764	8.7	Ro	2	3	2	2	
BD−13°3407							
HD 156074	7.7	Ro	2	3	2	2	
BD+42°2811		R1*					
HD 52432	7.5	R5	4	2	1:†	‡	HD: prototype of R5
BD−3°1685							
HD 76396	8.8	R5	2	1	2	2	
BD+51°1462							
HD 79319	8.9	R5	5	4	1	1	
BD+14°2048		R4*					
HD 112869	9.2–9.6	Na	5	3	‡	3	
BD+28°2389		R6p*					
HD 25408	7.9	R8	4	3	‡	1	HD: prototype of R8
BD+61°667							
HD 59643	8.2	R8	4	2	1:	1	
BD+24°1686		R9*					

* Reclassification of some spectra after Shane.

† Estimated band intensities marked : are doubtful.

‡ Blank spaces indicate that the estimate is impossible because of plate defects, underexposure, or overexposure.

estimates of band intensities given in this table were made on an arbitrary scale of five steps. Naturally, the estimates referring to different molecules cannot be compared directly, as the appearance of the narrow bands of *CH* and *NH* differs widely from that of the degraded bands of C_2 and *CN*. There is no clear-cut correlation between the *NH* intensities and the spectral subclass of the stars. The wide and irregular scattering of the intensities of C_2 and *CH* has already been pointed out by Shane. Of particular interest is the star HD 76396, R5, whose ultraviolet continuum is at least as strong as that of an Ro star. Also, the band intensities, estimated by the writer from three spectrograms, suggest an earlier subclass, although the conspicuous faintness of the *CN* bands remains puzzling.

The wide scattering of the intensity estimates collected in Table 1 leaves little hope that band intensities will afford suitable parameters for the subclassification of R stars but rather would seem to indicate a considerable variation of the relative abundance of hydrogen, carbon, and nitrogen. In principle, it should be possible to determine from the band intensities of the four species of molecules the relative abundance of the three constituent elements. The practical solution of this problem is vitiated by the lack of any theory of atmospheric opacity applicable to late-type stars and by the absence of any detailed information on the oscillator strengths of the molecules involved. A reliable determination of the relative abundance of hydrogen, carbon, and nitrogen would be of the greatest interest in view of the carbon-cycle theory of stellar energy production. This theory makes certain quantitative predictions concerning these abundance ratios, which could be tested by observations. Strictly, the theory does not claim to apply to giant stars, but it would seem profitable to extend the study of the *NH* bands to main-sequence stars.

The writer is greatly indebted to Dr. O. Struve for the hospitality shown to him at the McDonald Observatory, and he also gratefully acknowledges the assistance given to him by members of the staff.

RUPERT WILDT

PRINCETON UNIVERSITY OBSERVATORY
December 1940

A NOTE ON THE SPECTRUM OF 17 LEPORIS (BS 2148)

The large violet displacements of the strong absorption lines of 17 Leporis have been interpreted as a consequence of radial expansion of a tenuous shell around a normal A-type star which produces an undisplaced line of *Mg* II 4481 and undisplaced wings of the hydrogen lines.[1] The line *Hα* is strong in emission.[2] On a few plates there is a faint, rather narrow, emission line[3] on the red side of the core of *Hβ*. I have often suspected the existence of weak emission borders on the red sides of the strongest metallic lines, but the evidence was not entirely conclusive. On a spectrogram obtained by Dr. Popper with the glass Cassegrain spectrograph of the McDonald Observatory (dispersion 20 A/mm at λ 3933) on January 1, 1940, at 6^h30^m U.T. the absorption lines were in their double stage.[4] The strong lines of *Ti* II, λ 3761 and λ 3742 clearly show an emission border on the red sides of the red absorption components. This establishes the P Cygni character of the absorption lines and confirms the earlier interpretation. There is probably also an emission border at λ 3759, and its effect is to weaken the violet absorption component of λ 3761.

It is of interest to notice that, while in *Ti* II and *Fe* II the red absorption component is a little stronger than the violet, in the Balmer lines the violet components are much stronger than the red components.

The weaker metallic lines are always faint in the double stage. But the hydrogen lines are strong.[4] We see now that the strongest metallic lines also remain very intense. For example, both components of *Ti* II 3759 are strong, while those of *Fe* II 3814 are weak. This suggests that we are here concerned, at least in part, with an effect of the curve of growth. Nearly all metallic lines observed between λ 4000 and λ 4900 on the old Yerkes spectrograms fall upon the steep linear part of the curve.[5] Hence, they are very sensitive

[1] *Ap. J.*, **76**, 85, 1932.

[2] *Ibid.*, **90**, 727, 1939.

[3] *Ibid.*, **76**, 88, 1932.

[4] *Ibid.*, p. 86, 1932.

[5] *Ibid.*, **79**, 428, 1934.

PLATE XX

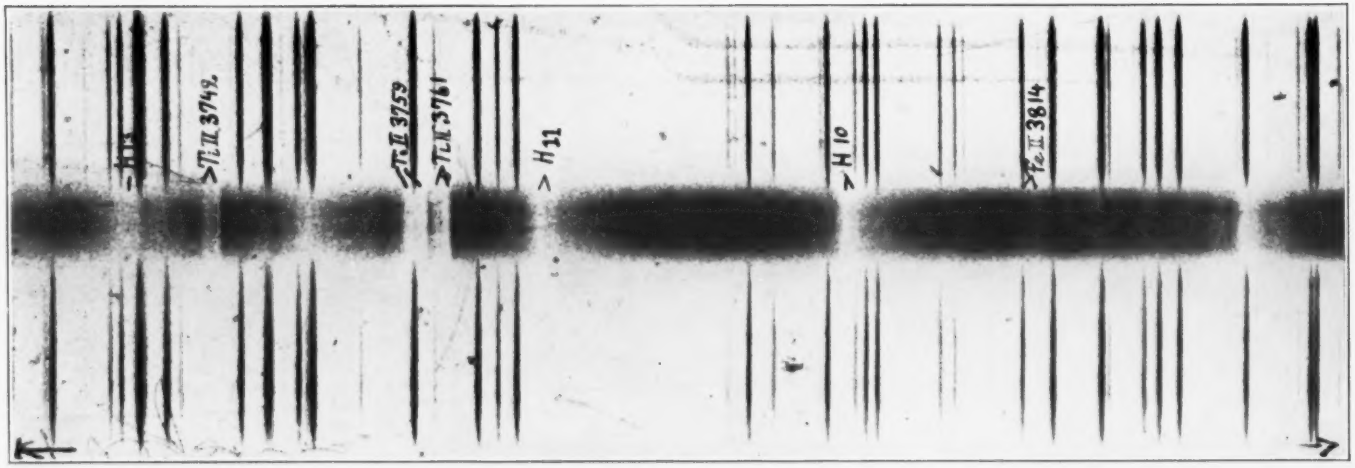

THE SPECTRUM OF 17 LEPORIS ON JANUARY 1, 1940

UNIV. OF MICH.

to changes in the numbers of atoms. The strongest metallic lines and the cores of the Balmer lines fall upon the flat portion of the curve of growth and are quite insensitive to changes in the numbers of atoms.

OTTO STRUVE

McDONALD OBSERVATORY
January 8, 1941

TEMPERATURE VARIATIONS OF γ CASSIOPEIAE

Since September, 1939, the Boe star γ Cassiopeiae has been on the author's program of color-temperature determinations of Be stars. Three comparisons with ϵ Cassiopeiae were obtained in 1939, five in 1940, and, to date, four in 1941. The plates taken in 1939 were measured with a Moll microphotometer and were reduced at eleven wave lengths between λ 6360 and λ 4050. All subsequent plates were measured with the direct-intensity microphotometer of the Observatory of the University of Michigan at forty-four wave lengths with the exception of plates 135 and 151; these were measured at thirty-one

TABLE 1

Plate No.	Date	$\Delta\Phi$	Φ	T_c
111	1939 Sept. 21	−0.21	0.74	34,000
124	Nov. 12	−0.10	0.85	24,500
126	26	−0.12	0.83	25,500
135	1940 July 13	−0.15	0.80	28,000
141	Oct. 30	−0.18	0.77	30,500
144	Nov. 7	−0.13	0.82	26,000
145	13	−0.18	0.77	30,500
149	Dec. 14	−0.22	0.73	35,500
150	1941 Jan. 3	−0.03	0.92	20,500
151	20	+0.13	1.08	16,000
152	Feb. 3	−0.04	0.91	21,000
153	9	−0.11	0.84	25,000

and twenty-four wave lengths, respectively. The results of the observations are recorded in Table 1. In the first column are the numbers of the plates, in the second are the dates of the observations, in the third are the observed values of the relative gradients in the sense γ Cas − ϵ Cas. It has been found[1] that the average scatter of relative gradient measures performed at Ann Arbor is of the order of 0.03. In the fourth column are the absolute gradients of γ Cassiopeiae referred to Williams' value[2] for the gradient of the zero point of the color-temperature scale. The gradient of ϵ Cassiopeiae relative to this zero point is taken as −0.20.[3] In the fifth column are the color temperatures corresponding to the absolute gradients in the preceding column. It is seen that no significant change in gradient was observed from September, 1939, to January, 1941, when the gradient suddenly increased and then fell. The observations will be continued.

W. ALBERT HILTNER

THE OBSERVATORY
UNIVERSITY OF MICHIGAN
February 17, 1941

[1] Williams, *Pub. Obs. U. of Michigan*, **7**, 166, 1939.

[2] *Ibid.*, p. 156.

[3] *M.N.*, **100**, 190, 1940.

PHOTOGRAPHS OF THE MILKY WAY IN CYGNUS AND SCORPIUS

Plate XXI shows two photographs of the region near γ Cygni, obtained with an f/1 Schmidt camera. The upper plate was obtained with an exposure of 20 minutes on Agfa Superpan Press film with a red filter; the lower with an exposure of 3 minutes on Eastman Ortho X film. The red-sensitive exposure shows a large amount of nebulosity centered along the Milky Way north and south of γ Cygni.

Plate XXII shows a region in Scorpius, α 17^h25^m, $\delta -38°$. The upper plate is an exposure of 20 minutes on Agfa Superpan Press film with a red filter; the lower one of 3 minutes on Eastman Ortho X film.

HAROLD A. LOWER

NOTE ON ECLIPSING VARIABLES

The card catalogue of references on eclipsing variables, which has been maintained at the Princeton University Observatory for a considerable time by Professor Raymond S. Dugan, is being continued by the present writer. Receipt of reprints of papers about eclipsing variables, particularly of those papers which appear in publications not regularly received by the Observatory, will be greatly appreciated. This catalogue is, of course, available for reference to any astronomer working on these stars.

NEWTON L. PIERCE

PRINCETON UNIVERSITY OBSERVATORY
January 15, 1941

THE GRATING INFRARED SOLAR SPECTRUM

I. ROTATIONAL STRUCTURE OF THE HEAVY WATER (*HDO*) BAND ν_2 AT 7.12 μ

ABSTRACT

The absorption band ν_2 of the heavy water vapor molecule *HDO* appears in the infrared solar spectrum at 7.12 μ. The amount of *HDO* vapor in the earth's atmosphere is exceedingly minute. Rotational structure of ν_2 (*HDO*) appears in the grating solar spectrum, while the "doublet" envelope of the band appears in the prismatic solar spectrum. The band ν_2 (*HDO*) is but rarely to be found in the solar spectrum, lying, as it does, in a region which is reduced to zero intensity by the *HHO* vapor normally resident in the atmosphere.

In a continuation and extension of work begun at the University of Michigan the author has recently mapped the infrared solar spectrum from 14 μ to 2 μ with an echelette grating having 2400 lines per inch.[1] The present note concerns a portion of the rotational structure of ν_2 (*HDO*). Discovery of the rotational structure in the grating solar spectrum led to a search for the band envelope of ν_2 (*HDO*) in the prismatic solar spectrum. It was quickly located in work already published.[2]

The envelope of ν_2 (*HDO*) is shown in Figure 1 in relation to the envelopes of ν_2 (*HHO*) and ν_1 (*NNO*).

The central portion of Figure 2 is a reproduction of the grating solar spectrum from 7.435 to 7.269 μ, deflection plotted upward. Below this curve is the corresponding region of ν_2 (*HDO*) observed by E. F. Barker and W. W. Sleator, who used a laboratory

[1] *Bulletin of the American Physical Society, Washington, D.C., Meeting, May 1, 2, 3, 1941.*

[2] See, e.g., curves 5 and 6 of Fig. 1 in Arthur Adel and C. O. Lampland, *Ap. J.*, **91**, 1, 1940.

PLATE XXI

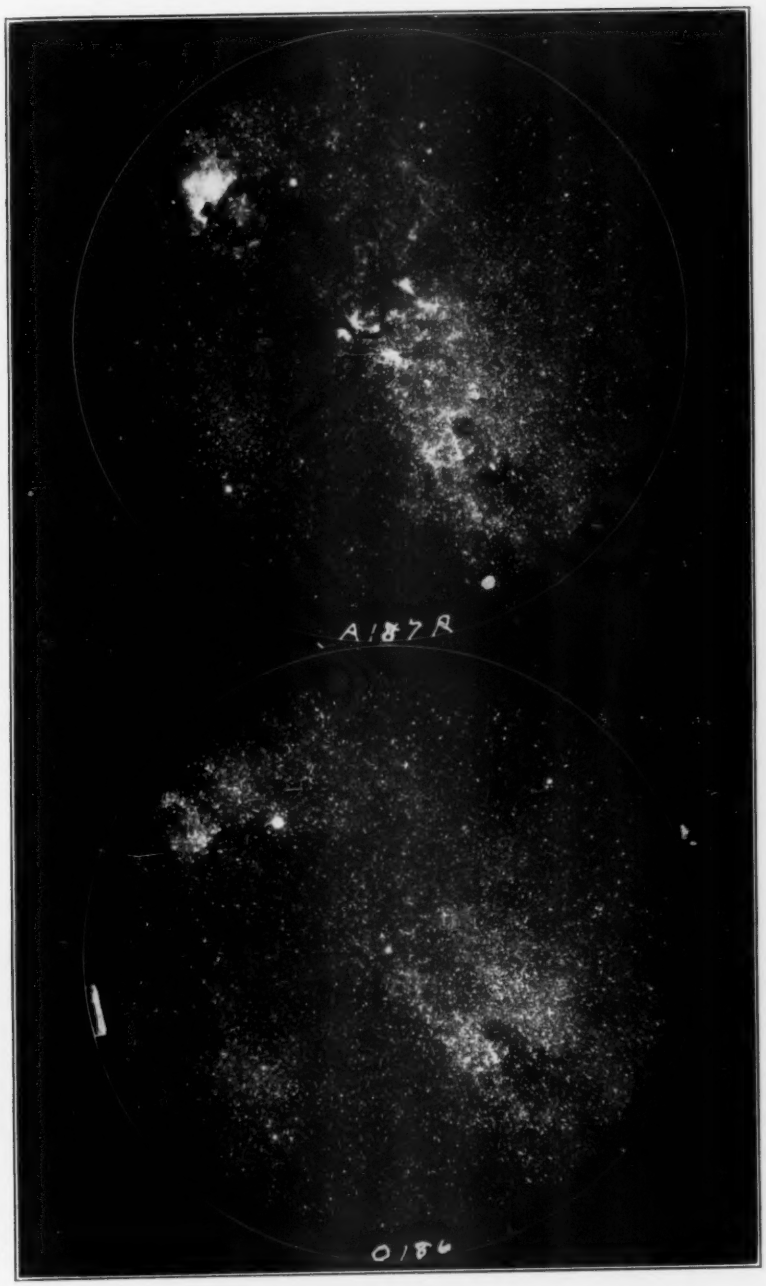

a

Red

b

Blue

REGION IN CYGNUS

UNIV. OF MICH.

PLATE XXII

a

Red

b

Blue

REGION IN SCORPIUS

UNIV. OF MICH.

FIG. 1.—Prismatic solar spectrum. Absorption by atmospheric *HDO* is shown in relation to absorption by atmospheric *HHO* and *NNO*.

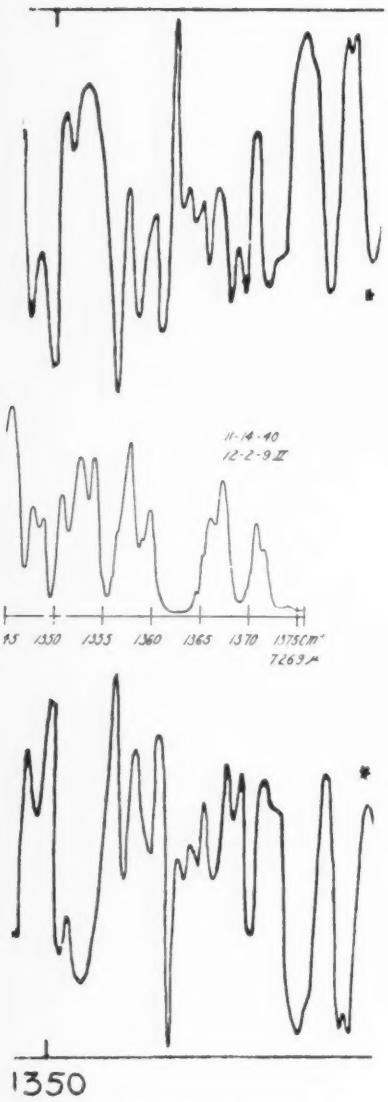

FIG. 2.—Rotational structure of *HDO* in the grating solar spectrum.

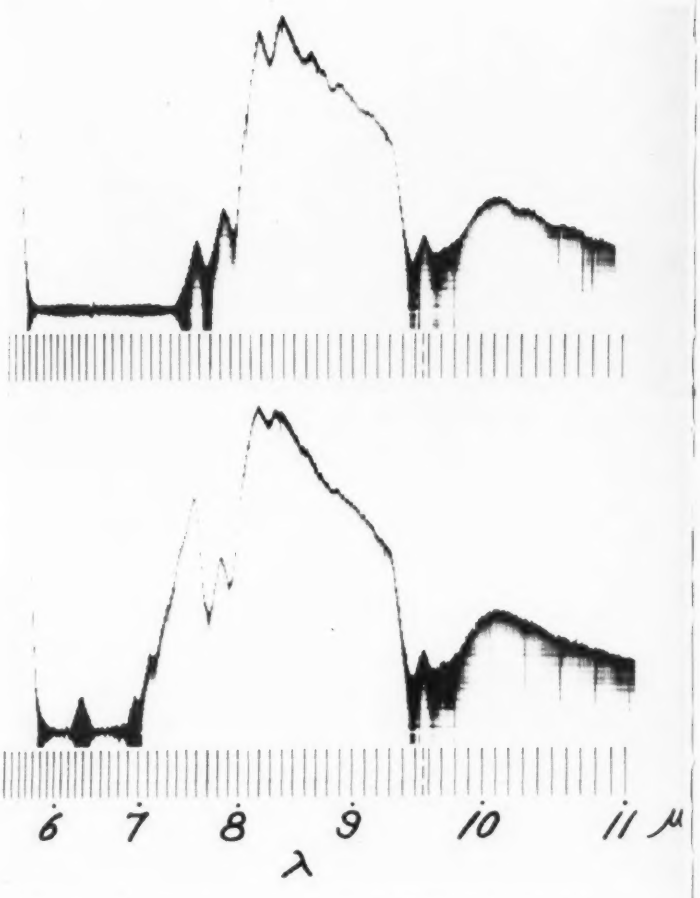

FIG. 3.—Occasional appearance of the *HDO* band in the solar spectrum

concentration of the heavy vapor.[1] They have plotted absorption upward. For convenience, therefore, their curve has been inverted and placed above the grating solar spectrum. Of course, other absorbing constituents of the earth's atmosphere are operative in this region of the spectrum also. Some of the ν_2 (*HDO*) lines are quite unaffected by this additional absorption; others are nearly obliterated. The agreement between the atmospheric and laboratory observations is, nevertheless, clear.

From Figure 3 it can be seen that the appearance of ν_2 (*HDO*) in the solar spectrum is a rare phenomenon. The band ν_2 (*HDO*) appears in the lower of the two curves, which was made with the precipitable water vapor (*HHO*) content of the atmosphere in the neighborhood of 1 mm liquid water equivalent. The upper curve was made with approximately 1 cm liquid water equivalent in the atmosphere. In this curve the region of 7.12 μ has been completely absorbed by ν_2 (*HHO*). Because of this circumstance ν_2 (*HDO*) must be sought in the solar spectrum at its very weakest, that is, when the atmosphere is driest.

Future observations of precipitable atmospheric water vapor by Fowle's method and simultaneous measurement of atmospheric absorption in ν_2 (*HDO*) should, in combination with calibrated absorption of ν_2 (*HDO*) in the laboratory, provide good determinations of the atmospheric abundance ratio *HDO*/*HHO*.

ARTHUR ADEL

LOWELL OBSERVATORY
FLAGSTAFF, ARIZONA
April 1941

THE GRATING INFRARED SOLAR SPECTRUM

II. ROTATIONAL STRUCTURE OF THE NITROUS OXIDE (*NNO*) BAND ν_1 AT 7.78 μ

ABSTRACT

Rotational structure of the atmospheric band ν_1 (*NNO*) has been obtained with a 2400-line grating.

The existence of an atmospheric layer of nitrous oxide (*NNO*) was established by the author in 1939.[2] The identification was accomplished through a comparison of the solar prismatic spectrum with the prismatic spectrum of nitrous oxide (Figure 1 on page 510).

In the same manner we may compare the grating solar spectrum[3] with the grating spectrum of nitrous oxide. Figure 2 is a reproduction of the grating solar spectrum from 7.924 to 7.692 μ, intensity plotted upward. Figure 3 shows the negative branch of ν_1 (*NNO*) as produced by approximately 1 cm *NNO* (N.T.P.).[4] Figures 2 and 3 were made in the first order of an echelette grating having 2400 lines per inch. In Figure 4, Figures 2 and 3 have been placed in correspondence. The rotational structure of ν_1 (*NNO*) is apparent in the grating solar spectrum despite the complex background due to other atmospheric constituents.

ARTHUR ADEL

LOWELL OBSERVATORY
FLAGSTAFF, ARIZONA
April 1941

[1] *J. Chem. Phys.*, **3**, 660, 1935.

[2] *Ap. J.*, **90**, 627, 1939.

[3] *Bulletin of the American Physical Society, Washington, D.C., Meeting, May 1, 2, 3, 1941.*

[4] The nitrous oxide bands were first resolved in the laboratory by E. K. Plyler and E. F. Barker, *Phys. Rev.*, **38**, 1827, 1931.

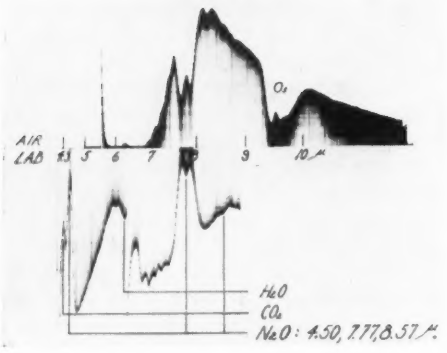

FIG. 1.—Prismatic identification of atmospheric nitrous oxide

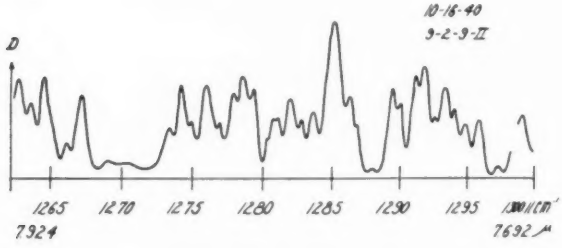

FIG. 2.—Grating solar spectrum, 7.924 to 7.692 μ

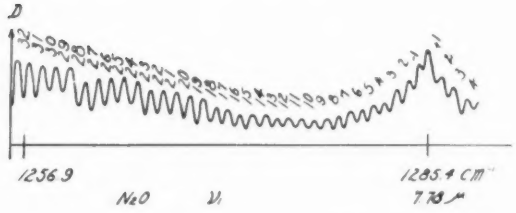

FIG. 3.—Negative branch of the *NNO* band at 7.78 μ

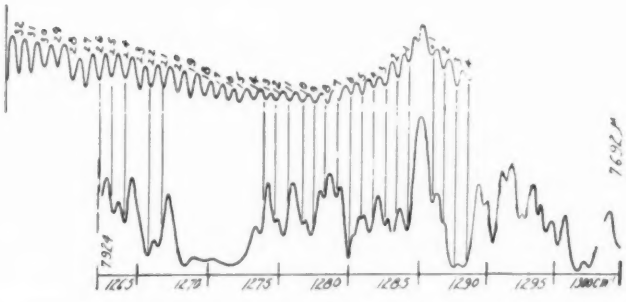

FIG. 4.—Grating identification of atmospheric nitrous oxide

A SIMPLE DEMONSTRATION OF STAR STREAMING

The existence of star streaming has been quantitatively established, and the constants of the velocity ellipsoid have been determined by statistical treatment of the extensive data on the radial velocities and proper motions of stars. While such elaborate discussions are necessary to utilize to the fullest extent the available information, such treatments are likely to obscure the essentially elementary character of the phenomenon that is being considered. Star streaming merely implies that the distribution of velocities in any given direction is Gaussian but with a modulus of precision which is a function of direction, and this should be capable of being demonstrated with a comparatively small amount of data.

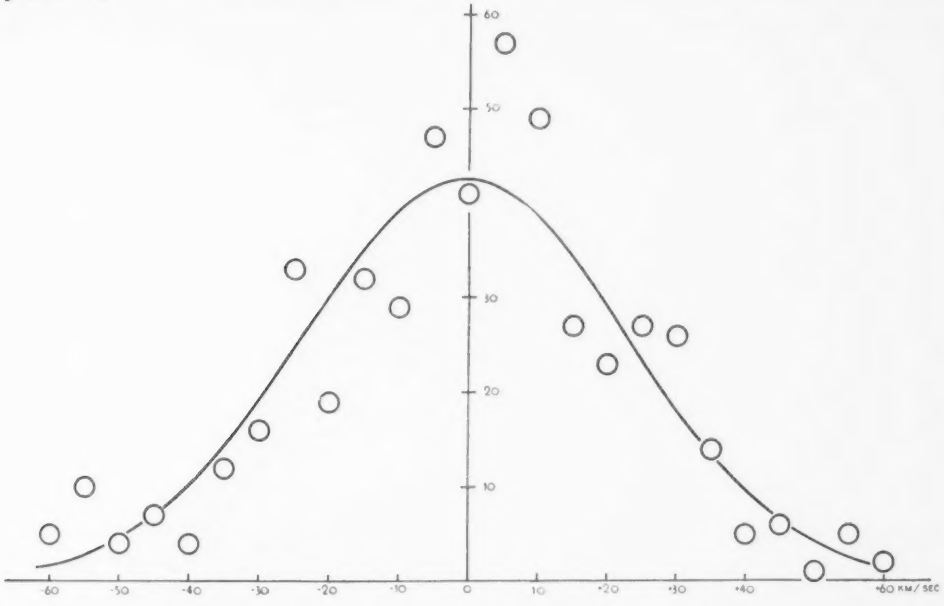

FIG. 1.—The distribution of the radial components of the peculiar velocities of stars near the vertex of star-streaming ($\alpha = 18^h16^m$; $\delta = -12°$). The full-line curve represents a Gaussian curve with the same first and second moments as the observed distribution. It is found that the first and the second moments are −0.3 and 23.4 km/sec, respectively; the latter gives the dispersion of the velocities in the direction considered.

It is clear that the most direct method of verifying the existence of star streaming would be to plot the distribution functions of the peculiar velocities of the stars in two different regions of the sky and to determine whether the resulting curves are Gaussian and what their moduli of precision are. Further, if one selects regions near the axes of the velocity ellipsoid, the radial velocities of the stars will be just the desired components parallel to the axes, and a discussion of these radial velocities should be sufficient to demonstrate the phenomenon.

In order to exhibit this, the Lick catalogue of radial velocities (*Pub. Lick Obs.*, **18**, 1932) has been used. One of the regions selected comprised an area of about 1600 square degrees, centered at $\alpha = 18^h16^m$, $\delta = -12°$, and a similar area exactly opposite to this. The other contained an area of about 1000 square degrees and was centered near $\alpha = 22^h$, $\delta = +55°$. All stars of spectral type later than B3 were used. There were 502 stars in the first group and 366 in the second. Reduction of the radial velocities to the local standard was accomplished by computing the corrections for the centers of regions about 15° square and applying them to all the stars in the square.

The figures show the observed frequency distributions for the two regions. For purposes of comparison the curves have been adjusted so as to contain equal numbers of stars. The calculated Gaussian distributions obtained by computing first and second moments are also shown. The difference in the dispersions in the two distributions is immediately obvious.

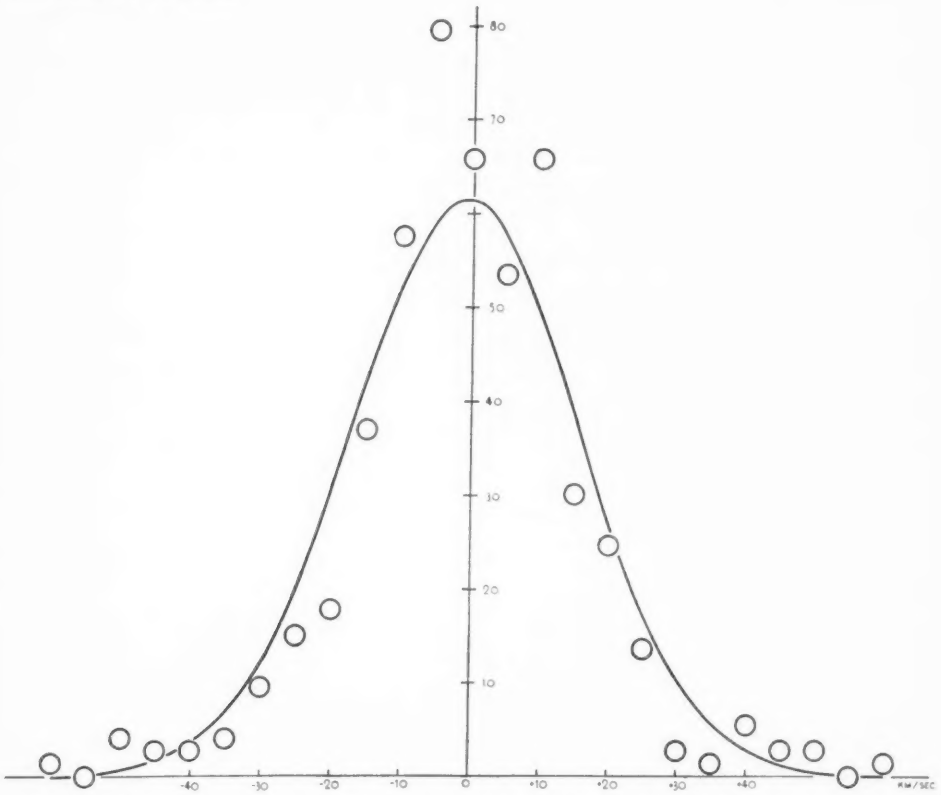

FIG. 2.—The distribution of the radial components of the peculiar velocities of stars approximately 90° from the vertex of star-streaming, and in the galactic plane ($\alpha = 22^h$; $\delta = +55°$.) The full-line curve represents a Gaussian curve with the same first and second moments as the observed distribution. It is found that the first and the second moments are −0.7 and 16.3 km/sec, respectively; the latter gives the dispersion of the velocities in the direction considered.

The fact that the first moments are less than 1 km/sec indicates that, even from so small a number of stars, the components of solar motion in these directions may be determined with fair accuracy. The second moments, which give the axes of the velocity ellipsoid, are 23.4 km/sec and 16.3 km/sec; these are within a few tenths of the values derived from more detailed investigations.

It is a pleasure to thank Dr. S. Chandrasekhar for having suggested the treatment embodied in this note.

RALPH E. WILLIAMSON

YERKES OBSERVATORY
April 2, 1941

ERRATUM

In the September issue, Vol. **90**, No. 2, p. 304, in Table 1, No. 78, under "Identification" for "140 mm from right" read "140 mm from left."

REVIEWS

The Principles of Statistical Mechanics. By RICHARD C. TOLMAN. ("International Series of Monographs on Physics.") Oxford: Clarendon Press, 1938. Pp. 661. $9.00.

To describe the purpose of this book I can do no better than quote its opening paragraph:

> It is the purpose of this book to expound the fundamental principles of statistical mechanics. Only incidental discussion of the application of statistical methods to the problems of usual physical-chemical interest will be given. It is hoped, however, that the exposition of underlying assumptions and general methods will be sufficient to give a real insight into the physical nature and mathematical apparatus of statistical mechanics.

After a description of general classical dynamics Tolman introduces the uniform, microcanonical, and canonical ensembles of Gibbs and discusses the validity of statistical mechanics. Tolman then takes up the Maxwell-Boltzmann distribution law, collisions as a mechanism of change, and Boltzmann's *H*-Theorem, of which the discussion is very satisfying. After a fairly complete description of the principles of quantum mechanics, including transformation theory, some applications of quantum mechanics are considered; then the density matrix is taken up, and the uniform, microcanonical, and canonical ensembles in quantum mechanics. The classical, Einstein-Bose, and Fermi-Dirac distributions are derived as the most probable distributions in microcanonical ensembles, and there follow chapters on the changes in quantum mechanical systems, on the quantum mechanical *H*-Theorem, and on the relationship of thermodynamics to classical and quantum statistical mechanics. There are two appendixes, subject index, and an index of authors. The book is not written concisely, and each of its many pages reads fairly rapidly. The book is somewhat awkwardly thick—a defect which could have been avoided by the use of thinner paper.

I quote the last paragraph:

> It is hoped, however, that our exposition of theory has been sufficiently sound and complete to solve our main task of giving a true insight into the methods that must be employed when we wish to predict the behaviour of a mechanical system on the basis of less knowledge as to its actual state than would in principle be allowable and possible. Such partial knowledge of state is in reality all that we ever do have, and the discipline of statistical mechanics must always remain necessary, whatever changes we may have to make in pure mechanics itself from classical to quantum or to any future form.

I think that Professor Tolman's purpose has been most successfully accomplished. He never allows himself to be distracted from it, and the book is therefore of quite a different character from R. H. Fowler's *Statistical Mechanics* (2d ed.; Cambridge, 1936), in which the author takes up successively the actual applications of statistical mechanics to many specific physical situations. The two books, Tolman's and Fowler's, are mutually complementary: the former with its emphasis on fundamental conceptions and meanings, the latter with its emphasis on applications. Neither can fully replace the other. Fowler's is better suited for a student or worker who is interested mainly in getting "results"; and if a person wishes merely to get correct results in statistical problems it is not necessary for him to read the book under review. Many physicists will fall into this category, and probably most astrophysicists, both observational and theoretical. Tolman's book is aimed, rather, at the person who wonders about the nature and validity of the fundamental conceptions and assumptions which underlie statistical mechanics. A person broadly interested in the logical basis of modern statistical mechanics, both classical and quantum, will find in this work probably the most satisfying discussions that have as yet been brought together in book form.

THEODORE E. STERNE

INDEX TO VOLUME 93

INDEX TO SUBJECTS

PAGE

Z Andromedae, The Evolution of a Peculiar Stellar Spectrum: *P. Swings and O. Struve* . 356

RT Aurigae. *Arthur L. Bennett* 52

ζ Aurigae, On the Atmospheric Structure of. *F. E. Roach* 1

B Stars, Interstellar Line Intensities and the Distances of the. *John W. Evans* . . . 275

B-Type Stars, Studies of Faint. *Carl K. Seyfert and Daniel M. Popper* 461

c Stars, The Luminosities of the Nonvariable. *Ralph E. Wilson* 212

29 Canis Majoris, The Light-Curve of the Eclipsing Variable. *Carl K. Seyfert* . . . 442

29 Canis Majoris, The Spectroscopic Binary. *Otto Struve and Frances Sherman* . . . 84

γ Cassiopeiae, The Recent Shell Spectrum of. *Ralph B. Baldwin* 333

γ Cassiopeiae, Temperature Variations of. *W. Albert Hiltner* 505

Coudé Spectrograph of the Mount Wilson Observatory, Some Results with the. *Walter S. Adams* 11

Cyanogen Criterion of Stellar Luminosity, The Extension to the Supergiants of the. *Philip C. Keenan* 475

Diffuse Radiation in the Galaxy. *L. G. Henyey and J. L. Greenstein* 70

Erratum. *Z. Kopal* 368

Erratum. *O. Struve, C. T. Elvey, and W. Linke* 512

Errors in the Spectroscopic Absolute Magnitudes of Dwarf Stars of Types F, Late K, and M, Systematic and Accidental. *Gustaf Strömberg* 33

Fowle, Frederick Eugene. *C. G. Abbot* 209

Heavy Water (*HDO*) Band ν_2 at 7.12 μ, The Grating Infrared Solar Spectrum. I. Rotational Structure of the. *Arthur Adel* 506

Hydrogen, The Continuous Spectrum of Stellar Atmospheres Consisting Only of Atoms and Negative Ions of. *Rupert Wildt* 47

Interstellar Absorption near the North Pole of Rotation. *Philip C. Keenan and Horace W. Babcock* 64

Interstellar Absorption to Reddening, The Ratio of. *J. L. Greenstein and L. G. Henyey* . 327

Interstellar Line Intensities and the Distances of the B Stars. *John W. Evans* . . . 275

PAGE

Interstellar Medium. I. Local Equilibrium, The Dynamics of the. *Lyman Spitzer, Jr.* . 369

17 Leporis (BS 2148), A Note on the Spectrum of. *Otto Struve* 504

β Lyrae and other Close Binaries, On the Interpretation of. *Gerard P. Kuiper* . . . 133

β Lyrae, Some Line Intensities in. *Jocelyn R. Gill* 118

β Lyrae, On the Nature of the System of. *Zdenek Kopal* 92

β Lyrae, The Spectrum of. *Otto Struve* 104

β Lyrae in the Visual Region, The Spectrum of. *J. L. Greenstein and T. L. Page* . . 128

Milky Way in Cygnus and Scorpius, Photographs of the. *Harold A. Lower* 506

Nebulae. XI. Physical Processes in Gaseous. *G. H. Shortley, L. H. Aller, J. G. Baker, and D. H. Menzel* 178

Nebulae. XII. Physical Processes in Gaseous. *Donald H. Menzel and Lawrence H. Aller* 195

Nebulae. XIII. Physical Processes in Gaseous. *Donald H. Menzel, Lawrence H. Aller, and Malcolm H. Hebb* 230

Nebulae. XIV. Physical Processes in Gaseous. *Lawrence H. Aller* 236

Nebulae. XV. Physical Processes in Gaseous. *Leo Goldberg* 244

Nebulae, Reynolds' Numbers for Extragalactic. *F. Zwicky* 411

NH Molecule in Spectra of Class R, The Resonance Bands of the. *Rupert Wildt* . . . 502

Night Sky, The Spectrum of the. *C. T. Elvey, P. Swings, and Walter Linke* 337

Nitrous Oxide (*NNO*) Band ν_1 at 7.37 μ, The Grating Infrared Solar Spectrum. II. Rotational Structure of the. *Arthur Adel* 509

Novae, The Distances and Luminosities of Three. *Dean B. McLaughlin* 417

Photometry, The Reciprocity Principle in Lunar. *M. Minnaert* 403

Planetary Atmospheres and Water-Cell Temperatures. *Arthur Adel and C. O. Lampland* 391

Planets, On the Theory of the Origin of the. *R. A. Lyttleton* 267

Pleione, The Spectrum of the Shell of. *Otto Struve and P. Swings* 446

Pleione, The Visual Spectrum of. *Jesse L. Greenstein* 453

Radiation Pressure in the Convective Stellar Model. *Louis R. Henrich* 483

Reviews:

Baker, Robert H. *An Introduction to Astronomy* 368

Stratton, F. J. M., and W. H. Manning. *Atlas of Spectra of Nova Herculis 1934* (W. W. Morgan) 368

Tolman, Richard C. *The Principles of Statistical Mechanics* (T. E. Sterne) 513

Solar Hydrogen Vortices, The Nature of. *R. S. Richardson* 24

PAGE

Spectra of B 1985 and WY Geminorum, The Emission Lines in the. *P. Swings and O. Struve* . . . 455

Spectra of Class R, The Resonance Bands of the NH Molecules in. *Rupert Wildt* . . . 502

Spectra of Gases in the Extreme Ultraviolet, Absorption. *Toshio Takamine and Yoshio Tanaka* . . . 386

Spectra of Long-Period Variables, Displacements of Lines in the. *P. W. Merrill* . . . 380

Spectra of Me Variables, Ultraviolet Emission Lines in the. *Paul W. Merrill* . . . 40

Spectra of Two Peculiar Stars: MWC 17 and CD -27° 11944, The. *P. Swings and O. Struve* . . . 349

Spectral Classifications of Faint Stars, Intercomparison of Various. *Alexander N. Vyssotsky* . . . 425

Spectrohelioscope for the Observation of Spectra of Chromospheric Erruptions, Use of the Hale. *W. Dodson* . . . 208

Spectroscopic Absolute Magnitudes of Dwarf Stars of Types F, Late K, and M, Systematic and Accidental Errors in the. *Gustaf Strömberg* . . . 33

Spectroscopic Binaries, On the Determination of Mass Ratios of. *O. C. Wilson* . . . 29

Spectroscopic Binary 29 Canis Majoris, The. *Otto Struve and Frances Sherman* . . . 84

Spectrum. I. Rotational Structure of the Heavy Water (*HDO*) Band ν_2 at 7.12 μ, The Grating Infrared Solar. *Arthur Adel* . . . 506

Spectrum. II. Rotational Structure of the Nitrous Oxide (*NNO*) Band ν_1 at 7.37 μ, The Grating Infrared Solar. *Arthur Adel* . . . 509

Spectrum: Z Andromedae, The Evolution of a Peculiar Stellar. *P. Swings and O. Struve* 356

Spectrum of γ Cassiopeiae, The Recent Shell. *Ralph B. Baldwin.* . . . 333

Spectrum of 17 Leporis (BS 2148), A Note on the. *Otto Struve* . . . 504

Spectrum of β Lyrae, The. *Otto Struve* . . . 104

Spectrum of β Lyrae in the Visual Region, The. *J. L. Greenstein and T. L. Page* . . . 128

Spectrum of the Night Sky, The. *C. T. Elvey, P. Swings, and Walter Linke* . . . 337

Spectrum of Pleione, The Visual. *Jesse L. Greenstein* . . . 453

Spectrum of the Shell of Pleione, The. *Otto Struve and P. Swings* . . . 446

Spectrum of Stellar Atmospheres Consisting only of Atoms and Negative Ions of Hydrogen, The Continuous. *Rupert Wildt* . . . 47

Spectrum of ζ Tauri, The 1914 Shell. *Ralph B. Baldwin* . . . 420

Star-streaming, A Simple Demonstration of. *Ralph E. Williamson* . . . 511

Stellar Motions in Terms of a Nonsteady-State Model for the Galaxy, An Interpretation of. *John Titus* . . . 57

PAGE

Stellar Systems. I. The Time of Relaxation of. *S. Chandrasekhar* 285

Stellar Systems. II. The Time of Relaxation of. *Ralph E. Williamson and S. Chandrasekhar* 305

Stellar Systems. III. The Time of Relaxation of. *S. Chandrasekhar* 323

Stream-Motions of 92,656 Stars, The. *W. J. Luyten* 250

ζ Tauri, The 1914 Shell Spectrum of. *Ralph B. Baldwin* 420

Temperature Radiation from Venus, The Importance of Certain Carbon Dioxide Bands in the. *Arthur Adel* 397

Temperatures, Planetary Atmospheres and Water-Cell. *Arthur Adel and C. O. Lampland* 391

Variable, 29 Canis Majoris, The Light-Curve of the Eclipsing. *Carl K. Seyfert* . . . 442

Variables, Note on Eclipsing. *Newton L. Pierce* 506

Venus. Comments on Dr. Adel's Paper, On the Observable Radiation from the Carbon Dioxide in the Atmosphere of. *C. O. Lampland* 401

Venus, The Importance of Certain Carbon Dioxide Bands in the Temperature Radiation from. *Arthur Adel* 397

Wolf-Rayet Eclipsing Binary: HV 11111 = BD+38°4010 = HD 193576, The Absolute Dimensions of a. *Sergei Gaposchkin* 202

INDEX OF AUTHORS

PAGE

ABBOT, C. G. Frederick Eugene Fowle 209

ADAMS, WALTER S. Some Results with the Coudé Spectrograph of the Mount Wilson Observatory 11

ADEL, ARTHUR. The Grating Infrared Solar Spectrum. I. Rotational Structure of Heavy Water (*HDO*) Band ν_2 at 7.12 μ 506

ADEL, ARTHUR. The Grating Infrared Solar Spectrum. II. Rotational Structure of the Nitrous Oxide (*NNO*) Band ν_1 at 7.37 μ 509

ADEL, ARTHUR. The Importance of Certain Carbon Dioxide Bands in the Temperature Radiation from Venus 397

ADEL, ARTHUR, and C. O. LAMPLAND. Planetary Atmospheres and Water-Cell Temperatures 391

ALLER, LAWRENCE H. Physical Processes in Gaseous Nebulae. XIV 236

ALLER, L. H., J. G. BAKER, D. H. MENZEL, and G. H. SHORTLEY. Physical Processes in Gaseous Nebulae. XI 178

ALLER, LAWRENCE H., MALCOLM H. HEBB, and DONALD H. MENZEL. Physical Processes in Gaseous Nebulae. XIII 230

ALLER, LAWRENCE H., and DONALD H. MENZEL. Physical Processes in Gaseous Nebulae. XII 195

BABCOCK, HORACE W., and PHILIP C. KEENAN. Interstellar Absorption near the North Pole of Rotation 64

BAKER, J. G., D. H. MENZEL, G. H. SHORTLEY, and L. H. ALLER. Physical Processes in Gaseous Nebulae. XI 178

BALDWIN, RALPH B. The Recent Shell Spectrum of γ Cassiopeiae 333

BALDWIN, RALPH B. The 1914 Shell Spectrum of ζ Tauri 420

BENNETT, ARTHUR L. RT Aurigae 52

CHANDRASEKHAR, S. The Time of Relaxation of Stellar Systems. I 285

CHANDRASEKHAR, S. The Time of Relaxation of Stellar Systems. III 323

CHANDRASEKHAR, S., and RALPH E. WILLIAMSON. The Time of Relaxation of Stellar Systems. II 305

DODSON, HELEN W. Use of the Hale Spectrohelioscope for the Observation of Spectra of Chromospheric Eruptions 208

ELVEY, C. T., P. SWINGS, and WALTER LINKE. The Spectrum of the Night Sky . . . 337

PAGE

EVANS, JOHN W. Interstellar Line Intensities and the Distances of the B Stars . . . 275

GAPOSCHKIN, SERGEI. The Absolute Dimensions of a Wolf-Rayet Eclipsing Binary: HV 11111 = BD+38°4010 = HD 193576 202

GILL, JOCELYN R. Some Line Intensities in β Lyrae 118

GOLDBERG, LEO. Physical Processes in Gaseous Nebulae. XV 244

GREENSTEIN, JESSE L. The Visual Spectrum of Pleione 453

GREENSTEIN, J. L., and L. G. HENYEY. Diffuse Radiation in the Galaxy 70

GREENSTEIN, J. L., and L. G. HENYEY. The Ratio of Interstellar Absorption to Reddening 327

GREENSTEIN, J. L., and T. L. PAGE. The Spectrum of β Lyrae in the Visual Region . . 128

HEBB, MALCOLM H., DONALD H. MENZEL, and LAWERNCE H. ALLER. Physical Processes in Gaseous Nebulae. XIII 230

HENRICH, LOUIS R. Radiation Pressure in the Convective Stellar Model 483

HENYEY, L. G., and J. L. GREENSTEIN. Diffuse Radiation in the Galaxy 70

HENYEY, L. G., and J. L. GREENSTEIN. The Ratio of Interstellar Absorption to Reddening 327

HILTNER, W. ALBERT. Temperature Variations of γ Cassiopeiae 505

KEENAN, PHILIP C. The Extension to the Supergiants of the Cyanogen Criterion of Stellar Luminosity 475

KEENAN, PHILIP C., and HORACE W. BABCOCK. Interstellar Absorption near the North Pole of Rotation 64

KOPAL, Z. Erratum 368

KOPAL, ZDENĚK. On the Nature of the System of β Lyrae 92

KUIPER, GERARD P. On the Interpretation of β Lyrae and Other Close Binaries . . . 133

LAMPLAND, C. O. On the Observable Radiation from the Carbon Dioxide in the Atmosphere of Venus. Comments on Dr. Adel's Paper 401

LAMPLAND, C. O., and ARTHUR ADEL. Planetary Atmospheres and Water-Cell Temperatures 301

LINKE, WALTER, C. T. ELVEY, and P. SWINGS. The Spectrum of the Night Sky . . . 337

LOWER, HAROLD A. Photographs of the Milky Way in Cygnus and Scorpius 506

LUYTEN, W. J. The Stream-Motions of 92,656 Stars 250

LYTTLETON, R. A. On the Theory of the Origin of the Planets 267

MCLAUGHLIN, DEAN B. The Distances and Luminosities of Three Novae 417

PAGE

MENZEL, DONALD H., and LAWRENCE H. ALLER. Physical Processes in Gaseous Nebulae. XII . . . 195

MENZEL, DONALD H., LAWRENCE H. ALLER, and MALCOLM H. HEBB. Physical Processes in Gaseous Nebulae. XIII . . . 230

MENZEL, D. H., G. H. SHORTLEY, L. H. ALLER, and J. G. BAKER. Physical Processes in Gaseous Nebulae. XI . . . 178

MERRILL, P. W. Displacements of Lines in the Spectra of Long-Period Variables . . . 380

MERRILL, PAUL W. Ultraviolet Emission Lines in the Spectra of Me Variables 40

MINNAERT, M. The Reciprocity Principle in Lunar Photometry . . . 403

MORGAN, W. W. Review of: *Atlas of Spectra of Nova Herculis 1934*, F. J. M. Stratton and W. H. Manning . . . 368

PAGE, T. L., and J. L. GREENSTEIN. The Spectrum of β Lyrae in the Visual Region . . 128

PIERCE, NEWTON L. Note on Eclipsing Variables . . . 506

POPPER, DANIEL M., and CARL K. SEYFERT. Studies of Faint B-Type Stars . . . 461

RICHARDSON, R. S. The Nature of Solar Hydrogen Vortices . . . 24

ROACH, F. E. On the Atmospheric Structure of ζ Aurigae . . . 1

SEYFERT, CARL K. The Light-Curve of the Eclipsing Variable, 29 Canis Majoris . . . 442

SEYFERT, CARL K., and DANIEL M. POPPER. Studies of Faint B-Type Stars . . . 461

SHERMAN, FRANCES, and OTTO STRUVE. The Spectroscopic Binary 29 Canis Majoris . 84

SHORTLEY, G. H., L. H. ALLER, J. G. BAKER, and D. H. MENZEL. Physical Processes in Gaseous Nebulae. XI . . . 178

SPITZER, LYMAN, JR. The Dynamics of the Interstellar Medium. I. Local Equilibrium . 369

STERNE, T. E. Review of: *The Principles of Statistical Mechanics*, Richard C. Tolman . 513

STRÖMBERG, GUSTAF. Systematic and Accidental Errors in the Spectroscopic Absolute Magnitudes of Dwarf Stars of Types F, Late K, and M . . . 33

STRUVE, OTTO. A Note on the Spectrum of 17 Leporis (BS 2148) . . . 504

STRUVE, OTTO. The Spectrum of β Lyrae . . . 104

STRUVE, O., C. T. ELVEY, and W. LINKE. Erratum . . . 512

STRUVE, OTTO, and FRANCES SHERMAN. The Spectroscopic Binary 29 Canis Majoris . 84

STRUVE, O., and P. SWINGS. The Emission Lines in the Spectra of B 1985 and WY Geminorum . . . 455

STRUVE, O., and P. SWINGS. The Evolution of a Peculiar Stellar Spectrum: Z Andromedae 356

STRUVE, O., and P. SWINGS. The Spectra of Two Peculiar Stars: MWC 17 and CD $-27^{\circ}11944$ . . . 349

PAGE

STRUVE, OTTO, and P. SWINGS. The Spectrum of the Shell of Pleione 446

SWINGS, P., C. T. ELVEY, and WALTER LINKE. The Spectrum of the Night Sky . . . 337

SWINGS, P., and O. STRUVE. The Emission Lines in the Spectra of B 1985 and WY Geminorum 455

SWINGS, P., and O. STRUVE. The Evolution of a Peculiar Spectrum: Z Andromedae . . 356

SWINGS, P., and O. STRUVE. The Spectra of Two Peculiar Stars: MWC 17 and CD $-27^{\circ}11944$ 349

SWINGS, P., and OTTO STRUVE. The Spectrum of the Shell of Pleione 446

TAKAMINE, TOSHIO, and YOSHIO TANAKA. Absorption Spectra of Gases in the Extreme Ultraviolet 386

TANAKA, YOSHIO, and TOSHIO TAKAMINE. Absorption Spectra of Gases in the Extreme Ultraviolet 386

TITUS, JOHN. An Interpretation of Stellar Motions in Terms of a Nonsteady-State Model for the Galaxy 57

VYSSOTSKY, ALEXANDER N. Intercomparison of Various Spectral Classifications of Faint Stars 425

WILDT, RUPERT. The Continuous Spectrum of Stellar Atmospheres Consisting Only of Atoms and Negative Ions of Hydrogen 47

WILDT, RUPERT. The Resonance Bands of the *NH* Molecule in Spectra of Class R . . 502

WILLIAMSON, RALPH E. A Simple Demonstration of Star-streaming 511

WILLIAMSON, RALPH E., and S. CHANDRASEKHAR. The Time Relaxation of Stellar Systems. II 305

WILSON, O. C. On the Determination of Mass Ratios of Spectroscopic Binaries . . . 29

WILSON, RALPH E. The Luminosities of the Nonvariable c Stars 212

ZWICKY, F. Reynolds' Numbers for Extragalactic Nebulae 411